

9. QUANTUM CHROMODYNAMICS

9.1. The QCD Lagrangian

Revised September 2003 by I. Hinchliffe (LBNL).

Quantum Chromodynamics (QCD), the gauge field theory which describes the strong interactions of colored quarks and gluons, is one of the components of the $SU(3) \times SU(2) \times U(1)$ Standard Model. A quark of specific flavor (such as a charm quark) comes in 3 colors; gluons come in eight colors; hadrons are color-singlet combinations of quarks, anti-quarks, and gluons. The Lagrangian describing the interactions of quarks and gluons is (up to gauge-fixing terms)

$$L_{\text{QCD}} = -\frac{1}{4} F_{\mu\nu}^{(a)} F^{(a)\mu\nu} + i \sum_q \bar{\psi}_q^i \gamma^\mu (D_\mu)_{ij} \psi_q^j - \sum_q m_q \bar{\psi}_q^i \psi_{qi}, \quad (9.1)$$

$$F_{\mu\nu}^{(a)} = \partial_\mu A_\nu^a - \partial_\nu A_\mu^a - g_s f_{abc} A_\mu^b A_\nu^c, \quad (9.2)$$

$$(D_\mu)_{ij} = \delta_{ij} \partial_\mu + i g_s \sum_a \frac{\lambda_{ij}^a}{2} A_\mu^a, \quad (9.3)$$

where g_s is the QCD coupling constant, and the f_{abc} are the structure constants of the $SU(3)$ algebra (the λ matrices and values for f_{abc} can be found in “SU(3) Isoscalar Factors and Representation Matrices,” Sec. 36 of this *Review*). The $\psi_q^i(x)$ are the 4-component Dirac spinors associated with each quark field of (3) color i and flavor q , and the $A_\mu^a(x)$ are the (8) Yang-Mills (gluon) fields. A complete list of the Feynman rules which derive from this Lagrangian, together with some useful color-algebra identities, can be found in Ref. 1.

The principle of “asymptotic freedom” determines that the renormalized QCD coupling is small only at high energies, and it is only in this domain that high-precision tests—similar to those in QED—can be performed using perturbation theory. Nonetheless, there has been in recent years much progress in understanding and quantifying the predictions of QCD in the nonperturbative domain, for example, in soft hadronic processes and on the lattice [2]. This short review will concentrate on QCD at short distances (large momentum transfers), where perturbation theory is the standard tool. It will discuss the processes that are used to determine the coupling constant of QCD. Other recent reviews of the coupling constant measurements may be consulted for a different perspective [3–5].

9.2. The QCD coupling and renormalization scheme

The renormalization scale dependence of the effective QCD coupling $\alpha_s = g_s^2/4\pi$ is controlled by the β -function:

$$\mu \frac{d\alpha_s}{d\mu} = 2\beta(\alpha_s) = -\frac{\beta_0}{2\pi} \alpha_s^2 - \frac{\beta_1}{4\pi^2} \alpha_s^3 - \frac{\beta_2}{64\pi^3} \alpha_s^4 - \dots, \quad (9.4a)$$

$$\beta_0 = 11 - \frac{2}{3} n_f, \quad (9.4b)$$

$$\beta_1 = 51 - \frac{19}{3} n_f, \quad (9.4c)$$

$$\beta_2 = 2857 - \frac{5033}{9} n_f + \frac{325}{27} n_f^2; \quad (9.4d)$$

where n_f is the number of quarks with mass less than the energy scale μ . The expression for the next term in this series (β_3) can be found in Ref. 7. In solving this differential equation for α_s , a constant of integration is introduced. This constant is the one fundamental constant of QCD that must be determined from experiment. The most sensible choice for this constant is the value of α_s at a fixed-reference scale μ_0 . It has become standard to choose $\mu_0 = M_Z$. The value at other values of μ can be obtained from $\log(\mu^2/\mu_0^2) = \int_{\alpha_s(\mu_0)}^{\alpha_s(\mu)} \frac{d\alpha}{\beta(\alpha)}$. It is also convenient to introduce the dimensional parameter Λ , since this provides a parameterization of the μ dependence of α_s . The definition of Λ is arbitrary. One way to define it (adopted here) is to write a solution of Eq. (9.4) as an expansion in inverse powers of $\ln(\mu^2)$:

$$\alpha_s(\mu) = \frac{4\pi}{\beta_0 \ln(\mu^2/\Lambda^2)} \left[1 - \frac{2\beta_1}{\beta_0^2} \frac{\ln[\ln(\mu^2/\Lambda^2)]}{\ln(\mu^2/\Lambda^2)} + \frac{4\beta_2^2}{\beta_0^4 \ln^2(\mu^2/\Lambda^2)} \right. \\ \left. \times \left(\left[\ln[\ln(\mu^2/\Lambda^2)] - \frac{1}{2} \right]^2 + \frac{\beta_2\beta_0}{8\beta_1^2} - \frac{5}{4} \right) \right]. \quad (9.5)$$

This solution illustrates the *asymptotic freedom* property: $\alpha_s \rightarrow 0$ as $\mu \rightarrow \infty$ and shows that QCD becomes strongly coupled at $\mu \sim \Lambda$.

Consider a “typical” QCD cross section which, when calculated perturbatively [6], starts at $\mathcal{O}(\alpha_s)$:

$$\sigma = A_1 \alpha_s + A_2 \alpha_s^2 + \dots \quad (9.6)$$

The coefficients A_1, A_2 come from calculating the appropriate Feynman diagrams. In performing such calculations, various divergences arise, and these must be regulated in a consistent way. This requires a particular renormalization scheme (RS). The most commonly used one is the modified minimal subtraction ($\overline{\text{MS}}$) scheme [8]. This involves continuing momentum integrals from 4 to $4-2\epsilon$ dimensions, and then subtracting off the resulting $1/\epsilon$ poles and also $(\ln 4\pi - \gamma_E)$, which is an artifact of continuing the dimension. (Here γ_E is the Euler-Mascheroni constant.) To preserve the dimensionless nature of the coupling, a mass scale μ must also be introduced: $g \rightarrow \mu^\epsilon g$. The finite coefficients A_i ($i \geq 2$) thus obtained depend implicitly on the renormalization convention used and explicitly on the scale μ .

The first two coefficients (β_0, β_1) in Eq. (9.4) are independent of the choice of RS’s. In contrast, the coefficients of terms proportional to α_s^n for $n > 3$ are RS-dependent. The form given above for β_2 is in the $\overline{\text{MS}}$ scheme.

The fundamental theorem of RS dependence is straightforward. Physical quantities, such as the cross section calculated to all orders in perturbation theory, do not depend on the RS. It follows that a truncated series *does* exhibit RS dependence. In practice, QCD cross sections are known to leading order (LO), or to next-to-leading order (NLO), or in some cases, to next-to-next-to-leading order (NNLO); and it is only the latter two cases, which have reduced RS dependence, that are useful for precision tests. At NLO the RS dependence is completely given by one condition which can be taken to be the value of the renormalization scale μ . At NNLO this is not sufficient, and μ is no longer equivalent to a choice of scheme; both must now be specified. One, therefore, has to address the question of what is the “best” choice for μ within a given scheme, usually $\overline{\text{MS}}$. There is no definite answer to this question—higher-order corrections do not “fix” the scale, rather they render the theoretical predictions less sensitive to its variation.

One should expect that choosing a scale μ characteristic of the typical energy scale (E) in the process would be most appropriate. In general, a poor choice of scale generates terms of order $\ln(E/\mu)$ in the A_i ’s. Various methods have been proposed including choosing the scale for which the next-to-leading-order correction vanishes (“Fastest Apparent Convergence [9]”); the scale for which the next-to-leading-order prediction is stationary [10], (*i.e.*, the value of μ where $d\sigma/d\mu = 0$); or the scale dictated by the effective charge scheme [11] or by the BLM scheme [12]. By comparing the values of α_s that different reasonable schemes give, an estimate of theoretical errors can be obtained. It has also been suggested to replace the perturbation series by its Padé approximant [13]. Results obtained using this method have, in certain cases, a reduced scale dependence [14,15]. One can also attempt to determine the scale from data by allowing it to vary and using a fit to determine it. This method can allow a determination of the error due to the scale choice and can give more confidence in the end result [16]. In many of the cases discussed below this scale uncertainty is the dominant error.

An important corollary is that if the higher-order corrections are naturally small, then the additional uncertainties introduced by the μ dependence are likely to be small. There are some processes, however, for which the choice of scheme *can* influence the extracted value of $\alpha_s(M_Z)$. There is no resolution to this problem other than to try to calculate even more terms in the perturbation series. It is important to note that, since the perturbation series is an asymptotic expansion, there is a limit to the precision with which any theoretical quantity can be calculated. In some processes, the highest-order perturbative terms may be comparable in size to nonperturbative corrections (sometimes called higher-twist or renormalon effects, for a discussion see [17]); an estimate of these terms and their uncertainties is required if a value of α_s is to be extracted.

Cases occur where there is more than one large scale, say μ_1 and μ_2 . In these cases, terms appear of the form $\log(\mu_1/\mu_2)$. If the ratio μ_1/μ_2 is large, these logarithms can render naive perturbation theory unreliable and a modified perturbation expansion that takes these terms into account must be used. A few examples are discussed below.

In the cases where the higher-order corrections to a process are known and are large, some caution should be exercised when quoting the value of α_s . In what follows, we will attempt to indicate the size of the theoretical uncertainties on the extracted value of α_s . There are two simple ways to determine this error. First, we can estimate it by comparing the value of $\alpha_s(\mu)$ obtained by fitting data using the QCD formula to highest known order in α_s , and then comparing it with the value obtained using the next-to-highest-order formula (μ is chosen as the typical energy scale in the process). The corresponding Λ 's are then obtained by evolving $\alpha_s(\mu)$ to $\mu = M_Z$ using Eq. (9.4) to the same order in α_s as the fit. Alternatively, we can vary the value of μ over a reasonable range, extracting a value of Λ for each choice of μ . This method is by its nature imprecise, since "reasonable" involves a subjective judgment. In either case, if the perturbation series is well behaved, the resulting error on $\alpha_s(M_Z)$ will be small.

In the above discussion we have ignored quark-mass effects, *i.e.*, we have assumed an idealized situation where quarks of mass greater than μ are neglected completely. In this picture, the β -function coefficients change by discrete amounts as flavor thresholds (a quark of mass M) are crossed when integrating the differential equation for α_s . Now imagine an experiment at energy scale μ ; for example, this could be $e^+e^- \rightarrow$ hadrons at center-of-mass energy μ . If $\mu \gg M$, the mass M is negligible and the process is well described by QCD with n_f massless flavors and its parameter $\alpha_{(n_f)}$ up to terms of order M^2/μ^2 . Conversely if $\mu \ll M$, the heavy quark plays no role and the process is well described by QCD with $n_f - 1$ massless flavors and its parameter $\alpha_{(n_f-1)}$ up to terms of order μ^2/M^2 . If $\mu \sim M$, the effects of the quark mass are process-dependent and cannot be absorbed into the running coupling. The values of $\alpha_{(n_f)}$ and $\alpha_{(n_f-1)}$ are related so that a physical quantity calculated in both "theories" gives the same result [18]. This implies, for $\mu = M$

$$\alpha_{(n_f)}(M) = \alpha_{(n_f-1)}(M) - \frac{11}{72\pi^2} \alpha_{(n_f-1)}^3(M) + \mathcal{O}(\alpha_{(n_f-1)}^4) \quad (9.7)$$

which is almost identical to the naive result $\alpha_{(n_f)}(M) = \alpha_{(n_f-1)}(M)$. Here M is the mass of the value of the running quark mass defined in the $\overline{\text{MS}}$ scheme (see the note on "Quark Masses" in the Particle Listings for more details), *i.e.*, where $M_{\overline{\text{MS}}}(M) = M$.

It also follows that, for a relationship such as Eq. (9.5) to remain valid for all values of μ , Λ must also change as flavor thresholds are crossed, the value corresponds to an effective number of massless quarks: $\Lambda \rightarrow \Lambda^{(n_f)}$ [18,19]. The formulae are given in the 1998 edition of this review.

Data from deep-inelastic scattering are in a range of energy where the bottom quark is not readily excited, and hence, these experiments quote $\Lambda_{\overline{\text{MS}}}^{(4)}$. Most data from PEP, PETRA, TRISTAN, LEP, and SLC quote a value of $\Lambda_{\overline{\text{MS}}}^{(5)}$ since these data are in an energy range where the bottom quark is light compared to the available energy. We have converted it to $\Lambda_{\overline{\text{MS}}}^{(4)}$ as required. A few measurements, including the lattice gauge theory values from the J/ψ system, and from τ decay are at sufficiently low energy that $\Lambda_{\overline{\text{MS}}}^{(3)}$ is appropriate.

In order to compare the values of α_s from various experiments, they must be evolved using the renormalization group to a common scale. For convenience, this is taken to be the mass of the Z boson. This evolution uses third-order perturbation theory and can introduce additional errors particularly if extrapolation from very small scales is used. The variation in the charm and bottom quark masses ($M_b = 4.3 \pm 0.2$ GeV and $M_c = 1.3 \pm 0.3$ GeV are used [20]) can also introduce errors. These result in a fixed value of $\alpha_s(2$ GeV) giving an uncertainty in $\alpha_s(M_Z) = \pm 0.001$ if only perturbative evolution is used. There could be additional errors from nonperturbative effects that enter at low energy.

9.3. QCD in deep-inelastic scattering

The original and still one of the most powerful quantitative tests of perturbative QCD is the breaking of Bjorken scaling in deep-inelastic lepton-hadron scattering. The review "Structure Functions," (Sec. 16 of this *Review*) describes the basic formalism and reviews the data. α_s is obtained together with the structure functions. The global fit from MRS T03 [30] of (Sec. 16) gives $\alpha_s(M_Z) = 0.1165 \pm 0.004$ from NLO and $\alpha_s(M_Z) = 0.1153 \pm 0.004$ from NNLO. Other fits are consistent with these values but cannot be averaged as they use overlapping data sets. The good agreement between the NLO and NNLO fits indicates that the theoretical uncertainties are under control. The NNLO result is used in the average below.

Nonsinglet structure function offers in principle the most precise test of the theory, since the Q^2 evolution is independent of the gluon distribution which is much more poorly constrained. The CCFR collaboration fit to the Gross-Llewellyn Smith sum rule [22] which is known to order α_s^3 [23,24](NNLO); estimates of the order α_s^4 term are available [25].

$$\int_0^1 dx \left(F_3^{\overline{p}p}(x, Q^2) + F_3^{\nu p}(x, Q^2) \right) = 3 \left[1 - \frac{\alpha_s}{\pi} \left(1 + 3.58 \frac{\alpha_s}{\pi} + 19.0 \left(\frac{\alpha_s}{\pi} \right)^2 \right) - \Delta HT \right], \quad (9.8)$$

where the higher-twist contribution ΔHT is estimated to be $(0.09 \pm 0.045)/Q^2$ in Refs. 23,26 and to be somewhat smaller by Ref. 27. The CCFR collaboration [28], combines their data with that from other experiments [29] and gives $\alpha_s(\sqrt{3}$ GeV) = 0.28 ± 0.035 (expt.) ± 0.05 (sys) $^{+0.035}_{-0.03}$ (theory). The error from higher-twist terms (assumed to be $\Delta HT = 0.05 \pm 0.05$) dominates the theoretical error. If the higher twist result of Ref. 27 is used, the central value increases to 0.31 in agreement with the fit of [30]. This value corresponds to $\alpha_s(M_Z) = 0.118 \pm 0.011$. Fits of the Q^2 evolution [31] of $x F_3$ using the CCFR data using NNLO and estimates of NNNLO QCD and higher twist terms enables the effect of these terms to be studied.

The spin-dependent structure functions, measured in polarized lepton-nucleon scattering, can also be used to test QCD and to determine α_s . Note that these experiments measure asymmetries and rely on measurements of unpolarized data to extract the spin-dependent structure functions. Here the values of $Q^2 \sim 2.5$ GeV² are small, particularly for the E143 data [32], and higher-twist corrections are important. A fit [33] by an experimental group using the measured spin dependent structure functions for several experiments Refs. 32,34 as well as their own data has been made. When data from HERMES [35] and SMC are included [36] $\alpha_s(M_Z) = 0.120 \pm 0.009$ is obtained: this is used in the final average.

α_s can also be determined from the Bjorken spin sum rule [37]; a fit gives [38] $\alpha_s(M_Z) = 0.118^{+0.019}_{-0.024}$, consistent with an earlier determination [39], the larger error being due to the extrapolation into the (unmeasured) small x region. Theoretically, the sum rule is preferable as the perturbative QCD result is known to higher order and these terms are important at the low Q^2 involved. It has been shown that the theoretical errors associated with the choice of scale are considerably reduced by the use of Padé approximants [14] which results in $\alpha_s(1.7$ GeV) = 0.328 ± 0.03 (expt.) ± 0.025 (theory) corresponding to $\alpha_s(M_Z) = 0.116^{+0.003}_{-0.005}$ (expt.) ± 0.003 (theory). No error is included from the extrapolation into the region of x that is unmeasured. Should data become available at smaller values of x so that this extrapolation could be more tightly constrained, the sum rule method could provide a better determination of α_s .

9.4. QCD in decays of the τ lepton

The semi-leptonic branching ratio of the tau ($\tau \rightarrow \nu_\tau +$ hadrons, R_τ) is an inclusive quantity. It is related to the contribution of hadrons to the imaginary part of the W self energy ($\text{Im}(\Pi(s))$). It is sensitive to a range of energies since it involves an integral

$$R_\tau \sim \int_0^{m_\tau^2} \frac{ds}{m_\tau^2} \left(1 - \frac{s}{m_\tau^2} \right)^2 \text{Im}(\Pi(s)). \quad (9.9)$$

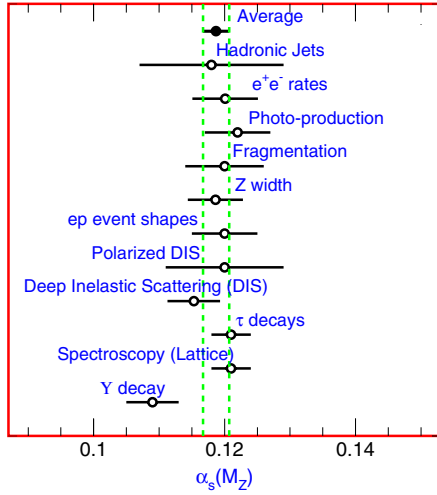


Figure 9.1: Summary of the value of $\alpha_s(M_Z)$ from various processes. The values shown indicate the process and the measured value of α_s extrapolated to $\mu = M_Z$. The error shown is the *total* error including theoretical uncertainties. The average quoted in this report which comes from these measurements is also shown. See text for discussion of errors.

Since the scale involved is low, one must take into account nonperturbative (higher-twist) contributions which are suppressed by powers of the τ mass.

$$R_\tau = 3.058 \left[1 + \frac{\alpha_s(m_\tau)}{\pi} + 5.2 \left(\frac{\alpha_s(m_\tau)}{\pi} \right)^2 + 26.4 \left(\frac{\alpha_s(m_\tau)}{\pi} \right)^3 + a \frac{m^2}{m_\tau^2} + b \frac{m\psi\bar{\psi}}{m_\tau^4} + c \frac{\psi\bar{\psi}\psi\bar{\psi}}{m_\tau^6} + \dots \right]. \quad (9.10)$$

Here $a, b,$ and c are dimensionless constants and m is a light quark mass. The term of order $1/m_\tau^2$ is a kinematical effect due to the light quark masses and is consequently very small. The nonperturbative terms are estimated using sum rules [40]. In total, they are estimated to be -0.014 ± 0.005 [41,42]. This estimate relies on there being no term of order Λ^2/m_τ^2 . Λ^2/m_τ^2 (note that $\frac{\alpha_s(m_\tau)}{\pi} \sim (\frac{0.5 \text{ GeV}}{m_\tau})^2$).

The $a, b,$ and c can be determined from the data [43] by fitting to moments of the $\Pi(s)$ and separately to the final states accessed by the vector and axial parts of the W coupling. The values so extracted [44,45] are consistent with the theoretical estimates. If the nonperturbative terms are omitted from the fit, the extracted value of $\alpha_s(m_\tau)$ decreases by ~ 0.02 .

For $\alpha_s(m_\tau) = 0.35$ the perturbative series for R_τ is $R_\tau \sim 3.058(1 + 0.112 + 0.064 + 0.036)$. The size (estimated error) of the nonperturbative term is 20% (7%) of the size of the order α_s^3 term. The perturbation series is not very well convergent; if the order α_s^3 term is omitted, the extracted value of $\alpha_s(m_\tau)$ increases by 0.05. The order α_s^4 term has been estimated [46] and attempts made to resum the entire series [47,48]. These estimates can be used to obtain an estimate of the errors due to these unknown terms [49,50]. We assign an uncertainty of ± 0.02 to $\alpha_s(m_\tau)$ from these sources.

R_τ can be extracted from the semi-leptonic branching ratio from the relation $R_\tau = 1/(B(\tau \rightarrow e\nu\bar{\nu}) - 1.97256)$; where $B(\tau \rightarrow e\nu\bar{\nu})$ is measured directly or extracted from the lifetime, the muon mass, and the muon lifetime assuming universality of lepton couplings. Using the average lifetime of 290.6 ± 1.1 fs and a τ mass of 1776.99 ± 0.29 MeV from the PDG fit gives $R_\tau = 3.645 \pm 0.020$. The direct measurement of $B(\tau \rightarrow e\nu\bar{\nu})$ can be combined with $B(\tau \rightarrow \mu\nu\bar{\nu})$ to give $B(\tau \rightarrow e\nu\bar{\nu}) = 0.1785 \pm 0.0005$ which gives $R_\tau = 3.629 \pm 0.015$.

Averaging these yields $\alpha_s(m_\tau) = 0.353 \pm 0.007$ using the experimental error alone. We assign a theoretical error equal to 40% of the contribution from the order α^3 term and all of the nonperturbative contributions. This then gives $\alpha_s(m_\tau) = 0.35 \pm 0.03$ for the final result. This corresponds to $\alpha_s(M_Z) = 0.121 \pm 0.003$. This result is consistent with that obtained by using the moments [51] and is used in the average below.

9.5. QCD in high-energy hadron collisions

There are many ways in which perturbative QCD can be tested in high-energy hadron colliders. The quantitative tests are only useful if the process in question has been calculated beyond leading order in QCD perturbation theory. The production of hadronic jets with large transverse momentum in hadron-hadron collisions provides a direct probe of the scattering of quarks and gluons: $qq \rightarrow qq, gg \rightarrow gg, gg \rightarrow gg, \text{ etc.}$ Higher-order QCD calculations of the jet rates [52] and shapes are in impressive agreement with data [53]. This agreement has led to the proposal that these data could be used to provide a determination of α_s [54]. A set of structure functions is assumed and jet data are fitted over a very large range of transverse momenta to the QCD prediction for the underlying scattering process that depends on α_s . The evolution of the coupling over this energy range (40 to 250 GeV) is therefore tested in the analysis. CDF obtains $\alpha_s(M_Z) = 0.1178 \pm 0.0001$ (stat.) ± 0.0085 (syst.) [55]. Estimation of the theoretical errors is not straightforward. The structure functions used depend implicitly on α_s and an iteration procedure must be used to obtain a consistent result; different sets of structure functions yield different correlations between the two values of α_s . CDF includes a scale error of 4% and a structure function error of 5% in the determination of α_s . Ref. 54 estimates the error from unknown higher order QCD corrections to be ± 0.005 . Combining these then gives $\alpha_s(M_Z) = 0.118 \pm 0.011$ which is used in the final average. Data are also available on the angular distribution of jets; these are also in agreement with QCD expectations [56,57].

QCD corrections to Drell-Yan type cross sections (*i.e.*, the production in hadron collisions by quark-antiquark annihilation of lepton pairs of invariant mass Q from virtual photons, or of real W or Z bosons), are known [58]. These $\mathcal{O}(\alpha_s)$ QCD corrections are sizable at small values of Q . The correction to W and Z production, as measured in $p\bar{p}$ collisions at $\sqrt{s} = 0.63$ TeV and $\sqrt{s} = 1.8$ TeV, is of order 30%. The NNLO corrections to this process are known [59].

The production of W and Z bosons and photons at large transverse momentum can also be used to test QCD. The leading-order QCD subprocesses are $q\bar{q} \rightarrow Vg$ and $gq \rightarrow Vq$ ($V = W, Z, \gamma$). If the parton distributions are taken from other processes and a value of α_s assumed, then an absolute prediction is obtained. Conversely, the data can be used to extract information on quark and gluon distributions and on the value of α_s . The next-to-leading-order QCD corrections are known [60,61] (for photons), and for W/Z production [62], and so a precision test is possible. Data exist on photon production from the CDF and DØ collaborations [63,64] and from fixed target experiments [65]. Detailed comparisons with QCD predictions [66] may indicate an excess of the data over the theoretical prediction at low value of transverse momenta, although other authors [67] find smaller excesses.

The UA2 collaboration [68] extracted a value of $\alpha_s(M_W) = 0.123 \pm 0.018$ (stat.) ± 0.017 (syst.) from the measured ratio $R_W = \frac{\sigma(W + 1\text{jet})}{\sigma(W + 0\text{jet})}$. The result depends on the algorithm used to define a jet, and the dominant systematic errors due to fragmentation and corrections for underlying events (the former causes jet energy to be lost, the latter causes it to be increased) are connected to the algorithm. There is also dependence on the parton distribution functions, and hence, α_s appears explicitly in the formula for R_W , and implicitly in the distribution functions. The UA2 result is not used in the final average. Data from CDF and DØ on the $W p_T$ distribution [69] are in agreement with QCD but are not able to determine α_s with sufficient precision to have any weight in a global average.

In the region of low p_t , fixed order perturbation theory is not applicable; one must sum terms of order $\alpha_s^n \ln^n(p_t/M_W)$ [70]. Data from $D\bar{O}$ [71] on the p_t distribution of Z bosons agree well with these predictions.

The production rates of b quarks in $p\bar{p}$ have been used to determine α_s [72]. The next-to-leading-order QCD production processes [73] have been used. By selecting events where the b quarks are back-to-back in azimuth, the next-to-leading-order calculation can be used to compare rates to the measured value and a value of α_s extracted. The errors are dominated by the measurement errors, the choice of μ and the scale at which the structure functions are evaluated, and uncertainties in the choice of structure functions. The last were estimated by varying the structure functions used. The result is $\alpha_s(M_Z) = 0.113^{+0.009}_{-0.013}$, which is not included in the final average, as the measured $b\bar{b}$ cross section is in poor agreement with perturbative QCD [74] and it is therefore difficult to interpret this result.

9.6. QCD in heavy-quarkonium decay

Under the assumption that the hadronic and leptonic decay widths of heavy $Q\bar{Q}$ resonances can be factorized into a nonperturbative part—dependent on the confining potential—and a calculable perturbative part, the ratios of partial decay widths allow measurements of α_s at the heavy-quark mass scale. The most precise data come from the decay widths of the $1^{--} J/\psi(1S)$ and Υ resonances. The total decay width of the Υ is predicted by perturbative QCD [75,76]

$$\begin{aligned} R_\mu(\Upsilon) &= \frac{\Gamma(\Upsilon \rightarrow \text{hadrons})}{\Gamma(\Upsilon \rightarrow \mu^+\mu^-)} \\ &= \frac{10(\pi^2 - 9)\alpha_s^3(M_b)}{9\pi\alpha_{\text{em}}^2} \\ &\quad \times \left[1 + \frac{\alpha_s}{\pi} \left(-19.36 + \frac{3\beta_0}{2} \left(1.161 + \ln\left(\frac{2M}{M_T}\right) \right) \right) \right]. \end{aligned} \quad (9.11)$$

Data are available for the Υ , Υ' , Υ'' , and J/ψ . The result is very sensitive to α_s and the data are sufficiently precise ($R_\mu(\Upsilon) = 39.11 \pm 0.4$) [77] that the theoretical errors will dominate. There are theoretical corrections to this formula due to the relativistic nature of the $Q\bar{Q}$ system which have been calculated [76] to order v^2/c^2 . These corrections are more severe for the J/ψ . There are also nonperturbative corrections arising from annihilation from higher Fock states (“color octet” contribution) which can only be estimated [78]; again these are more severe for the J/ψ . The Υ gives $\alpha_s(M_b) = 0.177 \pm 0.01$, where the error includes that from the “color octet” term and the choice of scale which together dominate. The ratio of widths $\frac{\Upsilon \rightarrow \gamma g g}{\Upsilon \rightarrow g g g}$ has been measured by the CLEO collaboration and can be used to determine $\alpha_s(M_b) = 0.189 \pm 0.01 \pm 0.01$. The error is dominated by theoretical uncertainties associated with the scale choice; the uncertainty due to the “color octet” piece is not present in this case [79]. The theoretical uncertainties due to the production of photons in fragmentation [80] are small [81]. Higher order QCD calculations of the photon energy distribution are available [82]; this distribution could now be used to further test the theory. The width $\Gamma(\Upsilon \rightarrow e^+e^-)$ can also be used to determine α_s by using

moments of the quantity $R_b(s) = \frac{\sigma(e^+e^- \rightarrow b\bar{b})}{\sigma(e^+e^- \rightarrow \mu^+\mu^-)}$ defined by

$M_n = \int_0^\infty \frac{R_b(s)}{s^{n+1}} [83]$. At large values of n , M_n is dominated by $\Gamma(\Upsilon \rightarrow e^+e^-)$. Higher order corrections are available and the method gives [84] $\alpha_s(M_b) = 0.220 \pm 0.027$. The dominant error is theoretical and is dominated by the choice of scale and by uncertainties in Coulomb corrections. These various Υ decay measurements can be combined and give $\alpha_s(M_b) = 0.185 \pm 0.01$ corresponding to $\alpha_s(M_Z) = 0.109 \pm 0.004$ which is used in the final average [79]

9.7. Perturbative QCD in e^+e^- collisions

The total cross section for $e^+e^- \rightarrow$ hadrons is obtained (at low values of \sqrt{s}) by multiplying the muon-pair cross section by the factor $R = 3\Sigma_q e_q^2$. The higher-order QCD corrections to this quantity have been calculated, and the results can be expressed in terms of the factor:

$$R = R^{(0)} \left[1 + \frac{\alpha_s}{\pi} + C_2 \left(\frac{\alpha_s}{\pi} \right)^2 + C_3 \left(\frac{\alpha_s}{\pi} \right)^3 + \dots \right], \quad (9.12)$$

where $C_2 = 1.411$ and $C_3 = -12.8$ [85].

$R^{(0)}$ can be obtained from the formula for $d\sigma/d\Omega$ for $e^+e^- \rightarrow f\bar{f}$ by integrating over Ω . The formula is given in Sec. 39.2 of this *Review*. This result is only correct in the zero-quark-mass limit. The $\mathcal{O}(\alpha_s)$ corrections are also known for massive quarks [86]. The principal advantage of determining α_s from R in e^+e^- annihilation is that there is no dependence on fragmentation models, jet algorithms, *etc.*

A measurement by CLEO [87] at $\sqrt{s} = 10.52$ GeV yields $\alpha_s(10.52 \text{ GeV}) = 0.20 \pm 0.01 \pm 0.06$, which corresponds to $\alpha_s(M_Z) = 0.13 \pm 0.005 \pm 0.03$. A comparison of the theoretical prediction of Eq. (9.12) (corrected for the b -quark mass), with all the available data at values of \sqrt{s} between 20 and 65 GeV, gives [88] $\alpha_s(35 \text{ GeV}) = 0.146 \pm 0.030$. The size of the order α_s^3 term is of order 40% of that of the order α_s^2 and 3% of the order α_s . If the order α_s^3 term is not included, a fit to the data yields $\alpha_s(35 \text{ GeV}) = 0.142 \pm 0.03$, indicating that the theoretical uncertainty is smaller than the experimental error.

Measurements of the ratio of hadronic to leptonic width of the Z at LEP and SLC, Γ_h/Γ_μ probe the same quantity as R . Using the average of $\Gamma_h/\Gamma_\mu = 20.783 \pm 0.025$ gives $\alpha_s(M_Z) = 0.1224 \pm 0.0038$ [89]. There are theoretical errors arising from the values of top-quark and Higgs masses which enter due to electroweak corrections to the Z width and from the choice of scale. While this method has small theoretical uncertainties from QCD itself, it relies sensitively on the electroweak couplings of the Z to quarks [90]. The presence of new physics which changes these couplings via electroweak radiative corrections would invalidate the value of $\alpha_s(M_Z)$. An illustration of the sensitivity can be obtained by comparing this value with the one obtained from the global fits [89] of the various precision measurements at LEP/SLC and the W and top masses: $\alpha_s(M_Z) = 0.1186 \pm 0.0027$. The difference between these two values may be accounted for by systematic uncertainties as large as ± 0.003 [89], therefore $\alpha_s(M_Z) = 0.1186 \pm 0.0042$ will be used in the final average.

An alternative method of determining α_s in e^+e^- annihilation is from measuring quantities that are sensitive to the relative rates of two-, three-, and four-jet events. A review should be consulted for more details [91] of the issues mentioned briefly here. In addition to simply counting jets, there are many possible choices of such “shape variables”: thrust [92], energy-energy correlations [93], average jet mass, *etc.* All of these are infrared safe, which means they can be reliably calculated in perturbation theory. The starting point for all these quantities is the multijet cross section. For example, at order α_s , for the process $e^+e^- \rightarrow q\bar{q}g$: [94]

$$\frac{1}{\sigma} \frac{d^2\sigma}{dx_1 dx_2} = \frac{2\alpha_s}{3\pi} \frac{x_1^2 + x_2^2}{(1-x_1)(1-x_2)}, \quad (9.13)$$

$$x_i = \frac{2E_i}{\sqrt{s}} \quad (9.14)$$

where x_i are the center-of-mass energy fractions of the final-state (massless) quarks. A distribution in a “three-jet” variable, such as those listed above, is obtained by integrating this differential cross section over an appropriate phase space region for a fixed value of the variable. The order α_s^2 corrections to this process have been computed, as well as the 4-jet final states such as $e^+e^- \rightarrow q\bar{q}gg$ [95].

There are many methods used by the e^+e^- experimental groups to determine α_s from the event topology. The jet-counting algorithm, originally introduced by the JADE collaboration [96], has been used

by many other groups. Here, particles of momenta p_i and p_j are combined into a pseudo-particle of momentum $p_i + p_j$ if the invariant mass of the pair is less than $y_0\sqrt{s}$. The process is iterated until all pairs of particles or pseudoparticles have a mass-measure that exceeds $y_0\sqrt{s}$; the remaining number is then defined to be the jet multiplicity. The remaining number is then defined to be the number of jets in the event, and can be compared to the QCD prediction. The Durham algorithm is slightly different: in combining a pair of partons, it uses $M^2 = 2\min(E_i^2, E_j^2)(1 - \cos\theta_{ij})$ for partons of energies E_i and E_j separated by angle θ_{ij} [97].

There are theoretical ambiguities in the way this process is carried out. Quarks and gluons are massless, whereas the observed hadrons are not, so that the massive jets that result from this scheme cannot be compared directly to the massless jets of perturbative QCD. Different recombination schemes have been tried, for example combining 3-momenta and then rescaling the energy of the cluster so that it remains massless. These schemes result in the same data giving slightly different values [98,99] of α_s . These differences can be used to determine a systematic error. In addition, since what is observed are hadrons rather than quarks and gluons, a model is needed to describe the evolution of a partonic final state into one involving hadrons, so that detector corrections can be applied. The QCD matrix elements are combined with a parton-fragmentation model. This model can then be used to correct the data for a direct comparison with the parton calculation. The different hadronization models that are used [100–103] model the dynamics that are controlled by nonperturbative QCD effects which we cannot yet calculate. The fragmentation parameters of these Monte Carlos are tuned to get agreement with the observed data. The differences between these models contribute to the systematic errors. The systematic errors from recombination schemes and fragmentation effects dominate over the statistical and other errors of the LEP/SLD experiments.

The scale M at which $\alpha_s(M)$ is to be evaluated is not clear. The invariant mass of a typical jet (or $\sqrt{s}y_0$) is probably a more appropriate choice than the e^+e^- center-of-mass energy. While there is no justification for doing so, if the value is allowed to float in the fit to the data, the fit improves and the data tend to prefer values of order $\sqrt{s}/10$ GeV for some variables [99,104]; the exact value depends on the variable that is fitted.

The perturbative QCD formulae can break down in special kinematical configurations. For example, the thrust (T) distribution contains terms of the type $\alpha_s \ln^2(1 - T)$. The higher orders in the perturbation expansion contain terms of order $\alpha_s^n \ln^m(1 - T)$. For $T \sim 1$ (the region populated by 2-jet events), the perturbation expansion is unreliable. The terms with $n \leq m$ can be summed to all orders in α_s [105]. If the jet recombination methods are used higher-order terms involve $\alpha_s^n \ln^m(y_0)$, these too can be resummed [106]. The resummed results give better agreement with the data at large values of T . Some caution should be exercised in using these resummed results because of the possibility of overcounting; the showering Monte Carlos that are used for the fragmentation corrections also generate some of these leading-log corrections. Different schemes for combining the order α_s^2 and the resummations are available [107]. These different schemes result in shifts in α_s of order ± 0.002 . The use of the resummed results improves the agreement between the data and the theory. An average of results at the Z resonance from SLD [99], OPAL [108], L3 [109], ALEPH [110], and DELPHI [111], using the combined α_s^2 and resummation fitting to a large set of shape variables, gives $\alpha_s(M_Z) = 0.122 \pm 0.007$. The errors in the values of $\alpha_s(M_Z)$ from these shape variables are totally dominated by the theoretical uncertainties associated with the choice of scale, and the effects of hadronization Monte Carlos on the different quantities fitted.

Estimates are available for the nonperturbative corrections to the mean value of $1 - T$ [112]. These are of order $1/E$ and involve a single parameter to be determined from experiment. These corrections can then be used as an alternative to those modeled by the fragmentation Monte Carlos. The DELPHI collaboration has fitted its data using an additional parameter to take into account these $1/E$ effects [113] and quotes for the MSbar scheme $\alpha_s = 0.1217 \pm 0.0046$ and a significant

$1/E$ term. This term vanishes in the RGI/ECH scheme and the data are well described by pure perturbation theory with consistent $\alpha_s = 0.1201 \pm 0.0020$.

Studies have been carried out at energies between ~ 130 GeV [114] and ~ 200 GeV [115]. These can be combined to give $\alpha_s(130 \text{ GeV}) = 0.114 \pm 0.008$ and $\alpha_s(189 \text{ GeV}) = 0.1104 \pm 0.005$. The dominant errors are theoretical and systematic and, most of these are in common at the two energies. These data and those at the Z resonance and below provide clear confirmation of the expected decrease in α_s as the energy is increased.

The LEP QCD working group [116] uses all LEP data Z mass and higher energies to perform a global fit using a large number of shape variables. It determines $\alpha_s(M_Z) = 0.1201 \pm 0.0003(\text{stat}) \pm 0.0048(\text{sys})$, (result quoted in Ref. 5) the error being dominated by theoretical uncertainties which are the most difficult to quantify.

Similar studies on event shapes have been undertaken at lower energies at TRISTAN, PEP/PETRA, and CLEO. A combined result from various shape parameters by the TOPAZ collaboration gives $\alpha_s(58 \text{ GeV}) = 0.125 \pm 0.009$, using the fixed order QCD result, and $\alpha_s(58 \text{ GeV}) = 0.132 \pm 0.008$ (corresponding to $\alpha_s(M_Z) = 0.123 \pm 0.007$), using the same method as in the SLD and LEP average [117]. The measurements of event shapes at PEP/PETRA are summarized in earlier editions of this note. A recent reevaluation of the JADE data [118] obtained using resummed QCD results with modern models of jet fragmentation and by averaging over several shape variables gives $\alpha_s(22 \text{ GeV}) = 0.151 \pm 0.004(\text{expt}) \pm 0.014(\text{theory})$ which is used in the final average. These results also attempt to constrain the non-perturbative parameters and show a remarkable agreement with QCD even at low energies [119]. An analysis by the TPC group [120] gives $\alpha_s(29 \text{ GeV}) = 0.160 \pm 0.012$, using the same method as TOPAZ.

The CLEO collaboration fits to the order α_s^2 results for the two jet fraction at $\sqrt{s} = 10.53$ GeV, and obtains $\alpha_s(10.53 \text{ GeV}) = 0.164 \pm 0.004$ (expt.) ± 0.014 (theory) [121]. The dominant systematic error arises from the choice of scale (μ), and is determined from the range of α_s that results from fit with $\mu = 10.53$ GeV, and a fit where μ is allowed to vary to get the lowest χ^2 . The latter results in $\mu = 1.2$ GeV. Since the quoted result corresponds to $\alpha_s(1.2 \text{ GeV}) = 0.35$, it is by no means clear that the perturbative QCD expression is reliable and the resulting error should, therefore, be treated with caution. A fit to many different variables as is done in the LEP/SLC analyses would give added confidence to the quoted error.

All these measurements are consistent with the LEP average quoted above which has the smallest statistical error; the systematic errors being mostly theoretical are likely to be strongly correlated between the measurements. The value of $\alpha_s(M_Z) = 0.1201 \pm 0.005$ is used in the final average.

9.8. Scaling violations in fragmentation functions

Measurements of the fragmentation function $d_i(z, E)$, (the probability that a hadron of type i be produced with energy zE in e^+e^- collisions at $\sqrt{s} = 2E$) can be used to determine α_s . (Detailed definitions and a discussion of the properties of fragmentation functions can be found in Sec. 17 of this *Review*). As in the case of scaling violations in structure functions, QCD predicts only the E dependence. Hence, measurements at different energies are needed to extract a value of α_s . Because the QCD evolution mixes the fragmentation functions for each quark flavor with the gluon fragmentation function, it is necessary to determine each of these before α_s can be extracted.

The ALEPH collaboration has used data from energies ranging from $\sqrt{s} = 22$ GeV to $\sqrt{s} = 91$ GeV. A flavor tag is used to discriminate between different quark species, and the longitudinal and transverse cross sections are used to extract the gluon fragmentation function [122]. The result obtained is $\alpha_s(M_Z) = 0.126 \pm 0.007$ (expt.) ± 0.006 (theory) [123]. The theory error is due mainly to the choice of scale. The OPAL collaboration [124] has also extracted the separate fragmentation functions. DELPHI [125] has also performed a similar analysis using data from other experiments at lower energy with the result $\alpha_s(M_Z) = 0.124 \pm 0.007 \pm 0.009$ (theory).

The larger theoretical error is due to the larger range of scales that were used in the fit. These results can be combined to give $\alpha_s(M_Z) = 0.125 \pm 0.005 \pm 0.008$ (theory).

A global analysis [126] uses data on the production of π, K, p , and \bar{p} from SLC [127], DELPHI [128], OPAL [129], ALEPH [130], and lower-energy data from the TPC collaboration [131]. A flavor tag and a three-jet analysis is used to disentangle the quark and gluon fragmentation functions. The value $\alpha_s(M_Z) = 0.117^{+0.0035+0.0017}_{-0.0069-0.0025}$ is obtained. The second error is a theoretical one arising from the choice of scale. The fragmentation functions resulting from this fit are consistent with a recent fit of Ref. 132.

It is unclear how to combine the measurements discussed in the two previous paragraphs as much of the data used are common to both. If the theoretical errors dominate then a simple average is appropriate as the methods are different. For want of a better solution, the naive average of $\alpha_s(M_Z) = 0.1201 \pm 0.006$ is used for in the average value quoted below.

9.9. Photon structure functions

e^+e^- can also be used to study photon-photon interactions, which can be used to measure the structure function of a photon [133], by selecting events of the type $e^+e^- \rightarrow e^+e^- + \text{hadrons}$ which proceeds via two photon scattering. If events are selected where one of the photons is almost on mass shell and the other has a large invariant mass Q , then the latter probes the photon structure function at scale Q ; the process is analogous to deep inelastic scattering where a highly virtual photon is used to probe the proton structure. This process was included in earlier versions of this *Review* which can be consulted for details on older measurements [134–137]. A review of the data can be found in Ref. 138. Data are available from LEP [139–143] and from TRISTAN [144,145] which extend the range of Q^2 to of order 300 GeV² and x as low as 2×10^{-3} and show Q^2 dependence of the structure function that is consistent with QCD expectations. There is evidence for a hadronic (non-perturbative) component to the photon structure function that complicates attempts to extract a value of α_s from the data.

Reference [146] uses data from PETRA, TRISTAN, and LEP to perform a combined fit. The higher data from LEP extend to higher Q^2 (< 780 GeV²) and enable a measurement: $\alpha_s(m_Z) = 0.1198 \pm 0.0054$ which now is competitive with other results.

Experiments at HERA can also probe the photon structure function by looking at jet production in γp collisions; this is analogous to the jet production in hadron-hadron collisions which is sensitive to hadron structure functions. The data [147] are consistent with theoretical models [148].

9.10. Jet rates in ep collisions

At lowest order in α_s , the ep scattering process produces a final state of (1+1) jets, one from the proton fragment and the other from the quark knocked out by the process $e + \text{quark} \rightarrow e + \text{quark}$. At next order in α_s , a gluon can be radiated, and hence a (2+1) jet final state produced. By comparing the rates for these (1+1) and (2+1) jet processes, a value of α_s can be obtained. A NLO QCD calculation is available [149]. The basic methodology is similar to that used in the jet counting experiments in e^+e^- annihilation discussed above. Unlike those measurements, the ones in ep scattering are not at a fixed value of Q^2 . In addition to the systematic errors associated with the jet definitions, there are additional ones since the structure functions enter into the rate calculations. Results from H1 [150] and ZEUS [152] can be combined to give [4] $\alpha_s(M_Z) = 0.120 \pm 0.002$ (expt.) ± 0.004 (theor.), which is used in the final average. The theoretical errors arise from scale choice, structure functions, and jet definitions.

Photoproduction of two or more jets via processes such as $\gamma + g \rightarrow g\bar{q}$ can also be observed at HERA. The process is similar to jet production in hadron-hadron collisions. Agreement with perturbative QCD is excellent and ZEUS [151] quotes $\alpha_s(M_Z) = 0.1224 \pm 0.0020$ (expt) ± 0.0050 (theory) which is used in the average below.

9.11. QCD in diffractive events

In approximately 10% of the deep-inelastic scattering events at HERA a rapidity gap is observed [153]; that is events are seen where there are almost no hadrons produced in the direction of the incident proton. This was unexpected; QCD based models of the final state predicted that the rapidity interval between the quark that is hit by the electron and the proton remnant should be populated approximately evenly by the hadrons. Similar phenomena have been observed at the Tevatron in W and jet production. For a review see Ref. 154.

9.12. Lattice QCD

Lattice gauge theory calculations can be used to calculate, using non-perturbative methods, a physical quantity that can be measured experimentally. The value of this quantity can then be used to determine the QCD coupling that enters in the calculation. For a review of the methodology see Ref. 155. For example, the energy levels of a $Q\bar{Q}$ system can be determined and then used to extract α_s . The masses of the $Q\bar{Q}$ states depend only on the quark mass and on α_s . A limitation until very recently is that calculations have not been performed for three light quark flavors. Results for zero ($n_f = 0$, quenched approximation) and two light flavors must be extrapolated to $n_f = 3$. The coupling constant so extracted is in a lattice renormalization scheme, and must be converted to the $\overline{\text{MS}}$ scheme for comparison with other results. Using the mass differences of Υ and Υ' and Υ'' and χ_b , Davies *et al.* [156] extract a value of $\alpha_s(M_Z) = 0.121 \pm 0.003$. This result is the first to have three light flavors and allows the strange quark to have a different mass from the up and down. This result supersedes earlier estimates although it should be pointed out that in an earlier paper [157] a result with a smaller error was given. A similar result with larger errors is reported by [158], whose results are consistent with $\alpha_s(M_Z) = 0.111 \pm 0.006$. The SESAM collaboration [159] uses the Υ and Υ' and χ_b masses to obtain $\alpha_s(M_Z) = 0.1118 \pm 0.0017$ using Wilson fermions. While this result agrees with that of Ref. 160 which also uses Wilson fermions, and is consistent with Ref. 167 which uses a similar method and results from quenched and two massless flavors to get $\alpha_s(M_Z) = 0.1076 \pm 0.0038$, these authors point out that their result is more than 3σ from that of Davies *et al.* [157] which uses Kogut-Susskind fermions. Note that a combination of the older results from quenched [161] and ($n_f = 2$) [162] gives $\alpha_s(M_Z) = 0.116 \pm 0.003$ [163] which is remarkably consistent with the newer values. The ALPHA collaboration [164] who use the strength of the QCD potential from the Υ system inferred by Ref. 165 have begun to probe the systematic errors in detail for simulations involving two flavors of massless quarks.

There have also been investigations of the running of α_s [166]. These show remarkable agreement with the two loop perturbative result of Eq. (9.5).

There are several sources of error in these estimates of $\alpha_s(M_Z)$. The experimental error associated with the measurements of the particle masses is negligible. The conversion from the lattice coupling constant to the $\overline{\text{MS}}$ constant is obtained using a perturbative expansion where one coupling expanded as a power series in the other. The series is known to third order [168]. The effect of the third-order term is a shift in the extracted value of $\alpha_s(M_Z)$ of $+0.002$. Other theoretical errors arising from the limited statistics of the Monte-Carlo calculation, extrapolation in n_f which is not needed in latest results [156], and corrections for light quark masses are smaller than this.

In this review, we will use only the new result [156] of $\alpha_s(M_Z) = 0.121 \pm 0.003$. It should be noted that this is 2σ away from the value $\alpha_s(M_Z) = 0.1134 \pm 0.003$ in the last version of this review that was obtained by averaging Refs. [157,159,160,161,167]

In addition to the strong coupling constant other quantities can be determined. Of particular interest are the decay constants of charmed and bottom mesons. These are required, for example, to facilitate the extraction of CKM elements from measurements of charm and bottom decay rates. See Ref. 169 for a recent review.

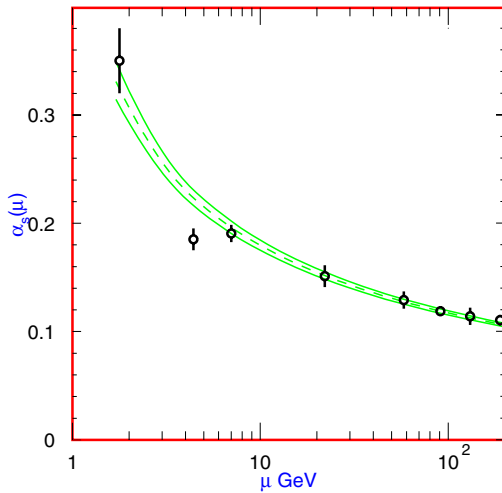


Figure 9.2: Summary of the values of $\alpha_s(\mu)$ at the values of μ where they are measured. The lines show the central values and the $\pm 1\sigma$ limits of our average. The figure clearly shows the decrease in $\alpha_s(\mu)$ with increasing μ . The data are, in increasing order of μ , τ width, Z decays, deep inelastic scattering, e^+e^- event shapes at 22 GeV from the JADE data, shapes at TRISTAN at 58 GeV, Z width, and e^+e^- event shapes at 135 and 189 GeV.

9.13. Conclusions

The need for brevity has meant that many other important topics in QCD phenomenology have had to be omitted from this review. One should mention in particular the study of exclusive processes (form factors, elastic scattering, ...), the behavior of quarks and gluons in nuclei, the spin properties of the theory, and QCD effects in hadron spectroscopy.

We have focused on those high-energy processes which currently offer the most quantitative tests of perturbative QCD. Figure 9.1 shows the values of $\alpha_s(M_Z)$ deduced from the various experiments. Figure 9.2 shows the values and the values of Q where they are measured. This figure clearly shows the experimental evidence for the variation of $\alpha_s(Q)$ with Q .

An average of the values in Fig. 9.1 gives $\alpha_s(M_Z) = 0.1187$, with a total χ^2 of 9 for eleven fitted points, showing good consistency among the data. The error on this average, assuming that all of the errors in the contributing results are uncorrelated, is ± 0.0013 , and may be an underestimate. Almost all of the values used in the average are dominated by systematic, usually theoretical, errors. Only some of these, notably from the choice of scale, are correlated. The average is not dominated by a single measurement; there are several results with comparable small errors: these are the ones from τ decay, lattice gauge theory, deep inelastic scattering, upsiion decay and the Z^0 width. We quote our average value as $\alpha_s(M_Z) = 0.1187 \pm 0.002$, which corresponds to $\Lambda^{(5)} = 217_{-23}^{+25}$ MeV using Eq. (9.5). Note that the average has moved by less than 1σ from the last version of this review. Future experiments can be expected to improve the measurements of α_s somewhat. Precision at the 1% level may be achievable if the systematic and theoretical errors can be reduced [170].

The value of α_s at any scale corresponding to our average can be obtained from <http://www-theory.lbl.gov/~ianh/alpha/alpha.html> which uses Eq. (9.5) to interpolate.

References:

1. R.K. Ellis, W.J. Stirling, and B.R. Webber, "QCD and Collider Physics" (Cambridge 1996).

2. For reviews see, for example, A.S. Kronfeld and P.B. Mackenzie, *Ann. Rev. Nucl. and Part. Sci.* **43**, 793 (1993); H. Wittig, *Int. J. Mod. Phys.* **A12**, 4477 (1997).
3. For example see, P. Gambino, *International Conference on Lepton Photon Interactions*, Fermilab, USA, (2003).
4. S. Bethke, [hep-ex/0211012](https://arxiv.org/abs/hep-ex/0211012); M. Davier, *33rd Rencontres de Moriond: Electroweak Interactions and Unified Theories*, Les Arcs, France (14–21 Mar. 1998); S. Bethke, *J. Phys.* **G26**, R27 (2000).
5. R. Hirsosky, *International Conference on Lepton Photon Interactions*, Fermilab, USA, (2003).
6. See, for example, J. Collins "Renormalization: an introduction to renormalization, the renormalization group and the operator product expansion," (Cambridge University Press, Cambridge, 1984). "QCD and Collider Physics" (Cambridge 1996).
7. S.A. Larin, T. van Ritbergen, and J.A.M. Vermaseren, *Phys. Lett.* **B400**, 379 (1997).
8. W.A. Bardeen *et al.*, *Phys. Rev.* **D18**, 3998 (1978).
9. G. Grunberg, *Phys. Lett.* **95B**, 70 (1980); *Phys. Rev.* **D29**, 2315 (1984).
10. P.M. Stevenson, *Phys. Rev.* **D23**, 2916 (1981); and *Nucl. Phys.* **B203**, 472 (1982).
11. S. Brodsky and H.J. Lu, SLAC-PUB-6389 (Nov. 1993).
12. S. Brodsky, G.P. Lepage, and P.B. Mackenzie, *Phys. Rev.* **D28**, 228 (1983).
13. M.A. Samuel, G. Li, and E. Steinfelds, *Phys. Lett.* **B323**, 188 (1994); M.A. Samuel, J. Ellis, and M. Karliner, *Phys. Rev. Lett.* **74**, 4380 (1995).
14. J. Ellis *et al.*, *Phys. Rev.* **D54**, 6986 (1996).
15. P.N. Burrows *et al.*, *Phys. Lett.* **B382**, 157 (1996).
16. P. Abreu *et al.*, *Z. Phys.* **C54**, 55 (1992).
17. A.H. Mueller, *Phys. Lett.* **B308**, 355, (1993).
18. W. Bernreuther, *Annals of Physics* **151**, 127 (1983); Erratum *Nucl. Phys.* **B513**, 758 (1998); S.A. Larin, T. van Ritbergen, and J.A.M. Vermaseren, *Nucl. Phys.* **B438**, 278 (1995).
19. K.G. Chetyrkin, B.A. Kniehl, and M. Steinhauser, *Phys. Rev. Lett.* **79**, 2184 (1997); K.G. Chetyrkin, B.A. Kniehl, and M. Steinhauser, *Nucl. Phys.* **B510**, 61 (1998).
20. See the Review on the "Quark Mass" in the Particle Listings for *Review of Particle Physics*.
21. A.D. Martin *et al.*, [hep-ph/0307262](https://arxiv.org/abs/hep-ph/0307262).
22. D. Gross and C.H. Llewellyn Smith, *Nucl. Phys.* **B14**, 337 (1969).
23. J. Chyla and A.L. Kataev, *Phys. Lett.* **B297**, 385 (1992).
24. S.A. Larin and J.A.M. Vermaseren, *Phys. Lett.* **B259**, 345 (1991).
25. A.L. Kataev and V.V. Starchenko, *Mod. Phys. Lett.* **A10**, 235 (1995).
26. V.M. Braun and A.V. Kolesnichenko, *Nucl. Phys.* **B283**, 723 (1987).
27. M. Dasgupta and B. Webber, *Phys. Lett.* **B382**, 273 (1993).
28. J. Kim *et al.*, *Phys. Rev. Lett.* **81**, 3595 (1998).
29. D. Allasia *et al.*, *Z. Phys.* **C28**, 321 (1985); K. Varvell *et al.*, *Z. Phys.* **C36**, 1 (1987); V.V. Ammosov *et al.*, *Z. Phys.* **C30**, 175 (1986); P.C. Bosetti *et al.*, *Nucl. Phys.* **B142**, 1 (1978).
30. A.L. Kataev *et al.*, *Nucl. Phys.* **A666 & 667**, 184 (2000); *Nucl. Phys.* **B573**, 405 (2000).
31. A.L. Kataev, G. Parente, and A.V. Sidorov, [hep-ph/0106224](https://arxiv.org/abs/hep-ph/0106224); A.L. Kataev, G. Parente, and A.V. Sidorov, *Nucl. Phys. Proc. Suppl.* **116**, 105 (2003) [hep-ph/0211151](https://arxiv.org/abs/hep-ph/0211151).

32. K. Abe *et al.*, Phys. Rev. Lett. **74**, 346 (1995); Phys. Lett. **B364**, 61 (1995); Phys. Rev. Lett. **75**, 25 (1995);
P.L. Anthony *et al.*, Phys. Rev. **D54**, 6620 (1996).
33. B. Adeva *et al.*, Phys. Rev. **D58**, 112002 (1998), Phys. Lett. **B420**, 180 (1998).
34. D. Adams *et al.*, Phys. Lett. **B329**, 399 (1995); Phys. Rev. **D56**, 5330 (1998); Phys. Rev. **D58**, 1112001 (1998);
K. Ackerstaff *et al.*, Phys. Lett. **B464**, 123 (1999).
35. P.L. Anthony *et al.*, Phys. Lett. **B463**, 339 (1999); Phys. Lett. **B493**, 19 (2000).
36. J. Blümlein and H. Böttcher, Nucl. Phys. **B636**, 225 (2002).
37. J.D. Bjorken, Phys. Rev. **148**, 1467 (1966).
38. G. Altarelli *et al.*, Nucl. Phys. **B496**, 337 (1997).
39. J. Ellis and M. Karliner, Phys. Lett. **B341**, 397 (1995).
40. M.A. Shifman, A.I. Vainshtein, and V.I. Zakharov, Nucl. Phys. **B147**, 385 (1979).
41. S. Narison and A. Pich, Phys. Lett. **B211**, 183 (1988);
E. Braaten, S. Narison, and A. Pich, Nucl. Phys. **B373**, 581 (1992).
42. M. Neubert, Nucl. Phys. **B463**, 511 (1996).
43. F. Le Diberder and A. Pich, Phys. Lett. **B289**, 165 (1992).
44. R. Barate *et al.*, Z. Phys. **C76**, 1 (1997); Z. Phys. **C76**, 15 (1997);
K. Ackerstaff *et al.*, Eur. Phys. J. **C7**, 571 (1999).
45. T. Coan *et al.*, Phys. Lett. **B356**, 580 (1995).
46. A.L. Kataev and V.V. Starshenko, Mod. Phys. Lett. **A10**, 235 (1995).
47. F. Le Diberder and A. Pich, Phys. Lett. **B286**, 147 (1992).
48. C.J. Maxwell and D.J. Tong, Nucl. Phys. **B481**, 681 (1996).
49. G. Altarelli, Nucl. Phys. **B40**, 59 (1995);
G. Altarelli, P. Nason, and G. Ridolfi, Z. Phys. **C68**, 257 (1995).
50. S. Narison, Nucl. Phys. **B40**, 47 (1995).
51. S. Menke, hep-ex/0106011.
52. S.D. Ellis, Z. Kunszt, and D.E. Soper, Phys. Rev. Lett. **64**, 2121 (1990);
F. Aversa *et al.*, Phys. Rev. Lett. **65**, 401 (1990);
W.T. Giele, E.W.N. Glover, and D. Kosower, Phys. Rev. Lett. **73**, 2019 (1994);
S. Frixione, Z. Kunszt, and A. Signer, Nucl. Phys. **B467**, 399 (1996).
53. F. Abe *et al.*, Phys. Rev. Lett. **77**, 438 (1996);
B. Abbott *et al.*, Phys. Rev. Lett. **86**, 1707 (2001).
54. W.T. Giele, E.W.N. Glover, and J. Yu, Phys. Rev. **D53**, 120 (1996).
55. T. Affolder *et al.*, Phys. Rev. Lett. **88**, 042001 (2002).
56. UA1 Collaboration: G. Arnison *et al.*, Phys. Lett. **B177**, 244 (1986).
57. F. Abe *et al.*, Phys. Rev. Lett. **77**, 533 (1996);
ibid., erratum Phys. Rev. Lett. **78**, 4307 (1997);
B. Abbott, Phys. Rev. Lett. **80**, 666 (1998);
S. Abachi *et al.*, Phys. Rev. **D53**, 6000 (1996).
58. G. Altarelli, R.K. Ellis, and G. Martinelli, Nucl. Phys. **B143**, 521 (1978).
59. R. Hamberg, W.L. Van Neerven, and T. Matsuura, Nucl. Phys. **B359**, 343 (1991).
60. P. Aurenche, R. Baier, and M. Fontannaz, Phys. Rev. **D42**, 1440 (1990);
P. Aurenche *et al.*, Phys. Lett. **140B**, 87 (1984);
P. Aurenche *et al.*, Nucl. Phys. **B297**, 661 (1988).
61. H. Baer, J. Ohnemus, and J.F. Owens, Phys. Lett. **B234**, 127 (1990).
62. H. Baer and M.H. Reno, Phys. Rev. **D43**, 2892 (1991);
P.B. Arnold and M.H. Reno, Nucl. Phys. **B319**, 37 (1989).
63. F. Abe *et al.*, Phys. Rev. Lett. **73**, 2662 (1994).
64. B. Abbott *et al.*, Phys. Rev. Lett. **84**, 2786 (2001);
V.M. Abazov *et al.*, Phys. Rev. Lett. **87**, 251805 (2001).
65. G. Alverson *et al.*, Phys. Rev. **D48**, 5 (1993).
66. L. Apanasevich *et al.*, Phys. Rev. **D59**, 074007 (1999); Phys. Rev. Lett. **81**, 2642 (1998).
67. W. Vogelsang and A. Vogt, Nucl. Phys. **B453**, 334 (1995);
P. Aurenche *et al.*, Eur. Phys. J. **C9**, 107 (1999).
68. J. Alitti *et al.*, Phys. Lett. **B263**, 563 (1991).
69. S. Abachi *et al.*, Phys. Rev. Lett. **75**, 3226 (1995);
J. Womersley, private communication;
J. Huston, in the *Proceedings to the 29th International Conference on High-Energy Physics (ICHEP98)*, Vancouver, Canada (23–29 Jul 1998) hep-ph/9901352.
70. R.K. Ellis and S. Veseli, Nucl. Phys. **B511**, 649 (1998);
C.T. Davies, B.R. Webber, and W.J. Stirling, Nucl. Phys. **B256**, 413 (1985);
G. Parisi and R. Petronzio, Nucl. Phys. **B154**, 427 (1979);
J.C. Collins, D.E. Soper, G. Sterman, Nucl. Phys. **B250**, 199 (1985).
71. DØ Collaboration: B. Abbott *et al.*, Phys. Rev. **D61**, 032004 (2000);
T. Affolder *et al.*, FERMILAB-PUB-99/220.
72. C. Albajar *et al.*, Phys. Lett. **B369**, 46 (1996).
73. M.L. Mangano, P. Nason, and G. Ridolfi, Nucl. Phys. **B373**, 295 (1992).
74. D. Acosta *et al.*, Phys. Rev. **D65**, 052005 (2002).
75. R. Barbieri *et al.*, Phys. Lett. **95B**, 93 (1980);
P.B. Mackenzie and G.P. Lepage, Phys. Rev. Lett. **47**, 1244 (1981).
76. G.T. Bodwin, E. Braaten, and G.P. Lepage, Phys. Rev. **D51**, 1125 (1995).
77. *The Review of Particle Physics*, D.E. Groom *et al.*, Eur. Phys. J. **C15**, 1 (2000) and 2001 off-year partial update for the 2002 edition available on the PDG WWW pages (URL: <http://pdg.lbl.gov/>).
78. M. Gremm and A. Kapustin, Phys. Lett. **B407**, 323 (1997).
79. I. Hinchliffe and A.V. Manohar, Ann. Rev. Nucl. Part. Sci. **50**, 643 (2000).
80. S. Catani and F. Hautmann, Nucl. Phys. **B** (Proc. Supp.), vol. **39BC**, 359 (1995).
81. B. Nemati *et al.*, Phys. Rev. **D55**, 5273 (1997).
82. M. Kramer, Phys. Rev. **D60**, 111503 (1999).
83. M. Voloshin, Int. J. Mod. Phys. **A10**, 2865 (1995).
84. M. Jamin and A. Pich, Nucl. Phys. **B507**, 334 (1997).
85. S.G. Gorishny, A. Kataev, and S.A. Larin, Phys. Lett. **B259**, 144 (1991);
L.R. Surguladze and M.A. Samuel, Phys. Rev. Lett. **66**, 560 (1991).
86. K.G. Chetyrkin and J.H. Kuhn, Phys. Lett. **B308**, 127 (1993).
87. R. Ammar *et al.*, Phys. Rev. **D57**, 1350 (1998).
88. D. Haidt, in *Directions in High Energy Physics*, vol. 14, p. 201, ed. P. Langacker (World Scientific, 1995).
89. G. Quast, presented at the *International Europhysics Conference on High Energy Physics, EPS-HEP03*, Aachen Germany (July 2003);
D. Abbaneo, *et al.*, LEPEWWG/2003-01.

90. A. Blondel and C. Verzegrassi, Phys. Lett. **B311**, 346 (1993); G. Altarelli *et al.*, Nucl. Phys. **B405**, 3 (1993).
91. G. Dissertori, I. Knowles, and M. Schmelling: "Quantum Chromodynamics: High Energy Experiments and Theory" (Oxford University Press, 2003).
92. E. Farhi, Phys. Rev. Lett. **39**, 1587 (1977).
93. C.L. Basham *et al.*, Phys. Rev. **D17**, 2298 (1978).
94. J. Ellis, M.K. Gaillard, and G. Ross, Nucl. Phys. **B111**, 253 (1976);
ibid., erratum Nucl. Phys. **B130**, 516 (1977);
P. Hoyer *et al.*, Nucl. Phys. **B161**, 349 (1979).
95. R.K. Ellis, D.A. Ross, A.E. Terrano, Phys. Rev. Lett. **45**, 1226 (1980);
Z. Kunszt and P. Nason, ETH-89-0836 (1989).
96. S. Bethke *et al.*, Phys. Lett. **B213**, 235 (1988).
97. S. Bethke *et al.*, Nucl. Phys. **B370**, 310 (1992).
98. M.Z. Akrawy *et al.*, Z. Phys. **C49**, 375 (1991).
99. K. Abe *et al.*, Phys. Rev. Lett. **71**, 2578 (1993); Phys. Rev. **D51**, 962 (1995).
100. B. Andersson *et al.*, Phys. Reports **97**, 33 (1983).
101. A. Ali *et al.*, Nucl. Phys. **B168**, 409 (1980);
A. Ali and R. Barreiro, Phys. Lett. **118B**, 155 (1982).
102. B.R. Webber, Nucl. Phys. **B238**, 492 (1984);
G. Marchesini *et al.*, Phys. Comm. **67**, 465 (1992).
103. T. Sjostrand and M. Bengtsson, Comp. Phys. Comm. **43**, 367 (1987);
T. Sjostrand, CERN-TH-7112/93 (1993).
104. O. Adriani *et al.*, Phys. Lett. **B284**, 471 (1992);
M. Akrawy *et al.*, Z. Phys. **C47**, 505 (1990);
B. Adeva *et al.*, Phys. Lett. **B248**, 473 (1990);
D. Decamp *et al.*, Phys. Lett. **B255**, 623 (1991).
105. S. Catani *et al.*, Phys. Lett. **B263**, 491 (1991).
106. S. Catani *et al.*, Phys. Lett. **B269**, 432 (1991);
S. Catani, B.R. Webber, and G. Turnock, Phys. Lett. **B272**, 368 (1991);
N. Brown and J. Stirling, Z. Phys. **C53**, 629 (1992).
107. S. Catani *et al.*, Phys. Lett. **B269**, 432 (1991); Phys. Lett. **B295**, 269 (1992); Nucl. Phys. **B607**, 3 (1993); Phys. Lett. **B269**, 432 (1991).
108. P.D. Acton *et al.*, Z. Phys. **C55**, 1 (1992); Z. Phys. **C58**, 386 (1993).
109. O. Adriani *et al.*, Phys. Lett. **B284**, 471 (1992).
110. D. Decamp *et al.*, Phys. Lett. **B255**, 623 (1992); Phys. Lett. **B257**, 479 (1992).
111. P. Abreu *et al.*, Z. Phys. **C59**, 21 (1993); Phys. Lett. **B456**, 322 (1999);
M. Acciarri *et al.*, Phys. Lett. **B404**, 390 (1997).
112. Y.L. Dokshitzer and B.R. Webber Phys. Lett. **B352**, 451 (1995);
Y.L. Dokshitzer *et al.*, Nucl. Phys. **B511**, 396 (1997);
Y.L. Dokshitzer *et al.*, JHEP **9801**, 011 (1998).
113. J. Abdallah *et al.*, [DELPHI Collaboration], Eur. Phys. J. **C29**, 285 (2003).
114. D. Buskulic *et al.*, Z. Phys. **C73**, 409 (1997); Z. Phys. **C73**, 229 (1997).
115. H. Stenzel *et al.* [ALEPH Collaboration], CERN-OPEN-99-303(1999);
DELPHI Collaboration: Eur. Phys. J. **C14**, 557 (2000);
M. Acciarri *et al.* [L3 Collaboration], Phys. Lett. **B489**, 65 (2000);
OPAL Collaboration, PN-403 (1999); all submitted to *International Conference on Lepton Photon Interactions*, Stanford, USA (Aug. 1999);
M. Acciarri *et al.* OPAL Collaboration], Phys. Lett. **B371**, 137 (1996); Z. Phys. **C72**, 191 (1996);
K. Ackerstaff *et al.*, Z. Phys. **C75**, 193 (1997);
ALEPH Collaboration: ALEPH 98-025 (1998).
116. <http://lepqcd.web.cern.ch/LEPQCD/annihilations/welcome.html>.
117. Y. Ohnishi *et al.*, Phys. Lett. **B313**, 475 (1993).
118. P.A. Movilla Fernandez *et al.*, Eur. Phys. J. **C1**, 461 (1998);
O. Biebel *et al.*, Phys. Lett. **B459**, 326 (1999).
119. S. Kluth *et al.*, [JADE Collaboration], hep-ex/0305023.
120. D.A. Bauer *et al.*, SLAC-PUB-6518.
121. L. Gibbons *et al.*, CLNS 95-1323 (1995).
122. P. Nason and B.R. Webber, Nucl. Phys. **B421**, 473 (1994).
123. D. Buskulic *et al.*, Phys. Lett. **B357**, 487 (1995);
ibid., erratum Phys. Lett. **B364**, 247 (1995).
124. R. Akers *et al.*, Z. Phys. **C68**, 203 (1995).
125. P. Abreu *et al.*, Phys. Lett. **B398**, 194 (1997).
126. B.A. Kniehl, G. Kramer, and B. Potter, Phys. Rev. Lett. **85**, 5288 (2000).
127. K. Abe *et al.*, [SLD Collaboration], Phys. Rev. **D59**, 052001 (1999).
128. P. Abreu *et al.*, [DELPHI Collaboration], Eur. Phys. J. **C5**, 585 (1998).
129. G. Abbiendi *et al.*, [OPAL Collaboration], Eur. Phys. J. **C11**, 217 (1999).
130. D. Buskulic *et al.*, [ALEPH Collaboration], Z. Phys. **C66**, 355 (1995);
R. Barate *et al.*, Eur. Phys. J. **C17**, 1 (2000).
131. H. Aihara, *et al.*, LBL-23737 (1988) (Unpublished).
132. L. Bourhis, M. Fontannaz, J.P. Guillet, and M. Werlen, Eur. Phys. J. **C19**, 89 (2001).
133. E. Witten, Nucl. Phys. **B120**, 189 (1977).
134. C. Berger *et al.*, Nucl. Phys. **B281**, 365 (1987).
135. H. Aihara *et al.*, Z. Phys. **C34**, 1 (1987).
136. M. Althoff *et al.*, Z. Phys. **C31**, 527 (1986).
137. W. Bartel *et al.*, Z. Phys. **C24**, 231 (1984).
138. M. Erdmann, *International Conference on Lepton Photon Interactions*, Rome Italy (Aug. 2001).
139. K. Ackerstaff *et al.*, Phys. Lett. **B412**, 225 (1997); Phys. Lett. **B411**, 387 (1997).
140. G. Abbiendi *et al.*, [OPAL Collaboration], Eur. Phys. J. **C18**, 15 (2000).
141. R. Barate *et al.*, Phys. Lett. **B458**, 152 (1999).
142. M. Acciarri *et al.*, Phys. Lett. **B436**, 403 (1998); Phys. Lett. **B483**, 373 (2000).
143. P. Abreu *et al.*, Z. Phys. **C69**, 223 (1996).
144. K. Muramatsu *et al.*, Phys. Lett. **B332**, 477 (1994).
145. S.K. Sahu *et al.*, Phys. Lett. **B346**, 208 (1995).
146. S. Albino, M. Klasen and S. Soldner-Rembold, Phys. Rev. Lett. **89**, 122004 (2002).
147. C. Adloff *et al.*, Eur. Phys. J. **C13**, 397 (2000);
J. Breitweg *et al.*, Eur. Phys. J. **C11**, 35 (1999).
148. S. Frixione, Nucl. Phys. **B507**, 295 (1997);
B.W. Harris and J.F. Owens, Phys. Rev. **D56**, 4007 (1997);
M. Klasen and G. Kramer, Z. Phys. **C72**, 107 (1996).
149. D. Graudenz, Phys. Rev. **D49**, 3921 (1994);
J.G. Korner, E. Mirkes, and G.A. Schuler, Int. J. Mod. Phys. **A4**, 1781, (1989);
S. Catani and M. Seymour, Nucl. Phys. **B485**, 291 (1997);
M. Dasgupta and B.R. Webber, Eur. Phys. J. **C1**, 539 (1998);
E. Mirkes and D. Zeppenfeld, Phys. Lett. **B380**, 205 (1996).

-
150. C. Adloff *et al.*, Eur. Phys. J. **C19**, 289 (2001);
T. Ahmed *et al.*, Phys. Lett. **B346**, 415 (1995); Eur. Phys. J. **C5**,
575 (1998).
151. ZEUS Collaboration: Phys. Lett. **B560**, 7 (2003).
152. ZEUS Collaboration: S. Chekanov *et al.*, Phys. Lett. **B558**, 41
(2003);
E. Tassi at DIS2001 Conference, Bologna (April 2001).
153. M. Derrick *et al.*, Phys. Lett. **B**, 369 (1996);
T. Ahmed *et al.*, Nucl. Phys. **B435**, 3 (1995).
154. D.M. Janson, M. Albrow, and R. Brugnera, hep-ex/9905537.
155. P. Weisz, Nucl. Phys. **B** (Proc. Supp.) **47**, 71 (1996).
156. C.T.H. Davies *et al.*, hep-lat/0304004.
157. C.T.H. Davies *et al.*, Phys. Rev. **D56**, 2755 (1997).
158. S. Aoki *et al.*, Phys. Rev. Lett. **74**, 222 (1995).
159. A. Spitz *et al.*, Phys. Rev. **D60**, 074502 (1999).
160. P. Boucaud *et al.*, JHEP **0201**, 046 (2002).
161. A.X. El-Khadra *et al.*, Phys. Rev. Lett. **69**, 729 (1992);
A.X. El-Khadra *et al.*, FNAL 94-091/T (1994);
A.X. El-Khadra *et al.*, hep-ph/9608220.
162. S. Collins *et al.*, cited by Ref. 163.
163. J. Shigemitsu, Nucl. Phys. **B** (Proc. Supp.) **53**, 16 (1997).
164. A. Bode *et al.*, [ALPHA Collaboration], Phys. Lett. **B515**, 4
(2001).
165. R. Sommer, Nucl. Phys. **B411**, (1994).
166. G. de Divitiis *et al.*, Nucl. Phys. **B437**, 447 (1995);
M. Luscher *et al.*, Nucl. Phys. **B413**, 481 (1994).
167. S. Booth *et al.*, [QCDSF-UKQCD Collaboration], Phys. Lett.
B519, 229 (2001).
168. M. Luscher and P. Weisz, Nucl. Phys. **B452**, 234 (1995);
C. Christou *et al.*, Nucl. Phys. **B525**, 387 (1998); and erratum
Nucl. Phys. **B608**, 479 (2001).
169. C.T. Sachrajda, *International Conference on Lepton Photon
Interactions*, Rome Italy (Aug. 2001);
P. Lepage *International Conference on Lepton Photon Interac-
tions*, Fermilab (Aug. 2003).
170. P.N. Burrows *et al.*, in *Proceedings of 1996 DPF/DPB Snowmass
Summer Study*, ed. D. Cassel *et al.*, (1997).

10. ELECTROWEAK MODEL AND CONSTRAINTS ON NEW PHYSICS

Revised December 2003 by J. Erler (U. Mexico) and P. Langacker (Univ. of Pennsylvania).

- 10.1 Introduction
- 10.2 Renormalization and radiative corrections
- 10.3 Cross-section and asymmetry formulas
- 10.4 W and Z decays
- 10.5 Experimental results
- 10.6 Constraints on new physics

10.1. Introduction

The standard electroweak model (SM) is based on the gauge group [1] $SU(2) \times U(1)$, with gauge bosons W_μ^i , $i = 1, 2, 3$, and B_μ for the $SU(2)$ and $U(1)$ factors, respectively, and the corresponding gauge coupling constants g and g' . The left-handed fermion fields $\psi_i = \begin{pmatrix} \nu_i \\ \ell_i^- \end{pmatrix}$ and $\begin{pmatrix} u_i \\ d_i^- \end{pmatrix}$ of the i^{th} fermion family transform as doublets under $SU(2)$, where $d_i^- \equiv \sum_j V_{ij} d_j$, and V is the Cabibbo-Kobayashi-Maskawa mixing matrix. (Constraints on V and tests of universality are discussed in Ref. 2 and in the Section on the Cabibbo-Kobayashi-Maskawa mixing matrix.) The right-handed fields are $SU(2)$ singlets. In the minimal model there are three fermion families and a single complex Higgs doublet $\phi \equiv \begin{pmatrix} \phi^+ \\ \phi^0 \end{pmatrix}$.

After spontaneous symmetry breaking the Lagrangian for the fermion fields is

$$\begin{aligned} \mathcal{L}_F = & \sum_i \bar{\psi}_i \left(i \not{\partial} - m_i - \frac{g m_i H}{2M_W} \right) \psi_i \\ & - \frac{g}{2\sqrt{2}} \sum_i \bar{\psi}_i \gamma^\mu (1 - \gamma^5) (T^+ W_\mu^+ + T^- W_\mu^-) \psi_i \\ & - e \sum_i q_i \bar{\psi}_i \gamma^\mu \psi_i A_\mu \\ & - \frac{g}{2 \cos \theta_W} \sum_i \bar{\psi}_i \gamma^\mu (g_V^i - g_A^i \gamma^5) \psi_i Z_\mu. \end{aligned} \quad (10.1)$$

$\theta_W \equiv \tan^{-1}(g'/g)$ is the weak angle; $e = g \sin \theta_W$ is the positron electric charge; and $A \equiv B \cos \theta_W + W^3 \sin \theta_W$ is the (massless) photon field. $W^\pm \equiv (W^1 \mp i W^2)/\sqrt{2}$ and $Z \equiv -B \sin \theta_W + W^3 \cos \theta_W$ are the massive charged and neutral weak boson fields, respectively. T^+ and T^- are the weak isospin raising and lowering operators. The vector and axial-vector couplings are

$$g_V^i \equiv t_{3L}(i) - 2q_i \sin^2 \theta_W, \quad (10.2a)$$

$$g_A^i \equiv t_{3L}(i), \quad (10.2b)$$

where $t_{3L}(i)$ is the weak isospin of fermion i (+1/2 for u_i and ν_i ; -1/2 for d_i and e_i) and q_i is the charge of ψ_i in units of e .

The second term in \mathcal{L}_F represents the charged-current weak interaction [3,4]. For example, the coupling of a W to an electron and a neutrino is

$$-\frac{e}{2\sqrt{2} \sin \theta_W} \left[W_\mu^- \bar{\nu} \gamma^\mu (1 - \gamma^5) \nu + W_\mu^+ \bar{\nu} \gamma^\mu (1 - \gamma^5) e \right]. \quad (10.3)$$

For momenta small compared to M_W , this term gives rise to the effective four-fermion interaction with the Fermi constant given (at tree level, *i.e.*, lowest order in perturbation theory) by $G_F/\sqrt{2} = g^2/8M_W^2$. CP violation is incorporated in the SM by a single observable phase in V_{ij} . The third term in \mathcal{L}_F describes electromagnetic interactions (QED), and the last is the weak neutral-current interaction.

In Eq. (10.1), m_i is the mass of the i^{th} fermion ψ_i . For the quarks these are the current masses. For the light quarks, as described in the Particle Listings, $\hat{m}_u \approx 1.5\text{--}4.5$ MeV, $\hat{m}_d \approx 5\text{--}8.5$ MeV, and $\hat{m}_s \approx 80\text{--}155$ MeV. These are running $\overline{\text{MS}}$ masses evaluated at the scale $\mu = 2$ GeV. (In this Section we denote quantities defined in the $\overline{\text{MS}}$ scheme by a caret; the exception is the strong coupling constant, α_s , which will always correspond to the $\overline{\text{MS}}$ definition and where the caret will be dropped.) For the heavier

quarks we use QCD sum rule constraints [5] and recalculate their masses in each call of our fits to account for their direct α_s dependence. We find, $\hat{m}_c(\mu = \hat{m}_c) = 1.290_{-0.045}^{+0.040}$ GeV and $\hat{m}_b(\mu = \hat{m}_b) = 4.206 \pm 0.031$ GeV, with a correlation of 29%. The top quark ‘‘pole’’ mass, $m_t = 177.9 \pm 4.4$ GeV, is an average of CDF results from run I [6] and run II [7], as well as the $D\bar{0}$ dilepton [8] and lepton plus jets [9] channels. The latter has been recently reanalyzed, leading to a somewhat higher value. We computed the covariance matrix accounting for correlated systematic uncertainties between the different channels and experiments according to Refs. 6 and 10. Our covariance matrix also accounts for a common 0.6 GeV uncertainty (the size of the three-loop term [11]) due to the conversion from the pole mass to the $\overline{\text{MS}}$ mass. We are using a BLM optimized [12] version of the two-loop perturbative QCD formula [13] which should correspond approximately to the kinematic mass extracted from the collider events. The three-loop formula [11] gives virtually identical results. We use $\overline{\text{MS}}$ masses in all expressions to minimize theoretical uncertainties. We will use above value for m_t (together with $M_H = 117$ GeV) for the numerical values quoted in Sec. 10.2–Sec. 10.4. See ‘‘The Note on Quark Masses’’ in the Particle Listings for more information. In the presence of right-handed neutrinos, Eq. (10.1) gives rise also to Dirac neutrino masses. The possibility of Majorana masses is discussed in ‘‘Neutrino mass’’ in the Particle Listings.

H is the physical neutral Higgs scalar which is the only remaining part of ϕ after spontaneous symmetry breaking. The Yukawa coupling of H to ψ_i , which is flavor diagonal in the minimal model, is $g m_i/2M_W$. In non-minimal models there are additional charged and neutral scalar Higgs particles [14].

10.2. Renormalization and radiative corrections

The SM has three parameters (not counting the Higgs boson mass, M_H , and the fermion masses and mixings). A particularly useful set is:

- (a) The fine structure constant $\alpha = 1/137.03599911(46)$, determined from the e^\pm anomalous magnetic moment, the quantum Hall effect, and other measurements [15]. In most electroweak renormalization schemes, it is convenient to define a running α dependent on the energy scale of the process, with $\alpha^{-1} \sim 137$ appropriate at very low energy. (The running has also been observed directly [16].) For scales above a few hundred MeV this introduces an uncertainty due to the low-energy hadronic contribution to vacuum polarization. In the modified minimal subtraction ($\overline{\text{MS}}$) scheme [17] (used for this *Review*), and with $\alpha_s(M_Z) = 0.120$ for the QCD coupling at M_Z , we have $\hat{\alpha}(m_\tau)^{-1} = 133.498 \pm 0.017$ and $\hat{\alpha}(M_Z)^{-1} = 127.918 \pm 0.018$. These values are updated from Ref. 18 and account for the latest results from τ decays and a reanalysis of the CMD 2 collaboration results after correcting a radiative correction [19]. See Ref. 20 for a discussion in the context of the anomalous magnetic moment of the muon. The correlation of the latter with $\hat{\alpha}(M_Z)$, as well as the non-linear α_s dependence of $\hat{\alpha}(M_Z)$ and the resulting correlation with the input variable α_s , are fully taken into account in the fits. The uncertainty is from e^+e^- annihilation data below 1.8 GeV and τ decay data, from isospin breaking effects (affecting the interpretation of the τ data), from uncalculated higher order perturbative and non-perturbative QCD corrections, and from the $\overline{\text{MS}}$ quark masses. Such a short distance mass definition (unlike the pole mass) is free from non-perturbative and renormalon uncertainties. Various recent evaluations of the contributions of the five light quark flavors, $\Delta\alpha_{\text{had}}^{(5)}$, to the conventional (on-shell) QED coupling, $\alpha(M_Z) = \frac{\alpha}{1 - \Delta\alpha}$, are summarized in Table 10.1. Most of the older results relied on $e^+e^- \rightarrow$ hadrons cross-section measurements up to energies of 40 GeV, which were somewhat higher than the QCD prediction, suggested stronger running, and were less precise. The most recent results typically assume the validity of perturbative QCD (PQCD) at scales of 1.8 GeV and above, and are in reasonable agreement with each other.

(Evaluations in the on-shell scheme utilize resonance data from BES [36] as further input.) There is, however, some discrepancy between analyzes based on $e^+e^- \rightarrow$ hadrons cross-section data

Table 10.1: Recent evaluations of the on-shell $\Delta\alpha_{\text{had}}^{(5)}(M_Z)$. For better comparison we adjusted central values and errors to correspond to a common and fixed value of $\alpha_s(M_Z) = 0.120$. References quoting results without the top quark decoupled are converted to the five flavor definition. Ref. [31] uses $A_{\text{QCD}} = 380 \pm 60$ MeV; for the conversion we assumed $\alpha_s(M_Z) = 0.118 \pm 0.003$.

Reference	Result	Comment
Martin & Zeppenfeld [21]	0.02744 ± 0.00036	PQCD for $\sqrt{s} > 3$ GeV
Eidelman & Jegerlehner [22]	0.02803 ± 0.00065	PQCD for $\sqrt{s} > 40$ GeV
Geshkenbein & Morgunov [23]	0.02780 ± 0.00006	$\mathcal{O}(\alpha_s)$ resonance model
Burkhardt & Pietrzyk [24]	0.0280 ± 0.0007	PQCD for $\sqrt{s} > 40$ GeV
Swartz [25]	0.02754 ± 0.00046	use of fitting function
Aleman, Davier, Höcker [26]	0.02816 ± 0.00062	includes τ decay data
Krasnikov & Rodenberg [27]	0.02737 ± 0.00039	PQCD for $\sqrt{s} > 2.3$ GeV
Davier & Höcker [28]	0.02784 ± 0.00022	PQCD for $\sqrt{s} > 1.8$ GeV
Kühn & Steinhauser [29]	0.02778 ± 0.00016	complete $\mathcal{O}(\alpha_s^2)$
Erler [18]	0.02779 ± 0.00020	converted from $\overline{\text{MS}}$ scheme
Davier & Höcker [30]	0.02770 ± 0.00015	use of QCD sum rules
Groote <i>et al.</i> [31]	0.02787 ± 0.00032	use of QCD sum rules
Martin, Outhwaite, Ryskin [32]	0.02741 ± 0.00019	includes new BES data
Burkhardt & Pietrzyk [33]	0.02763 ± 0.00036	PQCD for $\sqrt{s} > 12$ GeV
de Troconiz & Yndurain [34]	0.02754 ± 0.00010	PQCD for $s > 2$ GeV ²
Jegerlehner [35]	0.02766 ± 0.00013	converted from MOM scheme

and those based on τ decay spectral functions [20]. The latter imply lower central values for the extracted M_H of $\mathcal{O}(10$ GeV). Further improvement of this dominant theoretical uncertainty in the interpretation of precision data will require better measurements of the cross-section for $e^+e^- \rightarrow$ hadrons below the charmonium resonances, as well as in the threshold region of the heavy quarks (to improve the precision in $\hat{m}_c(\hat{m}_c)$ and $\hat{m}_b(\hat{m}_b)$). As an alternative to cross-section scans, one can use the high statistics radiative return events [37] at e^+e^- accelerators operating at resonances such as the Φ or the $\Upsilon(4S)$. The method is systematics dominated. First preliminary results have been presented by the KLOE collaboration [38].

- (b) The Fermi constant, $G_F = 1.16637(1) \times 10^{-5}$ GeV⁻², determined from the muon lifetime formula [39,40],

$$\tau_\mu^{-1} = \frac{G_F^2 m_\mu^5}{192\pi^3} F\left(\frac{m_e}{m_\mu}\right) \left(1 + \frac{3}{5} \frac{m_\mu^2}{M_W^2}\right) \times \left[1 + \left(\frac{25}{8} - \frac{\pi^2}{2}\right) \frac{\alpha(m_\mu)}{\pi} + C_2 \frac{\alpha^2(m_\mu)}{\pi^2}\right], \quad (10.4a)$$

where

$$F(x) = 1 - 8x + 8x^3 - x^4 - 12x^2 \ln x, \quad (10.4b)$$

$$C_2 = \frac{156815}{5184} - \frac{518}{81}\pi^2 - \frac{895}{36}\zeta(3) + \frac{67}{720}\pi^4 + \frac{53}{6}\pi^2 \ln(2), \quad (10.4c)$$

and

$$\alpha(m_\mu)^{-1} = \alpha^{-1} - \frac{2}{3\pi} \ln\left(\frac{m_\mu}{m_e}\right) + \frac{1}{6\pi} \approx 136. \quad (10.4d)$$

The $\mathcal{O}(\alpha^2)$ corrections to μ decay have been completed recently [40]. The remaining uncertainty in G_F is from the experimental input.

- (c) The Z boson mass, $M_Z = 91.1876 \pm 0.0021$ GeV, determined from the Z -lineshape scan at LEP 1 [41].

With these inputs, $\sin^2\theta_W$ and the W boson mass, M_W , can be calculated when values for m_t and M_H are given; conversely (as is done at present), M_H can be constrained by $\sin^2\theta_W$ and M_W . The value of $\sin^2\theta_W$ is extracted from Z -pole observables and neutral-current processes [41,42], and depends on the renormalization prescription. There are a number of popular schemes [44–50] leading to values which differ by small factors depending on m_t and M_H . The notation for these schemes is shown in Table 10.2. Discussion of the schemes follows the table.

Table 10.2: Notations used to indicate the various schemes discussed in the text. Each definition of $\sin\theta_W$ leads to values that differ by small factors depending on m_t and M_H .

Scheme	Notation
On-shell	$s_W = \sin\theta_W$
NOV	$s_{M_Z} = \sin\theta_W$
$\overline{\text{MS}}$	$\hat{s}_Z = \sin\theta_W$
$\overline{\text{MS}}$ ND	$\hat{s}_{\text{ND}} = \sin\theta_W$
Effective angle	$\bar{s}_f = \sin\theta_W$

- (i) The on-shell scheme [44] promotes the tree-level formula $\sin^2\theta_W = 1 - M_W^2/M_Z^2$ to a definition of the renormalized $\sin^2\theta_W$ to all orders in perturbation theory, *i.e.*, $\sin^2\theta_W \rightarrow s_W^2 \equiv 1 - M_W^2/M_Z^2$:

$$M_W = \frac{A_0}{s_W(1 - \Delta r)^{1/2}}, \quad (10.5a)$$

$$M_Z = \frac{M_W}{c_W}, \quad (10.5b)$$

where $c_W \equiv \cos\theta_W$, $A_0 = (\pi\alpha/\sqrt{2}G_F)^{1/2} = 37.2805(2)$ GeV, and Δr includes the radiative corrections relating α , $\alpha(M_Z)$, G_F , M_W , and M_Z . One finds $\Delta r \sim \Delta r_0 - \rho_t/\tan^2\theta_W$, where $\Delta r_0 = 1 - \alpha/\hat{\alpha}(M_Z) = 0.06654(14)$ is due to the running of α , and $\rho_t = 3G_F m_t^2/8\sqrt{2}\pi^2 = 0.00992(m_t/177.9 \text{ GeV})^2$ represents the dominant (quadratic) m_t dependence. There are additional contributions to Δr from bosonic loops, including those which depend logarithmically on M_H . One has $\Delta r = 0.03434 \mp 0.0017 \pm 0.00014$, where the second uncertainty is from $\alpha(M_Z)$. Thus the value of s_W^2 extracted from M_Z includes an uncertainty (∓ 0.00054) from the currently allowed range of m_t . This scheme is simple conceptually. However, the relatively large ($\sim 3\%$) correction from ρ_t causes large spurious contributions in higher orders.

- (ii) A more precisely determined quantity $s_{M_Z}^2$ can be obtained from M_Z by removing the (m_t, M_H) dependent term from Δr [45], *i.e.*,

$$s_{M_Z}^2 c_{M_Z}^2 \equiv \frac{\pi\alpha(M_Z)}{\sqrt{2}G_F M_Z^2}. \quad (10.6)$$

Using $\alpha(M_Z)^{-1} = 128.91 \pm 0.02$ yields $s_{M_Z}^2 = 0.23108 \mp 0.00005$. The small uncertainty in $s_{M_Z}^2$ compared to other schemes is because most of the m_t dependence has been removed by definition. However, the m_t uncertainty reemerges when other

quantities (e.g., M_W or other Z -pole observables) are predicted in terms of M_Z .

Both s_W^2 and $s_{M_Z}^2$ depend not only on the gauge couplings but also on the spontaneous-symmetry breaking, and both definitions are awkward in the presence of any extension of the SM which perturbs the value of M_Z (or M_W). Other definitions are motivated by the tree-level coupling constant definition $\theta_W = \tan^{-1}(g'/g)$.

- (iii) In particular, the modified minimal subtraction ($\overline{\text{MS}}$) scheme introduces the quantity $\sin^2 \hat{\theta}_W(\mu) \equiv \hat{g}'^2(\mu)/[\hat{g}^2(\mu) + \hat{g}'^2(\mu)]$, where the couplings \hat{g} and \hat{g}' are defined by modified minimal subtraction and the scale μ is conveniently chosen to be M_Z for many electroweak processes. The value of $\hat{s}_Z^2 = \sin^2 \hat{\theta}_W(M_Z)$ extracted from M_Z is less sensitive than s_W^2 to m_t (by a factor of $\tan^2 \theta_W$), and is less sensitive to most types of new physics than s_W^2 or $s_{M_Z}^2$. It is also very useful for comparing with the predictions of grand unification. There are actually several variant definitions of $\sin^2 \hat{\theta}_W(M_Z)$, differing according to whether or how finite $\alpha \ln(m_t/M_Z)$ terms are decoupled (subtracted from the couplings). One cannot entirely decouple the $\alpha \ln(m_t/M_Z)$ terms from all electroweak quantities because $m_t \gg m_b$ breaks SU(2) symmetry. The scheme that will be adopted here decouples the $\alpha \ln(m_t/M_Z)$ terms from the γ - Z mixing [17,46], essentially eliminating any $\ln(m_t/M_Z)$ dependence in the formulae for asymmetries at the Z -pole when written in terms of \hat{s}_Z^2 . (A similar definition is used for $\hat{\alpha}$.) The various definitions are related by

$$\hat{s}_Z^2 = c(m_t, M_H) s_W^2 = \bar{c}(m_t, M_H) s_{M_Z}^2, \quad (10.7)$$

where $c = 1.0381 \pm 0.0019$ and $\bar{c} = 1.0003 \mp 0.0006$. The quadratic m_t dependence is given by $c \sim 1 + \rho_t / \tan^2 \theta_W$ and $\bar{c} \sim 1 - \rho_t / (1 - \tan^2 \theta_W)$, respectively. The expressions for M_W and M_Z in the $\overline{\text{MS}}$ scheme are

$$M_W = \frac{A_0}{\hat{s}_Z(1 - \Delta\hat{r}_W)^{1/2}}, \quad (10.8a)$$

$$M_Z = \frac{M_W}{\hat{\rho}^{1/2} c_Z}, \quad (10.8b)$$

and one predicts $\Delta\hat{r}_W = 0.06976 \pm 0.00006 \pm 0.00014$. $\Delta\hat{r}_W$ has no quadratic m_t dependence, because shifts in M_W are absorbed into the observed G_F , so that the error in $\Delta\hat{r}_W$ is dominated by $\Delta r_0 = 1 - \alpha/\hat{\alpha}(M_Z)$ which induces the second quoted uncertainty. The quadratic m_t dependence has been shifted into $\hat{\rho} \sim 1 + \rho_t$, where including bosonic loops, $\hat{\rho} = 1.0110 \pm 0.0005$.

- (iv) A variant $\overline{\text{MS}}$ quantity \hat{s}_{ND}^2 (used in the 1992 edition of this *Review*) does not decouple the $\alpha \ln(m_t/M_Z)$ terms [47]. It is related to \hat{s}_Z^2 by

$$\hat{s}_Z^2 = \hat{s}_{\text{ND}}^2 / \left(1 + \frac{\hat{\alpha}}{\pi} d\right), \quad (10.9a)$$

$$d = \frac{1}{3} \left(\frac{1}{\hat{s}^2} - \frac{8}{3} \right) \left[\left(1 + \frac{\alpha_s}{\pi}\right) \ln \frac{m_t}{M_Z} - \frac{15\alpha_s}{8\pi} \right], \quad (10.9b)$$

Thus, $\hat{s}_Z^2 - \hat{s}_{\text{ND}}^2 \sim -0.0002$ for $m_t = 177.9$ GeV.

- (v) Yet another definition, the effective angle [48–50] \hat{s}_f^2 for the Z vector coupling to fermion f , is described in Sec. 10.3.

Experiments are at a level of precision that complete $\mathcal{O}(\alpha)$ radiative corrections must be applied. For neutral-current and Z -pole processes, these corrections are conveniently divided into two classes:

1. QED diagrams involving the emission of real photons or the exchange of virtual photons in loops, but not including vacuum polarization diagrams. These graphs often yield finite and gauge-invariant contributions to observable processes. However, they are dependent on energies, experimental cuts, etc., and must be calculated individually for each experiment.
2. Electroweak corrections, including $\gamma\gamma$, γZ , ZZ , and WW vacuum polarization diagrams, as well as vertex corrections, box graphs,

etc., involving virtual W 's and Z 's. Many of these corrections are absorbed into the renormalized Fermi constant defined in Eq. (10.4). Others modify the tree-level expressions for Z -pole observables and neutral-current amplitudes in several ways [42]. One-loop corrections are included for all processes. In addition, certain two-loop corrections are also important. In particular, two-loop corrections involving the top quark modify ρ_t in $\hat{\rho}$, Δr , and elsewhere by

$$\rho_t \rightarrow \rho_t [1 + R(M_H, m_t) \rho_t / 3]. \quad (10.10)$$

$R(M_H, m_t)$ is best described as an expansion in M_Z^2/m_t^2 . The unsuppressed terms were first obtained in Ref. 51, and are known analytically [52]. Contributions suppressed by M_Z^2/m_t^2 were first studied in Ref. 53 with the help of small and large Higgs mass expansions, which can be interpolated. These contributions are about as large as the leading ones in Refs. 51 and 52. In addition, the complete two-loop calculation of diagrams containing at least one fermion loop and contributing to Δr has been performed without further approximation in Ref. 54. The two-loop evaluation of Δr was completed with the purely bosonic contributions in Ref. 55. For M_H above its lower direct limit, $-17 < R \leq -13$. Mixed QCD-electroweak loops of order $\alpha\alpha_s m_t^2$ [56] and $\alpha\alpha_s^2 m_t^2$ [57] increase the predicted value of m_t by 6%. This is, however, almost entirely an artifact of using the pole mass definition for m_t . The equivalent corrections when using the $\overline{\text{MS}}$ definition $\hat{m}_t(\hat{m}_t)$ increase m_t by less than 0.5%. The leading electroweak [51,52] and mixed [58] two-loop terms are also known for the $Z \rightarrow b\bar{b}$ vertex, but not the respective subleading ones. $\mathcal{O}(\alpha\alpha_s)$ -vertex corrections involving massless quarks have been obtained in Ref. [59]. Since they add coherently, the resulting effect is sizable, and shifts the extracted $\alpha_s(M_Z)$ by $\approx +0.0007$. Corrections of the same order to $Z \rightarrow b\bar{b}$ decays have also been completed [60].

Throughout this *Review* we utilize electroweak radiative corrections from the program GAPP [61], which works entirely in the $\overline{\text{MS}}$ scheme, and which is independent of the package ZFITTER [50].

10.3. Cross-section and asymmetry formulas

It is convenient to write the four-fermion interactions relevant to ν -hadron, ν -e, and parity violating e -hadron neutral-current processes in a form that is valid in an arbitrary gauge theory (assuming massless left-handed neutrinos). One has

$$-\mathcal{L}^{\nu\text{Hadron}} = \frac{G_F}{\sqrt{2}} \bar{\nu} \gamma^\mu (1 - \gamma^5) \nu \times \sum_i \left[\epsilon_L(i) \bar{q}_i \gamma_\mu (1 - \gamma^5) q_i + \epsilon_R(i) \bar{q}_i \gamma_\mu (1 + \gamma^5) q_i \right], \quad (10.11)$$

$$-\mathcal{L}^{\nu e} = \frac{G_F}{\sqrt{2}} \bar{\nu}_\mu \gamma^\mu (1 - \gamma^5) \nu_\mu \bar{e} \gamma_\mu (g_V^{\nu e} - g_A^{\nu e} \gamma^5) e \quad (10.12)$$

(for ν_e -e or $\bar{\nu}_e$ -e, the charge-current contribution must be included), and

$$-\mathcal{L}^{e\text{Hadron}} = -\frac{G_F}{\sqrt{2}}$$

$$\times \sum_i \left[C_{1i} \bar{e} \gamma_\mu \gamma^5 e \bar{q}_i \gamma^\mu q_i + C_{2i} \bar{e} \gamma_\mu e \bar{q}_i \gamma^\mu \gamma^5 q_i \right]. \quad (10.13)$$

(One must add the parity-conserving QED contribution.)

The SM expressions for $\epsilon_{L,R}(i)$, $g_{V,A}^{\nu e}$, and C_{ij} are given in Table 10.3. Note, that $g_{V,A}^{\nu e}$ and the other quantities are coefficients of effective four-Fermi operators, which differ from the quantities defined in Eq. (10.2) in the radiative corrections and in the presence of possible physics beyond the SM.

A precise determination of the on-shell s_W^2 , which depends only very weakly on m_t and M_H , is obtained from deep inelastic neutrino scattering from (approximately) isoscalar targets [62]. The ratio $R_\nu \equiv \sigma_{\nu N}^{\text{NC}} / \sigma_{\nu N}^{\text{CC}}$ of neutral- to charged-current cross-sections has been measured to 1% accuracy by the CDHS [63] and CHARM [64]

collaborations at CERN, and the CCFR [65] collaboration at Fermilab has obtained an even more precise result, so it is important to obtain theoretical expressions for R_ν and $R_{\bar{\nu}} \equiv \sigma_{\bar{\nu}N}^{NC}/\sigma_{\bar{\nu}N}^{CC}$ to comparable accuracy. Fortunately, most of the uncertainties from the strong interactions and neutrino spectra cancel in the ratio. The largest theoretical uncertainty is associated with the c -threshold, which mainly affects σ^{CC} . Using the slow rescaling prescription [66] the central value of $\sin^2 \theta_W$ from CCFR varies as $0.0111(m_c [\text{GeV}] - 1.31)$, where m_c is the effective mass which is numerically close to the $\overline{\text{MS}}$ mass $\widehat{m}_c(\widehat{m}_c)$, but their exact relation is unknown at higher orders. For $m_c = 1.31 \pm 0.24$ GeV (determined from ν -induced dimuon production [67]) this contributes ± 0.003 to the total uncertainty $\Delta \sin^2 \theta_W \sim \pm 0.004$. (The experimental uncertainty is also ± 0.003 .) This uncertainty largely cancels, however, in the Paschos-Wolfenstein ratio [68],

$$R^- = \frac{\sigma_{\nu N}^{NC} - \sigma_{\bar{\nu} N}^{NC}}{\sigma_{\nu N}^{CC} - \sigma_{\bar{\nu} N}^{CC}}. \quad (10.14)$$

It was measured recently by the NuTeV collaboration [69] for the first time, and required a high-intensity and high-energy anti-neutrino beam.

Table 10.3: Standard Model expressions for the neutral-current parameters for ν -hadron, ν - e , and e -hadron processes. At tree level, $\rho = \kappa = 1$, $\lambda = 0$. If radiative corrections are included, $\rho_{\nu N}^{NC} = 1.0086$, $\widehat{\kappa}_{\nu N}(\langle Q^2 \rangle = -12 \text{ GeV}^2) = 0.9978$, $\widehat{\kappa}_{\nu N}(\langle Q^2 \rangle = -35 \text{ GeV}^2) = 0.9965$, $\lambda_{uL} = -0.0031$, $\lambda_{dL} = -0.0025$, and $\lambda_{dR} = 2\lambda_{uR}R = 7.5 \times 10^{-5}$. For ν - e scattering, $\rho_{\nu e} = 1.0132$ and $\widehat{\kappa}_{\nu e} = 0.9967$ (at $\langle Q^2 \rangle = 0$). For atomic parity violation and the SLAC polarized electron experiment, $\rho_{eq} = 0.9881$, $\rho_{eq} = 1.0011$, $\widehat{\kappa}'_{eq} = 1.0027$, $\widehat{\kappa}_{eq} = 1.0300$, $\lambda_{1d} = -2\lambda_{1u} = 3.7 \times 10^{-5}$, $\lambda_{2u} = -0.0121$ and $\lambda_{2d} = 0.0026$. The dominant m_t dependence is given by $\rho \sim 1 + \rho_t$, while $\widehat{\kappa} \sim 1$ ($\overline{\text{MS}}$) or $\kappa \sim 1 + \rho_t/\tan^2 \theta_W$ (on-shell).

Quantity	Standard Model Expression
$\epsilon_L(u)$	$\rho_{\nu N}^{NC} \left(\frac{1}{2} - \frac{2}{3} \widehat{\kappa}_{\nu N} \widehat{s}_Z^2 \right) + \lambda_{uL}$
$\epsilon_L(d)$	$\rho_{\nu N}^{NC} \left(-\frac{1}{2} + \frac{1}{3} \widehat{\kappa}_{\nu N} \widehat{s}_Z^2 \right) + \lambda_{dL}$
$\epsilon_R(u)$	$\rho_{\nu N}^{NC} \left(-\frac{2}{3} \widehat{\kappa}_{\nu N} \widehat{s}_Z^2 \right) + \lambda_{uR}$
$\epsilon_R(d)$	$\rho_{\nu N}^{NC} \left(\frac{1}{3} \widehat{\kappa}_{\nu N} \widehat{s}_Z^2 \right) + \lambda_{dR}$
g_V^{ve}	$\rho_{\nu e} \left(-\frac{1}{2} + 2\widehat{\kappa}_{\nu e} \widehat{s}_Z^2 \right)$
g_A^{ve}	$\rho_{\nu e} \left(-\frac{1}{2} \right)$
C_{1u}	$\rho'_{eq} \left(-\frac{1}{2} + \frac{4}{3} \widehat{\kappa}'_{eq} \widehat{s}_Z^2 \right) + \lambda_{1u}$
C_{1d}	$\rho'_{eq} \left(\frac{1}{2} - \frac{2}{3} \widehat{\kappa}'_{eq} \widehat{s}_Z^2 \right) + \lambda_{1d}$
C_{2u}	$\rho_{eq} \left(-\frac{1}{2} + 2\widehat{\kappa}_{eq} \widehat{s}_Z^2 \right) + \lambda_{2u}$
C_{2d}	$\rho_{eq} \left(\frac{1}{2} - 2\widehat{\kappa}_{eq} \widehat{s}_Z^2 \right) + \lambda_{2d}$

A simple zeroth-order approximation is

$$R_\nu = g_L^2 + g_R^2, \quad (10.15a)$$

$$R_{\bar{\nu}} = g_L^2 + \frac{g_R^2}{r}, \quad (10.15b)$$

$$R^- = g_L^2 - g_R^2, \quad (10.15c)$$

where

$$g_L^2 \equiv \epsilon_L(u)^2 + \epsilon_L(d)^2 \approx \frac{1}{2} - \sin^2 \theta_W + \frac{5}{9} \sin^4 \theta_W, \quad (10.16a)$$

$$g_R^2 \equiv \epsilon_R(u)^2 + \epsilon_R(d)^2 \approx \frac{5}{9} \sin^4 \theta_W, \quad (10.16b)$$

and $r \equiv \sigma_{\bar{\nu}N}^{CC}/\sigma_{\nu N}^{CC}$ is the ratio of $\bar{\nu}$ and ν charged-current cross-sections, which can be measured directly. (In the simple parton model, ignoring hadron energy cuts, $r \approx (\frac{1}{3} + \epsilon)/(1 + \frac{1}{3}\epsilon)$, where $\epsilon \sim 0.125$ is the ratio of the fraction of the nucleon's momentum carried by antiquarks to that carried by quarks.) In practice, Eq. (10.15) must be corrected for quark mixing, quark sea effects, c -quark threshold effects, non-isoscalarity, W - Z propagator differences, the finite muon mass, QED and electroweak radiative corrections. Details of the neutrino spectra, experimental cuts, x and Q^2 dependence of structure functions, and longitudinal structure functions enter only at the level of these corrections and therefore lead to very small uncertainties. The CCFR group quotes $s_W^2 = 0.2236 \pm 0.0041$ for $(m_t, M_H) = (175, 150)$ GeV with very little sensitivity to (m_t, M_H) . The NuTeV collaboration finds $s_W^2 = 0.2277 \pm 0.0016$ (for the same reference values) which is 3.0σ higher than the SM prediction. The discrepancy is in the left-handed coupling, $g_L^2 = 0.3000 \pm 0.0014$, which is 2.9σ low, while $g_R^2 = 0.0308 \pm 0.0011$ is 0.6σ high. It is conceivable that the effect is caused by an asymmetric strange sea [70]. A preliminary analysis of dimuon data [71] in the relevant kinematic regime, however, indicates an asymmetric strange sea with the wrong sign to explain the discrepancy [72]. Another possibility is that the parton distribution functions (PDFs) violate isospin symmetry at levels much stronger than generally expected. Isospin breaking, nuclear physics, and higher order QCD effects seem unlikely explanations of the NuTeV discrepancy but need further study. The extracted $g_{L,R}^2$ may also shift if analyzed using the most recent set of QED and electroweak radiative corrections [73].

The laboratory cross-section for $\nu_\mu e \rightarrow \nu_\mu e$ or $\bar{\nu}_\mu e \rightarrow \bar{\nu}_\mu e$ elastic scattering is

$$\frac{d\sigma_{\nu_\mu, \bar{\nu}_\mu}}{dy} = \frac{G_F^2 m_e E_\nu}{2\pi} \times \left[(g_V^{ve} \pm g_A^{ve})^2 + (g_V^{ve} \mp g_A^{ve})^2 (1-y)^2 - (g_V^{ve2} - g_A^{ve2}) \frac{y m_e}{E_\nu} \right], \quad (10.17)$$

where the upper (lower) sign refers to $\nu_\mu(\bar{\nu}_\mu)$, and $y \equiv E_e/E_\nu$ (which runs from 0 to $(1 + m_e/2E_\nu)^{-1}$) is the ratio of the kinetic energy of the recoil electron to the incident ν or $\bar{\nu}$ energy. For $E_\nu \gg m_e$ this yields a total cross-section

$$\sigma = \frac{G_F^2 m_e E_\nu}{2\pi} \left[(g_V^{ve} \pm g_A^{ve})^2 + \frac{1}{3} (g_V^{ve} \mp g_A^{ve})^2 \right]. \quad (10.18)$$

The most accurate leptonic measurements [74–77] of $\sin^2 \theta_W$ are from the ratio $R \equiv \sigma_{\nu_\mu e}/\sigma_{\bar{\nu}_\mu e}$ in which many of the systematic uncertainties cancel. Radiative corrections (other than m_t effects) are small compared to the precision of present experiments and have negligible effect on the extracted $\sin^2 \theta_W$. The most precise experiment (CHARM II) [76] determined not only $\sin^2 \theta_W$ but $g_{V,A}^{ve}$ as well. The cross-sections for $\nu_e e$ and $\bar{\nu}_e e$ may be obtained from Eq. (10.17) by replacing $g_{V,A}^{ve}$ by $g_{V,A}^{ve} + 1$, where the 1 is due to the charged-current contribution [77, 78].

The SLAC polarized-electron experiment [79] measured the parity-violating asymmetry

$$A = \frac{\sigma_R - \sigma_L}{\sigma_R + \sigma_L}, \quad (10.19)$$

where $\sigma_{R,L}$ is the cross-section for the deep-inelastic scattering of a right- or left-handed electron: $e_{R,L} N \rightarrow eX$. In the quark parton model

$$\frac{A}{Q^2} = a_1 + a_2 \frac{1 - (1-y)^2}{1 + (1-y)^2}, \quad (10.20)$$

where $Q^2 > 0$ is the momentum transfer and y is the fractional energy transfer from the electron to the hadrons. For the deuteron or other isoscalar targets, one has, neglecting the s -quark and antiquarks,

$$a_1 = \frac{3G_F}{5\sqrt{2}\pi\alpha} \left(C_{1u} - \frac{1}{2} C_{1d} \right) \approx \frac{3G_F}{5\sqrt{2}\pi\alpha} \left(-\frac{3}{4} + \frac{5}{3} \sin^2 \theta_W \right), \quad (10.21a)$$

$$a_2 = \frac{3G_F}{5\sqrt{2}\pi\alpha} \left(C_{2u} - \frac{1}{2}C_{2d} \right) \approx \frac{9G_F}{5\sqrt{2}\pi\alpha} \left(\sin^2\theta_W - \frac{1}{4} \right). \quad (10.21b)$$

There are now precise experiments measuring atomic parity violation [80] in cesium (at the 0.4% level) [81], thallium [82], lead [83], and bismuth [84]. The uncertainties associated with atomic wave functions are quite small for cesium [85], and have been reduced recently to about 0.4% [86]. In the past, the semi-empirical value of the tensor polarizability added another source of theoretical uncertainty [87]. The ratio of the off-diagonal hyperfine amplitude to the polarizability has now been measured directly by the Boulder group [86]. Combined with the precisely known hyperfine amplitude [88] one finds excellent agreement with the earlier results, reducing the overall theory uncertainty to only 0.5% (while slightly increasing the experimental error). An earlier 2.3 σ deviation from the SM (see the year 2000 edition of this *Review*) is now seen at the 1 σ level, after the contributions from the Breit interaction have been reevaluated [89], and after the subsequent inclusion of other large and previously underestimated effects [90] (*e.g.*, from QED radiative corrections), and an update of the SM calculation [91] resulted in a vanishing net effect. The theoretical uncertainties are 3% for thallium [92] but larger for the other atoms. For heavy atoms one determines the “weak charge”

$$Q_W = -2[C_{1u}(2Z + N) + C_{1d}(Z + 2N)] \\ \approx Z(1 - 4\sin^2\theta_W) - N. \quad (10.22)$$

The recent Boulder experiment in cesium also observed the parity-violating weak corrections to the nuclear electromagnetic vertex (the anapole moment [93]).

In the future it could be possible to reduce the theoretical wave function uncertainties by taking the ratios of parity violation in different isotopes [80,94]. There would still be some residual uncertainties from differences in the neutron charge radii, however [95].

The forward-backward asymmetry for $e^+e^- \rightarrow \ell^+\ell^-$, $\ell = \mu$ or τ , is defined as

$$A_{FB} \equiv \frac{\sigma_F - \sigma_B}{\sigma_F + \sigma_B}, \quad (10.23)$$

where $\sigma_F(\sigma_B)$ is the cross-section for ℓ^- to travel forward (backward) with respect to the e^- direction. A_{FB} and R , the total cross-section relative to pure QED, are given by

$$R = F_1, \quad (10.24)$$

$$A_{FB} = 3F_2/4F_1, \quad (10.25)$$

where

$$F_1 = 1 - 2\chi_0 g_V^e g_V^\ell \cos\delta_R + \chi_0^2 (g_V^e + g_A^e)^2 (g_V^\ell + g_A^\ell), \quad (10.26a)$$

$$F_2 = -2\chi_0 g_A^e g_A^\ell \cos\delta_R + 4\chi_0^2 g_A^e g_A^\ell g_V^e g_V^\ell, \quad (10.26b)$$

$$\tan\delta_R = \frac{M_Z \Gamma_Z}{M_Z^2 - s}, \quad (10.27)$$

$$\chi_0 = \frac{G_F}{2\sqrt{2}\pi\alpha} \frac{sM_Z^2}{[(M_Z^2 - s)^2 + M_Z^2 \Gamma_Z^2]^{1/2}}, \quad (10.28)$$

and \sqrt{s} is the CM energy. Eq. (10.26) is valid at tree level. If the data is radiatively corrected for QED effects (as described above), then the remaining electroweak corrections can be incorporated [96,97] (in an approximation adequate for existing PEP, PETRA, and TRISTAN data, which are well below the Z -pole) by replacing χ_0 by $\chi(s) \equiv (1 + \rho_t)\chi_0(s)\alpha/\alpha(s)$, where $\alpha(s)$ is the running QED coupling, and evaluating g_V in the $\overline{\text{MS}}$ scheme. Formulas for $e^+e^- \rightarrow$ hadrons may be found in Ref. 98.

At LEP and SLC, there were high-precision measurements of various Z -pole observables [41,99–105], as summarized in Table 10.4. These include the Z mass and total width, Γ_Z , and partial widths $\Gamma(f\bar{f})$ for $Z \rightarrow f\bar{f}$ where fermion $f = e, \mu, \tau$, hadrons, b , or c . It is convenient to use the variables M_Z , Γ_Z , $R_\ell \equiv \Gamma(\text{had})/\Gamma(\ell^+\ell^-)$, $\sigma_{\text{had}} \equiv 12\pi\Gamma(e^+e^-\Gamma(\text{had})/M_Z^2\Gamma_Z^2)$, $R_b \equiv \Gamma(b\bar{b})/\Gamma(\text{had})$, and $R_c \equiv$

$\Gamma(c\bar{c})/\Gamma(\text{had})$, most of which are weakly correlated experimentally. ($\Gamma(\text{had})$ is the partial width into hadrons.) $\mathcal{O}(\alpha^3)$ QED corrections introduce a large anticorrelation (-30%) between Γ_Z and σ_{had} [41], while the anticorrelation between R_b and R_c (-14%) is smaller than previously [100]. R_ℓ is insensitive to m_t except for the $Z \rightarrow b\bar{b}$ vertex and final state corrections and the implicit dependence through $\sin^2\theta_W$. Thus it is especially useful for constraining α_s . The width for invisible decays [41], $\Gamma(\text{inv}) = \Gamma_Z - 3\Gamma(\ell^+\ell^-) - \Gamma(\text{had}) = 499.0 \pm 1.5$ MeV, can be used to determine the number of neutrino flavors much lighter than $M_Z/2$, $N_\nu = \Gamma(\text{inv})/\Gamma^{\text{theory}}(\nu\bar{\nu}) = 2.983 \pm 0.009$ for $(m_t, M_H) = (177.9, 117)$ GeV.

There were also measurements of various Z -pole asymmetries. These include the polarization or left-right asymmetry

$$A_{LR} \equiv \frac{\sigma_L - \sigma_R}{\sigma_L + \sigma_R}, \quad (10.29)$$

where $\sigma_L(\sigma_R)$ is the cross-section for a left-(right)-handed incident electron. A_{LR} has been measured precisely by the SLD collaboration at the SLC [101], and has the advantages of being extremely sensitive to $\sin^2\theta_W$ and that systematic uncertainties largely cancel. In addition, the SLD collaboration has extracted the final-state couplings A_b , A_c [41], A_s [102], A_τ , and A_μ [103] from left-right forward-backward asymmetries, using

$$A_{LR}^{FB}(f) = \frac{\sigma_{LF}^f - \sigma_{LB}^f - \sigma_{RF}^f + \sigma_{RB}^f}{\sigma_{LF}^f + \sigma_{LB}^f + \sigma_{RF}^f + \sigma_{RB}^f} = \frac{3}{4}A_f, \quad (10.30)$$

where, for example, σ_{LF} is the cross-section for a left-handed incident electron to produce a fermion f traveling in the forward hemisphere. Similarly, A_τ is measured at LEP [41] through the negative total τ polarization, \mathcal{P}_τ , and A_e is extracted from the angular distribution of \mathcal{P}_τ . An equation such as (10.30) assumes that initial state QED corrections, photon exchange, γ - Z interference, the tiny electroweak boxes, and corrections for $\sqrt{s} \neq M_Z$ are removed from the data, leaving the pure electroweak asymmetries. This allows the use of effective tree-level expressions,

$$A_{LR} = A_e P_e, \quad (10.31)$$

$$A_{FB} = \frac{3}{4}A_f \frac{A_e + P_e}{1 + P_e A_e}, \quad (10.32)$$

where

$$A_f \equiv \frac{2\overline{g}_V^f \overline{g}_A^f}{\overline{g}_V^f{}^2 + \overline{g}_A^f{}^2}, \quad (10.33)$$

and

$$\overline{g}_V^f = \sqrt{\rho_f} t_{3L}^{(f)} - 2q_f \kappa_f \sin^2\theta_W, \quad (10.33b)$$

$$\overline{g}_A^f = \sqrt{\rho_f} t_{3L}^{(f)}. \quad (10.33c)$$

P_e is the initial e^- polarization, so that the second equality in Eq. (10.30) is reproduced for $P_e = 1$, and the Z -pole forward-backward asymmetries at LEP ($P_e = 0$) are given by $A_{FB}^{(0,f)} = \frac{3}{4}A_e A_f$ where $f = e, \mu, \tau, b, c, s$ [104], and g , and where $A_{FB}^{(0,q)}$ refers to the hadronic charge asymmetry. Corrections for t -channel exchange and s/t -channel interference cause $A_{FB}^{(0,e)}$ to be strongly anticorrelated with R_e (-37%). The initial state coupling, A_e , is also determined through the left-right charge asymmetry [105] and in polarized Bhabha scattering at the SLC [103].

The electroweak radiative corrections have been absorbed into corrections $\rho_f - 1$ and $\kappa_f - 1$, which depend on the fermion f and on the renormalization scheme. In the on-shell scheme, the quadratic m_t dependence is given by $\rho_f \sim 1 + \rho_t$, $\kappa_f \sim 1 + \rho_t/\tan^2\theta_W$, while in $\overline{\text{MS}}$, $\hat{\rho}_f \sim \hat{\kappa}_f \sim 1$, for $f \neq b$ ($\hat{\rho}_b \sim 1 - \frac{4}{3}\rho_t$, $\hat{\kappa}_b \sim 1 + \frac{2}{3}\rho_t$). In the $\overline{\text{MS}}$ scheme the normalization is changed according to $G_F M_Z^2/2\sqrt{2}\pi \rightarrow \hat{\alpha}/4\hat{s}_2^2 c_2^2$. (If one continues to normalize amplitudes by $G_F M_Z^2/2\sqrt{2}\pi$, as in the 1996 edition of this *Review*, then $\hat{\rho}_f$ contains an additional factor of $\hat{\rho}$.) In practice, additional bosonic and fermionic loops, vertex corrections, leading higher order contributions, *etc.*, must be included.

For example, in the \overline{MS} scheme one has $\widehat{\rho}_\ell = 0.9981$, $\widehat{\kappa}_\ell = 1.0013$, $\widehat{\rho}_b = 0.9861$, and $\widehat{\kappa}_b = 1.0071$. It is convenient to define an effective angle $\overline{s}_f^2 \equiv \sin^2 \overline{\theta}_{Wf} \equiv \widehat{\kappa}_f \widehat{s}_Z^2 = \kappa_f s_W^2$, in terms of which \overline{g}_V^f and \overline{g}_A^f are given by $\sqrt{\rho_f}$ times their tree-level formulae. Because \overline{g}_V^ℓ is very small, not only $A_{LR}^0 = A_e$, $A_{FB}^{(0,\ell)}$, and \mathcal{P}_τ , but also $A_{FB}^{(0,b)}$, $A_{FB}^{(0,c)}$, $A_{FB}^{(0,s)}$, and the hadronic asymmetries are mainly sensitive to \overline{s}_f^2 . One finds that $\widehat{\kappa}_f$ ($f \neq b$) is almost independent of (m_t, M_H) , so that one can write

$$\overline{s}_f^2 \sim \widehat{s}_Z^2 + 0.00029. \quad (10.34)$$

Thus, the asymmetries determine values of \overline{s}_ℓ^2 and \widehat{s}_Z^2 almost independent of m_t , while the κ 's for the other schemes are m_t dependent.

LEP 2 [41] has run at several energies above the Z -pole up to ~ 209 GeV. Measurements have been made of a number of observables, including the cross-sections for $e^+e^- \rightarrow f\bar{f}$ for $f = q, \mu^-, \tau^-$; the differential cross-sections and A_{FB} for μ and τ ; R and A_{FB} for b and c ; W branching ratios; and WW , $WW\gamma$, ZZ , single W , and single Z cross-sections. They are in agreement with the SM predictions, with the exceptions of the total hadronic cross-section (1.7 σ high), R_b (2.1 σ low), and $A_{FB}(b)$ (1.6 σ low). Also, the SM Higgs has been excluded below 114.4 GeV [106].

The Z -boson properties are extracted assuming the SM expressions for the γ - Z interference terms. These have also been tested experimentally by performing more general fits [107] to the LEP 1 and LEP 2 data. Assuming family universality this approach introduces three additional parameters relative to the standard fit [41], describing the γ - Z interference contribution to the total hadronic and leptonic cross-sections, $j_{\text{had}}^{\text{tot}}$ and j_ℓ^{tot} , and to the leptonic forward-backward asymmetry, j_ℓ^{fb} . For example,

$$j_{\text{had}}^{\text{tot}} \sim g_V^{\ell} g_V^{\text{had}} = 0.277 \pm 0.065, \quad (10.35)$$

which is in good agreement with the SM expectation [41] of $0.220_{-0.014}^{+0.003}$. Similarly, LEP data up to CM energies of 206 GeV were used to constrain the γ - Z interference terms for the heavy quarks. The results for j_b^{tot} , j_b^{fb} , j_c^{tot} , and j_c^{fb} were found in perfect agreement with the SM. These are valuable tests of the SM; but it should be cautioned that new physics is not expected to be described by this set of parameters, since (i) they do not account for extra interactions beyond the standard weak neutral-current, and (ii) the photonic amplitude remains fixed to its SM value.

Strong constraints on anomalous triple and quartic gauge couplings have been obtained at LEP 2 and at the Tevatron, as are described in the Particle Listings.

The left-right asymmetry in polarized Møller scattering $e^+e^- \rightarrow e^+e^-$ is being measured in the SLAC E158 experiment. A precision of better than ± 0.001 in $\sin^2 \theta_W$ at $Q^2 \sim 0.03$ GeV² is anticipated. The result of the first of three runs yields $\widehat{s}_Z^2 = 0.2279 \pm 0.0032$ [108]. In a similar experiment and at about the same Q^2 , Qweak at Jefferson Lab [109] will be able to measure $\sin^2 \theta_W$ in polarized ep scattering with a relative precision of 0.3%. These experiments will provide the most precise determinations of the weak mixing angle off the Z peak and will be sensitive to various types of physics beyond the SM.

The Belle [110], CLEO [111], and BaBar [112] collaborations reported precise measurements of the flavor changing transition $b \rightarrow s\gamma$. The signal efficiencies (including the extrapolation to the full photon spectrum) depend on the bottom pole mass, m_b . We adjusted the Belle and BaBar results to agree with the m_b value used by CLEO. In the case of CLEO, a 3.8% component from the model error of the signal efficiency is moved from the systematic error to the model error. The results for the branching fractions are then given by,

$$\mathcal{B}[\text{Belle}] = 3.05 \times 10^{-4} [1 \pm 0.158 \pm 0.124 \pm 0.202 \pm 0], \quad (10.36a)$$

$$\mathcal{B}[\text{CLEO}] = 3.21 \times 10^{-4} [1 \pm 0.134 \pm 0.076 \pm 0.059 \pm 0.016], \quad (10.36b)$$

$$\mathcal{B}[\text{BaBar}] = 3.86 \times 10^{-4} [1 \pm 0.090 \pm 0.093 \pm 0.074 \pm 0.016], \quad (10.36c)$$

where the first two errors are the statistical and systematic uncertainties (taken uncorrelated). The third error (taken 100%

correlated) accounts for the extrapolation from the finite photon energy cutoff (2.25 GeV, 2.0 GeV, and 2.1 GeV, respectively) to the full theoretical branching ratio [113]. The last error is from the correction for the $b \rightarrow d\gamma$ component which is common to CLEO and BaBar. It is advantageous [114] to normalize the result with respect to the semi-leptonic branching fraction, $\mathcal{B}(b \rightarrow X e \nu) = 0.1064 \pm 0.0023$, yielding,

$$R = \frac{\mathcal{B}(b \rightarrow s\gamma)}{\mathcal{B}(b \rightarrow X e \nu)} = (3.39 \pm 0.43 \pm 0.37) \times 10^{-3}. \quad (10.37)$$

In the fits we use the variable $\ln R = -5.69 \pm 0.17$ to assure an approximately Gaussian error [115]. We added an 11% theory uncertainty (excluding parametric errors such as from α_s) in the SM prediction which is based on the next-to-leading order calculations of Refs. 114,116.

The present world average of the muon anomalous magnetic moment,

$$a_\mu^{\text{exp}} = \frac{g_\mu - 2}{2} = (1165920.37 \pm 0.78) \times 10^{-9}, \quad (10.38)$$

is dominated by the 1999 and 2000 data runs of the E821 collaboration at BNL [117]. The final 2001 data run is currently being analyzed. The QED contribution has been calculated to four loops (fully analytically to three loops), and the leading logarithms are included to five loops [118]. The estimated SM electroweak contribution [119–121], $a_\mu^{\text{EW}} = (1.52 \pm 0.03) \times 10^{-9}$, which includes leading two-loop [120] and three-loop [121] corrections, is at the level of the current uncertainty. The limiting factor in the interpretation of the result is the uncertainty from the two-loop hadronic contribution [20], $a_\mu^{\text{had}} = (69.63 \pm 0.72) \times 10^{-9}$, which has been obtained using $e^+e^- \rightarrow$ hadrons cross-section data. The latter are dominated by the recently reanalyzed CMD 2 data [19]. This value suggests a 1.9 σ discrepancy between Eq. (10.38) and the SM prediction. In an alternative analysis, the authors of Ref. 20 use τ decay data and isospin symmetry (CVC) to obtain instead $a_\mu^{\text{had}} = (71.10 \pm 0.58) \times 10^{-9}$. This result implies no conflict (0.7 σ) with Eq. (10.38). Thus, there is also a discrepancy between the 2π spectral functions obtained from the two methods. For example, if one uses the e^+e^- data and CVC to predict the branching ratio for $\tau^- \rightarrow \nu_\tau \pi^- \pi^0$ decays one obtains $24.52 \pm 0.32\%$ [20] while the average of the measured branching ratios by DELPHI [122], ALEPH, CLEO, L3, and OPAL [20] yields $25.43 \pm 0.09\%$, which is 2.8 σ higher. It is important to understand the origin of this difference and to obtain additional experimental information (*e.g.*, from the radiative return method [37]). Fortunately, this problem is less pronounced as far as a_μ^{had} is concerned: due to the suppression at large s (from where the conflict originates) the difference is only 1.7 σ (or 1.9 σ if one adds the 4π channel which by itself is consistent between the two methods). Note also that a part of this difference is due to the older e^+e^- data [20], and the direct conflict between τ decay data and CMD 2 is less significant. Isospin violating corrections have been estimated in Ref. 123 and found to be under control. The largest effect is due to higher-order electroweak corrections [39] but introduces a negligible uncertainty [124]. In the following we view the 1.7 σ difference as a fluctuation and average the results. An additional uncertainty is induced by the hadronic three-loop light-by-light scattering contribution [125], $a_\mu^{\text{LBL}} = (+0.83 \pm 0.19) \times 10^{-9}$, which was estimated within a form factor approach. The sign of this effect is opposite to the one quoted in the 2002 edition of this *Review*, and has subsequently been confirmed by two other groups [126]. Other hadronic effects at three-loop order contribute [127], $a_\mu^{\text{had}} \left[\left(\frac{\alpha}{\pi} \right)^3 \right] = (-1.00 \pm 0.06) \times 10^{-9}$. Correlations with the two-loop hadronic contribution and with $\Delta\alpha(M_Z)$ (see Sec. 10.2) were considered in Ref. 128, which also contains analytic results for the perturbative QCD contribution. The SM prediction is

$$a_\mu^{\text{theory}} = (1165918.83 \pm 0.49) \times 10^{-9}, \quad (10.39)$$

where the error is from the hadronic uncertainties excluding parametric ones such as from α_s and the heavy quark masses. We estimate its correlation with $\Delta\alpha(M_Z)$ as 21%. The small overall discrepancy

between the experimental and theoretical values could be due to fluctuations or underestimates of the theoretical uncertainties. On the other hand, $g_\mu - 2$ is also affected by many types of new physics, such as supersymmetric models with large $\tan\beta$ and moderately light superparticle masses [129]. Thus, the deviation could also arise from physics beyond the SM.

Note added: After completion of this Section and the fits described here, the E821 collaboration announced its measurement on the anomalous magnetic moment of the negatively charged muon based on data taken in 2001 [130]. The result, $a_\mu^{\text{exp}} = (1165921.4 \pm 0.8 \pm 0.3) \times 10^{-9}$, is consistent with the results on positive muons and appears to confirm the deviation. There also appeared two new evaluations [131,132] of a_μ^{had} . They are based on e^+e^- data only and are generally in good agreement with each other and other e^+e^- based analyses. τ decay data are not used; it is argued [131] that CVC breaking effects (*e.g.*, through a relatively large mass difference between the ρ^\pm and ρ^0 vector mesons) may be larger than expected. This may also be relevant in the context of the NuTeV discrepancy discussed above [131].

10.4. W and Z decays

The partial decay width for gauge bosons to decay into massless fermions $f_1\bar{f}_2$ is

$$\Gamma(W^+ \rightarrow e^+\nu_e) = \frac{G_F M_W^3}{6\sqrt{2}\pi} \approx 226.56 \pm 0.24 \text{ MeV} \quad , \quad (10.47a)$$

$$\Gamma(W^+ \rightarrow u_i\bar{d}_j) = \frac{CG_F M_W^3}{6\sqrt{2}\pi} |V_{ij}|^2 \approx (707.1 \pm 0.7) |V_{ij}|^2 \text{ MeV} \quad , \quad (10.47b)$$

$$\Gamma(Z \rightarrow \psi_i\bar{\psi}_i) = \frac{CG_F M_Z^3}{6\sqrt{2}\pi} [g_V^i{}^2 + g_A^i{}^2] \quad (10.47c)$$

$$\approx \begin{cases} 300.4 \pm 0.2 \text{ MeV} & (u\bar{u}), \quad 167.29 \pm 0.07 \text{ MeV} & (\nu\bar{\nu}), \\ 383.2 \pm 0.2 \text{ MeV} & (d\bar{d}), \quad 84.03 \pm 0.04 \text{ MeV} & (e^+e^-), \\ 375.8 \pm 0.1 \text{ MeV} & (b\bar{b}). \end{cases}$$

For leptons $C = 1$, while for quarks $C = 3(1 + \alpha_s(M_V)/\pi + 1.409\alpha_s^2/\pi^2 - 12.77\alpha_s^3/\pi^3)$, where the 3 is due to color and the factor in parentheses represents the universal part of the QCD corrections [133] for massless quarks [134]. The $Z \rightarrow f\bar{f}$ widths contain a number of additional corrections: universal (non-singlet) top quark mass contributions [135]; fermion mass effects and further QCD corrections proportional to $\bar{m}_q^2(M_Z^2)$ [136] which are different for vector and axial-vector partial widths; and singlet contributions starting from two-loop order which are large, strongly top quark mass dependent, family universal, and flavor non-universal [137]. All QCD effects are known and included up to three-loop order. The QED factor $1 + 3\alpha q_f^2/4\pi$, as well as two-loop order $\alpha\alpha_s$ and α^2 self-energy corrections [138] are also included. Working in the on-shell scheme, *i.e.*, expressing the widths in terms of $G_F M_{W,Z}^3$, incorporates the largest radiative corrections from the running QED coupling [44,139]. Electroweak corrections to the Z widths are then incorporated by replacing $g_{V,A}^i{}^2$ by $\bar{g}_{V,A}^i{}^2$. Hence, in the on-shell scheme the Z widths are proportional to $\rho_i \sim 1 + \rho_i$. The $\overline{\text{MS}}$ normalization accounts also for the leading electroweak corrections [48]. There is additional (negative) quadratic m_t dependence in the $Z \rightarrow b\bar{b}$ vertex corrections [140] which causes $\Gamma(b\bar{b})$ to decrease with m_t . The dominant effect is to multiply $\Gamma(b\bar{b})$ by the vertex correction $1 + \delta\rho_{b\bar{b}}$,

where $\delta\rho_{b\bar{b}} \sim 10^{-2}(-\frac{m_t^2}{2M_Z^2} + \frac{1}{5})$. In practice, the corrections are included in ρ_b and κ_b , as discussed before.

For 3 fermion families the total widths are predicted to be

$$\Gamma_Z \approx 2.4968 \pm 0.0011 \text{ GeV} \quad , \quad (10.48)$$

$$\Gamma_W \approx 2.0936 \pm 0.0022 \text{ GeV} \quad . \quad (10.49)$$

We have assumed $\alpha_s(M_Z) = 0.1200$. An uncertainty in α_s of ± 0.0018 introduces an additional uncertainty of 0.05% in the hadronic

widths, corresponding to ± 0.9 MeV in Γ_Z . These predictions are to be compared with the experimental results $\Gamma_Z = 2.4952 \pm 0.0023$ GeV [41] and $\Gamma_W = 2.124 \pm 0.041$ GeV (see the Particle Listings for more details).

Table 10.4: Principal Z -pole and other observables, compared with the SM predictions for the global best fit values $M_Z = 91.1874 \pm 0.0021$ GeV, $M_H = 113_{-40}^{+56}$ GeV, $m_t = 176.9 \pm 4.0$ GeV, $\alpha_s(M_Z) = 0.1213 \pm 0.0018$, and $\hat{\alpha}(M_Z)^{-1} = 127.906 \pm 0.019$. The LEP averages of the ALEPH, DELPHI, L3, and OPAL results include common systematic errors and correlations [41]. The heavy flavor results of LEP and SLD are based on common inputs and correlated, as well [100]. $\bar{\alpha}_i^2(A_{FB}^{(0,q)})$ is the effective angle extracted from the hadronic charge asymmetry, which has some correlation with $A_{FB}^{(0,b)}$ which is currently neglected. The values of $\Gamma(\ell^+\ell^-)$, $\Gamma(\text{had})$, and $\Gamma(\text{inv})$ are not independent of Γ_Z , the R_ℓ , and σ_{had} . The m_t values are from the lepton plus jets channel of the CDF [6] and DØ [9] run I data, respectively. Results from the other channels and all correlations are also included. The first M_W value is from UA2, CDF, and DØ [141], while the second one is from LEP 2 [41]. The first M_W and M_Z are correlated, but the effect is negligible due to the tiny M_Z error. The three values of A_e are (i) from A_{LR} for hadronic final states [101]; (ii) from A_{LR} for leptonic final states and from polarized Bhabha scattering [103]; and (iii) from the angular distribution of the τ polarization. The two A_τ values are from SLD and the total τ polarization, respectively. g_L^2 and g_R^2 are from NuTeV [69] and have a very small (-1.7%) residual anticorrelation. The older deep-inelastic scattering (DIS) results from CDHS [63], CHARM [64], and CCFR [65] are included, as well, but not shown in the Table. The world averages for $g_{V,A}^{\nu e}$ are dominated by the CHARM II [76] results, $g_V^{\nu e} = -0.035 \pm 0.017$ and $g_A^{\nu e} = -0.503 \pm 0.017$. The errors in Q_W , DIS, $b \rightarrow s\gamma$, and $g_\mu - 2$ are the total (experimental plus theoretical) uncertainties. The τ_τ value is the τ lifetime world average computed by combining the direct measurements with values derived from the leptonic branching ratios [5]; the theory uncertainty is included in the SM prediction. In all other SM predictions, the uncertainty is from M_Z , M_H , m_t , m_b , m_c , $\hat{\alpha}(M_Z)$, and α_s , and their correlations have been accounted for. The SM errors in Γ_Z , $\Gamma(\text{had})$, R_ℓ , and σ_{had} are largely dominated by the uncertainty in α_s .

Quantity	Value	Standard Model	Pull
m_t [GeV]	176.1 ± 7.4	176.9 ± 4.0	-0.1
	180.1 ± 5.4		0.6
M_W [GeV]	80.454 ± 0.059	80.390 ± 0.018	1.1
	80.412 ± 0.042		0.5
M_Z [GeV]	91.1876 ± 0.0021	91.1874 ± 0.0021	0.1
Γ_Z [GeV]	2.4952 ± 0.0023	2.4972 ± 0.0012	-0.9
$\Gamma(\text{had})$ [GeV]	1.7444 ± 0.0020	1.7435 ± 0.0011	—
$\Gamma(\text{inv})$ [MeV]	499.0 ± 1.5	501.81 ± 0.13	—
$\Gamma(\ell^+\ell^-)$ [MeV]	83.984 ± 0.086	84.024 ± 0.025	—
σ_{had} [nb]	41.541 ± 0.037	41.472 ± 0.009	1.9
R_e	20.804 ± 0.050	20.750 ± 0.012	1.1
R_μ	20.785 ± 0.033	20.751 ± 0.012	1.0
R_τ	20.764 ± 0.045	20.790 ± 0.018	-0.7
R_b	0.21638 ± 0.00066	0.21564 ± 0.00014	1.1
R_c	0.1720 ± 0.0030	0.17233 ± 0.00005	-0.1
$A_{FB}^{(0,e)}$	0.0145 ± 0.0025	0.01626 ± 0.00025	-0.7
$A_{FB}^{(0,\mu)}$	0.0169 ± 0.0013		0.5
$A_{FB}^{(0,\tau)}$	0.0188 ± 0.0017		1.5
$A_{FB}^{(0,b)}$	0.0997 ± 0.0016	0.1032 ± 0.0008	-2.2

Table 10.4: (continued)

Quantity	Value	Standard Model	Pull
$A_{FB}^{(0,c)}$	0.0706 ± 0.0035	0.0738 ± 0.0006	-0.9
$A_{FB}^{(0,s)}$	0.0976 ± 0.0114	0.1033 ± 0.0008	-0.5
$\hat{s}_\ell^2(A_{FB}^{(0,q)})$	0.2324 ± 0.0012	0.23149 ± 0.00015	0.8
A_e	0.15138 ± 0.00216	0.1472 ± 0.0011	1.9
	0.1544 ± 0.0060		1.2
	0.1498 ± 0.0049		0.5
A_μ	0.142 ± 0.015		-0.4
A_τ	0.136 ± 0.015		-0.8
	0.1439 ± 0.0043		-0.8
A_b	0.925 ± 0.020	0.9347 ± 0.0001	-0.5
A_c	0.670 ± 0.026	0.6678 ± 0.0005	0.1
A_s	0.895 ± 0.091	0.9357 ± 0.0001	-0.4
g_L^2	0.30005 ± 0.00137	0.30397 ± 0.00023	-2.9
g_R^2	0.03076 ± 0.00110	0.03007 ± 0.00003	0.6
$g_V^{e\ell}$	-0.040 ± 0.015	-0.0397 ± 0.0003	-0.1
$g_A^{e\ell}$	-0.507 ± 0.014	-0.5065 ± 0.0001	0.0
$Q_W(\text{Cs})$	-72.69 ± 0.48	-73.19 ± 0.03	1.0
$Q_W(\text{Tl})$	-116.6 ± 3.7	-116.81 ± 0.04	0.1
$\frac{\Gamma(b \rightarrow s\gamma)}{\Gamma(b \rightarrow X e \nu)}$	$3.39^{+0.62}_{-0.54} \times 10^{-3}$	$(3.23 \pm 0.09) \times 10^{-3}$	0.3
$\frac{1}{2}(g_\mu - 2 - \frac{\alpha}{\pi})$	4510.64 ± 0.92	4509.13 ± 0.10	1.6
τ_τ [fs]	290.92 ± 0.55	291.83 ± 1.81	-0.4

10.5. Experimental results

The values of the principal Z -pole observables are listed in Table 10.4, along with the SM predictions for $M_Z = 91.1874 \pm 0.0021$ GeV, $M_H = 113^{+56}_{-40}$ GeV, $m_t = 176.9 \pm 4.0$ GeV, $\alpha_s(M_Z) = 0.1213 \pm 0.0018$, and $\hat{\alpha}(M_Z)^{-1} = 127.906 \pm 0.019$ ($\Delta\alpha_{\text{had}}^{(5)} \approx 0.02801 \pm 0.00015$). The values and predictions of M_W [41,141]; m_t [6,9]; the Q_W for cesium [81] and thallium [82]; deep inelastic [69] and ν_μ - e scattering [74–76]; the $b \rightarrow s\gamma$ observable [110–112]; the muon anomalous magnetic moment [117]; and the τ lifetime are also listed. The values of M_W and m_t differ from those in the Particle Listings because they include recent preliminary results. The agreement is excellent. Only g_L^2 from NuTeV is currently showing a large (2.9 σ) deviation. In addition, the hadronic peak cross-section, σ_{had} , and the A_{FB}^0 from hadronic final states differ by 1.9 σ . On the other hand, $A_{FB}^{(0,b)}$ (2.2 σ) and $g_\mu - 2$ (1.6 σ , see Sec. 10.3) both moved closer to the SM predictions by about one standard deviation compared to the 2002 edition of this *Review*, while M_W (LEP 2) has moved closer by 0.8 σ . Observables like $R_b = \Gamma(b\bar{b})/\Gamma(\text{had})$, $R_c = \Gamma(c\bar{c})/\Gamma(\text{had})$, and the combined value for M_W which showed significant deviations in the past, are now in reasonable agreement. In particular, R_b whose measured value deviated as much as 3.7 σ from the SM prediction is now only 1.1 σ (0.34%) high.

A_b can be extracted from $A_{FB}^{(0,b)}$ when $A_e = 0.1501 \pm 0.0016$ is taken from a fit to leptonic asymmetries (using lepton universality). The result, $A_b = 0.886 \pm 0.017$, is 2.9 σ below the SM prediction[†], and also 1.5 σ below $A_b = 0.925 \pm 0.020$ obtained from $A_{FB}^{(0,b)}$ at SLD. Thus, it appears that at least some of the problem in $A_{FB}^{(0,b)}$ is experimental.

Note, however, that the uncertainty in $A_{FB}^{(0,b)}$ is strongly statistics dominated. The combined value, $A_b = 0.902 \pm 0.013$ deviates by 2.5 σ . It would be extremely difficult to account for this 3.5% deviation by new physics radiative corrections since an order of 20% correction to $\hat{\alpha}_b$ would be necessary to account for the central value of A_b . If this deviation is due to new physics, it is most likely of tree-level type affecting differentially the third generation. Examples include the decay of a scalar neutrino resonance [142], mixing of the b quark with heavy exotics [143], and a heavy Z' with family-nonuniversal couplings [144]. It is difficult, however, to simultaneously account

for R_b , which has been measured on the Z peak and off-peak [145] at LEP 1. An average of R_b measurements at LEP 2 at energies between 133 and 207 GeV is 2.1 σ below the SM prediction, while $A_{FB}^{(b)}$ (LEP 2) is 1.6 σ low.

The left-right asymmetry, $A_{LR}^0 = 0.15138 \pm 0.00216$ [101], based on all hadronic data from 1992–1998 differs 1.9 σ from the SM expectation of 0.1472 ± 0.0011 . The combined value of $A_\ell = 0.1513 \pm 0.0021$ from SLD (using lepton-family universality and including correlations) is also 1.9 σ above the SM prediction; but there is now experimental agreement between this SLD value and the LEP value, $A_\ell = 0.1481 \pm 0.0027$, obtained from a fit to $A_{FB}^{(0,\ell)}$, $A_e(\mathcal{P}_\tau)$, and $A_\tau(\mathcal{P}_\tau)$, again assuming universality.

Despite these discrepancies the goodness of the fit to all data is excellent with a $\chi^2/\text{d.o.f.} = 45.5/45$. The probability of a larger χ^2 is 45%. The observables in Table 10.4, as well as some other less precise observables, are used in the global fits described below. The correlations on the LEP lineshape and τ polarization, the LEP/SLD heavy flavor observables, the SLD lepton asymmetries, the deep inelastic and ν - e scattering observables, and the m_t measurements, are included. The theoretical correlations between $\Delta\alpha_{\text{had}}^{(5)}$ and $g_\mu - 2$, and between the charm and bottom quark masses, are also accounted for.

Table 10.5: Values of \hat{s}_Z^2 , s_W^2 , α_s , and M_H [in GeV] for various (combinations of) observables. Unless indicated otherwise, the top quark mass, $m_t = 177.9 \pm 4.4$ GeV, is used as an additional constraint in the fits. The (†) symbol indicates a fixed parameter.

Data	\hat{s}_Z^2	s_W^2	$\alpha_s(M_Z)$	M_H
All data	0.23120(15)	0.2228(4)	0.1213(18)	113^{+56}_{-40}
All indirect (no m_t)	0.23116(17)	0.2229(4)	0.1213(18)	79^{+95}_{-38}
Z pole (no m_t)	0.23118(17)	0.2231(6)	0.1197(28)	79^{+94}_{-38}
LEP 1 (no m_t)	0.23148(20)	0.2237(7)	0.1210(29)	140^{+192}_{-74}
SLD + M_Z	0.23067(28)	0.2217(6)	0.1213 (†)	43^{+38}_{-23}
$A_{FB}^{(b,c)} + M_Z$	0.23185(28)	0.2244(8)	0.1213 (†)	408^{+317}_{-179}
$M_W + M_Z$	0.23089(37)	0.2221(8)	0.1213 (†)	67^{+77}_{-45}
M_Z	0.23117(15)	0.2227(5)	0.1213 (†)	117 (†)
DIS (isoscalar)	0.2359(16)	0.2274(16)	0.1213 (†)	117 (†)
Q_W (APV)	0.2292(19)	0.2207(19)	0.1213 (†)	117 (†)
polarized Møller	0.2292(42)	0.2207(43)	0.1213 (†)	117 (†)
elastic $\nu_\mu(\bar{\nu}_\mu)e$	0.2305(77)	0.2220(77)	0.1213 (†)	117 (†)
SLAC eD	0.222(18)	0.213(19)	0.1213 (†)	117 (†)
elastic $\nu_\mu(\bar{\nu}_\mu)p$	0.211(33)	0.203(33)	0.1213 (†)	117 (†)

The data allow a simultaneous determination of M_H , m_t , $\sin^2\theta_W$, and the strong coupling $\alpha_s(M_Z)$. (\hat{m}_c , \hat{m}_b , and $\Delta\alpha_{\text{had}}^{(5)}$ are also allowed to float in the fits, subject to the theoretical constraints [5,18] described in Sec. 10.1–Sec. 10.2. These are correlated with α_s .) α_s is determined mainly from R_ℓ , Γ_Z , σ_{had} , and τ_τ and is only weakly correlated with the other variables (except for a 10% correlation with \hat{m}_c). The global fit to all data, including the CDF/DØ average, $m_t = 177.9 \pm 4.4$ GeV, yields

$$\begin{aligned}
 M_H &= 113^{+56}_{-40} \text{ GeV} , \\
 m_t &= 176.9 \pm 4.0 \text{ GeV} , \\
 \hat{s}_Z^2 &= 0.23120 \pm 0.00015 , \\
 \alpha_s(M_Z) &= 0.1213 \pm 0.0018 .
 \end{aligned} \tag{10.50}$$

† Alternatively, one can use $A_\ell = 0.1481 \pm 0.0027$, which is from LEP alone and in excellent agreement with the SM, and obtain $A_b = 0.898 \pm 0.022$ which is 1.7 σ low. This illustrates that some of the discrepancy is related to the one in A_{LR} .

In the on-shell scheme one has $s_W^2 = 0.22280 \pm 0.00035$, the larger error due to the stronger sensitivity to m_t , while the corresponding effective angle is related by Eq. (10.34), *i.e.*, $\bar{s}_\ell^2 = 0.23149 \pm 0.00015$. The m_t pole mass corresponds to $\hat{m}_t(\hat{m}_t) = 166.8 \pm 3.8$ GeV. In all fits, the errors include full statistical, systematic, and theoretical uncertainties. The \hat{s}_Z^2 (\bar{s}_ℓ^2) error reflects the error on $\bar{s}_Z^2 = 0.23150 \pm 0.00016$ from a fit to the Z -pole asymmetries.

The weak mixing angle can be determined from Z -pole observables, M_W , and from a variety of neutral-current processes spanning a very wide Q^2 range. The results (for the older low-energy neutral-current data see [42,43]) shown in Table 10.5 are in reasonable agreement with each other, indicating the quantitative success of the SM. The largest discrepancy is the value $\hat{s}_Z^2 = 0.2358 \pm 0.0016$ from DIS which is 2.9σ above the value 0.23120 ± 0.00015 from the global fit to all data. Similarly, $\bar{s}_\ell^2 = 0.23185 \pm 0.00028$ from the forward-backward asymmetries into bottom and charm quarks, and $\hat{s}_Z^2 = 0.23067 \pm 0.00028$ from the SLD asymmetries (both when combined with M_Z) are 2.3σ high and 1.9σ low, respectively.

The extracted Z -pole value of $\alpha_s(M_Z)$ is based on a formula with negligible theoretical uncertainty (± 0.0005 in $\alpha_s(M_Z)$) if one assumes the exact validity of the SM. One should keep in mind, however, that this value, $\alpha_s = 0.1197 \pm 0.0028$, is very sensitive to such types of new physics as non-universal vertex corrections. In contrast, the value derived from τ decays, $\alpha_s(M_Z) = 0.1221^{+0.0026}_{-0.0023}$ [5], is theory dominated but less sensitive to new physics. The former is mainly due to the larger value of $\alpha_s(m_\tau)$, but just as the hadronic Z -width the τ lifetime is fully inclusive and can be computed reliably within the operator product expansion. The two values are in excellent agreement with each other. They are also in perfect agreement with other recent values, such as 0.1202 ± 0.0049 from jet-event shapes at LEP [146], and 0.121 ± 0.003 [147] from the most recent lattice calculation of the Υ spectrum. For more details and other determinations, see our Section 9 on “Quantum Chromodynamics” in this *Review*.

The data indicate a preference for a small Higgs mass. There is a strong correlation between the quadratic m_t and logarithmic M_H terms in $\hat{\rho}$ in all of the indirect data except for the $Z \rightarrow b\bar{b}$ vertex. Therefore, observables (other than R_b) which favor m_t values higher than the Tevatron range favor lower values of M_H . This effect is enhanced by R_b , which has little direct M_H dependence but favors the lower end of the Tevatron m_t range. M_W has additional M_H dependence through $\Delta\hat{r}_W$ which is not coupled to m_t^2 effects. The strongest individual pulls toward smaller M_H are from M_W and $A_{FB}^{(0b)}$, while $A_{FB}^{(0b)}$ and the NuTeV results favor high values. The difference in χ^2 for the global fit is $\Delta\chi^2 = \chi^2(M_H = 1000 \text{ GeV}) - \chi^2_{\min} = 34.6$. Hence, the data favor a small value of M_H , as in supersymmetric extensions of the SM. The central value of the global fit result, $M_H = 113^{+56}_{-40}$ GeV, is slightly below the direct lower bound, $M_H \geq 114.4$ GeV (95% CL) [106].

The 90% central confidence range from all precision data is

$$53 \text{ GeV} \leq M_H \leq 213 \text{ GeV} .$$

Including the results of the direct searches as an extra contribution to the likelihood function drives the 95% upper limit to $M_H \leq 241$ GeV. As two further refinements, we account for (i) theoretical uncertainties from uncalculated higher order contributions by allowing the T parameter (see next subsection) subject to the constraint $T = 0 \pm 0.02$, (ii) the M_H dependence of the correlation matrix which gives slightly more weight to lower Higgs masses [148]. The resulting limits at 95 (90, 99)% CL are

$$M_H \leq 246 \text{ (217, 311) GeV} ,$$

respectively. The extraction of M_H from the precision data depends strongly on the value used for $\alpha(M_Z)$. Upper limits, however, are more robust due to two compensating effects: the older results indicated more QED running and were less precise, yielding M_H distributions which were broader with centers shifted to smaller values. The hadronic contribution to $\alpha(M_Z)$ is correlated with $g_\mu - 2$ (see Sec. 10.3). The measurement of the latter is higher than the SM

prediction, and its inclusion in the fit favors a larger $\alpha(M_Z)$ and a lower M_H (by 4 GeV).

One can also carry out a fit to the indirect data alone, *i.e.*, without including the constraint, $m_t = 177.9 \pm 4.4$ GeV, obtained by CDF and DØ. (The indirect prediction is for the $\overline{\text{MS}}$ mass, $\hat{m}_t(\hat{m}_t) = 162.5^{+9.2}_{-6.9}$ GeV, which is in the end converted to the pole mass). One obtains $m_t = 172.4^{+9.8}_{-7.3}$ GeV, with little change in the $\sin^2 \theta_W$ and α_s values, in remarkable agreement with the direct CDF/DØ average. The relations between M_H and m_t for various observables are shown in Fig. 10.1.

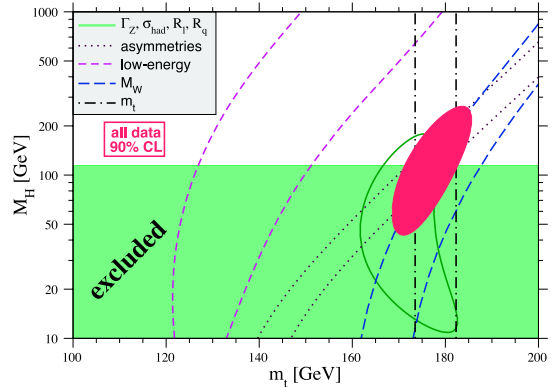


Figure 10.1: One-standard-deviation (39.35%) uncertainties in M_H as a function of m_t for various inputs, and the 90% CL region ($\Delta\chi^2 = 4.605$) allowed by all data. $\alpha_s(M_Z) = 0.120$ is assumed except for the fits including the Z -lineshape data. The 95% direct lower limit from LEP 2 is also shown. See full-color version on color pages at end of book.

Using $\alpha(M_Z)$ and \hat{s}_Z^2 as inputs, one can predict $\alpha_s(M_Z)$ assuming grand unification. One predicts [149] $\alpha_s(M_Z) = 0.130 \pm 0.001 \pm 0.01$ for the simplest theories based on the minimal supersymmetric extension of the SM, where the first (second) uncertainty is from the inputs (thresholds). This is slightly larger, but consistent with the experimental $\alpha_s(M_Z) = 0.1213 \pm 0.0018$ from the Z lineshape and the τ lifetime, as well as with other determinations. Non-supersymmetric unified theories predict the low value $\alpha_s(M_Z) = 0.073 \pm 0.001 \pm 0.001$. See also the note on “Low-Energy Supersymmetry” in the Particle Listings.

One can also determine the radiative correction parameters Δr : from the global fit one obtains $\Delta r = 0.0347 \pm 0.0011$ and $\Delta\hat{r}_W = 0.06981 \pm 0.00032$. M_W measurements [41,141] (when combined with M_Z) are equivalent to measurements of $\Delta r = 0.0326 \pm 0.0021$, which is 1.2σ below the result from all indirect data, $\Delta r = 0.0355 \pm 0.0013$. Fig. 10.2 shows the 1σ contours in the $M_W - m_t$ plane from the direct and indirect determinations, as well as the combined 90% CL region. The indirect determination uses M_Z from LEP 1 as input, which is defined assuming an s -dependent decay width. M_W then corresponds to the s -dependent width definition, as well, and can be directly compared with the results from the Tevatron and LEP 2 which have been obtained using the same definition. The difference to a constant width definition is formally only of $\mathcal{O}(\alpha^2)$, but is strongly enhanced since the decay channels add up coherently. It is about 34 MeV for M_Z and 27 MeV for M_W . The residual difference between working consistently with one or the other definition is about 3 MeV, *i.e.*, of typical size for non-enhanced $\mathcal{O}(\alpha^2)$ corrections [54,55].

Most of the parameters relevant to ν -hadron, ν - e , e -hadron, and e^+e^- processes are determined uniquely and precisely from the data in “model-independent” fits (*i.e.*, fits which allow for an arbitrary electroweak gauge theory). The values for the parameters defined in Eqs. (10.11)–(10.13) are given in Table 10.6 along with the predictions of the SM. The agreement is reasonable, except for the values of g_W^2 and $\epsilon_L(u, d)$, which reflect the discrepancy in the recent NuTeV results. (The ν -hadron results without the new NuTeV data can be found in

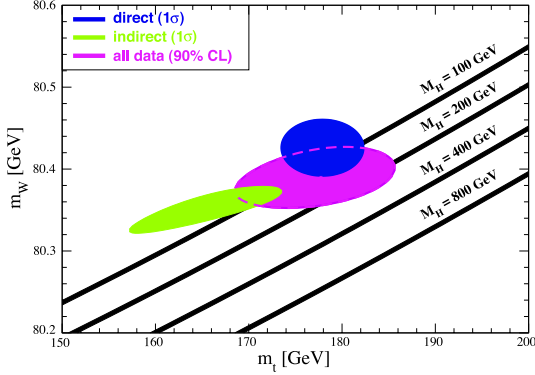


Figure 10.2: One-standard-deviation (39.35%) region in M_W as a function of m_t for the direct and indirect data, and the 90% CL region ($\Delta\chi^2 = 4.605$) allowed by all data. The SM prediction as a function of M_H is also indicated. The widths of the M_H bands reflect the theoretical uncertainty from $\alpha(M_Z)$. See full-color version on color pages at end of book.

Table 10.6: Values of the model-independent neutral-current parameters, compared with the SM predictions for the global best fit values $M_Z = 91.1874 \pm 0.0021$ GeV, $M_H = 113^{+56}_{-40}$ GeV, $m_t = 176.9 \pm 4.0$ GeV, $\alpha_s(M_Z) = 0.1213 \pm 0.0018$, and $\tilde{\alpha}(M_Z)^{-1} = 127.906 \pm 0.019$. There is a second $g_{V,A}^{e^c}$ solution, given approximately by $g_{V^c}^{e^+} \leftrightarrow g_{A^c}^{e^+}$, which is eliminated by e^+e^- data under the assumption that the neutral current is dominated by the exchange of a single Z . The ϵ_L , as well as the ϵ_R , are strongly correlated and non-Gaussian, so that for implementations we recommend the parametrization using g_i and $\theta_i = \tan^{-1}[\epsilon_i(u)/\epsilon_i(d)]$, $i = L$ or R . θ_R is only weakly correlated with the g_i , while the correlation coefficient between θ_R and θ_L is 0.27.

Quantity	Experimental Value	SM	Correlation		
$\epsilon_L(u)$	0.326 ± 0.013	0.3460(2)			
$\epsilon_L(d)$	-0.441 ± 0.010	$-0.4292(1)$	non-		
$\epsilon_R(u)$	$-0.175^{+0.013}_{-0.004}$	$-0.1551(1)$	Gaussian		
$\epsilon_R(d)$	$-0.022^{+0.072}_{-0.047}$	0.0776			
g_L^2	0.3005 ± 0.0012	0.3040(2)	-0.11	-0.21	-0.01
g_R^2	0.0311 ± 0.0010	0.0301		-0.02	-0.03
θ_L	2.51 ± 0.033	$2.4631(1)$			0.26
θ_R	$4.59^{+0.41}_{-0.28}$	5.1765			
$g_V^{e^c}$	-0.040 ± 0.015	$-0.0397(3)$			-0.05
$g_A^{e^c}$	-0.507 ± 0.014	$-0.5065(1)$			
$C_{1u} + C_{1d}$	0.148 ± 0.004	0.1529(1)	0.95	-0.55	-0.26
$C_{1u} - C_{1d}$	-0.597 ± 0.061	$-0.5299(4)$		-0.57	-0.27
$C_{2u} + C_{2d}$	0.62 ± 0.80	-0.0095			-0.38
$C_{2u} - C_{2d}$	-0.07 ± 0.12	$-0.0623(6)$			

the previous editions of this *Review*). The off Z -pole e^+e^- results are difficult to present in a model-independent way because Z -propagator effects are non-negligible at TRISTAN, PETRA, PEP, and LEP 2 energies. However, assuming e - μ - τ universality, the low-energy lepton asymmetries imply [98] $4(g_A^e)^2 = 0.99 \pm 0.05$, in good agreement with the SM prediction $\simeq 1$.

The results presented here are generally in reasonable agreement with the ones obtained by the LEP Electroweak Working Group [41]. We obtain higher best fit values for α_s and a higher and slightly more precise M_H . We trace most of the differences to be due to (i) the

inclusion of recent higher order radiative corrections, in particular, the leading $\mathcal{O}(\alpha_s^4)$ contribution to hadronic Z decays [150]; (ii) a different evaluation of $\alpha(M_Z)$ [18]; (iii) slightly different data sets (such as the recent $D\mathcal{O}$ m_t value); and (iv) scheme dependences. Taking into account these differences, the agreement is excellent.

10.6. Constraints on new physics

The Z -pole, W mass, and neutral-current data can be used to search for and set limits on deviations from the SM. In particular, the combination of these indirect data with the direct CDF and $D\mathcal{O}$ average for m_t allows one to set stringent limits on new physics. We will mainly discuss the effects of exotic particles (with heavy masses $M_{\text{new}} \gg M_Z$ in an expansion in M_Z/M_{new}) on the gauge boson self-energies. (Brief remarks are made on new physics which is not of this type.) Most of the effects on precision measurements can be described by three gauge self-energy parameters S , T , and U . We will define these, as well as related parameters, such as ρ_0 , ϵ_i , and $\tilde{\epsilon}_i$, to arise from new physics only. *I.e.*, they are equal to zero ($\rho_0 = 1$) exactly in the SM, and do not include any contributions from m_t or M_H , which are treated separately. Our treatment differs from most of the original papers.

Many extensions of the SM are described by the ρ_0 parameter,

$$\rho_0 \equiv M_W^2 / (M_Z^2 \tilde{c}_Z^2 \tilde{\rho}), \quad (10.51)$$

which describes new sources of $SU(2)$ breaking that cannot be accounted for by the SM Higgs doublet or m_t effects. In the presence of $\rho_0 \neq 1$, Eq. (10.51) generalizes Eq. (10.8b) while Eq. (10.8a) remains unchanged. Provided that the new physics which yields $\rho_0 \neq 1$ is a small perturbation which does not significantly affect the radiative corrections, ρ_0 can be regarded as a phenomenological parameter which multiplies G_F in Eqs. (10.11)–(10.13), (10.28), and Γ_Z in Eq. (10.47). There is enough data to determine ρ_0 , M_H , m_t , and α_s , simultaneously. From the global fit,

$$\rho_0 = 0.9998^{+0.0008}_{-0.0005}, \quad (10.52)$$

$$114.4 \text{ GeV} < M_H < 193 \text{ GeV}, \quad (10.53)$$

$$m_t = 178.0 \pm 4.1 \text{ GeV}, \quad (10.54)$$

$$\alpha_s(M_Z) = 0.1214 \pm 0.0018, \quad (10.55)$$

where the lower limit on M_H is the direct search bound. (If the direct limit is ignored one obtains $M_H = 66^{+86}_{-30}$ GeV and $\rho_0 = 0.9993^{+0.0010}_{-0.0008}$.) The error bar in Eq. (10.52) is highly asymmetric: at the 2σ level one has $\rho_0 = 0.9998^{+0.0025}_{-0.0010}$ and $M_H < 664$ GeV. Clearly, in the presence of ρ_0 upper limits on M_H become much weaker. The result in Eq. (10.52) is in remarkable agreement with the SM expectation, $\rho_0 = 1$. It can be used to constrain higher-dimensional Higgs representations to have vacuum expectation values of less than a few percent of those of the doublets. Indeed, the relation between M_W and M_Z is modified if there are Higgs multiplets with weak isospin $> 1/2$ with significant vacuum expectation values. In order to calculate to higher orders in such theories one must define a set of four fundamental renormalized parameters which one may conveniently choose to be α , G_F , M_Z , and M_W , since M_W and M_Z are directly measurable. Then \hat{s}_Z^2 and ρ_0 can be considered dependent parameters.

Eq. (10.52) can also be used to constrain other types of new physics. For example, non-degenerate multiplets of heavy fermions or scalars break the vector part of weak $SU(2)$ and lead to a decrease in the value of M_Z/M_W . A non-degenerate $SU(2)$ doublet ($\begin{smallmatrix} f_1 \\ f_2 \end{smallmatrix}$) yields a positive contribution to ρ_0 [151] of

$$\frac{CG_F}{8\sqrt{2}\pi^2} \Delta m^2, \quad (10.56)$$

where

$$\Delta m^2 \equiv m_1^2 + m_2^2 - \frac{4m_1^2 m_2^2}{m_1^2 - m_2^2} \ln \frac{m_1}{m_2} \geq (m_1 - m_2)^2, \quad (10.57)$$

and $C = 1$ (3) for color singlets (triplets). Thus, in the presence of such multiplets, one has

$$\frac{3G_F}{8\sqrt{2}\pi^2} \sum_i \frac{C_i}{3} \Delta m_i^2 = \rho_0 - 1, \quad (10.58)$$

where the sum includes fourth-family quark or lepton doublets, $(\begin{smallmatrix} t' \\ b' \end{smallmatrix})$ or $(\begin{smallmatrix} E^0 \\ E^- \end{smallmatrix})$, and scalar doublets such as $(\begin{smallmatrix} \hat{1} \\ \hat{2} \end{smallmatrix})$ in Supersymmetry (in the absence of $L - R$ mixing). This implies

$$\sum_i \frac{C_i}{3} \Delta m_i^2 \leq (85 \text{ GeV})^2 \quad (10.59)$$

at 95% CL. The corresponding constraints on non-degenerate squark and slepton doublets are even stronger, $\sum_i C_i \Delta m_i^2 / 3 \leq (59 \text{ GeV})^2$. This is due to the MSSM Higgs mass bound, $m_{h^0} < 150 \text{ GeV}$, and the very strong correlation between m_{h^0} and ρ_0 (79%).

Non-degenerate multiplets usually imply $\rho_0 > 1$. Similarly, heavy Z' bosons decrease the prediction for M_Z due to mixing and generally lead to $\rho_0 > 1$ [152]. On the other hand, additional Higgs doublets which participate in spontaneous symmetry breaking [153], heavy lepton doublets involving Majorana neutrinos [154], and the vacuum expectation values of Higgs triplets or higher-dimensional representations can contribute to ρ_0 with either sign. Allowing for the presence of heavy degenerate chiral multiplets (the S parameter, to be discussed below) affects the determination of ρ_0 from the data, at present leading to a smaller value (for fixed M_H).

A number of authors [155–160] have considered the general effects on neutral-current and Z and W boson observables of various types of heavy (*i.e.*, $M_{\text{new}} \gg M_Z$) physics which contribute to the W and Z self-energies but which do not have any direct coupling to the ordinary fermions. In addition to non-degenerate multiplets, which break the vector part of weak SU(2), these include heavy degenerate multiplets of chiral fermions which break the axial generators. The effects of one degenerate chiral doublet are small, but in Technicolor theories there may be many chiral doublets and therefore significant effects [155].

Such effects can be described by just three parameters, S , T , and U at the (electroweak) one-loop level. (Three additional parameters are needed if the new physics scale is comparable to M_Z [161].) T is proportional to the difference between the W and Z self-energies at $Q^2 = 0$ (*i.e.*, vector SU(2)-breaking), while S ($S + U$) is associated with the difference between the Z (W) self-energy at $Q^2 = M_Z^2$ ($Q^2 = 0$ (axial SU(2)-breaking)). Denoting the contributions of new physics to the various self-energies by Π_{ij}^{new} , we have

$$\hat{\alpha}(M_Z)T \equiv \frac{\Pi_{WW}^{\text{new}}(0)}{M_W^2} - \frac{\Pi_{ZZ}^{\text{new}}(0)}{M_Z^2}, \quad (10.60a)$$

$$\begin{aligned} \frac{\hat{\alpha}(M_Z)}{4\hat{s}_Z^2\hat{c}_Z^2}S &\equiv \frac{\Pi_{ZZ}^{\text{new}}(M_Z^2) - \Pi_{ZZ}^{\text{new}}(0)}{M_Z^2} \\ &- \frac{\hat{c}_Z^2 - \hat{s}_Z^2}{\hat{c}_Z\hat{s}_Z} \frac{\Pi_{Z\gamma}^{\text{new}}(M_Z^2)}{M_Z^2} - \frac{\Pi_{\gamma\gamma}^{\text{new}}(M_Z^2)}{M_Z^2}, \end{aligned} \quad (10.60b)$$

$$\begin{aligned} \frac{\hat{\alpha}(M_Z)}{4\hat{s}_Z^2}(S+U) &\equiv \frac{\Pi_{WW}^{\text{new}}(M_Z^2) - \Pi_{WW}^{\text{new}}(0)}{M_W^2} \\ &- \frac{\hat{c}_Z}{\hat{s}_Z} \frac{\Pi_{Z\gamma}^{\text{new}}(M_Z^2)}{M_Z^2} - \frac{\Pi_{\gamma\gamma}^{\text{new}}(M_Z^2)}{M_Z^2}. \end{aligned} \quad (10.60c)$$

S , T , and U are defined with a factor proportional to $\hat{\alpha}$ removed, so that they are expected to be of order unity in the presence of new physics. In the $\overline{\text{MS}}$ scheme as defined in Ref. 46, the last two terms in Eq. (10.60b) and Eq. (10.60c) can be omitted (as was done in some earlier editions of this *Review*). They are related to other parameters (S_i , h_i , \hat{e}_i) defined in [46,156,157] by

$$\begin{aligned} T &= h_V = \hat{e}_1/\alpha, \\ S &= h_{AZ} = S_Z = 4\hat{s}_Z^2\hat{e}_3/\alpha, \\ U &= h_{AW} - h_{AZ} = S_W - S_Z = -4\hat{s}_Z^2\hat{e}_2/\alpha. \end{aligned} \quad (10.61)$$

A heavy non-degenerate multiplet of fermions or scalars contributes positively to T as

$$\rho_0 - 1 = \frac{1}{1 - \alpha T} - 1 \simeq \alpha T, \quad (10.62)$$

where ρ_0 is given in Eq. (10.58). The effects of non-standard Higgs representations cannot be separated from heavy non-degenerate multiplets unless the new physics has other consequences, such as vertex corrections. Most of the original papers defined T to include the effects of loops only. However, we will redefine T to include all new sources of SU(2) breaking, including non-standard Higgs, so that T and ρ_0 are equivalent by Eq. (10.62).

A multiplet of heavy degenerate chiral fermions yields

$$S = C \sum_i (t_{3L}(i) - t_{3R}(i))^2 / 3\pi, \quad (10.63)$$

where $t_{3L,R}(i)$ is the third component of weak isospin of the left-(right-)handed component of fermion i and C is the number of colors. For example, a heavy degenerate ordinary or mirror family would contribute $2/3\pi$ to S . In Technicolor models with QCD-like dynamics, one expects [155] $S \sim 0.45$ for an iso-doublet of techni-fermions, assuming $N_{TC} = 4$ techni-colors, while $S \sim 1.62$ for a full techni-generation with $N_{TC} = 4$; T is harder to estimate because it is model dependent. In these examples one has $S \geq 0$. However, the QCD-like models are excluded on other grounds (flavor changing neutral-currents, and too-light quarks and pseudo-Goldstone bosons [162]). In particular, these estimates do not apply to models of walking Technicolor [162], for which S can be smaller or even negative [163]. Other situations in which $S < 0$, such as loops involving scalars or Majorana particles, are also possible [164]. The simplest origin of $S < 0$ would probably be an additional heavy Z' boson [152], which could mimic $S < 0$. Supersymmetric extensions of the SM generally give very small effects. See Refs. 115,165 and the Section on Supersymmetry in this *Review* for a complete set of references.

[115,165]. Most simple types of new physics yield $U = 0$, although there are counter-examples, such as the effects of anomalous triple gauge vertices [157].

The SM expressions for observables are replaced by

$$\begin{aligned} M_Z^2 &= M_{Z0}^2 \frac{1 - \alpha T}{1 - G_F M_{Z0}^2 S / 2\sqrt{2}\pi}, \\ M_W^2 &= M_{W0}^2 \frac{1}{1 - G_F M_{W0}^2 (S + U) / 2\sqrt{2}\pi}, \end{aligned} \quad (10.64)$$

where M_{Z0} and M_{W0} are the SM expressions (as functions of m_t and M_H) in the $\overline{\text{MS}}$ scheme. Furthermore,

$$\begin{aligned} \Gamma_Z &= \frac{1}{1 - \alpha T} M_Z^3 \beta_Z, \\ \Gamma_W &= M_W^3 \beta_W, \\ A_i &= \frac{1}{1 - \alpha T} A_{i0}, \end{aligned} \quad (10.65)$$

where β_Z and β_W are the SM expressions for the reduced widths Γ_{Z0}/M_{Z0}^3 and Γ_{W0}/M_{W0}^3 , M_Z and M_W are the physical masses, and A_i (A_{i0}) is a neutral-current amplitude (in the SM).

The data allow a simultaneous determination of \hat{s}_Z^2 (from the Z -pole asymmetries), S (from M_Z), U (from M_W), T (mainly from Γ_Z), α_s (from R_t , σ_{had} , and τ_τ), and m_t (from CDF and DØ), with little correlation among the SM parameters:

$$\begin{aligned} S &= -0.13 \pm 0.10 (-0.08), \\ T &= -0.17 \pm 0.12 (+0.09), \\ U &= 0.22 \pm 0.13 (+0.01), \end{aligned} \quad (10.66)$$

and $\hat{s}_Z^2 = 0.23119 \pm 0.00016$, $\alpha_s(M_Z) = 0.1222 \pm 0.0019$, $m_t = 177.2 \pm 4.2 \text{ GeV}$, where the uncertainties are from the inputs. The central values assume $M_H = 117 \text{ GeV}$, and in parentheses we show

the change for $M_H = 300$ GeV. As can be seen, the SM parameters (U) can be determined with no (little) M_H dependence. On the other hand, S , T , and M_H cannot be obtained simultaneously, because the Higgs boson loops themselves are resembled approximately by oblique effects. Eqs. (10.66) show that negative (positive) contributions to the S (T) parameter can weaken or entirely remove the strong constraints on M_H from the SM fits. Specific models in which a large M_H is compensated by new physics are reviewed in [166]. The parameters in Eqs. (10.66), which by definition are due to new physics only, all deviate by more than one standard deviation from the SM values of zero. However, these deviations are correlated. Fixing $U = 0$ (as is done in Fig. 10.3) will also move S and T to values compatible with zero within errors because the slightly high experimental value of M_W favors a positive value for $S + U$. Using Eq. (10.62) the value of ρ_0 corresponding to T is $0.9987 \pm 0.0009 (+0.0007)$. The values of the \hat{c} parameters defined in Eq. (10.61) are

$$\begin{aligned}\hat{c}_3 &= -0.0011 \pm 0.0008 (-0.0006), \\ \hat{c}_1 &= -0.0013 \pm 0.0009 (+0.0007), \\ \hat{c}_2 &= -0.0019 \pm 0.0011 (-0.0001).\end{aligned}\quad (10.67)$$

Unlike the original definition, we defined the quantities in Eqs. (10.67) to vanish identically in the absence of new physics and to correspond directly to the parameters S , T , and U in Eqs. (10.66). There is a strong correlation (80%) between the S and T parameters. The allowed region in $S - T$ is shown in Fig. 10.3. From Eqs. (10.66) one obtains $S \leq 0.03 (-0.05)$ and $T \leq 0.02 (0.11)$ at 95% CL for $M_H = 117$ GeV (300 GeV). If one fixes $M_H = 600$ GeV and requires the constraint $S \geq 0$ (as is appropriate in QCD-like Technicolor models) then $S \leq 0.09$ (Bayesian) or $S \leq 0.06$ (frequentist). This rules out simple Technicolor models with many techni-doublets and QCD-like dynamics.

An extra generation of ordinary fermions is excluded at the 99.95% CL on the basis of the S parameter alone, corresponding to $N_F = 2.92 \pm 0.27$ for the number of families. This result assumes that there are no new contributions to T or U and therefore that any new families are degenerate. In principle this restriction can be relaxed by allowing T to vary as well, since $T > 0$ is expected from a non-degenerate extra family. However, the data currently favor $T < 0$, thus strengthening the exclusion limits. A more detailed analysis is required if the extra neutrino (or the extra down-type quark) is close to its direct mass limit [167]. This can drive S to small or even negative values but at the expense of too-large contributions to T . These results are in agreement with a fit to the number of light neutrinos, $N_\nu = 2.986 \pm 0.007$ (which favors a larger value for $\alpha_s(M_Z) = 0.1228 \pm 0.0021$ mainly from R_ℓ and τ_τ). However, the S parameter fits are valid even for a very heavy fourth family neutrino.

There is no simple parametrization that is powerful enough to describe the effects of every type of new physics on every possible observable. The S , T , and U formalism describes many types of heavy physics which affect only the gauge self-energies, and it can be applied to all precision observables. However, new physics which couples directly to ordinary fermions, such as heavy Z' bosons [152] or mixing with exotic fermions [168] cannot be fully parametrized in the S , T , and U framework. It is convenient to treat these types of new physics by parametrizations that are specialized to that particular class of theories (e.g., extra Z' bosons), or to consider specific models (which might contain, e.g., Z' bosons and exotic fermions with correlated parameters). Constraints on various types of new physics are reviewed in Refs. [43,91,169,170]. Fits to models with (extended) Technicolor and Supersymmetry are described, respectively, in Refs. [171], and [115,172]. The effects of compactified extra spatial dimensions at the TeV scale have been reviewed in [173], and constraints on Little Higgs models in [174].

An alternate formalism [175] defines parameters, ϵ_1 , ϵ_2 , ϵ_3 , ϵ_b in terms of the specific observables M_W/M_Z , $\Gamma_{\ell\ell}$, $A_{FB}^{(0,\ell)}$, and R_b . The definitions coincide with those for \hat{c}_i in Eqs. (10.60) and (10.61) for physics which affects gauge self-energies only, but the ϵ 's now parametrize arbitrary types of new physics. However, the ϵ 's are not related to other observables unless additional model-dependent assumptions are made. Another approach [176–178] parametrizes new

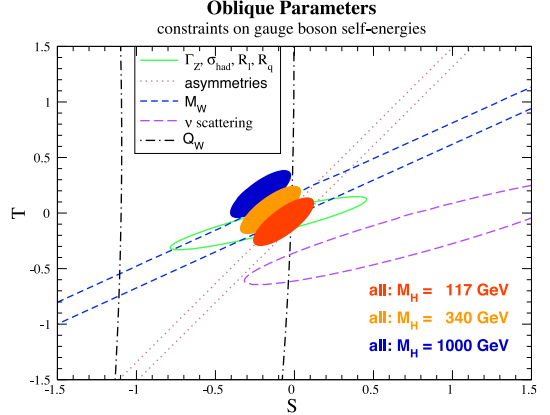


Figure 10.3: 1σ constraints (39.35%) on S and T from various inputs. S and T represent the contributions of new physics only. (Uncertainties from m_t are included in the errors.) The contours assume $M_H = 117$ GeV except for the central and upper 90% CL contours allowed by all data, which are for $M_H = 340$ GeV and 1000 GeV, respectively. Data sets not involving M_W are insensitive to U . Due to higher order effects, however, $U = 0$ has to be assumed in all fits. α_s is constrained using the τ lifetime as additional input in all fits. See full-color version on color pages at end of book.

physics in terms of gauge-invariant sets of operators. It is especially powerful in studying the effects of new physics on non-Abelian gauge vertices. The most general approach introduces deviation vectors [169]. Each type of new physics defines a deviation vector, the components of which are the deviations of each observable from its SM prediction, normalized to the experimental uncertainty. The length (direction) of the vector represents the strength (type) of new physics.

Table 10.7: 95% CL lower mass limits (in GeV) from low energy and Z pole data on various extra Z' gauge bosons, appearing in models of unification and string theory. ρ_0 free indicates a completely arbitrary Higgs sector, while $\rho_0 = 1$ restricts to Higgs doublets and singlets with still unspecified charges. The CDF bounds from searches for $\bar{p}p \rightarrow e^+e^-$, $\mu^+\mu^-$ [183] and the LEP 2 $e^+e^- \rightarrow f\bar{f}$ [41,184] bounds are listed in the last two columns, respectively. (The CDF bounds would be weakened if there are open supersymmetric or exotic decay channels.)

Z'	ρ_0 free	$\rho_0 = 1$	CDF (direct)	LEP 2
Z_χ	551	545	595	673
Z_ψ	151	146	590	481
Z_η	379	365	620	434
Z_{LR}	570	564	630	804
Z_{SM}	822	809	690	1787
Z_{string}	582	578	—	—

One of the best motivated kinds of physics beyond the SM besides Supersymmetry are extra Z' bosons. They do not spoil the observed approximate gauge coupling unification, and appear copiously in many Grand Unified Theories (GUTs), most Superstring models, as well as in dynamical symmetry breaking [171,179] and Little Higgs models [174]. For example, the $SO(10)$ GUT contains an extra $U(1)$ as can be seen from its maximal subgroup, $SU(5) \times U(1)_\chi$. Similarly, the E_6 GUT contains the subgroup $SO(10) \times U(1)_\psi$. The Z_ψ possesses only axial-vector couplings to the ordinary fermions, and its mass is generally less constrained. The Z_η boson is the linear combination $\sqrt{3/8}Z_\chi - \sqrt{5/8}Z_\psi$. The Z_{LR} boson occurs in left-right models with gauge group $SU(3)_C \times SU(2)_L \times SU(2)_R \times U(1)_{B-L} \subset SO(10)$.

The sequential Z_{SM} boson is defined to have the same couplings to fermions as the SM Z boson. Such a boson is not expected in the context of gauge theories unless it has different couplings to exotic fermions than the ordinary Z . However, it serves as a useful reference case when comparing constraints from various sources. It could also play the role of an excited state of the ordinary Z in models with extra dimensions at the weak scale. Finally, we consider a Superstring motivated Z_{string} boson appearing in a specific model [180]. The potential Z' boson is in general a superposition of the SM Z and the new boson associated with the extra U(1). The mixing angle θ satisfies,

$$\tan^2 \theta = \frac{M_{Z_0}^2 - M_Z^2}{M_{Z_1}^2 - M_{Z_0}^2},$$

where M_{Z_0} is the SM value for M_Z in the absence of mixing. Note, that $M_Z < M_{Z_1}$, and that the SM Z couplings are changed by the mixing. If the Higgs U(1)' quantum numbers are known, there will be an extra constraint,

$$\theta = C \frac{g_2}{g_1} \frac{M_Z^2}{M_{Z_1}^2}, \quad (10.68)$$

where $g_{1,2}$ are the U(1) and U(1)' gauge couplings with $g_2 = \sqrt{\frac{5}{3}} \sin \theta_W \sqrt{\lambda} g_1$. $\lambda \sim 1$ (which we assume) if the GUT group breaks directly to $SU(3) \times SU(2) \times U(1) \times U(1)'$. C is a function of vacuum expectation values. For minimal Higgs sectors it can be found in reference [152]. Table 10.7 shows the 95% CL lower mass limits obtained from a somewhat earlier data set [181] for ρ_0 free and $\rho_0 = 1$, respectively. In cases of specific minimal Higgs sectors where C is known, the Z' mass limits are generally pushed into the TeV region. The limits on $|\theta|$ are typically $< \text{few} \times 10^{-3}$. For more details see [181,182] and the Section on "The Z' Searches" in this Review. Also listed in Table 10.7 are the direct lower limits on Z' production from CDF [183] and LEP 2 bounds [41,184]. The final LEP 1 value for σ_{had} , some previous values for $Q_W(Cs)$, NuTeV, and $A_{FB}^{0,b}$ (for family-nonuniversal couplings [185]) modify the results and might even suggest the possible existence of a Z' [144,186].

References:

1. S. Weinberg, Phys. Rev. Lett. **19**, 1264 (1967);
A. Salam, p. 367 of *Elementary Particle Theory*, ed. N. Svartholm (Almqvist and Wiksells, Stockholm, 1969);
S.L. Glashow, J. Iliopoulos, and L. Maiani, Phys. Rev. **D2**, 1285 (1970).
2. H. Abele *et al.*, hep-ph/0312150.
3. For reviews, see G. Barbiellini and C. Santoni, Riv. Nuovo Cimento **9(2)**, 1 (1986);
E.D. Commins and P.H. Bucksbaum, *Weak Interactions of Leptons and Quarks*, (Cambridge Univ. Press, Cambridge, 1983);
W. Fetscher and H.J. Gerber, p. 657 of Ref. 4;
J. Deutsch and P. Quin, p. 706 of Ref. 4;
J.M. Conrad, M.H. Shaevitz, and T. Bolton, Rev. Mod. Phys. **70**, 1341 (1998).
4. *Precision Tests of the Standard Electroweak Model*, ed. P. Langacker (World Scientific, Singapore, 1995).
5. J. Erler and M. Luo, Phys. Lett. **B558**, 125 (2003).
6. CDF: T. Affolder *et al.*, Phys. Rev. **D63**, 032003 (2001).
7. E. Thomson for the CDF Collaboration, presented at the *31st SLAC Summer Institute* (SSI 2003, Menlo Park).
8. DØ: B. Abbott *et al.*, Phys. Rev. **D58**, 052001 (1998).
9. F. Caneili for the DØ Collaboration, presented at the *8th Conference on the Intersections of Particle and Nuclear Physics* (CIPANP 2003, New York).
10. L. Demortier *et al.*, preprint FERMILAB-TM-2084.
11. K. Melnikov and T. v. Ritbergen, Phys. Lett. **B482**, 99 (2000).
12. S.J. Brodsky, G.P. Lepage, and P.B. Mackenzie, Phys. Rev. **D28**, 228 (1983).
13. N. Gray *et al.*, Z. Phys. **C48**, 673 (1990).
14. For reviews, see the article on "The Higgs boson" in this Review; J. Gunion, H.E. Haber, G.L. Kane, and S. Dawson, *The Higgs Hunter's Guide*, (Addison-Wesley, Redwood City, 1990);
M. Sher, Phys. Reports **179**, 273 (1989);
M. Carena and H.E. Haber, Prog. Part. Nucl. Phys. **50**, 63 (2003).
15. P.J. Mohr and B.N. Taylor, Rev. Mod. Phys. **72**, 351 (2000).
16. TOPAZ: I. Levine *et al.*, Phys. Rev. Lett. **78**, 424 (1997);
VENUS: S. Okada *et al.*, Phys. Rev. Lett. **81**, 2428 (1998);
OPAL: G. Abbiendi *et al.*, Eur. Phys. J. **C13**, 553 (2000);
L3: M. Acciarri *et al.*, Phys. Lett. **B476**, 40 (2000).
17. S. Fanchiotti, B. Kniehl, and A. Sirlin, Phys. Rev. **D48**, 307 (1993) and references therein.
18. J. Erler, Phys. Rev. **D59**, 054008 (1999).
19. CMD 2: R.R. Akhmetshin *et al.*, hep-ex/0308008.
20. M. Davier, S. Eidelman, A. Höcker, and Z. Zhang, hep-ph/0308213.
21. A.D. Martin and D. Zeppenfeld, Phys. Lett. **B345**, 558 (1995).
22. S. Eidelman and F. Jegerlehner, Z. Phys. **C67**, 585 (1995).
23. B.V. Geshkenbein and V.L. Morgunov, Phys. Lett. **B340**, 185 (1995) and Phys. Lett. **B352**, 456 (1995).
24. H. Burkhardt and B. Pietrzyk, Phys. Lett. **B356**, 398 (1995).
25. M.L. Swartz, Phys. Rev. **D53**, 5268 (1996).
26. R. Alemany, M. Davier, and A. Höcker, Eur. Phys. J. **C2**, 123 (1998).
27. N.V. Krasnikov and R. Rodenberg, Nuovo Cimento **111A**, 217 (1998).
28. M. Davier and A. Höcker, Phys. Lett. **B419**, 419 (1998).
29. J.H. Kühn and M. Steinhauser, Phys. Lett. **B437**, 425 (1998).
30. M. Davier and A. Höcker, Phys. Lett. **B435**, 427 (1998).
31. S. Groote, J.G. Körner, K. Schilcher, N.F. Nasrallah, Phys. Lett. **B440**, 375 (1998).
32. A.D. Martin, J. Outhwaite, and M.G. Ryskin, Phys. Lett. **B492**, 69 (2000).
33. H. Burkhardt and B. Pietrzyk, Phys. Lett. **B513**, 46 (2001).
34. J.F. de Troconiz and F.J. Yndurain, Phys. Rev. **D65**, 093002 (2002).
35. F. Jegerlehner, hep-ph/0308117.
36. BES: J.Z. Bai *et al.*, Phys. Rev. Lett. **88**, 101802 (2002);
G.S. Huang, hep-ex/0105074.
37. S. Binner, J.H. Kühn, and K. Melnikov, Phys. Lett. **B459**, 279 (1999).
38. KLOE: A. Aloisio *et al.*, hep-ex/0307051.
39. W.J. Marciano and A. Sirlin, Phys. Rev. Lett. **61**, 1815 (1988).
40. T. van Ritbergen and R.G. Stuart, Phys. Rev. Lett. **82**, 488 (1999).
41. ALEPH, DELPHI, L3, OPAL, LEP Electroweak Working Group, and SLD Heavy Flavor Group, hep-ex/0212036 and <http://www.cern.ch/LEPEWWG/>.
42. Earlier analyses include U. Amaldi *et al.*, Phys. Rev. **D36**, 1385 (1987);
G. Costa *et al.*, Nucl. Phys. **B297**, 244 (1988);
Deep inelastic scattering is considered by G.L. Fogli and D. Haidt, Z. Phys. **C40**, 379 (1988);
P. Langacker and M. Luo, Phys. Rev. **D44**, 817 (1991);
For more recent analyses, see Ref. 43.
43. P. Langacker, p. 883 of Ref. 4;
J. Erler and P. Langacker, Phys. Rev. **D52**, 441 (1995);
Neutrino scattering is reviewed by J.M. Conrad *et al.* in Ref. 3;
Nonstandard neutrino interactions are surveyed in Z. Berezhiani and A. Rossi, Phys. Lett. **B535**, 207 (2002);
S. Davidson, C. Pena-Garay, N. Rius, and A. Santamaria, JHEP **0303**, 011 (2003).

44. A. Sirlin, Phys. Rev. **D22**, 971 (1980) and *ibid.* **29**, 89 (1984);
D.C. Kennedy *et al.*, Nucl. Phys. **B321**, 83 (1989);
D.C. Kennedy and B.W. Lynn, Nucl. Phys. **B322**, 1 (1989);
D.Yu. Bardin *et al.*, Z. Phys. **C44**, 493 (1989);
W. Hollik, Fortsch. Phys. **38**, 165 (1990);
For reviews, see the articles by W. Hollik, pp. 37 and 117, and
W. Marciano, p. 170 in Ref. 4. Extensive references to other
papers are given in Ref. 42.
45. W. Hollik in Ref. 44 and references therein;
V.A. Novikov, L.B. Okun, and M.I. Vysotsky, Nucl. Phys. **B397**,
35 (1993).
46. W.J. Marciano and J.L. Rosner, Phys. Rev. Lett. **65**, 2963 (1990).
47. G. Degrossi, S. Fanchiotti, and A. Sirlin, Nucl. Phys. **B351**, 49
(1991).
48. G. Degrossi and A. Sirlin, Nucl. Phys. **B352**, 342 (1991).
49. P. Gambino and A. Sirlin, Phys. Rev. **D49**, 1160 (1994).
50. ZFITTER: D. Bardin *et al.*, Comput. Phys. Commun. **133**, 229
(2001) and references therein.
51. R. Barbieri *et al.*, Phys. Lett. **B288**, 95 (1992);
R. Barbieri *et al.*, Nucl. Phys. **B409**, 105 (1993).
52. J. Fleischer, O.V. Tarasov, and F. Jegerlehner, Phys. Lett. **B319**,
249 (1993).
53. G. Degrossi, P. Gambino, and A. Vicini, Phys. Lett. **B383**, 219
(1996);
G. Degrossi, P. Gambino, and A. Sirlin, Phys. Lett. **B394**, 188
(1997).
54. A. Freitas, W. Hollik, W. Walter, and G. Weiglein, Phys. Lett.
B495, 338 (2000) and Nucl. Phys. **B632**, 189 (2002).
55. M. Awramik and M. Czakon, Phys. Rev. Lett. **89**, 241801 (2002);
A. Onishchenko and O. Veretin, Phys. Lett. **B551**, 111 (2003).
56. A. Djouadi and C. Verzegnassi, Phys. Lett. **B195**, 265 (1987);
A. Djouadi, Nuovo Cimento **100A**, 357 (1988);
B.A. Kniehl, Nucl. Phys. **B347**, 86 (1990);
A. Djouadi and P. Gambino, Phys. Rev. **D49**, 3499 (1994), **D49**,
4705 (1994), and **D53**, 4111(E) (1996).
57. K.G. Chetyrkin, J.H. Kühn, and M. Steinhauser, Phys. Lett.
B351, 331 (1995);
L. Avdeev *et al.*, Phys. Lett. **B336**, 560 (1994) and **B349**, 597(E)
(1995).
58. J. Fleischer *et al.*, Phys. Lett. **B293**, 437 (1992);
K.G. Chetyrkin, A. Kwiatkowski, and M. Steinhauser, Mod.
Phys. Lett. **A8**, 2785 (1993).
59. A. Czarnecki and J.H. Kühn, Phys. Rev. Lett. **77**, 3955 (1996).
60. R. Harlander, T. Seidensticker, and M. Steinhauser, Phys. Lett.
B426, 125 (1998);
J. Fleischer *et al.*, Phys. Lett. **B459**, 625 (1999).
61. J. Erler, hep-ph/0005084.
62. For reviews, see F. Perrier, p. 385 of Ref. 4;
J.M. Conrad *et al.* in Ref. 3.
63. CDHS: H. Abramowicz *et al.*, Phys. Rev. Lett. **57**, 298 (1986);
CDHS: A. Blondel *et al.*, Z. Phys. **C45**, 361 (1990).
64. CHARM: J.V. Allaby *et al.*, Phys. Lett. **B177**, 446 (1986);
CHARM: J.V. Allaby *et al.*, Z. Phys. **C36**, 611 (1987).
65. CCFR: C.G. Arroyo *et al.*, Phys. Rev. Lett. **72**, 3452 (1994);
CCFR: K.S. McFarland *et al.*, Eur. Phys. J. **C1**, 509 (1998).
66. R.M. Barnett, Phys. Rev. **D14**, 70 (1976);
H. Georgi and H.D. Politzer, Phys. Rev. **D14**, 1829 (1976).
67. LAB-E: S.A. Rabinowitz *et al.*, Phys. Rev. Lett. **70**, 134 (1993).
68. E.A. Paschos and L. Wolfenstein, Phys. Rev. **D7**, 91 (1973).
69. NuTeV: G. P. Zeller *et al.*, Phys. Rev. Lett. **88**, 091802 (2002).
70. S. Davidson *et al.*, JHEP **0202**, 037 (2002).
71. NuTeV: M. Goncharov *et al.*, Phys. Rev. **D64**, 112006 (2001).
72. NuTeV: G.P. Zeller *et al.*, Phys. Rev. **D65**, 111103 (2002);
NuTeV: R. H. Bernstein *et al.*, J. Phys. G **29**, 1919 (2003).
73. K.P.O. Diener, S. Dittmaier, and W. Hollik, hep-ph/0310364.
74. CHARM: J. Dorenbosch *et al.*, Z. Phys. **C41**, 567 (1989).
75. CALO: L.A. Ahrens *et al.*, Phys. Rev. **D41**, 3297 (1990).
76. CHARM II: P. Vilain *et al.*, Phys. Lett. **B335**, 246 (1994).
77. See also J. Panman, p. 504 of Ref. 4.
78. ILM: R.C. Allen *et al.*, Phys. Rev. **D47**, 11 (1993);
LSND: L.B. Auerbach *et al.*, Phys. Rev. **D63**, 112001 (2001).
79. SSF: C.Y. Prescott *et al.*, Phys. Lett. **B84**, 524 (1979);
For a review, see P. Souder, p. 599 of Ref. 4.
80. For reviews and references to earlier work, see M.A. Bouchiat and
L. Pottier, Science **234**, 1203 (1986);
B.P. Masterson and C.E. Wieman, p. 545 of Ref. 4.
81. Cesium (Boulder): C.S. Wood *et al.*, Science **275**, 1759 (1997).
82. Thallium (Oxford): N.H. Edwards *et al.*, Phys. Rev. Lett. **74**,
2654 (1995);
Thallium (Seattle): P.A. Vetter *et al.*, Phys. Rev. Lett. **74**, 2658
(1995).
83. Lead (Seattle): D.M. Meekhof *et al.*, Phys. Rev. Lett. **71**, 3442
(1993).
84. Bismuth (Oxford): M.J.D. MacPherson *et al.*, Phys. Rev. Lett.
67, 2784 (1991).
85. V.A. Dzuba, V.V. Flambaum, and O.P. Sushkov, Phys. Lett.
141A, 147 (1989);
S.A. Blundell, J. Sapirstein, and W.R. Johnson, Phys. Rev. Lett.
65, 1411 (1990) and Phys. Rev. **D45**, 1602 (1992);
For a review, see S.A. Blundell, W.R. Johnson, and J. Sapirstein,
p. 577 of Ref. 4.
86. S.C. Bennett and C.E. Wieman, Phys. Rev. Lett. **82**, 2484 (1999).
87. V.A. Dzuba, V.V. Flambaum, and O.P. Sushkov, Phys. Rev.
A56, R4357 (1997).
88. M.A. Bouchiat and J. Guéna, J. Phys. (France) **49**, 2037 (1988).
89. A. Derevianko, Phys. Rev. Lett. **85**, 1618 (2000);
V.A. Dzuba, C. Harabati, and W.R. Johnson, Phys. Rev. **A63**,
044103 (2001);
M.G. Kozlov, S.G. Porsev, and I.I. Tupitsyn, Phys. Rev. Lett. **86**,
3260 (2001).
90. A.I. Milstein and O.P. Sushkov, Phys. Rev. **A66**, 022108 (2002);
W.R. Johnson, I. Bednyakov, and G. Soff, Phys. Rev. Lett. **87**,
233001 (2001);
V.A. Dzuba, V.V. Flambaum, and J.S. Ginges, Phys. Rev. **D66**,
076013 (2002);
M.Y. Kuchiev and V.V. Flambaum, Phys. Rev. Lett. **89**, 283002
(2002);
A.I. Milstein, O.P. Sushkov, and I.S. Terekhov, Phys. Rev. Lett.
89, 283003 (2002);
For a recent review, see J.S.M. Ginges and V.V. Flambaum,
physics/0309054.
91. J. Erler, A. Kurylov, and M.J. Ramsey-Musolf, Phys. Rev. **D68**,
016006 (2003).
92. V.A. Dzuba *et al.*, J. Phys. **B20**, 3297 (1987).
93. Ya.B. Zel'dovich, Sov. Phys. JETP **6**, 1184 (1958);
For recent discussions, see V.V. Flambaum and D.W. Murray,
Phys. Rev. **C56**, 1641 (1997);
W.C. Haxton and C.E. Wieman, Ann. Rev. Nucl. Part. Sci. **51**,
261 (2001).
94. J.L. Rosner, Phys. Rev. **D53**, 2724 (1996).
95. S.J. Pollock, E.N. Fortson, and L. Willets, Phys. Rev. **C46**, 2587
(1992);
B.Q. Chen and P. Vogel, Phys. Rev. **C48**, 1392 (1993).
96. B.W. Lynn and R.G. Stuart, Nucl. Phys. **B253**, 216 (1985).

97. *Physics at LEP*, ed. J. Ellis and R. Peccei, CERN 86-02, Vol. 1.
98. C. Kiesling, *Tests of the Standard Theory of Electroweak Interactions*, (Springer-Verlag, New York, 1988);
R. Marshall, *Z. Phys.* **C43**, 607 (1989);
Y. Mori *et al.*, *Phys. Lett.* **B218**, 499 (1989);
D. Haidt, p. 203 of Ref. 4.
99. For reviews, see D. Schaale, p. 215, and A. Blondel, p. 277 of Ref. 4.
100. M. Elsing, presented at the *International Europhysics Conference on High Energy Physics* (EPS 2003, Aachen).
101. SLD: K. Abe *et al.*, *Phys. Rev. Lett.* **84**, 5945 (2000).
102. SLD: K. Abe *et al.*, *Phys. Rev. Lett.* **85**, 5059 (2000).
103. SLD: K. Abe *et al.*, *Phys. Rev. Lett.* **86**, 1162 (2001).
104. DELPHI: P. Abreu *et al.*, *Z. Phys.* **C67**, 1 (1995);
OPAL: K. Ackerstaff *et al.*, *Z. Phys.* **C76**, 387 (1997).
105. SLD: K. Abe *et al.*, *Phys. Rev. Lett.* **78**, 17 (1997).
106. ALEPH, DELPHI, L3, and OPAL Collaborations, and the LEP Working Group for Higgs Boson Searches: D. Abbaneo *et al.*, *Phys. Lett.* **B565**, 61 (2003).
107. A. Leike, T. Riemann, and J. Rose, *Phys. Lett.* **B273**, 513 (1991);
T. Riemann, *Phys. Lett.* **B293**, 451 (1992).
108. E158: P.L. Anthony *et al.*, hep-ex/0312035;
the implications are discussed in A. Czarnecki and W.J. Marciano, *Int. J. Mod. Phys. A* **15**, 2365 (2000).
109. G. S. Mitchell, hep-ex/0308049;
the implications are discussed in Ref. 91.
110. Belle: K. Abe *et al.*, *Phys. Lett.* **B511**, 151 (2001).
111. CLEO: S. Chen *et al.*, *Phys. Rev. Lett.* **87**, 251807 (2001).
112. BaBar: B. Aubert *et al.*, hep-ex/0207076.
113. A. Ali and C. Greub, *Phys. Lett.* **B259**, 182 (1991);
A.L. Kagan and M. Neubert, *Eur. Phys. J.* **C7**, 5 (1999).
114. A. Czarnecki and W.J. Marciano, *Phys. Rev. Lett.* **81**, 277 (1998).
115. J. Erler and D.M. Pierce, *Nucl. Phys.* **B526**, 53 (1998).
116. Y. Nir, *Phys. Lett.* **B221**, 184 (1989);
K. Adel and Y.P. Yao, *Phys. Rev.* **D49**, 4945 (1994);
C. Greub, T. Hurth, and D. Wyler, *Phys. Rev.* **D54**, 3350 (1996);
K.G. Chetyrkin, M. Misiak, and M. Münz, *Phys. Lett.* **B400**, 206 (1997);
C. Greub and T. Hurth, *Phys. Rev.* **D56**, 2934 (1997);
M. Ciuchini *et al.*, *Nucl. Phys.* **B527**, 21 (1998) and **B534**, 3 (1998);
F.M. Borzumati and C. Greub, *Phys. Rev.* **D58**, 074004 (1998) and **D59**, 057501 (1999);
A. Strumia, *Nucl. Phys.* **B532**, 28 (1998).
117. E821: H.N. Brown *et al.*, *Phys. Rev. Lett.* **86**, 2227 (2001);
E821: G.W. Bennett, *et al.*, *Phys. Rev. Lett.* **89**, 101804 (2002).
118. For reviews, see V.W. Hughes and T. Kinoshita, *Rev. Mod. Phys.* **71**, S133 (1999);
A. Czarnecki and W.J. Marciano, *Phys. Rev.* **D64**, 013014 (2001);
T. Kinoshita, *J. Phys.* **G29**, 9 (2003).
119. S.J. Brodsky and J.D. Sullivan, *Phys. Rev.* **D156**, 1644 (1967);
T. Burnett and M.J. Levine, *Phys. Lett.* **B24**, 467 (1967);
R. Jackiw and S. Weinberg, *Phys. Rev.* **D5**, 2473 (1972);
I. Bars and M. Yoshimura, *Phys. Rev.* **D6**, 374 (1972);
K. Fujikawa, B.W. Lee, and A.I. Sanda, *Phys. Rev.* **D6**, 2923 (1972);
G. Altarelli, N. Cabibbo, and L. Maiani, *Phys. Lett.* **B40**, 415 (1972);
W.A. Bardeen, R. Gastmans, and B.E. Laurup, *Nucl. Phys.* **B46**, 315 (1972).
120. T.V. Kukhto, E.A. Kuraev, A. Schiller, and Z.K. Silagadze, *Nucl. Phys.* **B371**, 567 (1992);
S. Peris, M. Perrottet, and E. de Rafael, *Phys. Lett.* **B355**, 523 (1995);
A. Czarnecki, B. Krause, and W.J. Marciano, *Phys. Rev.* **D52**, 2619 (1995) and *Phys. Rev. Lett.* **76**, 3267 (1996).
121. G. Degrassi and G. Giudice, *Phys. Rev.* **D58**, 053007 (1998).
122. F. Matorras (DELPHI), contributed paper to the *International Europhysics Conference on High Energy Physics* (EPS 2003, Aachen).
123. V. Cirigliano, G. Ecker and H. Neufeld, *JHEP* **0208**, 002 (2002).
124. J. Erler, hep-ph/0211345.
125. M. Knecht and A. Nyffeler, *Phys. Rev.* **D65**, 073034 (2002).
126. M. Hayakawa and T. Kinoshita, hep-ph/0112102;
J. Bijnens, E. Pallante and J. Prades, *Nucl. Phys.* **B626**, 410 (2002).
127. B. Krause, *Phys. Lett.* **B390**, 392 (1997).
128. J. Erler and M. Luo, *Phys. Rev. Lett.* **87**, 071804 (2001).
129. J.L. Lopez, D.V. Nanopoulos, and X. Wang, *Phys. Rev.* **D49**, 366 (1994);
for recent reviews, see Ref. 118.
130. E821: <http://www.g-2.bnl.gov/index.shtml/>.
131. S. Ghozzi and F. Jegerlehner, hep-ph/0310181.
132. K. Hagiwara, A.D. Martin, D. Nomura, and T. Teubner, hep-ph/0312250.
133. A comprehensive report and further references can be found in K.G. Chetyrkin, J.H. Kühn, and A. Kwiatkowski, *Phys. Reports* **277**, 189 (1996).
134. J. Schwinger, *Particles, Sources and Fields*, Vol. II, (Addison-Wesley, New York, 1973);
K.G. Chetyrkin, A.L. Kataev, and F.V. Tkachev, *Phys. Lett.* **B85**, 277 (1979);
M. Dine and J. Sapirstein, *Phys. Rev. Lett.* **43**, 668 (1979);
W. Celmaster, R.J. Gonsalves, *Phys. Rev. Lett.* **44**, 560 (1980);
S.G. Gorishnii, A.L. Kataev, and S.A. Larin, *Phys. Lett.* **B212**, 238 (1988) and **B259**, 144 (1991);
L.R. Surguladze and M.A. Samuel, *Phys. Rev. Lett.* **66**, 560 (1991) and 2416(E).
135. W. Bernreuther and W. Wetzel, *Z. Phys.* **11**, 113 (1981) and *Phys. Rev.* **D24**, 2724 (1982);
B.A. Kniehl, *Phys. Lett.* **B237**, 127 (1990);
K.G. Chetyrkin, *Phys. Lett.* **B307**, 169 (1993);
A.H. Hoang *et al.*, *Phys. Lett.* **B338**, 330 (1994);
S.A. Larin, T. van Ritbergen, and J.A.M. Vermaseren, *Nucl. Phys.* **B438**, 278 (1995).
136. T.H. Chang, K.J.F. Gaemers, and W.L. van Neerven, *Nucl. Phys.* **B202**, 407 (1980);
J. Jersak, E. Laermann, and P.M. Zerwas, *Phys. Lett.* **B98**, 363 (1981) and *Phys. Rev.* **D25**, 1218 (1982);
S.G. Gorishnii, A.L. Kataev, and S.A. Larin, *Nuovo Cimento* **92**, 117 (1986);
K.G. Chetyrkin and J.H. Kühn, *Phys. Lett.* **B248**, 359 (1990) and *ibid.* **406**, 102 (1997);
K.G. Chetyrkin, J.H. Kühn, and A. Kwiatkowski, *Phys. Lett.* **B282**, 221 (1992).
137. B.A. Kniehl and J.H. Kühn, *Phys. Lett.* **B224**, 229 (1990) and *Nucl. Phys.* **B329**, 547 (1990);
K.G. Chetyrkin and A. Kwiatkowski, *Phys. Lett.* **B305**, 285 (1993) and **B319**, 307 (1993);
S.A. Larin, T. van Ritbergen, and J.A.M. Vermaseren, *Phys. Lett.* **B320**, 159 (1994);
K.G. Chetyrkin and O.V. Tarasov, *Phys. Lett.* **B327**, 114 (1994).

138. A.L. Kataev, Phys. Lett. **B287**, 209 (1992).
139. D. Albert *et al.*, Nucl. Phys. **B166**, 460 (1980);
F. Jegerlehner, Z. Phys. **C32**, 425 (1986);
A. Djouadi, J.H. Kühn, and P.M. Zerwas, Z. Phys. **C46**, 411 (1990);
A. Borrelli *et al.*, Nucl. Phys. **B333**, 357 (1990).
140. A.A. Akhundov, D.Yu. Bardin, and T. Riemann, Nucl. Phys. **B276**, 1 (1986);
W. Beenakker and W. Hollik, Z. Phys. **C40**, 141 (1988);
B.W. Lynn and R.G. Stuart, Phys. Lett. **B352**, 676 (1990);
J. Bernabeu, A. Pich, and A. Santamaría, Nucl. Phys. **B363**, 326 (1991).
141. UA2: S. Alitti *et al.*, Phys. Lett. **B276**, 354 (1992);
CDF: T. Affolder *et al.*, Phys. Rev. **D64**, 052001 (2001);
DØ: V. M. Abazov *et al.*, Phys. Rev. **D66**, 012001 (2002);
CDF and DØ Collaborations: [hep-ex/0311039](#).
142. J. Erler, J.L. Feng, and N. Polonsky, Phys. Rev. Lett. **78**, 3063 (1997).
143. D. Choudhury, T.M.P. Tait and C.E.M. Wagner, Phys. Rev. **D65**, 053002 (2002).
144. J. Erler and P. Langacker, Phys. Rev. Lett. **84**, 212 (2000).
145. DELPHI: P. Abreu *et al.*, Z. Phys. **C**, 70 (1996);
DELPHI: P. Abreu *et al.*, in the Proceedings of the *International Europhysics Conference on High Energy Physics* (Jerusalem, 1997).
146. P. Schleper, presented at the *International Europhysics Conference on High Energy Physics* (EPS 2003, Aachen).
147. HPQCD: C.T. Davies *et al.*, [hep-lat/0304004](#).
148. J. Erler, Phys. Rev. **D63**, 071301 (2001).
149. P. Langacker and N. Polonsky, Phys. Rev. **D52**, 3081 (1995);
J. Bagger, K.T. Matchev, and D. Pierce, Phys. Lett. **B348**, 443 (1995).
150. A.L. Kataev and V.V. Starshenko, Mod. Phys. Lett. **A10**, 235 (1995).
151. M. Veltman, Nucl. Phys. **B123**, 89 (1977);
M. Chanowitz, M.A. Furman, and I. Hinchliffe, Phys. Lett. **B78**, 285 (1978).
152. P. Langacker and M. Luo, Phys. Rev. **D45**, 278 (1992) and references therein.
153. A. Denner, R.J. Guth, and J.H. Kühn, Phys. Lett. **B240**, 438 (1990).
154. S. Bertolini and A. Sirlin, Phys. Lett. **B257**, 179 (1991).
155. M. Peskin and T. Takeuchi, Phys. Rev. Lett. **65**, 964 (1990) and Phys. Rev. **D46**, 381 (1992);
M. Golden and L. Randall, Nucl. Phys. **B361**, 3 (1991).
156. D. Kennedy and P. Langacker, Phys. Rev. Lett. **65**, 2967 (1990) and Phys. Rev. **D44**, 1591 (1991).
157. G. Altarelli and R. Barbieri, Phys. Lett. **B253**, 161 (1990).
158. B. Holdom and J. Terning, Phys. Lett. **B247**, 88 (1990).
159. B.W. Lynn, M.E. Peskin, and R.G. Stuart, p. 90 of Ref. 97.
160. An alternative formulation is given by K. Hagiwara *et al.*, Z. Phys. **C64**, 559 (1994) and *ibid.* **C68**, 352(E) (1995);
K. Hagiwara, D. Haidt, and S. Matsumoto, Eur. Phys. J. **C2**, 95 (1998).
161. I. Maksymyk, C.P. Burgess, and D. London, Phys. Rev. **D50**, 529 (1994);
C.P. Burgess *et al.*, Phys. Lett. **B326**, 276 (1994).
162. K. Lane, in the Proceedings of the *27th International Conference on High Energy Physics* (Glasgow, 1994).
163. E. Gates and J. Terning, Phys. Rev. Lett. **67**, 1840 (1991);
R. Sundrum and S.D.H. Hsu, Nucl. Phys. **B391**, 127 (1993);
R. Sundrum, Nucl. Phys. **B395**, 60 (1993);
M. Luty and R. Sundrum, Phys. Rev. Lett. **70**, 529 (1993);
T. Appelquist and J. Terning, Phys. Rev. Lett. **B315**, 139 (1993).
164. H. Georgi, Nucl. Phys. **B363**, 301 (1991);
M.J. Dugan and L. Randall, Phys. Lett. **B264**, 154 (1991).
165. R. Barbieri *et al.*, Nucl. Phys. **B341**, 309 (1990).
166. M.E. Peskin and J.D. Wells, Phys. Rev. **D64**, 093003 (2001).
167. H.J. He, N. Polonsky, and S. Su, Phys. Rev. **D64**, 053004 (2001);
V.A. Novikov, L.B. Okun, A.N. Rozanov, and M.I. Vysotsky, Sov. Phys. JETP **76**, 127 (2002) and references therein.
168. For a review, see D. London, p. 951 of Ref. 4;
a recent analysis is M.B. Popovic and E.H. Simmons, Phys. Rev. **D58**, 095007 (1998);
for collider implications, see T.C. Andre and J.L. Rosner, [hep-ph/0309254](#).
169. P. Langacker, M. Luo, and A.K. Mann, Rev. Mod. Phys. **64**, 87 (1992);
M. Luo, p. 977 of Ref. 4.
170. F.S. Merritt *et al.*, p. 19 of *Particle Physics: Perspectives and Opportunities: Report of the DPF Committee on Long Term Planning*, ed. R. Peccei *et al.* (World Scientific, Singapore, 1995).
171. C.T. Hill and E.H. Simmons, Phys. Reports **381**, 235 (2003).
172. G. Altarelli *et al.*, JHEP **0106**, 018 (2001);
A. Kurylov, M.J. Ramsey-Musolf, and S. Su, Nucl. Phys. **B667**, 321 (2003) and Phys. Rev. **D68**, 035008 (2003);
W. de Boer and C. Sander, [hep-ph/0307049](#);
S. Heinemeyer and G. Weiglein, [hep-ph/0307177](#);
J.R. Ellis, K.A. Olive, Y. Santoso, and V.C. Spanos, [hep-ph/0310356](#).
173. K. Agashe, A. Delgado, M.J. May, and R. Sundrum, JHEP **0308**, 050 (2003);
M. Carena *et al.*, Phys. Rev. **D68**, 035010 (2003);
for reviews, see the articles on "Extra Dimensions" in this *Review* and I. Antoniadis, [hep-th/0102202](#).
174. J.L. Hewett, F.J. Petriello, and T.G. Rizzo, JHEP **0310**, 062 (2003);
C. Csaki *et al.*, Phys. Rev. **D67**, 115002 (2003) and *ibid.* **68**, 035009 (2003);
T. Gregoire, D.R. Smith, and J.G. Wacker, [hep-ph/0305275](#);
M. Perelstein, M.E. Peskin, and A. Pierce, [hep-ph/0310039](#);
R. Casalbuoni, A. Deandrea, and M. Oertel, [hep-ph/0311038](#);
W. Kilian and J. Reuter, [hep-ph/0311095](#).
175. G. Altarelli, R. Barbieri, and S. Jadach, Nucl. Phys. **B369**, 3 (1992) and **B376**, 444(E) (1992).
176. A. De Rújula *et al.*, Nucl. Phys. **B384**, 3 (1992).
177. K. Hagiwara *et al.*, Phys. Rev. **D48**, 2182 (1993).
178. C.P. Burgess and D. London, Phys. Rev. **D48**, 4337 (1993).
179. R.S. Chivukula and E.H. Simmons, Phys. Rev. **D66**, 015006 (2002).
180. S. Chaudhuri *et al.*, Nucl. Phys. **B456**, 89 (1995);
G. Cleaver *et al.*, Phys. Rev. **D59**, 055005 (1999).
181. J. Erler and P. Langacker, Phys. Lett. **B456**, 68 (1999).
182. T. Appelquist, B.A. Dobrescu, and A.R. Hopper, Phys. Rev. **D68**, 035012 (2003);
R.S. Chivukula, H.J. He, J. Howard, and E.H. Simmons, [hep-ph/0307209](#).
183. CDF: F. Abe *et al.*, Phys. Rev. Lett. **79**, 2192 (1997).
184. K.M. Cheung, Phys. Lett. **B517**, 167 (2001).
185. P. Langacker and M. Plümacher, Phys. Rev. **D62**, 013006 (2000).
186. R. Casalbuoni, S. De Curtis, D. Dominici, and R. Gatto, Phys. Lett. **B460**, 135 (1999);
J.L. Rosner, Phys. Rev. **D61**, 016006 (2000).

11. THE CABIBBO-KOBAYASHI-MASKAWA QUARK-MIXING MATRIX

Revised January 2004 by F.J. Gilman (Carnegie-Mellon University), K. Kleinknecht and B. Renk (Johannes-Gutenberg Universität Mainz).

In the Standard Model with $SU(2) \times U(1)$ as the gauge group of electroweak interactions, both the quarks and leptons are assigned to be left-handed doublets and right-handed singlets. The quark mass eigenstates are not the same as the weak eigenstates, and the matrix relating these bases was defined for six quarks and given an explicit parametrization by Kobayashi and Maskawa [1] in 1973. This generalizes the four-quark case, where the matrix is described by a single parameter, the Cabibbo angle [2].

By convention, the mixing is often expressed in terms of a 3×3 unitary matrix V operating on the charge $-e/3$ quark mass eigenstates (d , s , and b):

$$\begin{pmatrix} d' \\ s' \\ b' \end{pmatrix} = \begin{pmatrix} V_{ud} & V_{us} & V_{ub} \\ V_{cd} & V_{cs} & V_{cb} \\ V_{td} & V_{ts} & V_{tb} \end{pmatrix} \begin{pmatrix} d \\ s \\ b \end{pmatrix}. \quad (11.1)$$

The values of individual matrix elements can in principle all be determined from weak decays of the relevant quarks, or, in some cases, from deep inelastic neutrino scattering. Using the eight tree-level constraints discussed below together with unitarity, and assuming only three generations, the 90% confidence limits on the magnitude of the elements of the complete matrix are

$$\begin{pmatrix} 0.9739 \text{ to } 0.9751 & 0.221 \text{ to } 0.227 & 0.0029 \text{ to } 0.0045 \\ 0.221 \text{ to } 0.227 & 0.9730 \text{ to } 0.9744 & 0.039 \text{ to } 0.044 \\ 0.0048 \text{ to } 0.014 & 0.037 \text{ to } 0.043 & 0.9990 \text{ to } 0.9992 \end{pmatrix}. \quad (11.2)$$

The ranges shown are for the individual matrix elements. The constraints of unitarity connect different elements, so choosing a specific value for one element restricts the range of others.

There are several parametrizations of the Cabibbo-Kobayashi-Maskawa (CKM) matrix. We advocate a "standard" parametrization [3] of V that utilizes angles θ_{12} , θ_{23} , θ_{13} , and a phase, δ_{13}

$$V = \begin{pmatrix} c_{12}c_{13} & s_{12}c_{13} & s_{13}e^{-i\delta_{13}} \\ -s_{12}c_{23} - c_{12}s_{23}s_{13}e^{i\delta_{13}} & c_{12}c_{23} - s_{12}s_{23}s_{13}e^{i\delta_{13}} & s_{23}c_{13} \\ s_{12}s_{23} - c_{12}c_{23}s_{13}e^{i\delta_{13}} & -c_{12}s_{23} - s_{12}c_{23}s_{13}e^{i\delta_{13}} & c_{23}c_{13} \end{pmatrix}, \quad (11.3)$$

with $c_{ij} = \cos\theta_{ij}$ and $s_{ij} = \sin\theta_{ij}$ for the "generation" labels $i, j = 1, 2, 3$. This has distinct advantages of interpretation, for the rotation angles are defined and labeled in a way which relate to the mixing of two specific generations and if one of these angles vanishes, so does the mixing between those two generations; in the limit $\theta_{23} = \theta_{13} = 0$ the third generation decouples, and the situation reduces to the usual Cabibbo mixing of the first two generations with θ_{12} identified as the Cabibbo angle [2]. This parametrization is exact to all orders, and has four parameters; the real angles θ_{12} , θ_{23} , θ_{13} can all be made to lie in the first quadrant by an appropriate redefinition of quark field phases.

The matrix elements in the first row and third column, which have been directly measured in decay processes, are all of a simple form, and, as c_{13} is known to deviate from unity only in the sixth decimal place, $V_{ud} = c_{12}$, $V_{us} = s_{12}$, $V_{ub} = s_{13}e^{-i\delta_{13}}$, $V_{cb} = s_{23}$, and $V_{tb} = c_{23}$ to an excellent approximation. The phase δ_{13} lies in the range $0 \leq \delta_{13} < 2\pi$, with non-zero values breaking CP invariance for the weak interactions. The generalization to the n generation case contains $n(n-1)/2$ angles and $(n-1)(n-2)/2$ phases. Using tree-level processes as constraints only, the matrix elements in Eq. (11.2) correspond to values of the sines of the angles of $s_{12} = 0.2243 \pm 0.0016$, $s_{23} = 0.0413 \pm 0.0015$, and $s_{13} = 0.0037 \pm 0.0005$.

If we use the loop-level processes discussed below as additional constraints, the central values of the sines of the angles do not change, and the CKM phase, sometimes referred to as the angle $\gamma = \phi_3$ of the unitarity triangle, is restricted to $\delta_{13} = (1.05 \pm 0.24)$ radians $= 60^\circ \pm 14^\circ$.

Kobayashi and Maskawa [1] originally chose a parametrization involving the four angles θ_1 , θ_2 , θ_3 , and δ :

$$\begin{pmatrix} d' \\ s' \\ b' \end{pmatrix} = \begin{pmatrix} c_1 & -s_1c_3 & -s_1s_3 \\ s_1c_2 & c_1c_2c_3 - s_2s_3e^{i\delta} & c_1c_2s_3 + s_2c_3e^{i\delta} \\ s_1s_2 & c_1s_2c_3 + c_2s_3e^{i\delta} & c_1s_2s_3 - c_2c_3e^{i\delta} \end{pmatrix} \begin{pmatrix} d \\ s \\ b \end{pmatrix}, \quad (11.4)$$

where $c_i = \cos\theta_i$ and $s_i = \sin\theta_i$ for $i = 1, 2, 3$. In the limit $\theta_2 = \theta_3 = 0$, this reduces to the usual Cabibbo mixing with θ_1 identified (up to a sign) with the Cabibbo angle [2]. Note that in this case V_{ub} and V_{td} are real and V_{cb} complex, illustrating a different placement of the phase than in the standard parametrization.

An approximation to the standard parametrization proposed by Wolfenstein [4] emphasizes the hierarchy in the size of the angles, $s_{12} \gg s_{23} \gg s_{13}$. Setting $\lambda \equiv s_{12}$, the sine of the Cabibbo angle, one expresses the other elements in terms of powers of λ :

$$V = \begin{pmatrix} 1 - \lambda^2/2 & \lambda & A\lambda^3(\rho - i\eta) \\ -\lambda & 1 - \lambda^2/2 & A\lambda^2 \\ A\lambda^3(1 - \rho - i\eta) & -A\lambda^2 & 1 \end{pmatrix} + \mathcal{O}(\lambda^4). \quad (11.5)$$

with A , ρ , and η real numbers that were intended to be of order unity. This approximate form is widely used, especially for B -physics, but care must be taken, especially for CP -violating effects in K -physics, since the phase enters V_{cd} and V_{cs} through terms that are higher order in λ . These higher order terms up to order (λ^5) are given in [5].

Another parametrization has been advocated [6] that arises naturally where one builds models of quark masses in which initially $m_u = m_d = 0$. With no phases in the third row or third column, the connection between measurements of CP -violating effects for B mesons and single CKM parameters is less direct than in the standard parametrization.

Different parametrizations shuffle the placement of phases between particular tree and loop (e.g., neutral meson mixing) amplitudes. No physics can depend on which of the above parametrizations (or any other) is used, as long as a single one is used consistently and care is taken to be sure that no other choice of phases is in conflict.

Our present knowledge of the matrix elements comes from the following sources:

(1) $|V_{ud}|$: Analyses have been performed comparing nuclear beta decays that proceed through a vector current to muon decay. Radiative corrections are essential to extracting the value of the matrix element. They already include effects [7] of order $Z\alpha^2$, and most of the theoretical argument centers on the nuclear mismatch and structure-dependent radiative corrections, [8], [9].

Taking the complete data set on superallowed $0^+ \rightarrow 0^+$ beta decays, [10], a value of $|V_{ud}| = 0.9740 \pm 0.0005$ has been obtained [11]. Calculations taking into account core polarization effects and charge symmetry breaking as well as charge independence breaking forces on the mean field potentials [12] get close results. This contradicts earlier results about changes in the charge-symmetry violation for quarks inside nucleons in nuclear matter. Therefore we do not apply further additional uncertainties.

The theoretical uncertainties in extracting a value of $|V_{ud}|$ from neutron decays are significantly smaller than for decays of mirror nuclei, but the value depends on both the value of g_A/g_V and the neutron lifetime. Experimental progress has been made on g_A/g_V using very highly polarized cold neutrons together with improved detectors. The recent experimental result [13], $g_A/g_V = -1.2739 \pm 0.0019$, by itself has a better precision than the former world average and results in $|V_{ud}| = 0.9713 \pm 0.0013$ if taken alone. Averaging over all recent experiments using polarizations of more than 90% [14] gives $g_A/g_V = -1.2720 \pm 0.0018$ and results in $|V_{ud}| = 0.9725 \pm 0.0013$ from neutron decay.

Since most of the contributions to the errors in these two determinations of $|V_{ud}|$ are independent, we average them to obtain

$$|V_{ud}| = 0.9738 \pm 0.0005. \quad (11.6)$$

(2) $|V_{us}|$: The original analysis of K_{e3} decays yielded [15]

$$|V_{us}| = 0.2196 \pm 0.0023 . \quad (11.7)$$

With isospin violation taken into account in K^+ and K^0 decays, the extracted values of $|V_{us}|$ are in agreement at the 1% level. Radiative corrections have been recently calculated in chiral perturbation theory [16]. The combined effects of long-distance radiative corrections and nonlinear terms in the form factor can decrease the value of $|V_{us}|$ by up to 1% [17], and we take this into account by applying an additional correction of $(-0.5 \pm 0.5)\%$ which compensates the effect of radiative corrections in Ref. [16]. A new measurement of the K^+ semileptonic branching ratio [18] indicates a higher value of this quantity, in disagreement with the early measurements. It also would imply a contradiction to the value of $|V_{us}|$ derived from K^0 semileptonic decays. We average the new result with the older ones, leading mainly to an increase of the non-dominant experimental part of the uncertainty of $|V_{us}|$, and a slight increase of the derived value

$$|V_{us}| = 0.2200 \pm 0.0026 , \quad (11.8)$$

in very good agreement with the former analysis. New results on this will come from KLOE and NA48/2. The analysis [19] of hyperon decay data has larger theoretical uncertainties because of first order SU(3) symmetry breaking effects in the axial-vector couplings. This has been redone incorporating second order SU(3) symmetry breaking corrections in models [20] applied to the WA2 data [21] to give a value of $|V_{us}| = 0.2176 \pm 0.0026$, which is consistent with Eq. (11.8) using the “best-fit” model. A new analysis of the same hyperon decay data [22] yields $|V_{us}| = 0.2250 \pm 0.0027$, at variance with the earlier hyperon analysis. Since the values obtained in these models differ outside the errors and generally do not give good fits, we retain the value in Eq. (11.8) for $|V_{us}|$.

(3) $|V_{cd}|$: The magnitude of V_{cd} may be deduced from neutrino and antineutrino production of charm off valence d quarks. The dimuon production cross sections of the CDHS group [23] yield $\overline{B}_c |V_{cd}|^2 = (0.41 \pm 0.07) \times 10^{-2}$, where \overline{B}_c is the semileptonic branching fraction of the charmed hadrons produced. The corresponding value from the more recent CCFR Tevatron experiment [24], where a next-to-leading-order QCD analysis has been carried out, is $0.534 \pm 0.046^{+0.025}_{-0.051} \times 10^{-2}$, where the last error is from the scale uncertainty. Assuming a similar scale error for the CDHS measurement and averaging these two values with the result from the Charm II experiment [25] $\overline{B}_c |V_{cd}|^2 = (0.442 \pm 0.049) \times 10^{-2}$, we obtain as an average $(0.463 \pm 0.034) \times 10^{-2}$. Supplementing this with data [26,27,28] on the mix of charmed particle species produced by neutrinos and values for their semileptonic branching fractions (to give $\overline{B}_c = 0.0923 \pm 0.0073$), this yields

$$|V_{cd}| = 0.224 \pm 0.012 . \quad (11.9)$$

(4) $|V_{cs}|$: Values for $|V_{cs}|$ obtained from neutrino production of charm and from semileptonic D decays have errors due to theoretical uncertainties that exceed 10%, as discussed in previous editions of this review. They have been superseded by direct measurements [29] of $|V_{cs}|$ in charm-tagged W decays that give $|V_{cs}| = 0.97 \pm 0.09$ (stat.) ± 0.07 (syst.). A tighter determination follows from the ratio of hadronic W decays to leptonic decays, which has been measured at LEP with the result [30] that $\sum_{i,j} |V_{ij}|^2 = 2.039 \pm 0.025 \pm 0.001$, where the sum extends over $i = u, c$ and $j = d, s, b$ and the last error is from knowledge of α_s . With a three-generation CKM matrix, unitarity requires that this sum has the value 2. Since five of the six CKM matrix elements in the sum are well measured or contribute negligibly to the measured sum of the squares, it can be converted into a greatly improved result [30]:

$$|V_{cs}| = 0.996 \pm 0.013 . \quad (11.10)$$

(5) $|V_{cb}|$: The heavy quark effective theory [31] (HQET) provides a nearly model-independent treatment of B semileptonic decays to charmed mesons, assuming that both the b and c quarks are heavy enough for the theory to apply. Measurements of the exclusive decay

$B \rightarrow \overline{D}^* \ell^+ \nu_\ell$ have been used primarily to extract a value of $|V_{cb}|$ using corrections based on HQET. Exclusive $B \rightarrow \overline{D} \ell^+ \nu_\ell$ decays give a consistent, but less precise result. Analysis of inclusive decays, where the measured semileptonic bottom hadron partial width is assumed to be that of a b quark decaying through the usual $V-A$ interaction, depends on going from the quark to the hadron level and involves an assumption on the validity of quark-hadron duality. Improvements have been obtained in theoretical studies of the moments of inclusive semi leptonic and radiative decays and experimental measurements of such moments. The results for $|V_{cb}|$ from exclusive and inclusive decays generally are in good agreement. A more detailed discussion and references are found in a mini-review in the *Review of Particle Physics* [32]. We add an uncertainty due to the assumption of quark-hadron duality [32], [33] of 1% to the results from inclusive decays and average over the exclusive result $|V_{cb}| = (42.0 \pm 1.1 \pm 1.9) \times 10^{-3}$ and inclusive result $|V_{cb}| = (41.0 \pm 0.5 \pm 0.5 \pm 0.8) \times 10^{-3}$ with theoretical uncertainties combined linearly to obtain

$$|V_{cb}| = (41.3 \pm 1.5) \times 10^{-3} . \quad (11.11)$$

(6) $|V_{ub}|$: The decay $b \rightarrow u \ell \overline{\nu}_\ell$ and its charge conjugate can be observed in the semileptonic decay of B mesons produced on the $\Upsilon(4S)$ ($b\overline{b}$) resonance by measuring the lepton energy spectrum above the endpoint of the $b \rightarrow c \ell \overline{\nu}_\ell$ spectrum. There the $b \rightarrow u \ell \overline{\nu}_\ell$ decay rate can be obtained by subtracting the background from nonresonant $e^+ e^-$ reactions. This continuum background is determined from auxiliary measurements off the $\Upsilon(4S)$. The interpretation of this inclusive result in terms of $|V_{ub}|$ depends fairly strongly on the theoretical model used to generate the lepton energy spectrum, especially that for $b \rightarrow u$ transitions. At LEP, the separation between u -like and c -like decays is based on up to twenty different event parameters, and while the extraction of $|V_{ub}|$ is less sensitive to theoretical assumptions, it requires a detailed understanding of the decay $b \rightarrow c \ell \overline{\nu}_\ell$. The CLEO Collaboration [34] has recently employed an important technique that uses moments of measured distributions in $b \rightarrow s \gamma$ and $B \rightarrow D^* \ell \nu_\ell$ to fix the parameters in the inclusive distribution and thereby reduce the errors.

The huge data samples at the B factories, optimized cut variables which minimize theoretical uncertainties, measurements of spectral moments and event samples with fully reconstructed B decays contribute to an improved accuracy of $|V_{ub}|$.

The value of $|V_{ub}|$ can also be extracted from exclusive decays, such as $B \rightarrow \pi \ell \nu_\ell$ and $B \rightarrow \rho \ell \nu_\ell$, but there is an associated theoretical model dependence in the values of the matrix elements of the weak current between exclusive states. Detailed discussion and references on both the inclusive and exclusive analyses is found in the mini-review on $|V_{ub}|$ in the *Review of Particle Physics* [35]. They average the inclusive result $|V_{ub}| = (4.68 \pm 0.85) \times 10^{-3}$, with the exclusive result of $|V_{ub}| = (3.326 \pm 0.59) \times 10^{-3}$ to obtain a result dominated by the theoretical uncertainties,

$$|V_{ub}| = (3.67 \pm 0.47) \times 10^{-3} . \quad (11.12)$$

(7) V_{tb} : The discovery of the top quark by the CDF and D0 collaborations utilized in part the semileptonic decays of t to b . The CDF experiment has published a limit on the fraction of decays of the form $t \rightarrow b \ell^+ \nu_\ell$, as opposed to semileptonic t decays that involve the light s or d quarks, of [36]

$$\frac{|V_{tb}|^2}{|V_{td}|^2 + |V_{ts}|^2 + |V_{tb}|^2} = 0.94^{+0.31}_{-0.24} . \quad (11.13)$$

For most of the CKM matrix elements the principal error is no longer experimental, but rather theoretical. This arises from explicit dependence in interpreting inclusive data or in the direct use of specific hadronic matrix elements to relate decay rates for exclusive processes to weak transitions of quarks. This type of uncertainty often is even larger at present in extracting CKM matrix elements from loop diagrams, as discussed below. Such theoretical errors are not distributed in a Gaussian manner. We have judged what is a reasonable range in assigning the theoretical errors.

While we use the central values with the quoted errors in a consistent way [37] performing a random exploration of the full parameter space to make a best overall fit to the CKM matrix (interpreting a “1 σ ” range in a theoretical error as corresponding to a 68% confidence level that the true value lies within a range of “ $\pm 1 \sigma$ ” of the central value in making those fits), the result should be taken with appropriate care. The issue of how to use appropriate statistical methods to deal with these errors has been intensively discussed in the last few years by a number of authors [38]. The different fitting methods, if they use the same input parameters, give essentially the same result. Our limited knowledge of some of the theoretical uncertainties makes us cautious in extending this to results for multi-standard-deviation determinations of the allowed regions for CKM matrix elements.

We determine the best fit by searching for the minimum chi-squared by scanning the parameter spaces of the four angles. The results for three generations of quarks, from Eqs. (11.6), (11.8), (11.9), (11.10), (11.11), (11.12), and (11.13) plus unitarity, are summarized in the matrix in Eq. (11.2). The ranges given there are different from those given in Eqs. (11.6) – (11.13) because of the inclusion of unitarity, but are consistent with the one-standard-deviation errors on the input matrix elements. Note in particular that the unitarity constraint has pushed $|V_{ud}|$ about 1.4 standard deviations higher than given in Eq. (11.6). We observe a violation of unitarity in the first row of the CKM matrix by more than 2 standard deviations. While this bears watching and encourages another more accurate measurement of $|V_{us}|$ as well as more theoretical work, we do not see this as a major challenge to the validity of the three-generation Standard Model.

The data do not preclude there being more than three generations. Moreover, the entries deduced from unitarity might be altered when the CKM matrix is expanded to accommodate more generations. Conversely, the known entries restrict the possible values of additional generations. For example, unitarity and the known elements of the first row require that any additional element in the first row have a magnitude $|V_{ub}| < 0.08$. When there are more than three generations the allowed ranges (at 90% CL) of the matrix elements connecting the first three generations are

$$\begin{pmatrix} 0.9730 \text{ to } 0.9746 & 0.2174 \text{ to } 0.2241 & 0.0030 \text{ to } 0.0044 \dots \\ 0.213 & \text{to } 0.226 & 0.968 & \text{to } 0.975 & 0.039 & \text{to } 0.044 \dots \\ 0 & \text{to } 0.08 & 0 & \text{to } 0.11 & 0.07 & \text{to } 0.9993 \dots \\ \vdots & & \vdots & & \vdots & \end{pmatrix}, \quad (11.14)$$

where we have used unitarity (for the expanded matrix) and the measurements of the magnitudes of the CKM matrix elements (including the constraint from hadronic W decays), resulting in the weak bound $|V_{tb}| > 0.07$.

Direct and indirect information on the smallest matrix elements of the CKM matrix is neatly summarized in terms of the “unitarity triangle,” one of six such triangles that correspond to the unitarity condition applied to two different rows or columns of the CKM matrix. Unitarity applied to the first and third columns yields

$$V_{ud} V_{ub}^* + V_{cd} V_{cb}^* + V_{td} V_{tb}^* = 0. \quad (11.15)$$

The unitarity triangle is just a geometrical presentation of this equation in the complex plane [39], as in Fig. 11.1(a). We can always choose to orient the triangle so that $V_{cd} V_{cb}^*$ lies along the horizontal; in the standard parametrization, V_{cb} is real and V_{cd} is real to a very good approximation in any case. Setting cosines of small angles to unity, Eq. (11.15) becomes

$$V_{ub}^* + V_{td} \approx s_{12} V_{cb}^*, \quad (11.16)$$

which is shown as the unitarity triangle. The sides of this triangle are of order 1% of the diagonal elements of the CKM matrix, which highlights the precision we are aiming to achieve of knowing each of these sides in turn to a precision of a few percent.

The angles α , β and γ of the triangle are also referred to as ϕ_2 , ϕ_1 , and ϕ_3 , respectively, with β and $\gamma = \delta_{13}$ being the phases of the CKM elements V_{td} and V_{ub} as per

$$V_{td} = |V_{td}|e^{-i\beta}, V_{ub} = |V_{ub}|e^{-i\gamma}. \quad (11.17)$$

Rescaling the triangle so that the base is of unit length, the coordinates of the vertices A, B, and C become respectively:

$$(\text{Re}(V_{ud} V_{ub}^*)/|V_{cd} V_{cb}^*|, \text{Im}(V_{ud} V_{ub}^*)/|V_{cd} V_{cb}^*|), (1, 0), \text{ \& } (0, 0). \quad (11.18)$$

The coordinates of the apex of the rescaled unitarity triangle take the simple form $(\bar{\rho}, \bar{\eta})$, with $\bar{\rho} = \rho(1 - \lambda^2/2)$ and $\bar{\eta} = \eta(1 - \lambda^2/2)$ in the Wolfenstein approximation, [4] parametrization [4], as shown in Fig. 11.1(b).

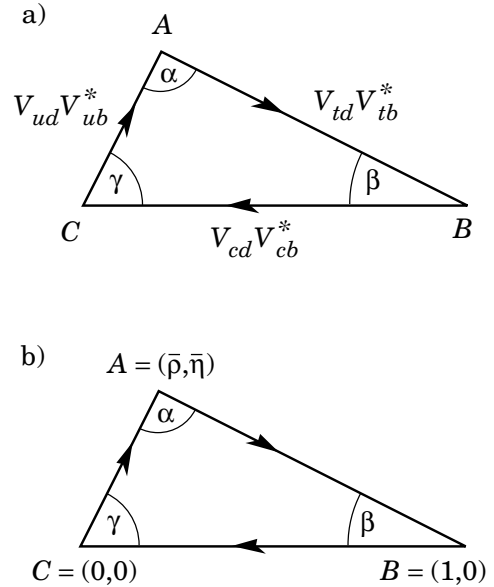


Figure 11.1: (a) Representation in the complex plane of the triangle formed by the CKM matrix elements $V_{ud} V_{ub}^*$, $V_{td} V_{tb}^*$, and $V_{cd} V_{cb}^*$. (b) Rescaled triangle with vertices A, B, and C at $(\bar{\rho}, \bar{\eta})$, $(1, 0)$, and $(0, 0)$, respectively.

CP -violating processes involve the phase in the CKM matrix, assuming that the observed CP violation is solely related to a nonzero value of this phase. More specifically, a necessary and sufficient condition for CP violation with three generations can be formulated in a parametrization-independent manner in terms of the non-vanishing of J , the determinant of the commutator of the mass matrices for the charge $2e/3$ and charge $-e/3$ quarks [40]. CP -violating amplitudes or differences of rates are all proportional to the product of CKM factors in this quantity, namely $s_{12}s_{13}s_{23}c_{12}^2c_{13}^2c_{23}\sin\delta_{13}$. This is just twice the area of the unitarity triangle.

Further information, particularly on CKM matrix elements involving the top quark, can be obtained from flavor-changing processes that occur at the one-loop level. We have not used this information up to this point since the derivation of values for V_{td} and V_{ts} in this manner from, for example, B mixing or $b \rightarrow s\gamma$, require an additional assumption that the top-quark loop, rather than new physics, gives the dominant contribution to the process in question. Conversely, when we find agreement between CKM matrix elements extracted from loop diagrams and the values above based on direct measurements plus the assumption of three generations, this can be used to place restrictions on new physics.

We first consider constraints from flavor-changing processes that are not CP -violating. The measured value [41] of $\Delta M_{B_d} = 0.502 \pm 0.007 \text{ ps}^{-1}$ from $B_d^0 - \bar{B}_d^0$ mixing can be turned into information on $|V_{tb}^* V_{td}|$, assuming that the dominant contribution to the mass difference arises from the matrix element between a B_d and a \bar{B}_d of an operator that corresponds to a box diagram with W bosons and top quarks as sides. Using the characteristic hadronic matrix element that then occurs, $\hat{B}_{B_d} \cdot f_{B_d}^2 = (1.26 \pm 0.10) \cdot (196 \pm 32 \text{ MeV})^2$ from lattice QCD calculations [42], next-to-leading-order QCD corrections ($\eta_{\text{QCD}} = 0.55$) [43], and the running top-quark mass, $\overline{m}_t(m_t) = (166 \pm 5) \text{ GeV}$ as input, we obtain

$$|V_{tb}^* \cdot V_{td}| = 0.0083 \pm 0.0016, \quad (11.19)$$

where the uncertainty comes primarily from that in the hadronic matrix elements, whose estimated errors are combined linearly.

In the ratio of B_s to B_d mass differences, many common factors (such as the QCD correction and dependence on the top-quark mass) cancel, and we have

$$\frac{\Delta M_{B_s}}{\Delta M_{B_d}} = \frac{M_{B_s}}{M_{B_d}} \frac{\hat{B}_{B_s} f_{B_s}^2}{\hat{B}_{B_d} f_{B_d}^2} \frac{|V_{tb}^* \cdot V_{ts}|^2}{|V_{tb}^* \cdot V_{td}|^2}. \quad (11.20)$$

With the experimentally measured masses, $\hat{B}_{B_s} f_{B_s}^2 / (\hat{B}_{B_d} f_{B_d}^2) = 1.56 \pm 0.26$ [42], and the experimental lower limit [41] at 95% CL of $\Delta M_{B_s} > 14.4 \text{ ps}^{-1}$ based on published data,

$$|V_{td}|/|V_{ts}| < 0.25. \quad (11.21)$$

Since with three generations, $|V_{ts}| \approx |V_{cb}|$, this result converts to $|V_{td}| < 0.011$, which is a significant constraint by itself (see Figure 2).

The CLEO observation [44] of $b \rightarrow s\gamma$, confirmed by BELLE and BaBar [45], is in agreement with the Standard Model prediction. This observation can be restated, assuming the Standard Model, as a constraint [46]

$$V_{tb} V_{td}^* = (-47 \pm 8) \times 10^{-3}. \quad (11.22)$$

This is consistent in both sign and magnitude with the value that follows from the measured magnitudes of CKM matrix elements and the assumption of three generations, but has a much larger uncertainty.

In $K^+ \rightarrow \pi^+ \nu \bar{\nu}$ there are significant contributions from loop diagrams involving both charm and top quarks. Experiment is just beginning to probe the level predicted in the Standard Model [47].

All these additional indirect constraints are consistent with the CKM elements obtained from the direct measurements plus unitarity, assuming three generations. Adding the results on B mixing together with theoretical improvements in lattice calculations reduces the range allowed for $|V_{td}|$.

Now we turn to CP -violating processes. Just the added constraint from CP violation in the neutral kaon system, taken together with the restrictions above on the magnitudes of the CKM matrix elements, is tight enough to restrict considerably the range of angles and the phase of the CKM matrix. For example, the constraint obtained from the CP -violating parameter ϵ in the neutral K system corresponds to the vertex A of the unitarity triangle lying on a hyperbola for fixed values of the (imprecisely known) hadronic matrix elements [48], [49].

In addition, following the initial evidence [50], it is now established that direct CP violation in the weak transition from a neutral K to two pions exists, i.e., that the parameter ϵ' is non-zero [51]. While theoretical uncertainties in hadronic matrix elements of canceling amplitudes presently preclude this measurement from giving a significant constraint on the unitarity triangle, it supports the assumption that the observed CP violation is related to a non-zero value of the CKM phase.

Ultimately in the neutral K system, the CP -violating process $K_L \rightarrow \pi^0 \nu \bar{\nu}$ offers the possibility of a theoretically clean, high precision measurement of the imaginary part of $V_{td} \cdot V_{ts}^*$ and the area of the unitarity triangle. Given $|V_{ts}|$, this will yield the altitude of the

unitarity triangle. However, the experimental upper limit is presently many orders of magnitude away from the required sensitivity.

Turning to the B -meson system, for CP -violating asymmetries of neutral B mesons decaying to CP eigenstates, the interference between mixing and a single weak decay amplitude for certain final states directly relates the asymmetry in a given decay to $\sin 2\phi$, where $\phi = \alpha, \beta, \gamma$ is an appropriate angle of the unitarity triangle [39]. A new generation of experiments has established a non-vanishing asymmetry in the decays $B_d(\bar{B}_d) \rightarrow \psi K_S$ and in other B_d decay modes where the asymmetry is given by $\sin 2\beta$. The present experimental results from BaBar [52] and BELLE [53], when averaged yield

$$\sin 2\beta = 0.736 \pm 0.049. \quad (11.23)$$

While the limits on the leptonic charge asymmetry for $B_d - \bar{B}_d$ mixing (measuring the analogue of $2\text{Re } \epsilon$ in the neutral K system) have been reduced to the 1% level [41], this is still roughly an order of magnitude greater than the value expected without new physics. It provides no significant constraints on the CKM matrix for now [54].

The constraints on the apex of the unitarity triangle that follow from Eqs. (11.12), (11.19), (11.21), (11.23), and ϵ are shown in Fig. 11.2. Both the limit on ΔM_s and the value of ΔM_d indicate that the apex lies in the first rather than the second quadrant.

All constraints nicely overlap in one small area in the first quadrant with the sign of ϵ measured in the K system agreeing with the sign of $\sin 2\beta$ measured in the B system.

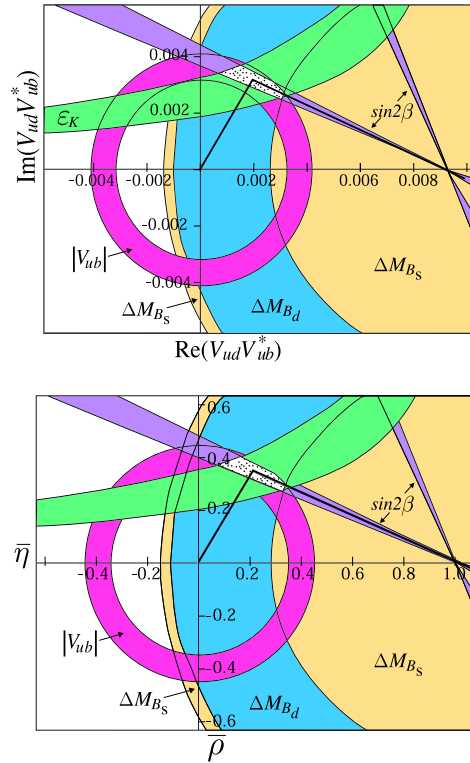


Figure 11.2: Constraints from the text on the position of the apex, A, of the unitarity triangle following from the position of $|V_{ub}|$, B mixing, ϵ , and $\sin 2\beta$. A possible unitarity triangle is shown with A in the preferred region. See full-color version on color pages at end of book.

The situation with regard to the unitarity triangle has changed qualitatively in the past few years. Both the constraints from the lengths of the sides (from $|V_{ub}|$, $|V_{cb}|$, and $|V_{td}|$) and independently

those from CP -violating processes (ϵ from the K system and $\sin 2\beta$ from the B system) indicate the same region for the apex of the triangle. The first major test of the full CKM picture and CP violation has been passed successfully.

From a combined fit using the direct measurements, B mixing, ϵ , and $\sin 2\beta$, we obtain:

$$\text{Re } V_{td} = 0.0067 \pm 0.0008, \quad (11.24)$$

$$\text{Im } V_{td} = -0.0031 \pm 0.0004, \quad (11.25)$$

$$\bar{\rho} = 0.20 \pm 0.09, \quad (11.26)$$

$$\bar{\eta} = 0.33 \pm 0.05. \quad (11.27)$$

All processes can be quantitatively understood by one value of the CKM phase $\delta_{13} = \gamma = 60^\circ \pm 14^\circ$. The value of $\beta = 23.4^\circ \pm 2^\circ$ from the overall fit is consistent with the value from the CP -asymmetry measurements of $23.7^\circ \pm 2.1^\circ$. The invariant measure of CP violation is $J = (2.88 \pm 0.33) \times 10^{-5}$.

The limit in Eq. (11.21) is not far from the value we would expect from the other information on the unitarity triangle. This limit is more robust theoretically since it depends on ratios (rather than absolute values) of hadronic matrix elements and is independent of the top mass or QCD corrections (which cancel in the ratio). Thus, the significant increase in experimental sensitivity to B_s mixing that should become available in the CDF and D0 experiments in the next few years will lead either to an observation of mixing as predicted by our knowledge to date or to an indication of physics beyond the Standard Model.

Other experimental progress in the next few years includes: checking the unitarity of the first row of the CKM matrix by new precise measurements of $|V_{us}|$ in semileptonic decays of charged and neutral kaons; resolution of the apparent inconsistency between BELLE and BaBar in the measurement of the time-dependent particle-antiparticle asymmetry in the decay $B_d(\bar{B}_d) \rightarrow \phi K_S$; searches for direct CP violation in B decay modes; and measurement of the Dalitz plot asymmetry in $K^+(K^-) \rightarrow 3\pi$ at the 10^{-4} level by NA48/2.

Longer range, the frontiers are: extraction of the angle $\alpha = \phi_2$ from measurements of decays of B_d mesons; determination of the angle $\gamma = \phi_3$ from measurements of both B_d and B_s decays; and the pursuit of the CP -violating rare decay $K_L \rightarrow \pi^0 \nu \bar{\nu}$.

Acknowledgment:

This research work is supported in part by the Department of Energy under Grant No. DE-FG02-91ER40682 and by the Bundesministerium für Bildung und Forschung under Grant No. 05HE1UMA/3.

References:

1. M. Kobayashi and T. Maskawa, *Prog. Theor. Phys.* **49**, 652 (1973).
2. N. Cabibbo, *Phys. Rev. Lett.* **10**, 531 (1963).
3. L.-L. Chau and W.-Y. Keung, *Phys. Rev. Lett.* **53**, 1802 (1984); H. Harari and M. Leurer, *Phys. Lett.* **B181**, 123 (1986); H. Fritzsch and J. Plankl, *Phys. Rev.* **D35**, 1732 (1987); F.J. Botella and L.-L. Chau, *Phys. Lett.* **B168**, 97 (1986).
4. L. Wolfenstein, *Phys. Rev. Lett.* **51**, 1945 (1983).
5. A. Buras *et al.*, *Phys. Rev.* **D50**, 3433 (1994); see also M. Schmidtler and K. Schubert, *Z. Phys.* **C53**, 347, (1992).
6. C.D. Froggatt and H.B. Nielsen, *Nucl. Phys.* **B147**, 277 (1979); H. Fritzsch, *Nucl. Phys.* **B155**, 189 (1979); S. Dimopoulos, L.J. Hall, and S. Rabi, *Phys. Rev. Lett.* **68**, 1984 (1992); H. Fritzsch and Z.-Z. Xing, *Phys. Lett.* **B413**, 396 (1997).
7. W.J. Marciano and A. Sirlin, *Phys. Rev. Lett.* **56**, 22 (1986); A. Sirlin and R. Zucchini, *Phys. Rev. Lett.* **57**, 1994 (1986); W. Jaus and G. Rasche, *Phys. Rev.* **D35**, 3420 (1987); A. Sirlin, *Phys. Rev.* **D35**, 3423 (1987).
8. B.A. Brown and W.E. Ormand, *Phys. Rev. Lett.* **62**, 866 (1989).
9. F.C. Barker *et al.*, *Nucl. Phys.* **A540**, 501 (1992); F.C. Barker *et al.*, *Nucl. Phys.* **A579**, 62 (1994).
10. G. Savard *et al.*, *Phys. Rev. Lett.* **74**, 1521 (1995).
11. J.C. Hardy and I.S. Towner, talk at WEIN98, Santa Fe, June 14-21, 1998 and [nucl-th/9809087](#).
12. H. Sagawa, Proc. of the Workshop "Quark-Mixing, CKM Unitarity", 2002, Heidelberg, 162.
13. H. Abele *et al.*, *Phys. Rev. Lett.* **88**, 211801 (2002) as a final result of J. Reich *et al.*, *Nucl. Instrum. Methods* **A440**, 535 (2000), and H. Abele *et al.*, *Nucl. Phys.* **A612**, 53 (1997).
14. Yu. A. Mostovoi *et al.*, *Phys. Atomic Nucl.* **64**, 1955 (2001); P. Liaud, *Nucl. Phys.* **A612**, 53 (1997).
15. H. Leutwyler and M. Roos, *Z. Phys.* **C25**, 91 (1984); See also the work of R.E. Shrock and L.-L. Wang, *Phys. Rev. Lett.* **41**, 1692 (1978).
16. V. Cirigliano *et al.*, *Eur. Phys. J.* **C23**, 121 (2002).
17. G. Calderon and G. Lopez Castro, *Phys. Rev.* **D65**, 073032 (2002).
18. J. Thompson, talk given at CKM03 workshop, Durham, UK, April 5th to 9th, (2003), [hep-ex/0307053](#).
19. J.F. Donoghue, B.R. Holstein, and S.W. Klimt, *Phys. Rev.* **D35**, 934 (1987).
20. R. Flores-Mendietta, A. Garcia, and G. Sanchez-Col'on, *Phys. Rev.* **D54**, 6855 (1996).
21. M. Bourquin *et al.*, *Z. Phys.* **C21**, 27 (1983).
22. N. Cabibbo *et al.*, [hep-ph/0307214](#); [hep-ph/0307298](#), to be published in *Ann. Rev. Nucl. Part. Sci.*, Vol. 53 (2003).
23. H. Abramowicz *et al.*, *Z. Phys.* **C15**, 19 (1982).
24. S.A. Rabinowitz *et al.*, *Phys. Rev. Lett.* **70**, 134 (1993); A.O. Bazarko *et al.*, *Z. Phys.* **C65**, 189 (1995).
25. P. Vilain *et al.*, *Eur. Phys. J.* **C11**, 19 (1999).
26. N. Ushida *et al.*, *Phys. Lett.* **B206**, 375 (1988).
27. T. Bolton, [hep-ex/9708014](#) (1997).
28. A. Kayis-Topasku *et al.*, *Phys. Lett.* **B549**, 48 (2002).
29. P. Abreu *et al.*, *Phys. Lett.* **B439**, 209 (1998); R. Barate *et al.*, *Phys. Lett.* **B465**, 349 (1999).
30. The LEP Collaborations, the LEP Electroweak Working Group and the SLD Heavy Flavour and Electroweak Groups, [hep-ex/0112021v2](#) (2002).
31. N. Isgur and M.B. Wise, *Phys. Lett.* **B232**, 113 (1989), and *Phys. Lett.* **B237**, 527 (1990) E; E. Eichten and B. Hill, *Phys. Lett.* **B234**, 511 (1990); M.E. Luke, *Phys. Lett.* **B252**, 447 (1990).
32. See the review on "Determination of $|V_{cb}|$ " by M. Artuso and E. Barberio in this *Review*.
33. A. Falk, presentation at the Fifth KEK Topical Conference, Tsukuba, Japan, November 20-22, 2001 and [hep-ph/0201094](#).
34. A. Bornheim *et al.* (CLEO Collaboration), [hep-ex/0202019](#), 2002.
35. See the review on "Determination of $|V_{ub}|$ " by M. Battaglia and L. Gibbons in this *Review*.
36. T. Affolder *et al.*, *Phys. Rev. Lett.* **86**, 3233 (2001).
37. K. Kleinknecht and B. Renk, *Phys. Lett.* **86**, 130B (1983); *Z. Phys.* **C34**, 209 (1987).
38. A. Hocker *et al.*, *Eur. Phys. J.* **C21**, 225 (2001); C. Ciuchini *et al.*, *JHEP* **0107**, 013 (2001).
39. L.-L. Chau and W.Y. Keung, Ref. 3;

- J.D. Bjorken, private communication and Phys. Rev. **D39**, 1396 (1989);
C. Jarlskog and R. Stora, Phys. Lett. **B208**, 268 (1988);
J.L. Rosner, A.I. Sanda, and M.P. Schmidt, in *Proceedings of the Workshop on High Sensitivity Beauty Physics at Fermilab*, Fermilab, November 11–14, 1987, edited by A.J. Slaughter, N. Lockyer, and M. Schmidt (Fermilab, Batavia, 1988), p. 165;
C. Hamzaoui, J.L. Rosner, and A.I. Sanda, *ibid.*, p. 215.
40. C. Jarlskog, Phys. Rev. Lett. **55**, 1039 (1985) and Z. Phys. **C29**, 491 (1985).
41. See the review on “ B - \bar{B} Mixing” by O. Schneider in this *Review*.
42. A. Kronfeld, hep-lat/0310063v1.
43. A.J. Buras *et al.*, Nucl. Phys. **B347**, 491 (1990).
44. M. S. Alam *et al.* (CLEO Collab.), Phys. Rev. Lett. **74**, 2885 (1995);
S. Chen *et al.* (CLEO Collab.), Phys. Rev. Lett. **87**, 1807 (2001).
45. K. Abe *et al.* (BELLE Collab.), Phys. Lett. **B511**, 157 (2001);
B. Aubert *et al.* (BaBar Collab.), hep-ex/0207074 and hep-ex/0207076 (2002).
46. A. Ali and M. Misiak, hep-ph/0304132, (2003).
47. S. Adler *et al.*, hep-ex/0111091 (2001).
48. The relevant QCD corrections in leading order in F.J. Gilman and M.B. Wise Phys. Lett. **B93**, 129 (1980), and Phys. Rev. **D27**, 1128 (1983), have been extended to next-to-leading-order by A. Buras *et al.*, Ref. 43;
S. Herrlich and U. Nierste Nucl. Phys. **B419**, 292 (1992) and Nucl. Phys. **B476**, 27 (1996).
49. The limiting curves in Fig. 11.2 arising from the value of $|\epsilon|$ correspond to values of the hadronic matrix element expressed in terms of the renormalization group invariant parameter \widehat{B}_K from 0.68 to 1.06. See, for example, D. Becirevic, plenary talk at Lattice 2003, Tsukuba, Japan, July 15 - 19, 2003.
50. H. Burkhardt *et al.*, Phys. Lett. **B206**, 169 (1988).
51. G.D. Barr *et al.*, Phys. Lett. **B317**, 233 (1993);
L.K. Gibbons *et al.*, Phys. Rev. Lett. **70**, 1203 (1993);
V. Fanti *et al.*, Phys. Lett. **B465**, 335 (1999);
A. Alavi-Harati *et al.*, Phys. Rev. Lett. **83**, 22 (1999);
A. Lai *et al.*, Eur. Phys. J. **C22**, 231 (2001);
J.R. Batley *et al.*, Phys. Lett. **B544**, 97 (2002).
52. B. Aubert *et al.*, Phys. Rev. Lett. **89**, 201802 (2002).
53. K. Abe *et al.* Belle-CONF-0353, LP’03 (2003).
54. S. Laplace *et al.*, Phys. Rev. **D65**, 094040 (2002).

12. CP VIOLATION IN MESON DECAYS

Written December 2003 by D. Kirkby (UC, Irvine) and Y. Nir (Weizmann Inst.).

The *CP* transformation combines charge conjugation *C* with parity *P*. Under *C*, particles and antiparticles are interchanged, by conjugating all internal quantum numbers, e.g., $Q \rightarrow -Q$ for electromagnetic charge. Under *P*, the handedness of space is reversed, $\vec{x} \rightarrow -\vec{x}$. Thus, for example, a left-handed electron e_L^- is transformed under *CP* into a right-handed positron, e_R^+ .

If *CP* were an exact symmetry, the laws of Nature would be the same for matter and for antimatter. We observe that most phenomena are *C*- and *P*-symmetric, and therefore, also *CP*-symmetric. In particular, these symmetries are respected by the gravitational, electromagnetic, and strong interactions. The weak interactions, on the other hand, violate *C* and *P* in the strongest possible way. For example, the charged *W* bosons couple to left-handed electrons, e_L^- , and to their *CP*-conjugate right-handed positrons, e_R^+ , but to neither their *C*-conjugate left-handed positrons, e_L^+ , nor their *P*-conjugate right-handed electrons, e_R^- . While weak interactions violate *C* and *P* separately, *CP* is still preserved in most weak interaction processes. The *CP* symmetry is, however, violated in certain rare processes, as discovered in neutral *K* decays in 1964 [1], and recently observed in neutral *B* decays [2,3]. A K_L meson decays more often to $\pi^- e^+ \bar{\nu}_e$ than to $\pi^+ e^- \nu_e$, thus allowing electrons and positrons to be unambiguously distinguished, but the decay-rate asymmetry is only at the 0.003 level. The *CP*-violating effects observed in *B* decays are larger: the *CP* asymmetry in B^0/\bar{B}^0 meson decays to *CP* eigenstates like $J/\psi K_S$ is about 0.73. *CP* violation has not yet been observed in the decays of any charged mesons, or in neutral *D* or B_s mesons, or in the lepton sector.

In addition to parity and to continuous Lorentz transformations, there is one other spacetime operation that could be a symmetry of the interactions: time reversal *T*, $t \rightarrow -t$. Violations of *T* symmetry have been observed in neutral *K* decays [4], and are expected as a corollary of *CP* violation if the combined *CPT* transformation is a fundamental symmetry of Nature. All observations indicate that *CPT* is indeed a symmetry of Nature. Furthermore, one cannot build a Lorentz-invariant quantum field theory with a Hermitian Hamiltonian that violates *CPT*. (At several points in our discussion, we avoid assumptions about *CPT*, in order to identify cases where evidence for *CP* violation relies on assumptions about *CPT*.)

Within the Standard Model, *CP* symmetry is broken by complex phases in the Yukawa couplings (that is, the couplings of the Higgs scalar to quarks). When all manipulations to remove unphysical phases in this model are exhausted, one finds that there is a single *CP*-violating parameter [5]. In the basis of mass eigenstates, this single phase appears in the 3×3 unitary matrix that gives the *W*-boson couplings to an up-type antiquark and a down-type quark. (If the Standard Model is supplemented with Majorana mass terms for the neutrinos, the analogous mixing matrix for leptons has three *CP*-violating phases.) The beautifully consistent and economical Standard-Model description of *CP* violation in terms of Yukawa couplings, known as the Kobayashi-Maskawa (KM) mechanism [5], agrees with all measurements to date. In particular, one can account within this framework for the three measured *CP*-violating observables, ϵ and ϵ' in neutral *K* decays, and $S_{\psi K}$ in neutral *B* decays. This agreement implies that the matrix of three-generation quark mixing is, very likely, the dominant source of *CP* violation in meson decays.

The small number of observations, and the theoretical uncertainties involved in their interpretation, however, leave room for additional sources of *CP* violation from new physics. Indeed, almost all extensions of the Standard Model imply that there are such additional sources. Moreover, *CP* violation is a necessary condition for baryogenesis, the process of dynamically generating the matter-antimatter asymmetry of the Universe [6]. Despite the phenomenological success of the KM mechanism, it fails (by several orders of magnitude) to accommodate the observed asymmetry [7]. This discrepancy strongly suggests that Nature provides additional sources of *CP* violation beyond the KM

mechanism. (Recent evidence for neutrino masses implies that *CP* can be violated also in the lepton sector. This situation makes leptogenesis [8], a scenario where such phases play a crucial role in the generation of the baryon asymmetry, a very attractive possibility.) The expectation of new sources motivates the large ongoing experimental effort to find deviations from the predictions of the KM mechanism.

CP violation can be experimentally searched for in a variety of processes, such as meson decays, electric dipole moments of neutrons, electrons and nuclei, and neutrino oscillations. Meson decays probe flavor-changing *CP* violation. The search for electric dipole moments may find (or constrain) sources of *CP* violation that, unlike the KM phase, are not related to flavor changing couplings. Future searches for *CP* violation in neutrino oscillations might provide further input on leptogenesis.

The present measurements of *CP* asymmetries provide some of the strongest constraints on the weak couplings of quarks. Future measurements of *CP* violation in *K*, *D*, *B*, and B_s meson decays will provide additional constraints on the flavor parameters of the Standard Model, and can probe new physics. In this review, we give the formalism and basic physics that are relevant to present and near future measurements of *CP* violation in meson decays.

12.1. Formalism

The phenomenology of *CP* violation is superficially different in *K*, *D*, *B*, and B_s decays. This is primarily because each of these systems is governed by a different balance between decay rates, oscillations, and lifetime splitting. However, the underlying mechanisms of *CP* violation are identical for all pseudoscalar mesons.

In this section we present a general formalism for, and classification of, *CP* violation in the decay of a pseudoscalar meson *M* that might be a charged or neutral *K*, *D*, *B*, or B_s meson. Subsequent sections describe the *CP*-violating phenomenology, approximations, and alternate formalisms that are specific to each system.

12.1.1. Charged- and neutral-meson decays: We define decay amplitudes of *M* (which could be charged or neutral) and its *CP* conjugate \bar{M} to a multi-particle final state *f* and its *CP* conjugate \bar{f} as

$$\begin{aligned} A_f &= \langle f | \mathcal{H} | M \rangle \quad , \quad \bar{A}_f = \langle f | \mathcal{H} | \bar{M} \rangle \quad , \\ A_{\bar{f}} &= \langle \bar{f} | \mathcal{H} | M \rangle \quad , \quad \bar{A}_{\bar{f}} = \langle \bar{f} | \mathcal{H} | \bar{M} \rangle \quad , \end{aligned} \quad (12.1)$$

where \mathcal{H} is the Hamiltonian governing weak interactions. The action of *CP* on these states introduces phases ξ_M and ξ_f that depend on their flavor content, according to

$$CP|M\rangle = e^{+i\xi_M} |\bar{M}\rangle \quad , \quad CP|f\rangle = e^{+i\xi_f} |\bar{f}\rangle \quad , \quad (12.2)$$

with

$$CP|\bar{M}\rangle = e^{-i\xi_M} |M\rangle \quad , \quad CP|\bar{f}\rangle = e^{-i\xi_f} |f\rangle \quad (12.3)$$

so that $(CP)^2 = 1$. The phases ξ_M and ξ_f are arbitrary and unphysical because of the flavor symmetry of the strong interaction. If *CP* is conserved by the dynamics, $[CP, \mathcal{H}] = 0$, then A_f and $\bar{A}_{\bar{f}}$ have the same magnitude and an arbitrary unphysical relative phase

$$\bar{A}_{\bar{f}} = e^{i(\xi_f - \xi_M)} A_f \quad . \quad (12.4)$$

12.1.2. Neutral-meson mixing: A state that is initially a superposition of M^0 and \bar{M}^0 , say

$$|\psi(0)\rangle = a(0)|M^0\rangle + b(0)|\bar{M}^0\rangle \quad , \quad (12.5)$$

will evolve in time acquiring components that describe all possible decay final states $\{f_1, f_2, \dots\}$, that is,

$$|\psi(t)\rangle = a(t)|M^0\rangle + b(t)|\bar{M}^0\rangle + c_1(t)|f_1\rangle + c_2(t)|f_2\rangle + \dots \quad (12.6)$$

If we are interested in computing only the values of $a(t)$ and $b(t)$ (and not the values of all $c_i(t)$), and if the times t in which we are interested are much larger than the typical strong interaction scale, then we can use a much simplified formalism [9]. The simplified time evolution is determined by a 2×2 effective Hamiltonian \mathbf{H} that is not Hermitian, since otherwise the mesons would only oscillate and not decay. Any complex matrix, such as \mathbf{H} , can be written in terms of Hermitian matrices \mathbf{M} and $\mathbf{\Gamma}$ as

$$\mathbf{H} = \mathbf{M} - \frac{i}{2} \mathbf{\Gamma}. \quad (12.7)$$

\mathbf{M} and $\mathbf{\Gamma}$ are associated with $(M^0, \bar{M}^0) \leftrightarrow (M^0, \bar{M}^0)$ transitions via off-shell (dispersive), and on-shell (absorptive) intermediate states, respectively. Diagonal elements of \mathbf{M} and $\mathbf{\Gamma}$ are associated with the flavor-conserving transitions $M^0 \rightarrow M^0$ and $\bar{M}^0 \rightarrow \bar{M}^0$, while off-diagonal elements are associated with flavor-changing transitions $M^0 \leftrightarrow \bar{M}^0$.

The eigenvectors of \mathbf{H} have well-defined masses and decay widths. To specify the components of the strong interaction eigenstates, M^0 and \bar{M}^0 , in the light (M_L) and heavy (M_H) mass eigenstates, we introduce three complex parameters: p , q , and, for the case that both CP and CPT are violated in mixing, z :

$$\begin{aligned} |M_L\rangle &\propto p\sqrt{1-z}|M^0\rangle + q\sqrt{1+z}|\bar{M}^0\rangle \\ |M_H\rangle &\propto p\sqrt{1+z}|M^0\rangle - q\sqrt{1-z}|\bar{M}^0\rangle, \end{aligned} \quad (12.8)$$

with the normalization $|q|^2 + |p|^2 = 1$ when $z = 0$. (Another possible choice, which is in standard usage for K mesons, defines the mass eigenstates according to their lifetimes: K_S for the short-lived and K_L for the long-lived state. The K_L is the heavier state.)

The real and imaginary parts of the eigenvalues $\omega_{L,H}$ corresponding to $|M_{L,H}\rangle$ represent their masses and decay-widths, respectively. The mass and width splittings are

$$\begin{aligned} \Delta m &\equiv m_H - m_L = \mathcal{R}e(\omega_H - \omega_L), \\ \Delta\Gamma &\equiv \Gamma_H - \Gamma_L = -2\mathcal{I}m(\omega_H - \omega_L). \end{aligned} \quad (12.9)$$

Note that here Δm is positive by definition, while the sign of $\Delta\Gamma$ is to be experimentally determined. (Alternatively, one can use the states defined by their lifetimes to have $\Delta\Gamma \equiv \Gamma_S - \Gamma_L$ positive by definition.) Solving the eigenvalue problem for \mathbf{H} yields

$$\left(\frac{q}{p}\right)^2 = \frac{\mathbf{M}_{12}^* - (i/2)\mathbf{\Gamma}_{12}^*}{\mathbf{M}_{12} - (i/2)\mathbf{\Gamma}_{12}} \quad (12.10)$$

and

$$z \equiv \frac{\delta m - (i/2)\delta\Gamma}{\Delta m - (i/2)\Delta\Gamma}, \quad (12.11)$$

where

$$\delta m \equiv \mathbf{M}_{11} - \mathbf{M}_{22}, \quad \delta\Gamma \equiv \mathbf{\Gamma}_{11} - \mathbf{\Gamma}_{22} \quad (12.12)$$

are the differences in effective mass and decay-rate expectation values for the strong interaction states M^0 and \bar{M}^0 .

If either CP or CPT is a symmetry of \mathbf{H} (independently of whether T is conserved or violated), then the values of δm and $\delta\Gamma$ are both zero, and hence $z = 0$. We also find that

$$\omega_H - \omega_L = 2\sqrt{\left(\mathbf{M}_{12} - \frac{i}{2}\mathbf{\Gamma}_{12}\right)\left(\mathbf{M}_{12}^* - \frac{i}{2}\mathbf{\Gamma}_{12}^*\right)}. \quad (12.13)$$

If either CP or T is a symmetry of \mathbf{H} (independently of whether CPT is conserved or violated), then \mathbf{M}_{12} and $\mathbf{\Gamma}_{12}$ are relatively real, leading to

$$\left(\frac{q}{p}\right)^2 = e^{2i\xi_M} \Rightarrow \left|\frac{q}{p}\right| = 1, \quad (12.14)$$

where ξ_M is the arbitrary unphysical phase introduced in Eq. (12.3). If, and only if, CP is a symmetry of \mathbf{H} (independently of CPT and T), then both of the above conditions hold, with the result that the mass eigenstates are orthogonal

$$\langle M_H | M_L \rangle = |p|^2 - |q|^2 = 0. \quad (12.15)$$

12.1.3. CP -violating observables: All CP -violating observables in M and \bar{M} decays to final states f and \bar{f} can be expressed in terms of phase-convention-independent combinations of $A_f, \bar{A}_f, A_{\bar{f}}$, and $\bar{A}_{\bar{f}}$, together with, for neutral-meson decays only, q/p . CP violation in charged-meson decays depends only on the combination $|\bar{A}_{\bar{f}}/A_f|$, while CP violation in neutral-meson decays is complicated by $M^0 \leftrightarrow \bar{M}^0$ oscillations, and depends, additionally, on $|q/p|$ and on $\lambda_f \equiv (q/p)(\bar{A}_{\bar{f}}/A_f)$.

The decay-rates of the two neutral K mass eigenstates, K_S and K_L , are different enough ($\Gamma_S/\Gamma_L \sim 500$) that one can, in most cases, actually study their decays independently. For neutral D , B , and B_s mesons, however, values of $\Delta\Gamma/\Gamma$ (where $\Gamma \equiv (\Gamma_H + \Gamma_L)/2$) are relatively small, and so both mass eigenstates must be considered in their evolution. We denote the state of an initially pure $|M^0\rangle$ or $|\bar{M}^0\rangle$ after an elapsed proper time t as $|M_{\text{phys}}^0(t)\rangle$ or $|\bar{M}_{\text{phys}}^0(t)\rangle$, respectively. Using the effective Hamiltonian approximation, but not assuming CPT is a good symmetry, we obtain

$$\begin{aligned} |M_{\text{phys}}^0(t)\rangle &= (g_+(t) + z g_-(t)) |M^0\rangle - \sqrt{1-z^2} \frac{q}{p} g_-(t) |\bar{M}^0\rangle, \\ |\bar{M}_{\text{phys}}^0(t)\rangle &= (g_+(t) - z g_-(t)) |\bar{M}^0\rangle - \sqrt{1-z^2} \frac{p}{q} g_-(t) |M^0\rangle, \end{aligned} \quad (12.16)$$

where

$$g_{\pm}(t) \equiv \frac{1}{2} \left(e^{-im_H t - \frac{1}{2}\Gamma_H t} \pm e^{-im_L t - \frac{1}{2}\Gamma_L t} \right) \quad (12.17)$$

and $z = 0$ if either CPT or CP is conserved.

Defining $x \equiv \Delta m/\Gamma$ and $y \equiv \Delta\Gamma/(2\Gamma)$, and assuming $z = 0$, one obtains the following time-dependent decay rates:

$$\begin{aligned} \frac{d\Gamma [M_{\text{phys}}^0(t) \rightarrow f]/dt}{e^{-\Gamma t} \mathcal{N}_f} &= \\ & \left(|A_f|^2 + |(q/p)\bar{A}_{\bar{f}}|^2 \right) \cosh(y\Gamma t) + \left(|A_f|^2 - |(q/p)\bar{A}_{\bar{f}}|^2 \right) \cos(x\Gamma t) \\ & + 2\mathcal{R}e((q/p)A_f^* \bar{A}_{\bar{f}}) \sinh(y\Gamma t) - 2\mathcal{I}m((q/p)A_f^* \bar{A}_{\bar{f}}) \sin(x\Gamma t), \end{aligned} \quad (12.18)$$

$$\begin{aligned} \frac{d\Gamma [\bar{M}_{\text{phys}}^0(t) \rightarrow \bar{f}]/dt}{e^{-\Gamma t} \mathcal{N}_{\bar{f}}} &= \\ & \left(|(p/q)A_f|^2 + |\bar{A}_{\bar{f}}|^2 \right) \cosh(y\Gamma t) - \left(|(p/q)A_f|^2 - |\bar{A}_{\bar{f}}|^2 \right) \cos(x\Gamma t) \\ & + 2\mathcal{R}e((p/q)A_f \bar{A}_{\bar{f}}^*) \sinh(y\Gamma t) - 2\mathcal{I}m((p/q)A_f \bar{A}_{\bar{f}}^*) \sin(x\Gamma t), \end{aligned} \quad (12.19)$$

where \mathcal{N}_f is a common normalization factor. Decay rates to the CP -conjugate final state \bar{f} are obtained analogously, with $\mathcal{N}_f = \mathcal{N}_{\bar{f}}$ and the substitutions $A_f \rightarrow A_{\bar{f}}$ and $\bar{A}_{\bar{f}} \rightarrow \bar{A}_f$ in Eqs. (12.18,12.19). Terms proportional to $|A_f|^2$ or $|\bar{A}_{\bar{f}}|^2$ are associated with decays that occur without any net $M \leftrightarrow \bar{M}$ oscillation, while terms proportional to $|(q/p)\bar{A}_{\bar{f}}|^2$ or $|(p/q)A_f|^2$ are associated with decays following a net oscillation. The $\sinh(y\Gamma t)$ and $\sin(x\Gamma t)$ terms of Eqs. (12.18,12.19) are associated with the interference between these two cases. Note that, in multi-body decays, amplitudes are functions of phase-space variables. Interference may be present in some regions but not others, and is strongly influenced by resonant substructure.

When neutral pseudoscalar mesons are produced coherently in pairs from the decay of a vector resonance, $V \rightarrow M^0 \bar{M}^0$ (for example, $\Upsilon(4S) \rightarrow B^0 \bar{B}^0$ or $\phi \rightarrow K^0 \bar{K}^0$), the time-dependence of their subsequent decays to final states f_1 and f_2 has a similar form to Eqs. (12.18,12.19):

$$\begin{aligned} \frac{d\Gamma [V_{\text{phys}}(t_1, t_2) \rightarrow f_1 f_2]/dt}{e^{-\Gamma|\Delta t|} \mathcal{N}_{f_1 f_2}} &= \\ & \left(|a_+|^2 + |a_-|^2 \right) \cosh(y\Gamma \Delta t) + \left(|a_+|^2 - |a_-|^2 \right) \cos(x\Gamma \Delta t) \\ & - 2\mathcal{R}e(a_+^* a_-) \sinh(y\Gamma \Delta t) + 2\mathcal{I}m(a_+^* a_-) \sin(x\Gamma \Delta t), \end{aligned} \quad (12.20)$$

where $\Delta t \equiv t_2 - t_1$ is the difference in the production times, t_1 and t_2 , of f_1 and f_2 , respectively, and the dependence on the average decay time and on decay angles has been integrated out. The coefficients in Eq. (12.20) are determined by the amplitudes for no net oscillation from $t_1 \rightarrow t_2$, $\bar{A}_{f_1} A_{f_2}$ and $A_{f_1} \bar{A}_{f_2}$, and for a net oscillation, $(q/p)\bar{A}_{f_1} \bar{A}_{f_2}$ and $(p/q)A_{f_1} A_{f_2}$, via

$$a_+ \equiv \bar{A}_{f_1} A_{f_2} - A_{f_1} \bar{A}_{f_2}, \quad (12.21)$$

$$a_- \equiv -\sqrt{1-z^2} \left(\frac{q}{p} \bar{A}_{f_1} \bar{A}_{f_2} - \frac{p}{q} A_{f_1} A_{f_2} \right) + z (\bar{A}_{f_1} A_{f_2} + A_{f_1} \bar{A}_{f_2}).$$

Assuming *CPT* conservation, $z = 0$, and identifying $\Delta t \rightarrow t$ and $f_2 \rightarrow f$, we find that Eqs. (12.20) and (12.21) reduce to Eq. (12.18) with $A_{f_1} = 0$, $\bar{A}_{f_1} = 1$, or to Eq. (12.19) with $\bar{A}_{f_1} = 0$, $A_{f_1} = 1$. Indeed, such a situation plays an important role in experiments. Final states f_1 with $A_{f_1} = 0$ or $\bar{A}_{f_1} = 0$ are called tagging states, because they identify the decaying pseudoscalar meson as, respectively, \bar{M}^0 or M^0 . Before one of M^0 or \bar{M}^0 decays, they evolve in phase, so that there is always one M^0 and one \bar{M}^0 present. A tagging decay of one meson sets the clock for the time evolution of the other: it starts at t_1 as purely M^0 or \bar{M}^0 , with time evolution that depends only on $t_2 - t_1$.

When f_1 is a state that both M^0 and \bar{M}^0 can decay into, then Eq. (12.20) contains interference terms proportional to $A_{f_1} \bar{A}_{f_1} \neq 0$ that are not present in Eqs. (12.18, 12.19). Even when f_1 is dominantly produced by M^0 decays rather than \bar{M}^0 decays, or vice versa, $A_{f_1} \bar{A}_{f_1}$ can be non-zero owing to doubly-CKM-suppressed decays, and these terms should be considered for precision studies of *CP* violation in coherent $V \rightarrow M^0 \bar{M}^0$ decays [10].

12.1.4. Classification of *CP*-violating effects: We distinguish three types of *CP*-violating effects in meson decays:

- I. *CP* violation in decay is defined by

$$|\bar{A}_{\bar{f}}/A_f| \neq 1. \quad (12.22)$$

In charged meson decays, where mixing effects are absent, this is the only possible source of *CP* asymmetries:

$$A_{f\pm} \equiv \frac{\Gamma(M^- \rightarrow f^-) - \Gamma(M^+ \rightarrow f^+)}{\Gamma(M^- \rightarrow f^-) + \Gamma(M^+ \rightarrow f^+)} = \frac{|\bar{A}_{f^-}/A_{f^+}|^2 - 1}{|\bar{A}_{f^-}/A_{f^+}|^2 + 1}. \quad (12.23)$$

- II. *CP* (and *T*) violation in mixing is defined by

$$|q/p| \neq 1. \quad (12.24)$$

In charged-current semileptonic neutral meson decays $M, \bar{M} \rightarrow \ell^\pm X$ (taking $|A_{\ell^+ X}| = |\bar{A}_{\ell^- X}|$ and $A_{\ell^- X} = \bar{A}_{\ell^+ X} = 0$, as is the case in the Standard Model, to lowest order, and in most of its reasonable extensions), this is the only source of *CP* violation, and can be measured via the asymmetry of “wrong-sign” decays induced by oscillations:

$$A_{\text{SL}}(t) \equiv \frac{d\Gamma/dt[\bar{M}_{\text{phys}}^0(t) \rightarrow \ell^+ X] - d\Gamma/dt[M_{\text{phys}}^0(t) \rightarrow \ell^- X]}{d\Gamma/dt[\bar{M}_{\text{phys}}^0(t) \rightarrow \ell^+ X] + d\Gamma/dt[M_{\text{phys}}^0(t) \rightarrow \ell^- X]} = \frac{1 - |q/p|^4}{1 + |q/p|^4}. \quad (12.25)$$

Note that this asymmetry of time-dependent decay rates is actually time-independent.

- III. *CP* violation in interference between a decay without mixing, $M^0 \rightarrow f$, and a decay with mixing, $M^0 \rightarrow \bar{M}^0 \rightarrow f$ (such an effect occurs only in decays to final states that are common to M^0 and \bar{M}^0 , including all *CP* eigenstates), is defined by

$$\text{Im}(\lambda_f) \neq 0, \quad (12.26)$$

with

$$\lambda_f \equiv \frac{q \bar{A}_f}{p A_f}. \quad (12.27)$$

This form of *CP* violation can be observed, for example, using the asymmetry of neutral meson decays into final *CP* eigenstates f_{CP}

$$A_{f_{CP}}(t) \equiv \frac{d\Gamma/dt[\bar{M}_{\text{phys}}^0(t) \rightarrow f_{CP}] - d\Gamma/dt[M_{\text{phys}}^0(t) \rightarrow f_{CP}]}{d\Gamma/dt[\bar{M}_{\text{phys}}^0(t) \rightarrow f_{CP}] + d\Gamma/dt[M_{\text{phys}}^0(t) \rightarrow f_{CP}]}. \quad (12.28)$$

If $\Delta\Gamma = 0$ and $|q/p| = 1$, as expected to a good approximation for *B* mesons, but not for *K* mesons, then $A_{f_{CP}}$ has a particularly simple form (see Eq. (12.60), below). If, in addition, the decay amplitudes fulfill $|\bar{A}_{f_{CP}}| = |A_{f_{CP}}|$, the interference between decays with and without mixing is the only source of the asymmetry and $A_{f_{CP}}(t) = \text{Im}(\lambda_{f_{CP}}) \sin(\Gamma t)$.

Examples of these three types of *CP* violation will be given in Sections 12.4, 12.5, and 12.6.

12.2. Theoretical Interpretation: General Considerations

Consider the $M \rightarrow f$ decay amplitude A_f , and the *CP* conjugate process, $\bar{M} \rightarrow \bar{f}$, with decay amplitude $\bar{A}_{\bar{f}}$. There are two types of phases that may appear in these decay amplitudes. Complex parameters in any Lagrangian term that contributes to the amplitude will appear in complex conjugate form in the *CP*-conjugate amplitude. Thus, their phases appear in A_f and $\bar{A}_{\bar{f}}$ with opposite signs. In the Standard Model, these phases occur only in the couplings of the W^\pm bosons, and hence, are often called “weak phases”. The weak phase of any single term is convention-dependent. However, the difference between the weak phases in two different terms in A_f is convention-independent. A second type of phase can appear in scattering or decay amplitudes, even when the Lagrangian is real. Their origin is the possible contribution from intermediate on-shell states in the decay process. Since these phases are generated by *CP*-invariant interactions, they are the same in A_f and $\bar{A}_{\bar{f}}$. Usually the dominant rescattering is due to strong interactions; hence the designation “strong phases” for the phase shifts so induced. Again, only the relative strong phases between different terms in the amplitude are physically meaningful.

The ‘weak’ and ‘strong’ phases discussed here appear in addition to the ‘spurious’ *CP*-transformation phases of Eq. (12.4). Those spurious phases are due to an arbitrary choice of phase convention, and do not originate from any dynamics or induce any *CP* violation. For simplicity, we set them to zero from here on.

It is useful to write each contribution A_i to A_f in three parts: its magnitude $|a_i|$, its weak phase ϕ_i , and its strong phase δ_i . If, for example, there are two such contributions, $A_f = a_1 + a_2$, we have

$$A_f = |a_1|e^{i(\delta_1 + \phi_1)} + |a_2|e^{i(\delta_2 + \phi_2)}, \\ \bar{A}_{\bar{f}} = |a_1|e^{i(\delta_1 - \phi_1)} + |a_2|e^{i(\delta_2 - \phi_2)}. \quad (12.29)$$

Similarly, for neutral meson decays, it is useful to write

$$\mathbf{M}_{12} = |\mathbf{M}_{12}|e^{i\phi_M}, \quad \Gamma_{12} = |\Gamma_{12}|e^{i\phi_\Gamma}. \quad (12.30)$$

Each of the phases appearing in Eqs. (12.29, 12.30) is convention-dependent, but combinations such as $\delta_1 - \delta_2$, $\phi_1 - \phi_2$, $\phi_M - \phi_\Gamma$, and $\phi_M + \phi_1 - \bar{\phi}_1$ (where $\bar{\phi}_1$ is a weak phase contributing to $\bar{A}_{\bar{f}}$) are physical.

It is now straightforward to evaluate the various asymmetries in terms of the theoretical parameters introduced here. We will do so with approximations that are often relevant to the most interesting measured asymmetries.

1. The *CP* asymmetry in charged meson decays [Eq. (12.23)] is given by

$$A_{f\pm} = -\frac{2|a_1 a_2| \sin(\delta_2 - \delta_1) \sin(\phi_2 - \phi_1)}{|a_1|^2 + |a_2|^2 + 2|a_1 a_2| \cos(\delta_2 - \delta_1) \cos(\phi_2 - \phi_1)}. \quad (12.31)$$

The quantity of most interest to theory is the weak phase difference $\phi_2 - \phi_1$. Its extraction from the asymmetry requires, however, that the amplitude ratio and the strong phase are known. Both quantities depend on non-perturbative hadronic parameters that are difficult to calculate.

2. In the approximation that $|\Gamma_{12}/\mathbf{M}_{12}| \ll 1$ (valid for B and B_s mesons), the CP asymmetry in semileptonic neutral-meson decays [Eq. (12.25)] is given by

$$\mathcal{A}_{\text{SL}} = - \left| \frac{\Gamma_{12}}{\mathbf{M}_{12}} \right| \sin(\phi_M - \phi_\Gamma). \quad (12.32)$$

The quantity of most interest to theory is the weak phase $\phi_M - \phi_\Gamma$. Its extraction from the asymmetry requires, however, that $|\Gamma_{12}/\mathbf{M}_{12}|$ is known. This quantity depends on long distance physics that is difficult to calculate.

3. In the approximations that only a single weak phase contributes to decay, $A_f = |a_f|e^{i(\delta_f + \phi_f)}$, and that $|\Gamma_{12}/\mathbf{M}_{12}| = 0$, we obtain $|\lambda_f| = 1$, and the CP asymmetries in decays to a final CP eigenstate f [Eq. (12.28)] with eigenvalue $\eta_f = \pm 1$ are given by

$$A_{fCP}(t) = \mathcal{I}m(\lambda_f) \sin(\Delta m t) \quad \text{with} \quad \mathcal{I}m(\lambda_f) = \eta_f \sin(\phi_M + 2\phi_f). \quad (12.33)$$

Note that the phase so measured is purely a weak phase, and no hadronic parameters are involved in the extraction of its value from $\mathcal{I}m(\lambda_f)$.

The discussion above allows us to introduce another classification:

1. *Direct CP violation* is one that cannot be accounted for by just $\phi_M \neq 0$. CP violation in decay (type I) belongs to this class.
2. *Indirect CP violation* is consistent with taking $\phi_M \neq 0$ and setting all other CP violating phases to zero. CP violation in mixing (type II) belongs to this class.

As concerns type III CP violation, observing $\eta_{f_1} \mathcal{I}m(\lambda_{f_1}) \neq \eta_{f_2} \mathcal{I}m(\lambda_{f_2})$ (for the same decaying meson and two different final CP eigenstates f_1 and f_2) would establish direct CP violation. The significance of this classification is related to theory. In superweak models [11], CP violation appears only in diagrams that contribute to \mathbf{M}_{12} , hence they predict that there is no direct CP violation. In most models and, in particular, in the Standard Model, CP violation is both direct and indirect. The experimental observation of $\epsilon' \neq 0$ (see Section 12.4) excluded the superweak scenario.

12.3. Theoretical Interpretation: The KM Mechanism

Of all the Standard Model quark parameters, only the Kobayashi-Maskawa (KM) phase is CP violating. Having a single source of CP violation, the Standard Model is very predictive for CP asymmetries: some vanish, and those that do not are correlated.

To be precise, CP could be violated also by strong interactions. The experimental upper bound on the electric dipole moment of the neutron implies, however, that θ_{QCD} , the non-perturbative parameter that determines the strength of this type of CP violation, is tiny, if not zero. (The smallness of θ_{QCD} constitutes a theoretical puzzle, known as ‘the strong CP problem.’) In particular, it is irrelevant to our discussion of meson decays.

The charged current interactions (that is, the W^\pm interactions) for quarks are given by

$$-L_{W^\pm} = \frac{g}{\sqrt{2}} \bar{u}_L^i \gamma^\mu (V_{\text{CKM}})_{ij} d_{Lj} W_\mu^\pm + \text{h.c.} \quad (12.34)$$

Here $i, j = 1, 2, 3$ are generation numbers. The Cabibbo-Kobayashi-Maskawa (CKM) mixing matrix for quarks is a 3×3 unitary matrix [12]. Ordering the quarks by their masses, *i.e.* $(u_1, u_2, u_3) \rightarrow (u, c, t)$ and $(d_1, d_2, d_3) \rightarrow (d, s, b)$, the elements of V_{CKM} are written as follows:

$$V_{\text{CKM}} = \begin{pmatrix} V_{ud} & V_{us} & V_{ub} \\ V_{cd} & V_{cs} & V_{cb} \\ V_{td} & V_{ts} & V_{tb} \end{pmatrix}. \quad (12.35)$$

While a general 3×3 unitary matrix depends on three real angles and six phases, the freedom to redefine the phases of the quark mass eigenstates can be used to remove five of the phases, leaving a single physical phase, the Kobayashi-Maskawa phase, that is responsible for all CP violation in meson decays in the Standard Model.

The fact that one can parametrize V_{CKM} by three real and only one imaginary physical parameters can be made manifest by choosing an explicit parametrization. The Wolfenstein parametrization [13,14] is particularly useful:

$$V_{\text{CKM}} = \begin{pmatrix} 1 - \frac{1}{2}\lambda^2 - \frac{1}{8}\lambda^4 & \lambda & A\lambda^3(\rho - i\eta) \\ -\lambda + \frac{1}{2}A^2\lambda^5[1 - 2(\rho + i\eta)] & 1 - \frac{1}{2}\lambda^2 - \frac{1}{8}\lambda^4(1 + 4A^2) & A\lambda^2 \\ A\lambda^3[1 - (1 - \frac{1}{2}\lambda^2)(\rho + i\eta)] & -A\lambda^2 + \frac{1}{2}A\lambda^4[1 - 2(\rho + i\eta)] & 1 - \frac{1}{2}A^2\lambda^4 \end{pmatrix}. \quad (12.36)$$

Here $\lambda = |V_{us}| = 0.22$ (not to be confused with λ_f) plays the role of an expansion parameter, and η represents the CP violating phase. Terms of $\mathcal{O}(\lambda^6)$ were neglected.

The unitarity of the CKM matrix leads to various relations among the matrix elements; *e.g.*,

$$V_{ud}V_{ub}^* + V_{cd}V_{cb}^* + V_{td}V_{tb}^* = 0. \quad (12.37)$$

This relation requires the sum of three complex quantities to vanish and so can be geometrically represented in the complex plane as a triangle (see Fig. 12.1). The angles of this triangle,

$$\begin{aligned} \alpha &\equiv \varphi_2 \equiv \arg\left(-\frac{V_{td}V_{tb}^*}{V_{ud}V_{ub}^*}\right), \\ \beta &\equiv \varphi_1 \equiv \arg\left(-\frac{V_{cd}V_{cb}^*}{V_{td}V_{tb}^*}\right), \\ \gamma &\equiv \varphi_3 \equiv \arg\left(-\frac{V_{ud}V_{ub}^*}{V_{cd}V_{cb}^*}\right), \end{aligned} \quad (12.38)$$

are physical quantities and can, in principle, be independently measured by CP asymmetries in B decays. The notations (α, β, γ) and $(\varphi_1, \varphi_2, \varphi_3)$ are both in common usage.

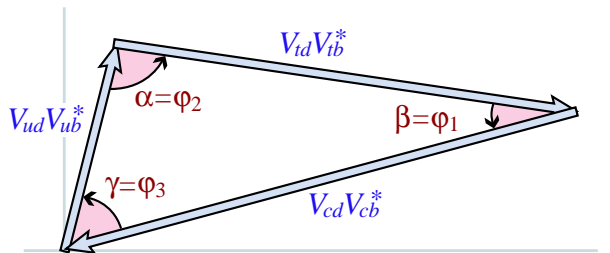


Figure 12.1: Graphical representation of the unitarity constraint $V_{ud}V_{ub}^* + V_{cd}V_{cb}^* + V_{td}V_{tb}^* = 0$ as a triangle in the complex plane.

All unitarity triangles that correspond to relations, such as Eq. (12.37) between two different columns or two different rows of the CKM matrix have the same area, commonly denoted by $J/2$ [15]. If CP is violated, J is different from zero and can be taken as the single CP -violating parameter. In the Wolfenstein parametrization of Eq. (12.36), $J \simeq \lambda^6 A^2 \eta$.

12.4. K Decays

CP violation was discovered in $K \rightarrow \pi\pi$ decays in 1964 [1]. The same mode provided the first evidence for direct CP violation [16–18].

The decay amplitudes actually measured in neutral K decays refer to the mass eigenstates K_L and K_S , rather than to the K and \bar{K} states referred to in Eq. (12.1). We define CP-violating amplitude ratios for two-pion final states,

$$\eta_{00} \equiv \frac{\langle \pi^0 \pi^0 | \mathcal{H} | K_L \rangle}{\langle \pi^0 \pi^0 | \mathcal{H} | K_S \rangle}, \quad \eta_{+-} \equiv \frac{\langle \pi^+ \pi^- | \mathcal{H} | K_L \rangle}{\langle \pi^+ \pi^- | \mathcal{H} | K_S \rangle}. \quad (12.39)$$

Another important observable is the asymmetry of time-integrated semileptonic decay rates:

$$\delta_L \equiv \frac{\Gamma(K_L \rightarrow \ell^+ \nu_\ell \pi^-) - \Gamma(K_L \rightarrow \ell^- \bar{\nu}_\ell \pi^+)}{\Gamma(K_L \rightarrow \ell^+ \nu_\ell \pi^-) + \Gamma(K_L \rightarrow \ell^- \bar{\nu}_\ell \pi^+)}. \quad (12.40)$$

CP violation has been observed as an appearance of K_L decays to two-pion final states [19],

$$\begin{aligned} |\eta_{00}| &= (2.276 \pm 0.014) \times 10^{-3} & \phi_{00} &= 43.7^\circ \pm 0.8^\circ \\ |\eta_{+-}| &= (2.286 \pm 0.014) \times 10^{-3} & \phi_{+-} &= 43.4^\circ \pm 0.7^\circ \\ |\eta_{00}/\eta_{+-}| &= 0.9950 \pm 0.0008 & \phi_{00} - \phi_{+-} &= 0.2^\circ \pm 0.4^\circ, \end{aligned} \quad (12.41)$$

where ϕ_{ij} is the phase of the amplitude ratio η_{ij} determined without assuming CPT invariance. (A fit that assumes CPT gives [19] $\phi_{00} = 43.49^\circ \pm 0.06^\circ$, $\phi_{+-} = 43.51^\circ \pm 0.05^\circ$ and $\phi_{00} - \phi_{+-} = -0.022^\circ \pm 0.020^\circ$.) CP violation has also been observed in semileptonic K_L decays [19]

$$\delta_L = (3.27 \pm 0.12) \times 10^{-3}, \quad (12.42)$$

where δ_L is a weighted average of muon and electron measurements, as well as in K_L decays to $\pi^+ \pi^- \gamma$ and $\pi^+ \pi^- e^+ e^-$ [19]. CP violation in $K \rightarrow 3\pi$ decays has not yet been observed [19,20].

Historically, CP violation in neutral K decays has been described in terms of parameters ϵ and ϵ' . The observables η_{00} , η_{+-} , and δ_L are related to these parameters, and to those of Section 12.1, by

$$\begin{aligned} \eta_{00} &= \frac{1 - \lambda_{\pi^0 \pi^0}}{1 + \lambda_{\pi^0 \pi^0}} = \epsilon - 2\epsilon', \\ \eta_{+-} &= \frac{1 - \lambda_{\pi^+ \pi^-}}{1 + \lambda_{\pi^+ \pi^-}} = \epsilon + \epsilon', \\ \delta_L &= \frac{1 - |q/p|^2}{1 + |q/p|^2} = \frac{2\mathcal{R}e(\epsilon)}{1 + |\epsilon|^2}, \end{aligned} \quad (12.43)$$

where, in the last line, we have assumed that $|A_{\ell^+ \nu_\ell \pi^-}| = |\bar{A}_{\ell^- \bar{\nu}_\ell \pi^+}|$ and $|A_{\ell^+ \nu_\ell \pi^-}| = |\bar{A}_{\ell^+ \nu_\ell \pi^-}| = 0$. (The convention-dependent parameter $\bar{\epsilon} \equiv (1 - q/p)/(1 + q/p)$, sometimes used in the literature, is, in general, different from ϵ but yields a similar expression, $\delta_L = 2\mathcal{R}e(\bar{\epsilon})/(1 + |\bar{\epsilon}|^2)$.) A fit to the $K \rightarrow \pi\pi$ data yields [19]

$$\begin{aligned} |\epsilon| &= (2.284 \pm 0.014) \times 10^{-3}, \\ \mathcal{R}e(\epsilon'/\epsilon) &= (1.67 \pm 0.26) \times 10^{-3}. \end{aligned} \quad (12.44)$$

In discussing two-pion final states, it is useful to express the amplitudes $A_{\pi^0 \pi^0}$ and $A_{\pi^+ \pi^-}$ in terms of their isospin components via

$$\begin{aligned} A_{\pi^0 \pi^0} &= \sqrt{\frac{1}{3}} |A_0| e^{i(\delta_0 + \phi_0)} - \sqrt{\frac{2}{3}} |A_2| e^{i(\delta_2 + \phi_2)}, \\ A_{\pi^+ \pi^-} &= \sqrt{\frac{2}{3}} |A_0| e^{i(\delta_0 + \phi_0)} + \sqrt{\frac{1}{3}} |A_2| e^{i(\delta_2 + \phi_2)}, \end{aligned} \quad (12.45)$$

where we parameterize the amplitude $A_I(\bar{A}_I)$ for $K^0(\bar{K}^0)$ decay into two pions with total isospin $I = 0$ or 2 as

$$\begin{aligned} A_I &\equiv \langle (\pi\pi)_I | \mathcal{H} | K^0 \rangle = |A_I| e^{i(\delta_I + \phi_I)}, \\ \bar{A}_I &\equiv \langle (\pi\pi)_I | \mathcal{H} | \bar{K}^0 \rangle = |\bar{A}_I| e^{i(\delta_I - \phi_I)}. \end{aligned} \quad (12.46)$$

The smallness of $|\eta_{00}|$ and $|\eta_{+-}|$ allows us to approximate

$$\epsilon \simeq \frac{1}{2}(1 - \lambda_{(\pi\pi)I=0}), \quad \epsilon' \simeq \frac{1}{6}(\lambda_{\pi^0 \pi^0} - \lambda_{\pi^+ \pi^-}). \quad (12.47)$$

The parameter ϵ represents indirect CP violation, while ϵ' parameterizes direct CP violation: $\mathcal{R}e(\epsilon')$ measures CP violation in decay (type I), $\mathcal{R}e(\epsilon)$ measures CP violation in mixing (type II), and $\mathcal{I}m(\epsilon)$ and $\mathcal{I}m(\epsilon')$ measure the interference between decays with and without mixing (type III).

The following expressions for ϵ and ϵ' are useful for theoretical evaluations:

$$\epsilon \simeq \frac{e^{i\pi/4}}{\sqrt{2}} \frac{\mathcal{I}m(\mathbf{M}_{12})}{\Delta m}, \quad \epsilon' = \frac{i}{\sqrt{2}} \frac{A_2}{A_0} |e^{i(\delta_2 - \delta_0)} \sin(\phi_2 - \phi_0)|. \quad (12.48)$$

The expression for ϵ is only valid in a phase convention where $\phi_2 = 0$, corresponding to a real $V_{ud} V_{us}^*$, and in the approximation that also $\phi_0 = 0$. The phase of ϵ , $\arg(\epsilon) \approx \arctan(-2\Delta m/\Delta\Gamma)$, is independent of the electroweak model and is experimentally determined to be about $\pi/4$. The calculation of ϵ benefits from the fact that $\mathcal{I}m(\mathbf{M}_{12})$ is dominated by short distance physics. Consequently, the main source of uncertainty in theoretical interpretations of ϵ are the values of matrix elements, such as $\langle K^0 | (\bar{s}d)_{V-A} (\bar{u}u)_{V-A} | \bar{K}^0 \rangle$. The expression for ϵ' is valid to first order in $|A_2/A_0| \sim 1/20$. The phase of ϵ' is experimentally determined, $\pi/2 + \delta_2 - \delta_0 \approx \pi/4$, and is independent of the electroweak model. Note that, accidentally, ϵ'/ϵ is real to a good approximation.

A future measurement of much interest is that of CP violation in the rare $K \rightarrow \pi\nu\bar{\nu}$ decays. The signal for CP violation is simply observing the $K_L \rightarrow \pi^0\nu\bar{\nu}$ decay. The effect here is that of interference between decays with and without mixing (type III) [21]:

$$\frac{\Gamma(K_L \rightarrow \pi^0\nu\bar{\nu})}{\Gamma(K^+ \rightarrow \pi^+\nu\bar{\nu})} = \frac{1}{2} [1 + |\lambda_{\pi\nu\bar{\nu}}|^2 - 2\mathcal{R}e(\lambda_{\pi\nu\bar{\nu}})] \simeq 1 - \mathcal{R}e(\lambda_{\pi\nu\bar{\nu}}), \quad (12.49)$$

where in the last equation we neglect CP violation in decay and in mixing (expected, model-independently, to be of order 10^{-5} and 10^{-3} , respectively). Such a measurement would be experimentally very challenging and theoretically very rewarding [22]. Similar to the CP asymmetry in $B \rightarrow J/\psi K_S$, the CP violation in $K \rightarrow \pi\nu\bar{\nu}$ decay is predicted to be large and can be very cleanly interpreted.

Within the Standard Model, the $K_L \rightarrow \pi^0\nu\bar{\nu}$ decay is dominated by an intermediate top quark contribution and, consequently, can be interpreted in terms of CKM parameters [23]. (For the charged mode, $K^+ \rightarrow \pi^+\nu\bar{\nu}$, the contribution from an intermediate charm quark is not negligible, and constitutes a source of hadronic uncertainty.) In particular, $B(K_L \rightarrow \pi^0\nu\bar{\nu})$ provides a theoretically clean way to determine the Wolfenstein parameter η [24]:

$$B(K_L \rightarrow \pi^0\nu\bar{\nu}) = \kappa_L X^2(m_t^2/m_W^2) A^4 \eta^2, \quad (12.50)$$

where $\kappa_L = 1.80 \times 10^{-10}$ incorporates the value of the four-fermion matrix element which is deduced, using isospin relations, from $B(K^+ \rightarrow \pi^0 e^+ \nu)$, and $X(m_t^2/m_W^2)$ is a known function of the top mass.

12.5. D Decays

Unlike the case of neutral K , B , and B_s mixing, $D^0 - \bar{D}^0$ mixing has not yet been observed [25]. Long-distance contributions make it difficult to calculate the Standard Model prediction for the $D^0 - \bar{D}^0$ mixing parameters. Therefore, the goal of the search for $D^0 - \bar{D}^0$ mixing is not to constrain the CKM parameters, but rather to probe new physics. Here CP violation plays an important role. Within the Standard Model, the CP-violating effects are predicted to be negligibly small, since the mixing and the relevant decays are described, to an excellent approximation, by physics of the first two generations. Observation of CP violation in $D^0 - \bar{D}^0$ mixing (at a level much higher than $\mathcal{O}(10^{-3})$) will constitute an unambiguous signal of new physics. At present, the most sensitive searches involve the $D \rightarrow K^+ K^-$ and $D \rightarrow K^\pm \pi^\mp$ modes.

The neutral D mesons decay via a singly-Cabibbo-suppressed transition to the CP eigenstate K^+K^- . Since the decay proceeds via a Standard-Model tree diagram, it is very likely unaffected by new physics and, furthermore, dominated by a single weak phase. It is safe then to assume that direct CP violation plays no role here. In addition, given the experimental bounds [26], $x \equiv \Delta m/\Gamma \lesssim 0.03$ and $y \equiv \Delta\Gamma/(2\Gamma) = 0.0045 \pm 0.0065$, we can expand the decay rates to first order in these parameters. Using Eq. (12.18) with these assumptions and approximations yields, for $xt, yt \lesssim \Gamma^{-1}$,

$$\begin{aligned} \Gamma[D_{\text{phys}}^0(t) \rightarrow K^+K^-] &= e^{-\Gamma t} |A_{KK}|^2 [1 - |q/p|(y \cos \phi_D - x \sin \phi_D)\Gamma t], \\ \Gamma[\overline{D}_{\text{phys}}^0(t) \rightarrow K^+K^-] &= e^{-\Gamma t} |A_{KK}|^2 [1 - |p/q|(y \cos \phi_D + x \sin \phi_D)\Gamma t], \end{aligned} \quad (12.51)$$

where ϕ_D is defined via $\lambda_{K^+K^-} = -|q/p|e^{i\phi_D}$. (In the limit of CP conservation, choosing $\phi_D = 0$ is equivalent to defining the mass eigenstates by their CP eigenvalue: $|D_{\mp}\rangle = p|D^0\rangle \pm q|\overline{D}^0\rangle$, with $D_-(D_+)$ being the CP -odd (CP -even) state; that is, the state that does not (does) decay into K^+K^- .) Given the small values of x and y , the time dependences of the rates in Eq. (12.51) can be recast into purely exponential forms, but with modified decay-rate parameters [27]:

$$\begin{aligned} \Gamma_{D^0 \rightarrow K^+K^-} &= \Gamma \times [1 + |q/p|(y \cos \phi_D - x \sin \phi_D)], \\ \Gamma_{\overline{D}^0 \rightarrow K^+K^-} &= \Gamma \times [1 + |p/q|(y \cos \phi_D + x \sin \phi_D)]. \end{aligned} \quad (12.52)$$

One can define CP -conserving and CP -violating combinations of these two observables (normalized to the true width Γ):

$$\begin{aligned} Y &\equiv \frac{\Gamma_{\overline{D}^0 \rightarrow K^+K^-} + \Gamma_{D^0 \rightarrow K^+K^-}}{2\Gamma} - 1 \\ &= \frac{|q/p| + |p/q|}{2} y \cos \phi_D - \frac{|q/p| - |p/q|}{2} x \sin \phi_D, \\ \Delta Y &\equiv \frac{\Gamma_{\overline{D}^0 \rightarrow K^+K^-} - \Gamma_{D^0 \rightarrow K^+K^-}}{2\Gamma} \\ &= \frac{|q/p| + |p/q|}{2} x \sin \phi_D - \frac{|q/p| - |p/q|}{2} y \cos \phi_D. \end{aligned} \quad (12.53)$$

In the limit of CP conservation (and, in particular, within the Standard Model), $Y = y$ and $\Delta Y = 0$.

The $K^{\pm}\pi^{\mp}$ states are not CP eigenstates, but they are still common final states for D^0 and \overline{D}^0 decays. Since $D^0(\overline{D}^0) \rightarrow K^-\pi^+$ is a Cabibbo-favored (doubly-Cabibbo-suppressed) process, these processes are particularly sensitive to x and/or $y = \mathcal{O}(\lambda^2)$. Taking into account that $|\lambda_{K^-\pi^+}|, |\lambda_{K^+\pi^-}^{-1}| \ll 1$ and $x, y \ll 1$, assuming that there is no direct CP violation (again, these are Standard Model tree level decays dominated by a single weak phase), and expanding the time-dependent rates for $xt, yt \lesssim \Gamma^{-1}$, one obtains

$$\begin{aligned} \frac{\Gamma[D_{\text{phys}}^0(t) \rightarrow K^+\pi^-]}{\Gamma[\overline{D}_{\text{phys}}^0(t) \rightarrow K^+\pi^-]} &= r_d^2 + r_d \left| \frac{q}{p} \right| (y' \cos \phi_D - x' \sin \phi_D)\Gamma t + \left| \frac{q}{p} \right|^2 \frac{y^2 + x^2}{4} (\Gamma t)^2, \\ \frac{\Gamma[\overline{D}_{\text{phys}}^0(t) \rightarrow K^-\pi^+]}{\Gamma[D_{\text{phys}}^0(t) \rightarrow K^-\pi^+]} &= r_d^2 + r_d \left| \frac{p}{q} \right| (y' \cos \phi_D + x' \sin \phi_D)\Gamma t + \left| \frac{p}{q} \right|^2 \frac{y^2 + x^2}{4} (\Gamma t)^2, \end{aligned} \quad (12.54)$$

where

$$\begin{aligned} y' &\equiv y \cos \delta - x \sin \delta, \\ x' &\equiv x \cos \delta + y \sin \delta. \end{aligned} \quad (12.55)$$

The weak phase ϕ_D is the same as that of Eq. (12.51) (a consequence of the absence of direct CP violation), δ is a strong phase difference for these processes, and $r_d = \mathcal{O}(\tan^2 \theta_c)$ is the amplitude ratio, $r_d = \left| \frac{\overline{A}_{K^-\pi^+}/A_{K^-\pi^+}}{A_{K^+\pi^-}/\overline{A}_{K^+\pi^-}} \right|$, that is, $\lambda_{K^-\pi^+} = r_d(q/p)e^{-i(\delta-\phi_D)}$ and $\lambda_{K^+\pi^-}^{-1} = r_d(p/q)e^{-i(\delta+\phi_D)}$. By fitting to the six coefficients of the various time-dependences, one can extract r_d , $|q/p|$, $(x^2 + y^2)$, $y' \cos \phi_D$, and $x' \sin \phi_D$. In particular, finding CP violation, that is, $|q/p| \neq 1$ and/or $\sin \phi_D \neq 0$, would constitute evidence for new physics.

More details on theoretical and experimental aspects of $D^0 - \overline{D}^0$ mixing can be found in [25]. Note that BABAR use $R_D \equiv r_d^2$ and $r_m \equiv |q/p|$. Belle use $R_m \equiv |q/p|$, $y_{CP} \equiv Y$, and $A_P \equiv -\Delta Y$.

12.6. B and B_s Decays

The upper bound on the CP asymmetry in semileptonic B decays [28] implies that CP violation in $B^0 - \overline{B}^0$ mixing is a small effect (we use $A_{\text{SL}}/2 \approx 1 - |q/p|$, see Eq. (12.25)):

$$A_{\text{SL}} = (0.3 \pm 1.3) \times 10^{-2} \implies |q/p| = 0.998 \pm 0.007. \quad (12.56)$$

The Standard Model prediction is

$$A_{\text{SL}} = \mathcal{O}\left(\frac{m_c^2}{m_t^2} \sin \beta\right) \lesssim 0.001. \quad (12.57)$$

In models where $\Gamma_{12}/\mathbf{M}_{12}$ is approximately real, such as the Standard Model, an upper bound on $\Delta\Gamma/\Delta m \approx \mathcal{R}e(\Gamma_{12}/\mathbf{M}_{12})$ provides yet another upper bound on the deviation of $|q/p|$ from one. This constraint does not hold if $\Gamma_{12}/\mathbf{M}_{12}$ is approximately imaginary. (An alternative parameterization uses $q/p = (1 - \bar{\epsilon}_B)/(1 + \bar{\epsilon}_B)$, leading to $A_{\text{SL}} \simeq 4\mathcal{R}e(\bar{\epsilon}_B)$.)

The small deviation (less than one percent) of $|q/p|$ from 1 implies that, at the present level of experimental precision, CP violation in B mixing is a negligible effect. Thus, for the purpose of analyzing CP asymmetries in hadronic B decays, we can use

$$\lambda_f = e^{-i\phi_{M(B)}} (\overline{A}_f/A_f), \quad (12.58)$$

where $\phi_{M(B)}$ refers to the phase of \mathbf{M}_{12} appearing in Eq. (12.30) that is appropriate for $B^0 - \overline{B}^0$ oscillations. Within the Standard Model, the corresponding phase factor is given by

$$e^{-i\phi_{M(B)}} = (V_{tb}^* V_{td}) / (V_{ub}^* V_{ud}). \quad (12.59)$$

Some of the most interesting decays involve final states that are common to B^0 and \overline{B}^0 [29,30]. It is convenient to rewrite Eq. (12.28) for B decays as [31,32,33]

$$\begin{aligned} A_f(t) &= S_f \sin(\Delta m t) - C_f \cos(\Delta m t), \\ S_f &\equiv \frac{2\mathcal{I}m(\lambda_f)}{1 + |\lambda_f|^2}, \quad C_f \equiv \frac{1 - |\lambda_f|^2}{1 + |\lambda_f|^2}, \end{aligned} \quad (12.60)$$

where we assume that $\Delta\Gamma = 0$ and $|q/p| = 1$. An alternative notation in use is $A_f \equiv -C_f$, but this A_f should not be confused with the A_f of Eq. (12.1).

The processes of interest proceed via quark transitions of the form $\bar{b} \rightarrow \bar{q}q'$ with $q' = s$ or d . For $q = c$ or u , there are contributions from both tree (t) and penguin (p^{qu}), where $q_u = u, c, t$ is the quark in the loop) diagrams (see Fig. 12.2) which carry different weak phases:

$$A_f = \left(V_{qb}^* V_{qq'} \right) t_f + \sum_{q_u=u,c,t} \left(V_{q_u b}^* V_{q_u q'} \right) p_f^{q_u}. \quad (12.61)$$

(The distinction between tree and penguin contributions is a heuristic one; the separation by the operator that enters is more precise. For a detailed discussion of the more complete operator product approach, which also includes higher order QCD corrections, see, for example, ref. [34].) Using CKM unitarity, these decay amplitudes can always

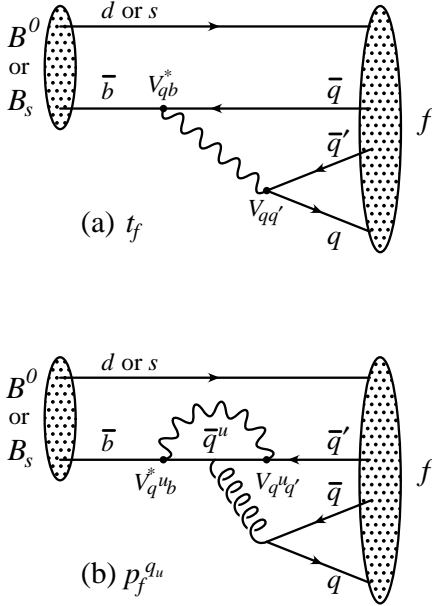


Figure 12.2: Feynman diagrams for (a) tree and (b) penguin amplitudes contributing to $B^0 \rightarrow f$ or $B_s \rightarrow f$ via a $\bar{b} \rightarrow \bar{q}q'$ quark-level process.

be written in terms of just two CKM combinations. For example, for $f = \pi\pi$, which proceeds via $\bar{b} \rightarrow \bar{u}u\bar{d}$ transition, we can write

$$A_{\pi\pi} = (V_{ub}^* V_{ud}) T_{\pi\pi} + (V_{tb}^* V_{td}) P_{\pi\pi}^t, \quad (12.62)$$

where $T_{\pi\pi} = t_{\pi\pi} + p_{\pi\pi}^c - p_{\pi\pi}^t$ and $P_{\pi\pi}^t = p_{\pi\pi}^t - p_{\pi\pi}^c$. CP -violating phases in Eq. (12.62) appear only in the CKM elements, so that

$$\frac{\bar{A}_{\pi\pi}}{A_{\pi\pi}} = \frac{(V_{ub} V_{ud}^*) T_{\pi\pi} + (V_{tb} V_{td}^*) P_{\pi\pi}^t}{(V_{ub}^* V_{ud}) T_{\pi\pi} + (V_{tb}^* V_{td}) P_{\pi\pi}^t}. \quad (12.63)$$

For $f = J/\psi K$, which proceeds via $\bar{b} \rightarrow \bar{c}c\bar{s}$ transition, we can write

$$A_{\psi K} = (V_{cb}^* V_{cs}) T_{\psi K} + (V_{ub}^* V_{us}) P_{\psi K}^u, \quad (12.64)$$

where $T_{\psi K} = t_{\psi K} + p_{\psi K}^c - p_{\psi K}^t$ and $P_{\psi K}^u = p_{\psi K}^u - p_{\psi K}^t$. A subtlety arises in this decay that is related to the fact that $B^0 \rightarrow J/\psi K^0$ and $\bar{B}^0 \rightarrow J/\psi \bar{K}^0$. A common final state, *e.g.*, $J/\psi K_S$, is reached only via $K^0 - \bar{K}^0$ mixing. Consequently, the phase factor (defined in Eq. (12.30)) corresponding to neutral K mixing, $e^{-i\phi_M(K)} = (V_{cd}^* V_{cs}) / (V_{cb}^* V_{cs})$, plays a role:

$$\frac{\bar{A}_{\psi K_S}}{A_{\psi K_S}} = -\frac{(V_{cb} V_{cs}^*) T_{\psi K} + (V_{ub} V_{us}^*) P_{\psi K}^u}{(V_{cb}^* V_{cs}) T_{\psi K} + (V_{ub}^* V_{us}) P_{\psi K}^u} \times \frac{V_{cd}^* V_{cs}}{V_{cb} V_{cs}^*}. \quad (12.65)$$

For $q = s$ or d , there are only penguin contributions to A_f , that is, $t_f = 0$ in Eq. (12.61). (The tree $\bar{b} \rightarrow \bar{u}u\bar{q}$ transition followed by $\bar{u}u \rightarrow \bar{q}q$ rescattering is included below in the P^u terms.) Again, CKM unitarity allows us to write A_f in terms of two CKM combinations. For example, for $f = \phi K_S$, which proceeds via $\bar{b} \rightarrow \bar{s}s\bar{s}$ transition, we can write

$$\frac{\bar{A}_{\phi K_S}}{A_{\phi K_S}} = -\frac{(V_{cb} V_{cs}^*) P_{\phi K}^c + (V_{ub} V_{us}^*) P_{\phi K}^u}{(V_{cb}^* V_{cs}) P_{\phi K}^c + (V_{ub}^* V_{us}) P_{\phi K}^u} \times \frac{V_{cd}^* V_{cs}}{V_{cb} V_{cs}^*}, \quad (12.66)$$

where $P_{\phi K}^c = p_{\phi K}^c - p_{\phi K}^t$ and $P_{\phi K}^u = p_{\phi K}^u - p_{\phi K}^t$.

Since the amplitude A_f involves two different weak phases, the corresponding decays can exhibit both CP violation in the interference of decays with and without mixing, $S_f \neq 0$, and CP violation in decays, $C_f \neq 0$. (At the present level of experimental precision, the contribution to C_f from CP violation in mixing is negligible, see Eq. (12.56).) If the contribution from a second weak phase is suppressed, then the interpretation of S_f in terms of Lagrangian CP -violating parameters is clean, while C_f is small. If such a second contribution is not suppressed, S_f depends on hadronic parameters and, if the relevant strong phase is large, C_f is large.

A summary of $\bar{b} \rightarrow \bar{q}q'q'$ modes with $q' = s$ or d is given in Table 12.1. The $\bar{b} \rightarrow \bar{d}d\bar{q}$ transitions lead to final states that are similar to the $\bar{b} \rightarrow \bar{u}u\bar{q}$ transitions and have similar phase dependence. Final states that consist of two vector-mesons ($\psi\phi$ and $\phi\phi$) are not CP eigenstates, and angular analysis will be needed to separate the CP -even from the CP -odd contributions.

Table 12.1: Summary of $\bar{b} \rightarrow \bar{q}q'$ modes with $q' = s$ or d . The second and third columns give examples of final hadronic states. The fourth column gives the CKM dependence of the amplitude A_f , using the notation of Eqs. (12.62, 12.64, 12.66), with the dominant term first and the sub-dominant second. The suppression factor of the second term compared to the first is given in the last column. ‘‘Loop’’ refers to a penguin tree suppression factor (it is mode-dependent and roughly $\mathcal{O}(0.2 - 0.3)$) and $\lambda = 0.22$ is the expansion parameter of Eq. (12.36).

$\bar{b} \rightarrow \bar{q}q'q'$	$B^0 \rightarrow f$	$B_s \rightarrow f$	CKM dependence of A_f	Suppression
$\bar{b} \rightarrow \bar{c}c\bar{s}$	ψK_S	$\psi\phi$	$(V_{cb}^* V_{cs})T + (V_{ub}^* V_{us})P^u$	loop $\times \lambda^2$
$\bar{b} \rightarrow \bar{s}s\bar{s}$	ϕK_S	$\phi\phi$	$(V_{cb}^* V_{cs})P^c + (V_{ub}^* V_{us})P^u$	λ^2
$\bar{b} \rightarrow \bar{u}u\bar{s}$	$\pi^0 K_S$	$K^+ K^-$	$(V_{cb}^* V_{cs})P^c + (V_{ub}^* V_{us})T$	λ^2/loop
$\bar{b} \rightarrow \bar{c}c\bar{d}$	$D^+ D^-$	ψK_S	$(V_{cb}^* V_{cd})T + (V_{tb}^* V_{td})P^t$	loop
$\bar{b} \rightarrow \bar{s}s\bar{d}$	$\phi\pi$	ϕK_S	$(V_{tb}^* V_{td})P^t + (V_{cb}^* V_{cd})P^c$	$\lesssim 1$
$\bar{b} \rightarrow \bar{u}u\bar{d}$	$\pi^+ \pi^-$	$\pi^0 K_S$	$(V_{ub}^* V_{ud})T + (V_{tb}^* V_{td})P^t$	loop

The cleanliness of the theoretical interpretation of S_f can be assessed from the information in the last column of Table 12.1. In case of small uncertainties, the expression for S_f in terms of CKM phases can be deduced from the fourth column of Table 12.1 in combination with Eq. (12.59) (and, for $b \rightarrow \bar{q}q's$ decays, the example in Eq. (12.65)). Here we consider several interesting examples.

For $B \rightarrow J/\psi K_S$ and other $\bar{b} \rightarrow \bar{c}c\bar{s}$ processes, we can neglect the P^u contribution to A_f , in the Standard Model, to an approximation that is better than one percent:

$$\lambda_{\psi K_S} = -e^{-2i\beta} \Rightarrow S_{\psi K_S} = \sin 2\beta, \quad C_{\psi K_S} = 0. \quad (12.67)$$

(Below the percent level, several effects have to be taken into account [35].) In the presence of new physics, A_f is still likely to be dominated by the T term, but the mixing amplitude might be modified. We learn that, model independently, $C_f \approx 0$ while S_f cleanly determines the mixing phase ($\phi_M - 2 \arg(V_{cb} V_{cd}^*)$). The experimental measurement [28], $S_{\psi K} = 0.731 \pm 0.056$, gave the first precision test of the Kobayashi-Maskawa mechanism, and its consistency with the predictions for $\sin 2\beta$ makes it very likely that this mechanism is indeed the dominant source of CP violation in meson decays.

For $B \rightarrow \phi K_S$ and other $\bar{b} \rightarrow \bar{s}s\bar{s}$ processes, we can neglect the P^u contribution to A_f , in the Standard Model, to an approximation that is good to order of a few percent:

$$\lambda_{\phi K_S} = -e^{-2i\beta} \Rightarrow S_{\phi K_S} = \sin 2\beta, \quad C_{\phi K_S} = 0. \quad (12.68)$$

In the presence of new physics, both A_f and M_{12} can get contributions that are comparable in size to those of the Standard Model and carry new weak phases. Such a situation gives several interesting consequences for $b \rightarrow \bar{s}s\bar{s}$ decays:

1. The value of S_f may be different from $S_{\psi K_S}$ by more than a few percent.
2. The values of S_f for different final states f may be different from each other by more than a few percent (for example, $S_{\phi K_S} \neq S_{\eta' K_S}$).
3. The value of C_f may be different from zero by more than a few percent.

While a clear interpretation of such signals in terms of Lagrangian parameters will be difficult because, under these circumstances, hadronic parameters do play a role, any of the above three options will clearly signal new physics. Present experimental results give [28] $S_{\eta' K} = 0.27 \pm 0.21$ and $S_{\phi K} = -1.0 \pm 0.5$. Thus, for this class of modes, neither $S_f \neq 0$ nor $S_f \neq S_{\psi K}$ is unambiguously established, but there is definitely still room for new physics.

For $B \rightarrow \pi\pi$ and other $\bar{b} \rightarrow \bar{u}ud$ processes, the penguin-to-tree ratio can be estimated using SU(3) relations and experimental data on related $B \rightarrow K\pi$ decays. The result is that the suppression is of order 0.2–0.3 and so cannot be neglected. The expressions for $S_{\pi\pi}$ and $C_{\pi\pi}$ to leading order in $R_{PT} \equiv (|V_{ub}V_{ud}|/|V_{ub}V_{ud}|)P_{\pi\pi}^t/(|V_{ub}V_{ud}|T_{\pi\pi})$ are:

$$\lambda_{\pi\pi} = e^{2i\alpha} \left[(1 - R_{PT} e^{-i\alpha}) / (1 - R_{PT} e^{+i\alpha}) \right] \Rightarrow$$

$$S_{\pi\pi} \approx \sin 2\alpha + 2\mathcal{R}e(R_{PT}) \cos 2\alpha \sin \alpha, \quad C_{\pi\pi} \approx 2\mathcal{I}m(R_{PT}) \sin \alpha. \quad (12.69)$$

Note that R_{PT} is mode-dependent and, in particular, could be different for $\pi^+\pi^-$ and $\pi^0\pi^0$. If strong phases can be neglected then R_{PT} is real, resulting in $C_{\pi\pi} = 0$. The size of $C_{\pi\pi}$ is an indicator of how large the strong phase is. The present experimental range is [28] $C_{\pi\pi} = -0.51 \pm 0.23$. As concerns $S_{\pi\pi}$, it is clear from Eq. (12.69) that the relative size and strong phase of the penguin contribution must be known to extract α . This is the problem of penguin pollution.

The cleanest solution involves isospin relations among the $B \rightarrow \pi\pi$ amplitudes [36]:

$$\frac{1}{\sqrt{2}}A_{\pi^+\pi^-} + A_{\pi^0\pi^0} = A_{\pi^+\pi^0}. \quad (12.70)$$

The method exploits the fact that the penguin contribution to $P_{\pi\pi}^t$ is pure $\Delta I = \frac{1}{2}$ (this is not true for the electroweak penguins which, however, are expected to be small), while the tree contribution to $T_{\pi\pi}$ contains pieces which are both $\Delta I = \frac{1}{2}$ and $\Delta I = \frac{3}{2}$. A simple geometric construction then allows one to find R_{PT} and extract α cleanly from $S_{\pi^+\pi^-}$. The key experimental difficulty is that one must measure accurately the separate rates for $B^0, \bar{B}^0 \rightarrow \pi^0\pi^0$. It has been noted that an upper bound on the average rate allows one to put a useful upper bound on the deviation of $S_{\pi^+\pi^-}$ from $\sin 2\alpha$ [37,38,39]. Parametrizing the asymmetry by $S_{\pi^+\pi^-} / \sqrt{1 - (C_{\pi^+\pi^-})^2} = \sin(2\alpha + 2\delta_{+-})$, the bound reads

$$\cos 2\delta_{+-} \geq \frac{1}{\sqrt{1 - (C_{\pi^+\pi^-})^2}} \left[1 - \frac{2B_{00}}{B_{+0}} + \frac{(B_{+-} - 2B_{+0} + 2B_{00})^2}{4B_{+-}B_{+0}} \right], \quad (12.71)$$

where B_{ij} are the averages over CP-conjugate branching ratios; e.g., $B_{00} = \frac{1}{2}[B(B^0 \rightarrow \pi^0\pi^0) + B(\bar{B}^0 \rightarrow \pi^0\pi^0)]$. CP asymmetries in $B \rightarrow \rho\pi$ and, in particular, in $B \rightarrow \rho\rho$ can also be used to determine α .

For B_s decays, one has to replace Eq. (12.59) with $e^{-i\phi_{M(B_s)}} = (V_{tb}^*V_{ts})/(V_{ub}^*V_{us})$. Note that one expects $\Delta\Gamma/\Gamma = \mathcal{O}(0.1)$, and therefore, y should not be put to zero in Eqs. (12.18,12.19), but $|q/p| = 1$ is expected to hold to an even better approximation than for B mesons. The CP asymmetry in $B_s \rightarrow J/\psi\phi$ will determine (with angular analysis to disentangle the CP-even and CP-odd components of the final state) $\sin 2\beta_s$, where

$$\beta_s \equiv \arg \left(-\frac{V_{ts}V_{cb}^*}{V_{cs}V_{tb}^*} \right). \quad (12.72)$$

Another class of interesting decay modes is that of the tree level decays of B_s and \bar{B}_s into $D_s^\pm K^\mp$. The quark sub-processes are $\bar{b} \rightarrow \bar{c}u\bar{s}$, $\bar{b} \rightarrow \bar{u}c\bar{s}$, and the two CP-conjugate processes. Measuring the four time dependent decay rates, one can cleanly extract the angle γ [40]. (Similarly, γ can be extracted from the time dependent rates of $B \rightarrow DK$ decays [41].)

12.7. Summary and Outlook

CP violation has been experimentally established in neutral K and B meson decays:

1. All three types of CP violation have been observed in $K \rightarrow \pi\pi$ decays:

$$\mathcal{R}e(\epsilon') = \frac{1}{6} \left(\left| \frac{\bar{A}_{\pi^0\pi^0}}{A_{\pi^0\pi^0}} \right| - \left| \frac{\bar{A}_{\pi^+\pi^-}}{A_{\pi^+\pi^-}} \right| \right) = (2.5 \pm 0.4) \times 10^{-6} \text{ (I)}$$

$$\mathcal{R}e(\epsilon) = \frac{1}{2} \left(1 - \left| \frac{q}{p} \right| \right) = (1.657 \pm 0.021) \times 10^{-3} \quad \text{(II)}$$

$$\mathcal{I}m(\epsilon) = -\frac{1}{2}\mathcal{I}m(\lambda_{(\pi\pi)_{I=0}}) = (1.572 \pm 0.022) \times 10^{-3} \quad \text{(III)} \quad (12.73)$$

2. CP violation in interference of decays with and without mixing has been observed in $B \rightarrow J/\psi K_S$ decays [28] (and related modes):

$$S_{\psi K} = \mathcal{I}m(\lambda_{\psi K}) = 0.731 \pm 0.056 \quad \text{(III)} \quad (12.74)$$

Searches for additional types of CP violation are ongoing in B , D , and K decays, and current limits are consistent with Standard Model expectations.

Beyond Standard Model predictions, observation of direct CP violation in B decays seems promising for the near future, followed later by CP violation observed in B_s decays and in the process $K \rightarrow \pi\nu\bar{\nu}$. Observables that are subject to clean theoretical interpretation, such as $S_{\psi K_S}$ and $\mathcal{B}(K_L \rightarrow \pi^0\nu\bar{\nu})$, are of particular value for constraining the values of the CKM parameters and probing the flavor sector of extensions to the Standard Model. Other probes of CP violation now being pursued experimentally include the electric dipole moments of the neutron and electron, and the decays of tau leptons. Additional processes that are likely to play an important role in future CP studies include top-quark production and decay, and neutrino oscillations.

All measurements of CP violation to date are consistent with the predictions of the Kobayashi-Maskawa mechanism of the Standard Model. However, a dynamically-generated matter-antimatter asymmetry of the universe requires additional sources of CP violation, and such sources are naturally generated by extensions to the Standard Model. New sources might eventually reveal themselves as small deviations from the predictions of the KM mechanism in meson decay rates, or else might not be observable in meson decays at all, but observable with future probes such as neutrino oscillations or electric dipole moments. We cannot guarantee that new sources of CP violation will ever be found experimentally, but the fundamental nature of CP violation demands a vigorous effort.

A number of excellent reviews of CP violation are available [42–45], where the interested reader may find a detailed discussion of the various topics that are briefly reviewed here. Another book on CP violation that will shortly appear is Ref. 46.

References:

1. J.H. Christenson *et al.*, Phys. Rev. Lett. **13**, 138 (1964).
2. B. Aubert *et al.* [BABAR Collaboration], Phys. Rev. Lett. **87**, 091801 (2001).
3. K. Abe *et al.* [Belle Collaboration], Phys. Rev. Lett. **87**, 091802 (2001).
4. See results on the ‘Time reversal invariance’ within the review on ‘Tests of conservation laws’ in this report.

5. M. Kobayashi and T. Maskawa, *Prog. Theor. Phys.* **49**, 652 (1973).
6. A.D. Sakharov, *Pisma Zh. Eksp. Teor. Fiz.* **5**, 32 (1967) [*Sov. Phys. JETP Lett.* **5**, 24 (1967)].
7. For a review, see *e.g.* A. Riotto, "Theories of baryogenesis," [arXiv:hep-ph/9807454](https://arxiv.org/abs/hep-ph/9807454).
8. M. Fukugita and T. Yanagida, *Phys. Lett.* **B174**, 45 (1986).
9. V. Weisskopf and E. P. Wigner, *Z. Phys.* **63**, 54 (1930); *Z. Phys.* **65**, 18 (1930). [See also Appendix A of P.K. Kabir, "The CP Puzzle: Strange Decays of the Neutral Kaon," Academic Press (1968)].
10. O. Long *et al.*, *Phys. Rev.* **D68**, 034010 (2003).
11. L. Wolfenstein, *Phys. Rev. Lett.* **13**, 562 (1964).
12. See the review on 'Cabibbo-Kobayashi-Maskawa mixing matrix' in this report.
13. L. Wolfenstein, *Phys. Rev. Lett.* **51**, 1945 (1983).
14. A.J. Buras, M.E. Lautenbacher, and G. Ostermaier, *Phys. Rev.* **D50**, 3433 (1994).
15. C. Jarlskog, *Phys. Rev. Lett.* **55**, 1039 (1985).
16. H. Burkhardt *et al.* [NA31 Collaboration], *Phys. Lett.* **B206**, 169 (1988).
17. V. Fanti *et al.* [NA48 Collaboration], *Phys. Lett.* **B465**, 335 (1999).
18. A. Alavi-Harati *et al.* [KTeV Collaboration], *Phys. Rev. Lett.* **83**, 22 (1999).
19. See the *K*-meson listings in this report.
20. See the review on '*CP* violation in $K_S \rightarrow 3\pi$ ' in this report.
21. Y. Grossman and Y. Nir, *Phys. Lett.* **B398**, 163 (1997).
22. L.S. Littenberg, *Phys. Rev.* **D39**, 3322 (1989).
23. A.J. Buras, *Phys. Lett.* **B333**, 476 (1994).
24. G. Buchalla and A.J. Buras, *Nucl. Phys.* **B400**, 225 (1993).
25. See the review on ' $D^0 - \bar{D}^0$ mixing' in this report.
26. See the *D*-meson listings in this report.
27. S. Bergmann *et al.*, *Phys. Lett.* **B486**, 418 (2000).
28. See the *B*-meson listings in this report.
29. A.B. Carter and A.I. Sanda, *Phys. Rev. Lett.* **45**, 952 (1980); *Phys. Rev.* **D23**, 1567 (1981).
30. I.I. Bigi and A.I. Sanda, *Nucl. Phys.* **B193**, 85 (1981).
31. I. Dunietz and J.L. Rosner, *Phys. Rev.* **D34**, 1404 (1986).
32. Ya.I. Azimov, N.G. Uraltsev, and V.A. Khoze, *Sov. J. Nucl. Phys.* **45**, 878 (1987) [*Yad. Fiz.* **45**, 1412 (1987)].
33. I.I. Bigi and A.I. Sanda, *Nucl. Phys.* **B281**, 41 (1987).
34. G. Buchalla, A.J. Buras, and M.E. Lautenbacher, *Rev. Mod. Phys.* **68**, 1125 (1996).
35. Y. Grossman, A.L. Kagan and Z. Ligeti, *Phys. Lett.* **B538**, 327 (2002).
36. M. Gronau and D. London, *Phys. Rev. Lett.* **65**, 3381 (1990).
37. Y. Grossman and H.R. Quinn, *Phys. Rev.* **D58**, 017504 (1998).
38. J. Charles, *Phys. Rev.* **D59**, 054007 (1999).
39. M. Gronau *et al.*, *Phys. Lett.* **B514**, 315 (2001).
40. R. Aleksan, I. Dunietz and B. Kayser, *Z. Phys.* **C54**, 653 (1992).
41. M. Gronau and D. Wyler, *Phys. Lett.* **B265**, 172 (1991).
42. G.C. Branco, L. Lavoura, and J.P. Silva, "*CP* violation," Oxford University Press, Oxford (1999).
43. I.I. Y. Bigi and A.I. Sanda, "*CP* Violation," Cambridge Monogr. Part. Phys. Nucl. Phys. Cosmol. **9**, 1 (2000).
44. P.F. Harrison and H.R. Quinn, editors [BABAR Collaboration], "The BABAR physics book: Physics at an asymmetric *B* factory," SLAC-R-0504.
45. K. Anikeev *et al.*, "*B* physics at the Tevatron: Run II and beyond," [arXiv:hep-ph/0201071](https://arxiv.org/abs/hep-ph/0201071).
46. K. Kleinknecht, "Uncovering *CP* Violation," Springer tracts in modern physics **195** (2003).

13. NEUTRINO MASS, MIXING, AND FLAVOR CHANGE

Revised November 2003 by B. Kayser (Fermilab).

There is now convincing evidence that both atmospheric and solar neutrinos change from one flavor to another. There is also very strong evidence that reactor anti-neutrinos do this, and interesting evidence that accelerator neutrinos do it as well. Barring exotic possibilities, neutrino flavor change implies that neutrinos have masses and that leptons mix. In this review, we discuss the physics of flavor change and the evidence for it, summarize what has been learned so far about neutrino masses and leptonic mixing, consider the relation between neutrinos and their antiparticles, and discuss the open questions about neutrinos to be answered by future experiments.

I. The physics of flavor change: If neutrinos have masses, then there is a spectrum of three or more neutrino mass eigenstates, $\nu_1, \nu_2, \nu_3, \dots$, that are the analogues of the charged-lepton mass eigenstates, e, μ , and τ . If leptons mix, the weak interaction coupling the W boson to a charged lepton, and a neutrino can couple any charged-lepton mass eigenstate ℓ_α to any neutrino mass eigenstate ν_i . Here, $\alpha = e, \mu$, or τ , and ℓ_e is the electron, *etc.*. Leptonic W^+ decay can yield a particular ℓ_α^+ in association with any ν_i . The amplitude for this decay to produce the specific combination $\ell_\alpha^+ + \nu_i$ is $U_{\alpha i}^*$, where U is the unitary leptonic mixing matrix [1]. Thus, the neutrino state created in the decay $W^+ \rightarrow \ell_\alpha^+ + \nu$ is the state

$$|\nu_\alpha\rangle = \sum_i U_{\alpha i}^* |\nu_i\rangle. \quad (13.1)$$

This superposition of neutrino mass eigenstates, produced in association with the charged lepton of “flavor” α , is the state we refer to as the neutrino of flavor α .

While there are only three (known) charged lepton mass eigenstates, the experimental results suggest that perhaps there are more than three neutrino mass eigenstates. If, for example, there are four ν_i , then one linear combination of them,

$$|\nu_s\rangle = \sum_i U_{s i}^* |\nu_i\rangle, \quad (13.2)$$

does not have a charged-lepton partner, and consequently does not couple to the Standard Model W boson. Indeed, since the decays $Z \rightarrow \nu_\alpha \bar{\nu}_\alpha$ of the Standard Model Z boson have been found to yield only three distinct neutrinos ν_α of definite flavor [2], ν_s does not couple to the Z boson either. Such a neutrino, which does not have any Standard Model weak couplings, is referred to as a “sterile” neutrino.

To understand neutrino flavor change, or “oscillation,” in vacuum, let us consider how a neutrino born as the ν_α of Eq. (13.1) evolves in time. First, we apply Schrödinger’s equation to the ν_i component of ν_α in the rest frame of that component. This tells us that

$$|\nu_i(\tau_i)\rangle = e^{-im_i\tau_i} |\nu_i(0)\rangle, \quad (13.3)$$

where m_i is the mass of ν_i , and τ_i is time in the ν_i frame. In terms of the time t and position L in the laboratory frame, the Lorentz-invariant phase factor in Eq. (13.3) may be written

$$e^{-im_i\tau_i} = e^{-i(E_i t - p_i L)}. \quad (13.4)$$

Here, E_i and p_i are respectively the energy and momentum of ν_i in the laboratory frame. In practice, our neutrino will be extremely relativistic, so we will be interested in evaluating the phase factor of Eq. (13.4) with $t \approx L$, where it becomes $\exp[-i(E_i - p_i)L]$.

Imagine now that our ν_α has been produced with a definite momentum p , so that all of its mass-eigenstate components have this common momentum. Then the ν_i component has $E_i = \sqrt{p^2 + m_i^2} \approx p + m_i^2/2p$, assuming that all neutrino masses m_i are small compared to the neutrino momentum. The phase factor of Eq. (13.4) is then approximately

$$e^{-i(m_i^2/2p)L}. \quad (13.5)$$

From this expression and Eq. (13.1), it follows that after a neutrino born as a ν_α has propagated a distance L , its state vector has become

$$|\nu_\alpha(L)\rangle \approx \sum_i U_{\alpha i}^* e^{-i(m_i^2/2E)L} |\nu_i\rangle. \quad (13.6)$$

Here, $E \simeq p$ is the average energy of the various mass eigenstate components of the neutrino. Using the unitarity of U to invert Eq. (13.1), and inserting the result in Eq. (13.6), we find that

$$|\nu_\alpha(L)\rangle \approx \sum_\beta \left[\sum_i U_{\alpha i}^* e^{-i(m_i^2/2E)L} U_{\beta i} \right] |\nu_\beta\rangle. \quad (13.7)$$

We see that our ν_α , in traveling the distance L , has turned into a superposition of all the flavors. The probability that it has flavor β , $P(\nu_\alpha \rightarrow \nu_\beta)$, is obviously $|\langle \nu_\beta | \nu_\alpha(L) \rangle|^2$. From Eq. (13.7) and the unitarity of U , we easily find that

$$\begin{aligned} P(\nu_\alpha \rightarrow \nu_\beta) &= \delta_{\alpha\beta} \\ &- 4 \sum_{i>j} \Re(U_{\alpha i}^* U_{\beta i} U_{\alpha j} U_{\beta j}^*) \sin^2[1.27 \Delta m_{ij}^2(L/E)] \\ &+ 2 \sum_{i>j} \Im(U_{\alpha i}^* U_{\beta i} U_{\alpha j} U_{\beta j}^*) \sin[2.54 \Delta m_{ij}^2(L/E)]. \end{aligned} \quad (13.8)$$

Here, $\Delta m_{ij}^2 \equiv m_i^2 - m_j^2$ is in eV^2 , L is in km, and E is in GeV. We have used the fact that when the previously omitted factors of \hbar and c are included,

$$\Delta m_{ij}^2(L/4E) \simeq 1.27 \Delta m_{ij}^2(\text{eV}^2) \frac{L(\text{km})}{E(\text{GeV})}. \quad (13.9)$$

The quantum mechanics of neutrino oscillation leading to the result Eq. (13.8) is somewhat subtle. To do justice to the physics requires a more refined treatment [3] than the one we have given. Sophisticated treatments continue to yield new insights [4].

Assuming that CPT invariance holds,

$$P(\bar{\nu}_\alpha \rightarrow \bar{\nu}_\beta) = P(\nu_\beta \rightarrow \nu_\alpha). \quad (13.10)$$

But, from Eq. (13.8) we see that

$$P(\nu_\beta \rightarrow \nu_\alpha; U) = P(\nu_\alpha \rightarrow \nu_\beta; U^*). \quad (13.11)$$

Thus, when CPT holds,

$$P(\bar{\nu}_\alpha \rightarrow \bar{\nu}_\beta; U) = P(\nu_\alpha \rightarrow \nu_\beta; U^*). \quad (13.12)$$

That is, the probability for oscillation of an anti-neutrino is the same as that for a neutrino, except that the mixing matrix U is replaced by its complex conjugate. Thus, if U is not real, the neutrino and anti-neutrino oscillation probabilities can differ by having opposite values of the last term in Eq. (13.8). When CPT holds, any difference between these probabilities indicates a violation of CP invariance.

As we shall see, the squared-mass splittings Δm_{ij}^2 called for by the various reported signals of oscillation are quite different from one another. It may be that one splitting, ΔM^2 , is much bigger than all the others. If that is the case, then for an oscillation experiment with L/E such that $\Delta M^2 L/E = \mathcal{O}(1)$, Eq. (13.8) simplifies considerably, becoming

$$P(\bar{\nu}_\alpha \rightarrow \bar{\nu}_\beta) \simeq S_{\alpha\beta} \sin^2[1.27 \Delta M^2(L/E)] \quad (13.13)$$

for $\beta \neq \alpha$, and

$$P(\bar{\nu}_\alpha \rightarrow \bar{\nu}_\alpha) \simeq 1 - 4 T_\alpha(1 - T_\alpha) \sin^2[1.27 \Delta M^2(L/E)]. \quad (13.14)$$

Here,

$$S_{\alpha\beta} \equiv 4 \left| \sum_{i \text{ U p}} U_{\alpha i}^* U_{\beta i} \right|^2 \quad (13.15)$$

and

$$T_\alpha \equiv \sum_{i \in \text{Up}} |U_{\alpha i}|^2, \quad (13.16)$$

where “ $i \in \text{Up}$ ” denotes a sum over only those neutrino mass eigenstates that lie *above* ΔM^2 or, alternatively, only those that lie *below* it. The unitarity of U guarantees that summing over either of these two clusters will yield the same results for $S_{\alpha\beta}$ and for $T_\alpha(1 - T_\alpha)$.

The situation described by Eqs. (13.13)–(13.16) may be called “quasi-two-neutrino oscillation.” It has also been called “one mass scale dominance” [5]. It corresponds to an experiment whose L/E is such that the experiment can “see” only the big splitting ΔM^2 . To this experiment, all the neutrinos above ΔM^2 appear to be a single neutrino, as do all those below ΔM^2 .

The relations of Eqs. (13.13)–(13.16) also apply to the special case where, to a good approximation, only two mass eigenstates, and two corresponding flavor eigenstates (or two linear combinations of flavor eigenstates), are relevant. One encounters this case when, for example, only two mass eigenstates couple significantly to the charged lepton with which the neutrino being studied is produced. When only two mass eigenstates count, there is only a single splitting, Δm^2 , and, omitting irrelevant phase factors, the unitary mixing matrix U takes the form

$$U = \begin{matrix} & \nu_1 & \nu_2 \\ \nu_\alpha & \begin{bmatrix} \cos\theta & \sin\theta \\ -\sin\theta & \cos\theta \end{bmatrix} \end{matrix}. \quad (13.17)$$

Here, the symbols above and to the left of the matrix label the columns and rows, and θ is referred to as the mixing angle. From Eqs. (13.15) and (13.16), we now have $S_{\alpha\beta} = \sin^2 2\theta$ and $4T_\alpha(1 - T_\alpha) = \sin^2 2\theta$, so that Eqs. (13.13) and (13.14) become, respectively,

$$P(\bar{\nu}_\alpha \rightarrow \bar{\nu}_\beta) = \sin^2 2\theta \sin^2[1.27 \Delta m^2 (L/E)] \quad (13.18)$$

with $\beta \neq \alpha$, and

$$P(\bar{\nu}_\alpha \rightarrow \bar{\nu}_\alpha) = 1 - \sin^2 2\theta \sin^2[1.27 \Delta m^2 (L/E)]. \quad (13.19)$$

Many experiments have been analyzed using these two expressions. Some of these experiments actually have been concerned with quasi-two-neutrino oscillation, rather than a genuinely two-neutrino situation. For these experiments, “ $\sin^2 2\theta$ ” and “ Δm^2 ” have the significance that follows from Eqs. (13.13)–(13.16).

When neutrinos travel through matter (*e.g.* in the Sun, Earth, or a supernova), their coherent forward scattering from particles they encounter along the way can significantly modify their propagation [6]. As a result, the probability for changing flavor can be rather different than it is in vacuum [7]. Flavor change that occurs in matter, and that grows out of the interplay between flavor-nonchanging neutrino-matter interactions and neutrino mass and mixing, is known as the Mikheyev-Smirnov-Wolfenstein (MSW) effect.

To a good approximation, one can describe neutrino propagation through matter via a Schrödinger-like equation. This equation governs the evolution of a neutrino state vector with several components, one for each flavor. The effective Hamiltonian in the equation, a matrix \mathcal{H} in neutrino flavor space, differs from its vacuum counterpart by the addition of interaction energies arising from the coherent forward neutrino scattering. For example, the ν_e - ν_e element of \mathcal{H} includes the interaction energy

$$V = \sqrt{2} G_F N_e, \quad (13.20)$$

arising from W -exchange-induced ν_e forward scattering from ambient electrons. Here, G_F is the Fermi constant, and N_e is the number of electrons per unit volume. In addition, the ν_e - ν_e , ν_μ - ν_μ , and ν_τ - ν_τ elements of \mathcal{H} all contain a common interaction energy growing out of Z -exchange-induced forward scattering. However, when one is not considering the possibility of transitions to sterile neutrino flavors, this common interaction energy merely adds to \mathcal{H} a multiple of the identity matrix, and such an addition has no effect on flavor transitions.

The effect of matter is illustrated by the propagation of solar neutrinos through solar matter. When combined with information

on atmospheric neutrino oscillation, the experimental bounds on short-distance ($L \lesssim 1$ km) oscillation of reactor $\bar{\nu}_e$ [8] tell us that, if there are no sterile neutrinos, then only two neutrino mass eigenstates, ν_1 and ν_2 , are significantly involved in the evolution of the solar neutrinos. Correspondingly, only two flavors are involved: the ν_e flavor with which every solar neutrino is born, and the effective flavor ν_x — some linear combination of ν_μ and ν_τ — which it may become. The Hamiltonian \mathcal{H} is then a 2×2 matrix in ν_e - ν_x space. Apart from an irrelevant multiple of the identity, for a distance r from the center of the Sun, \mathcal{H} is given by

$$\begin{aligned} \mathcal{H} &= \mathcal{H}_V + \mathcal{H}_M(r) \\ &= \frac{\Delta m_\odot^2}{4E} \begin{bmatrix} -\cos 2\theta_\odot & \sin 2\theta_\odot \\ \sin 2\theta_\odot & \cos 2\theta_\odot \end{bmatrix} + \begin{bmatrix} V(r) & 0 \\ 0 & 0 \end{bmatrix}. \end{aligned} \quad (13.21)$$

Here, the first matrix \mathcal{H}_V is the Hamiltonian in vacuum, and the second matrix $\mathcal{H}_M(r)$ is the modification due to matter. In \mathcal{H}_V , θ_\odot is the solar mixing angle defined by the two-neutrino mixing matrix of Eq. (13.17) with $\theta = \theta_\odot$, $\nu_\alpha = \nu_e$, and $\nu_\beta = \nu_x$. The splitting Δm_\odot^2 is $m_2^2 - m_1^2$, and for the present purpose we *define* ν_2 to be the heavier of the two mass eigenstates, so that Δm_\odot^2 is positive. In $\mathcal{H}_M(r)$, $V(r)$ is the interaction energy of Eq. (13.20) with the electron density $N_e(r)$ evaluated at distance r from the Sun’s center.

From Eqs. (13.18)–(13.19) (with $\theta = \theta_\odot$), we see that two-neutrino oscillation in vacuum cannot distinguish between a mixing angle θ_\odot and an angle $\theta'_\odot = \pi/2 - \theta_\odot$. But these two mixing angles represent physically different situations. Suppose, for example, that $\theta_\odot < \pi/4$. Then, from Eq. (13.17) we see that if the mixing angle is θ_\odot , the lighter mass eigenstate (defined to be ν_1) is more ν_e than ν_x , while if it is θ'_\odot , then this mass eigenstate is more ν_x than ν_e . While oscillation in vacuum cannot discriminate between these two possibilities, neutrino propagation through solar matter can do so. The neutrino interaction energy V of Eq. (13.20) is of definite, positive sign [9]. Thus, the ν_e - ν_e element of the solar \mathcal{H} , $-(\Delta m_\odot^2/4E) \cos 2\theta_\odot + V(r)$, has a different size when the mixing angle is $\theta'_\odot = \pi/2 - \theta_\odot$ than it does when this angle is θ_\odot . As a result, the flavor content of the neutrinos coming from the Sun can be different in the two cases [10].

Solar and long-baseline reactor neutrino data establish that the behavior of solar neutrinos is governed by a Large-Mixing-Angle (LMA) MSW effect (see Sec. II). Let us estimate the probability $P(\nu_e \rightarrow \nu_e)$ that a solar neutrino which undergoes the LMA-MSW effect in the Sun still has its original ν_e flavor when it arrives at the Earth. We focus on the neutrinos produced by ${}^8\text{B}$ decay, which are at the high-energy end of the solar neutrino spectrum. At $r \simeq 0$, where the solar neutrinos are created, the electron density $N_e \simeq 6 \times 10^{25}/\text{cm}^3$ [11] yields for the interaction energy V of Eq. (13.20) the value $0.75 \times 10^{-5} \text{ eV}^2/\text{MeV}$. Thus, for Δm_\odot^2 in the favored region, around $7 \times 10^{-5} \text{ eV}^2$, and E a typical ${}^8\text{B}$ neutrino energy (~ 6 - 7 MeV), \mathcal{H}_M dominates over \mathcal{H}_V . This means that, in first approximation, $\mathcal{H}(r \simeq 0)$ is diagonal. Thus, a ${}^8\text{B}$ neutrino is born not only in a ν_e flavor eigenstate, but also, again in first approximation, in an eigenstate of the Hamiltonian $\mathcal{H}(r \simeq 0)$. Since $V > 0$, the neutrino will be in the heavier of the two eigenstates. Now, under the conditions where the LMA-MSW effect occurs, the propagation of a neutrino from $r \simeq 0$ to the outer edge of the Sun is adiabatic. That is, $N_e(r)$ changes sufficiently slowly that we may solve Schrödinger’s equation for one r at a time, and then patch together the solutions. This means that our neutrino propagates outward through the Sun as one of the r -dependent eigenstates of the r -dependent $\mathcal{H}(r)$. Since the eigenvalues of $\mathcal{H}(r)$ do not cross at any r , and our neutrino is born in the heavier of the two $r = 0$ eigenstates, it emerges from the Sun in the heavier of the two \mathcal{H}_V eigenstates. The latter is the mass eigenstate we have called ν_2 , given according to Eq. (13.17) by

$$\nu_2 = \nu_e \sin \theta_\odot + \nu_x \cos \theta_\odot. \quad (13.22)$$

Since this is an eigenstate of the vacuum Hamiltonian, the neutrino remains in it all the way to the surface of the Earth. The probability of observing the neutrino as a ν_e on Earth is then just the probability that ν_2 is a ν_e . That is [cf. Eq. (13.22)] [12],

$$P(\nu_e \rightarrow \nu_e) = \sin^2 \theta_\odot. \quad (13.23)$$

We note that for $\theta_{\odot} < \pi/4$, this ν_e survival probability is less than 1/2. In contrast, when matter effects are negligible, the energy-averaged survival probability in two-neutrino oscillation cannot be less than 1/2 for any mixing angle [see Eq. (13.19)] [13].

II. The evidence for flavor metamorphosis: The persuasiveness of the evidence that neutrinos actually do change flavor in nature is summarized in Table 13.1. We discuss the different pieces of evidence.

Table 13.1: The persuasiveness of the evidence for neutrino flavor change. The symbol L denotes the distance travelled by the neutrinos. LSND is the Liquid Scintillator Neutrino Detector experiment.

Neutrinos	Evidence for Flavor Change
Atmospheric	Compelling
Accelerator ($L = 250$ km)	Interesting
Solar	Compelling
Reactor ($L \sim 180$ km)	Very Strong
From Stopped μ^+ Decay (LSND)	Unconfirmed

The atmospheric neutrinos are produced in the Earth's atmosphere by cosmic rays, and then detected in an underground detector. The flux of cosmic rays that lead to neutrinos with energies above a few GeV is isotropic, so that these neutrinos are produced at the same rate all around the Earth. This can easily be shown to imply that at any underground site, the downward- and upward-going fluxes of multi-GeV neutrinos of a given flavor must be equal. That is, unless some mechanism changes the flux of neutrinos of the given flavor as they propagate, the flux coming down from zenith angle θ_Z must equal that coming up from angle $\pi - \theta_Z$ [14].

The underground Super-Kamiokande (SK) detector finds that for multi-GeV atmospheric muon neutrinos [15],

$$\frac{\text{Flux Up}(-1.0 < \cos \theta_Z < -0.2)}{\text{Flux Down}(+0.2 < \cos \theta_Z < +1.0)} = 0.54 \pm 0.04, \quad (13.24)$$

in strong disagreement with equality of the upward and downward fluxes. Thus, some mechanism does change the ν_μ flux as the neutrinos travel to the detector. The most attractive candidate for this mechanism is the oscillation $\nu_\mu \rightarrow \nu_X$ of the muon neutrinos into neutrinos ν_X of another flavor. Since the upward-going muon neutrinos come from the atmosphere on the opposite side of the Earth from the detector, they travel much farther than the downward-going ones to reach the detector. Thus, they have more time to oscillate away into the other flavor, which explains why Flux Up < Flux Down. The null results of short-baseline reactor neutrino experiments [8] imply limits on $P(\bar{\nu}_e \rightarrow \bar{\nu}_\mu)$, which, assuming CPT invariance, are also limits on $P(\nu_\mu \rightarrow \nu_e)$. From the latter, we know that ν_X is not a ν_e , except possibly a small fraction of the time. Thus, ν_X is a ν_τ , a sterile neutrino ν_s , or sometimes one and sometimes the other. All of the voluminous, detailed SK atmospheric neutrino data are very well described by the hypothesis that the oscillation is purely $\nu_\mu \rightarrow \nu_\tau$, and that it is a quasi-two-neutrino oscillation with a splitting Δm_{atm}^2 and a mixing angle θ_{atm} that, at 90% CL, are in the ranges [16]

$$1.3 \times 10^{-3} \text{ eV}^2 \lesssim \Delta m_{\text{atm}}^2 \lesssim 3.0 \times 10^{-3} \text{ eV}^2, \quad (13.25)$$

and

$$\sin^2 2\theta_{\text{atm}} > 0.9. \quad (13.26)$$

Other experiments favor roughly similar regions of parameter space [17,18]. We note that the constraint (13.25) implies that at least one mass eigenstate ν_i has a mass exceeding 36 meV. From several pieces of evidence, the 90% CL upper limit on the fraction of ν_X that is sterile is 19% [19].

The oscillation interpretation of the atmospheric neutrino data has received support from the KEK to Kamioka (K2K) long-baseline experiment. This experiment produces a ν_μ beam using an accelerator, measures the beam intensity with a complex of near detectors, and then measures the ν_μ flux still in the beam 250 km away using the SK

detector. The L/E of this experiment is such that one expects to see an oscillation dominated by the atmospheric squared-mass splitting Δm_{atm}^2 . K2K has reported on two data samples. In the first, 80 ν_μ events would be expected in SK if there were no oscillation, but only 56 events are seen [20]. These data are well described by the same oscillation hypothesis that describes the atmospheric neutrino data, with the same parameters [16]. In the second, newer data sample, 26 events would be expected in the absence of oscillation, but only 16 events are seen [16]. This degree of ν_μ disappearance is quite consistent with that observed in the earlier data.

The neutrinos created in the Sun have been detected on Earth by several experiments, as discussed by K. Nakamura in this *Review*. The nuclear processes that power the Sun make only ν_e , not ν_μ or ν_τ . For years, solar neutrino experiments had been finding that the solar ν_e flux arriving at the Earth is below the one expected from neutrino production calculations. Now, thanks especially to the Sudbury Neutrino Observatory (SNO), we have compelling evidence that the missing ν_e have simply changed into neutrinos of other flavors.

SNO has studied the flux of high-energy solar neutrinos from ${}^8\text{B}$ decay. This experiment detects these neutrinos via the reactions

$$\nu + d \rightarrow e^- + p + p, \quad (13.27)$$

$$\nu + d \rightarrow \nu + p + n, \quad (13.28)$$

and

$$\nu + e^- \rightarrow \nu + e^-. \quad (13.29)$$

The first of these reactions, charged-current deuteron breakup, can be initiated only by a ν_e . Thus, it measures the flux $\phi(\nu_e)$ of ν_e from ${}^8\text{B}$ decay in the Sun. The second reaction, neutral-current deuteron breakup, can be initiated with equal cross sections by neutrinos of all active flavors. Thus, it measures $\phi(\nu_e) + \phi(\nu_{\mu,\tau})$, where $\phi(\nu_{\mu,\tau})$ is the flux of ν_μ and/or ν_τ from the Sun. Finally, the third reaction, neutrino electron elastic scattering, can be triggered by a neutrino of any active flavor, but $\sigma(\nu_{\mu,\tau} e \rightarrow \nu_{\mu,\tau} e) \simeq \sigma(\nu_e e \rightarrow \nu_e e)/6.5$. Thus, this reaction measures $\phi(\nu_e) + \phi(\nu_{\mu,\tau})/6.5$.

Recently, SNO has reported the results of measurements made with increased sensitivity to the neutral-current deuteron breakup [21]. From its observed rates for the two deuteron breakup reactions, SNO finds that [21]

$$\frac{\phi(\nu_e)}{\phi(\nu_e) + \phi(\nu_{\mu,\tau})} = 0.306 \pm 0.026 (\text{stat}) \pm 0.024 (\text{syst}). \quad (13.30)$$

Clearly, $\phi(\nu_{\mu,\tau})$ is not zero. This non-vanishing $\nu_{\mu,\tau}$ flux from the Sun is “smoking-gun” evidence that some of the ν_e produced in the solar core do indeed change flavor.

Corroborating information comes from the detection reaction $\nu e^- \rightarrow \nu e^-$, studied by both SNO and SK [22].

Change of neutrino flavor, whether in matter or vacuum, does not change the total neutrino flux. Thus, unless some of the solar ν_e are changing into sterile neutrinos, the total active high-energy flux measured by the neutral-current reaction (13.28) should agree with the predicted total ${}^8\text{B}$ solar neutrino flux based on calculations of neutrino production in the Sun. This predicted total is $(5.05_{-0.81}^{+1.01}) \times 10^6 \text{ cm}^{-2} \text{ s}^{-1}$ [23]. By comparison, the total active flux measured by reaction (13.28) is $[5.21 \pm 0.27 (\text{stat}) \pm 0.38 (\text{syst})] \times 10^6 \text{ cm}^{-2} \text{ s}^{-1}$, in good agreement. This agreement provides evidence that neutrino production in the Sun is correctly understood, further strengthens the evidence that neutrinos really do change flavor, and strengthens the evidence that the previously-reported deficits of solar ν_e flux are due to this change of flavor.

The strongly favored explanation of solar neutrino flavor change is the LMA-MSW effect. As pointed out after Eq. (13.23), a ν_e survival probability below 1/2, which is indicated by Eq. (13.30), requires that solar matter effects play a significant role [24]. The LMA-MSW interpretation of solar neutrino behavior implies that a substantial fraction of reactor $\bar{\nu}_e$ that travel more than a hundred kilometers should disappear into anti-neutrinos of other flavors. The KamLAND

experiment, which studies reactor $\bar{\nu}_e$ that typically travel ~ 180 km to reach the detector, finds that, indeed, the $\bar{\nu}_e$ flux at the detector is only 0.611 ± 0.085 (stat) ± 0.041 (syst) of what it would be if no $\bar{\nu}_e$ were vanishing [25]. The KamLAND data establish that the “solar” mixing angle θ_\odot is indeed large. In addition, KamLAND helps to confirm the LMA-MSW explanation of solar neutrino behavior since both the KamLAND result and all the solar neutrino data [26] can be described by the same neutrino parameters, in the LMA-MSW region. A global fit to both the solar and KamLAND data constrains these parameters, the solar Δm_\odot^2 and θ_\odot defined after Eq. (13.21), to lie in the region shown in Fig. 13.1 [27]. That θ_{atm} , Eq. (13.26), and θ_\odot , Fig. 13.1, are both large, in striking contrast to all quark mixing angles, is very interesting [28].

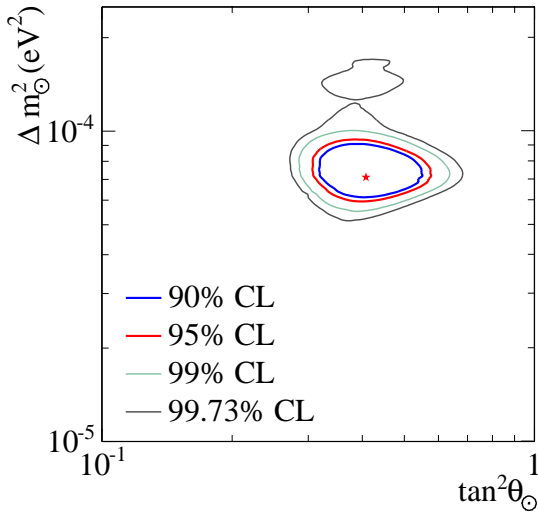


Figure 13.1: The region allowed for the neutrino parameters Δm_\odot^2 and θ_\odot by the solar and KamLAND data. The best-fit point, indicated by the star, is $\Delta m_\odot^2 = 7.1 \times 10^{-5} \text{ eV}^2$ and $\theta_\odot = 32.5^\circ$. See full-color version on color pages at end of book.

While the total active solar neutrino flux measured by SNO via neutral-current deuteron breakup is compatible with the theoretically predicted total ${}^8\text{B}$ neutrino production by the Sun, we have seen that the uncertainties in these quantities are not negligible. It remains possible that some of the solar ν_e that change their flavor become sterile. Taking into account both the solar and KamLAND data, but not assuming the total ${}^8\text{B}$ solar neutrino flux to be known from theory, it has been found that, at 90% CL, the sterile fraction of the non- ν_e solar neutrino flux at Earth is less than 36% [29].

The neutrinos studied by the LSND experiment [30] come from the decay $\mu^+ \rightarrow e^+ \nu_e \bar{\nu}_\mu$ of muons at rest. While this decay does not produce $\bar{\nu}_e$, an excess of $\bar{\nu}_e$ over expected background is reported by the experiment. This excess is interpreted as due to oscillation of some of the $\bar{\nu}_\mu$ produced by μ^+ decay into $\bar{\nu}_e$. The related Karlsruhe Rutherford Medium Energy Neutrino (KARMEN) experiment [31] sees no indication for such an oscillation. However, the LSND and KARMEN experiments are not identical; at LSND the neutrino travels a distance $L \approx 30$ m before detection, while at KARMEN it travels $L \approx 18$ m. The KARMEN results exclude a portion of the neutrino parameter region favored by LSND, but not all of it. A joint analysis [32] of the results of both experiments finds that a splitting $0.2 \lesssim \Delta m_{\text{LSND}}^2 \lesssim 1 \text{ eV}^2$ and mixing $0.003 \lesssim \sin^2 2\theta_{\text{LSND}} \lesssim 0.03$, or a splitting $\Delta m_{\text{LSND}}^2 \simeq 7 \text{ eV}^2$ and mixing $\sin^2 2\theta_{\text{LSND}} \simeq 0.004$, might explain both experiments.

The regions of neutrino parameter space favored or excluded by various neutrino oscillation experiments are shown in Fig. 13.2.

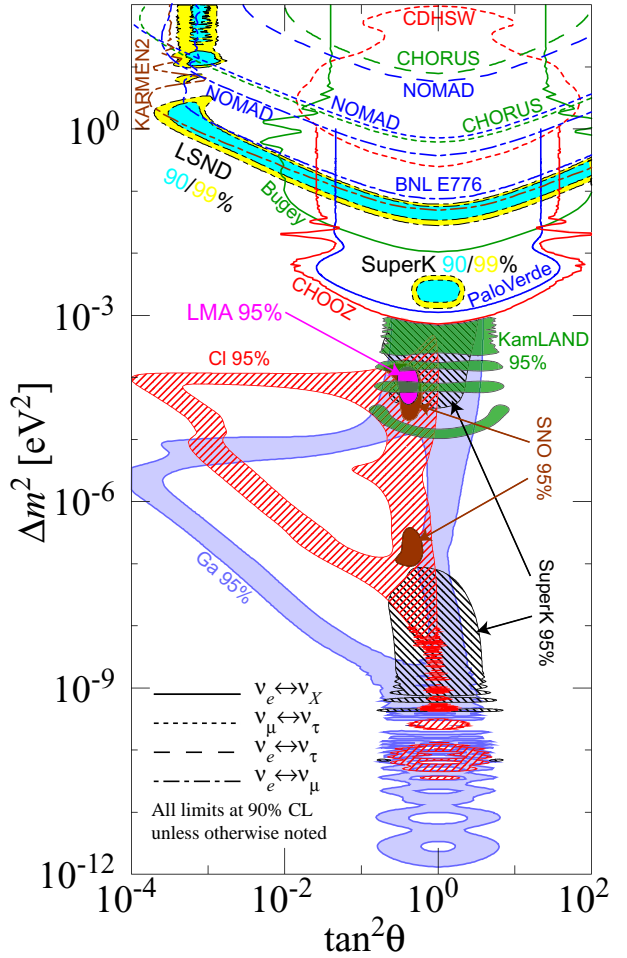


Figure 13.2: The regions of squared-mass splitting and mixing angle favored or excluded by various experiments. This figure was contributed by H. Murayama (University of California, Berkeley). References to the data used in the figure can be found at <http://hitoshi.berkeley.edu/neutrino/ref.html>. See full-color version on color pages at end of book.

III. Neutrino spectra and mixings: If there are only three neutrino mass eigenstates, ν_1, ν_2 and ν_3 , then there are only three mass splittings Δm_{ij}^2 , and they obviously satisfy

$$\Delta m_{32}^2 + \Delta m_{21}^2 + \Delta m_{13}^2 = 0. \quad (13.31)$$

However, as we have seen, the Δm^2 values required to explain the flavor changes of the atmospheric, solar, and LSND neutrinos are of three different orders of magnitude. Thus, they cannot possibly obey the constraint of Eq. (13.31). If all of the reported changes of flavor are genuine, then nature must contain at least four neutrino mass eigenstates [33]. As explained in Sec. I, one linear combination of these mass eigenstates would have to be sterile.

If the LSND oscillation is not confirmed, then nature may well contain only three neutrino mass eigenstates. The neutrino spectrum then contains two mass eigenstates separated by the splitting Δm_{\odot}^2 needed to explain the solar and KamLAND data, and a third eigenstate separated from the first two by the larger splitting Δm_{atm}^2 called for by the atmospheric and K2K data. Current experiments do not tell us whether the solar pair — the two eigenstates separated by Δm_{\odot}^2 — is at the bottom or the top of the spectrum. These two possibilities are usually referred to, respectively, as a normal and an inverted spectrum. The study of flavor changes of accelerator-generated neutrinos and anti-neutrinos that pass through matter can discriminate between these two spectra (see Sec. V). If the solar pair is at the bottom, then the spectrum is of the form shown in Fig. 13.3. There we include the approximate flavor content of each mass eigenstate, the flavor- α fraction of eigenstate ν_i being simply $|\langle \nu_{\alpha} | \nu_i \rangle|^2 = |U_{\alpha i}|^2$. The flavor content shown assumes that the atmospheric mixing angle of Eq. (13.26) is maximal (which gives the best fit to the atmospheric data [16]) and takes into account the now-established LMA-MSW explanation of solar neutrino behavior.

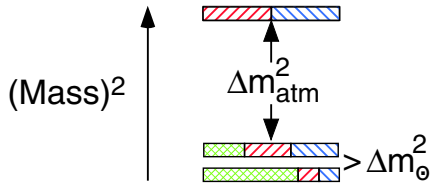


Figure 13.3: A three-neutrino squared-mass spectrum that accounts for the observed flavor changes of solar, reactor, atmospheric, and long-baseline accelerator neutrinos. The ν_e fraction of each mass eigenstate is crosshatched, the ν_{μ} fraction is indicated by right-leaning hatching, and the ν_{τ} fraction by left-leaning hatching.

When there are only three neutrino mass eigenstates, and the corresponding three familiar neutrinos of definite flavor, the leptonic mixing matrix U can be written as

$$U = \begin{array}{c} \nu_1 \qquad \qquad \nu_2 \qquad \qquad \nu_3 \\ \begin{array}{l} \nu_e \left[\begin{array}{ccc} c_{12}c_{13} & & s_{12}c_{13} \\ -s_{12}c_{23} - c_{12}s_{23}s_{13}e^{i\delta} & c_{12}c_{23} - s_{12}s_{23}s_{13}e^{i\delta} & s_{13}e^{-i\delta} \\ s_{12}s_{23} - c_{12}c_{23}s_{13}e^{i\delta} & -c_{12}s_{23} - s_{12}c_{23}s_{13}e^{i\delta} & c_{23}c_{13} \end{array} \right] \\ \nu_{\mu} \left[\begin{array}{ccc} c_{12}c_{13} & & s_{12}c_{13} \\ -s_{12}c_{23} - c_{12}s_{23}s_{13}e^{i\delta} & c_{12}c_{23} - s_{12}s_{23}s_{13}e^{i\delta} & s_{13}e^{-i\delta} \\ s_{12}s_{23} - c_{12}c_{23}s_{13}e^{i\delta} & -c_{12}s_{23} - s_{12}c_{23}s_{13}e^{i\delta} & c_{23}c_{13} \end{array} \right] \\ \nu_{\tau} \left[\begin{array}{ccc} c_{12}c_{13} & & s_{12}c_{13} \\ -s_{12}c_{23} - c_{12}s_{23}s_{13}e^{i\delta} & c_{12}c_{23} - s_{12}s_{23}s_{13}e^{i\delta} & s_{13}e^{-i\delta} \\ s_{12}s_{23} - c_{12}c_{23}s_{13}e^{i\delta} & -c_{12}s_{23} - s_{12}c_{23}s_{13}e^{i\delta} & c_{23}c_{13} \end{array} \right] \\ \times \text{diag}(e^{i\alpha_1/2}, e^{i\alpha_2/2}, 1) \end{array} \end{array} \quad (13.32)$$

Here, ν_1 and ν_2 are the members of the solar pair, with $m_2 > m_1$, and ν_3 is the isolated neutrino, which may be heavier or lighter than the solar pair. Inside the matrix, $c_{ij} \equiv \cos \theta_{ij}$ and $s_{ij} \equiv \sin \theta_{ij}$, where the three θ_{ij} 's are mixing angles. The quantities δ , α_1 , and α_2 are CP -violating phases. The phases α_1 and α_2 , known as Majorana phases, have physical consequences only if neutrinos are Majorana particles, identical to their antiparticles. Then these phases influence neutrinoless double beta decay [see Sec. IV] and other processes [34]. However, as we see from Eq. (13.8), α_1 and α_2 do not affect neutrino oscillation, regardless of whether neutrinos are Majorana particles. Apart from the phases α_1 , α_2 , which have no quark analogues, the parametrization of the leptonic mixing matrix in Eq. (13.32) is identical to that [35] advocated for the quark mixing matrix by Gilman, Kleinknecht, and Renk in their article in this *Review*.

From bounds on the short-distance oscillation of reactor $\bar{\nu}_e$ [8] and other data, at 3σ , $s_{13}^2 < 0.067$ [36]. Taking this and the LMA-MSW explanation of solar neutrino behavior into account, and assuming that atmospheric neutrino mixing is maximal, the U of Eq. (13.32) simplifies to

$$\begin{array}{ccc} \nu_1 & \nu_2 & \nu_3 \end{array}$$

$$U \simeq \begin{array}{l} \nu_e \left[\begin{array}{ccc} c e^{i\alpha_1/2} & s e^{i\alpha_2/2} & s_{13} e^{-i\delta} \\ -s e^{i\alpha_1/2}/\sqrt{2} & c e^{i\alpha_2/2}/\sqrt{2} & 1/\sqrt{2} \\ s e^{i\alpha_1/2}/\sqrt{2} & -c e^{i\alpha_2/2}/\sqrt{2} & 1/\sqrt{2} \end{array} \right] \end{array} \quad (13.33)$$

Here, $c \equiv \cos \theta_{\odot}$ and $s \equiv \sin \theta_{\odot}$, where θ_{\odot} is the solar mixing angle defined in Sec. I and constrained by Fig. 13.1. With θ_{13} small, $\theta_{\odot} \simeq \theta_{12}$. The illustrative flavor content shown in Fig. 13.3 is obtained from the U of Eq. (13.33) taking $s_{13}^2 \simeq 0$, $s^2 \simeq 0.3$.

If the LSND oscillation is confirmed, then, as already noted, there must be at least four mass eigenstates. If there are exactly four, then the spectrum is either of the kind depicted in Fig. 13.4a, or of the kind shown in Fig. 13.4b.

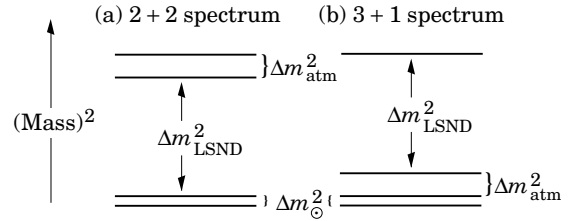


Figure 13.4: Possible four-neutrino squared-mass spectra.

In Fig. 13.4a, we have a “2+2” spectrum. This consists of a “solar pair” of eigenstates that are separated by the solar splitting Δm_{\odot}^2 and are the main contributors to the behavior of solar neutrinos, plus an “atmospheric pair” that are separated by the atmospheric splitting Δm_{atm}^2 and are the main contributors to the atmospheric $\nu_{\mu} \rightarrow \nu_{\tau}$ oscillation. From the bounds on reactor $\bar{\nu}_e$ short-distance oscillation [8], we know that the ν_e fraction of the atmospheric pair is less than a few percent. From bounds on accelerator ν_{μ} short-distance oscillation [37], we know that the ν_{μ} fraction of the solar pair is similarly limited. Thus, the atmospheric (solar) pair of eigenstates plays only a small role in the behavior of the solar ν_e (atmospheric ν_{μ}). The solar and atmospheric pairs are separated from each other by the large LSND splitting Δm_{LSND}^2 , making possible the LSND oscillation. The solar pair may lie below the atmospheric pair, as shown in Fig. 13.4a, or above it.

In Fig. 13.4b, we have a “3+1” spectrum. This includes a trio, consisting of a solar pair separated by Δm_{\odot}^2 , plus a third neutrino separated from the solar pair by Δm_{atm}^2 , and a fourth neutrino separated from the trio by Δm_{LSND}^2 . In the trio, the solar pair may lie below the third neutrino, as shown, or above it [38]. In addition, the fourth, isolated neutrino may lie above the other three, as shown, or below them. In the case of a 3+1 spectrum, the reactor $\bar{\nu}_e$ and accelerator ν_{μ} oscillation bounds mentioned previously imply that the isolated neutrino has very little ν_e or ν_{μ} flavor content. It is interesting to consider the possibility that it has very little ν_{τ} content as well, and consequently is largely sterile. Then, by unitarity, the other three neutrinos—the “3”—can have only very little sterile content. Those three neutrinos dominate the solar and atmospheric fluxes, so neither of these fluxes will contain sterile neutrinos to any significant degree. In contrast, it is characteristic of the 2+2 spectra that either the solar or atmospheric neutrino fluxes, or both, do include a substantial component of sterile neutrinos [39–40]. Thus, further information on the sterile neutrino content of these two fluxes can potentially discriminate between the 2+2 and 3+1 spectra.

Neither a 2+2 nor a 3+1 spectrum gives a statistically satisfactory fit to all the data. In particular, in the 3+1 spectra, there is tension between the bounds on short-baseline oscillation and the LSND signal for short-baseline oscillation [41]. However, if there are *at least* four neutrino mass eigenstates, there is no strong reason to believe that there are *exactly* four. The presence of more states may improve the quality of the fit. For example, it has been found that a “3+2”

spectrum fits all the short-baseline data significantly better than a 3+1 spectrum [42].

IV. The neutrino-anti-neutrino relation: Unlike quarks and charged leptons, neutrinos may be their own antiparticles. Whether they are depends on the nature of the physics that gives them mass.

In the Standard Model (SM), neutrinos are assumed to be massless. Now that we know they do have masses, it is straightforward to extend the SM to accommodate these masses in the same way that this model accommodates quark and charged lepton masses. When a neutrino ν is assumed to be massless, the SM does not contain the chirally right-handed neutrino field ν_R , but only the left-handed field ν_L that couples to the W and Z bosons. To accommodate the ν mass in the same manner as quark masses are accommodated, we add ν_R to the Model. Then we may construct the “Dirac mass term”

$$\mathcal{L}_D = -m_D \bar{\nu}_L \nu_R + h.c. \quad , \quad (13.34)$$

in which m_D is a constant. This term, which mimics the mass terms of quarks and charged leptons, conserves the lepton number L that distinguishes neutrinos and negatively-charged leptons on the one hand from anti-neutrinos and positively-charged leptons on the other. Since everything else in the SM also conserves L , we then have an L -conserving world. In such a world, each neutrino mass eigenstate ν_i differs from its antiparticle $\bar{\nu}_i$, the difference being that $L(\bar{\nu}_i) = -L(\nu_i)$. When $\bar{\nu}_i \neq \nu_i$, we refer to the $\nu_i - \bar{\nu}_i$ complex as a “Dirac neutrino.”

Once ν_R has been added to our description of neutrinos, a “Majorana mass term,”

$$\mathcal{L}_M = -m_R \bar{\nu}_R^c \nu_R + h.c. \quad , \quad (13.35)$$

can be constructed out of ν_R and its charge conjugate, ν_R^c . In this term, m_R is another constant. Since both ν_R and $\bar{\nu}_R^c$ absorb ν and create $\bar{\nu}$, \mathcal{L}_M mixes ν and $\bar{\nu}$. Thus, a Majorana mass term does not conserve L . There is then no conserved lepton number to distinguish a neutrino mass eigenstate ν_i from its antiparticle. Hence, when Majorana mass terms are present, $\bar{\nu}_i = \nu_i$. That is, for a given helicity h , $\bar{\nu}_i(h) = \nu_i(h)$. We then refer to ν_i as a “Majorana neutrino.”

Suppose the right-handed neutrinos required by Dirac mass terms have been added to the SM. If we insist that this extended SM conserve L , then, of course, Majorana mass terms are forbidden. However, if we do not impose L conservation, but require only the general principles of gauge invariance and renormalizability, then Majorana mass terms like that of Eq. (13.35) are expected to be present. As a result, L is violated, and neutrinos are Majorana particles [43].

In the see-saw mechanism [44], which is the most popular explanation of why neutrinos — although massive — are nevertheless so light, both Dirac and Majorana mass terms are present. Hence, the neutrinos are Majorana particles. However, while half of them are the familiar light neutrinos, the other half are extremely heavy Majorana particles referred to as the N_i , with masses possibly as large as the GUT scale. The N_i may have played a crucial role in baryogenesis in the early universe, as we shall discuss in Sec. V.

How can the theoretical expectation that L is violated and neutrinos are Majorana particles be confirmed experimentally? The interactions of neutrinos are well described by the SM, and the SM interactions conserve L . If we may neglect any non-SM L -violating interactions, then the only sources of L violation are the neutrino Majorana mass terms. This means that all L -violating effects disappear in the limit of vanishing neutrino masses. Thus, any experimental approach to confirming the violation of L , and the consequent Majorana character of neutrinos, must be able to see an L violation that is going to be very small because of the smallness of the neutrino masses that drive it. One approach that shows great promise is the search for neutrinoless double beta decay ($0\nu\beta\beta$). This is the process $(A, Z) \rightarrow (A, Z+2) + 2e^-$, in which a nucleus containing A nucleons, Z of which are protons, decays to a nucleus containing $Z+2$ protons by emitting two electrons. This process manifestly violates L conservation, so we expect it to be suppressed. However, if (A, Z) is a nucleus that is stable against single β (and α and γ) decay, then it

can decay only via the process we are seeking, and the L -conserving two-neutrino process $(A, Z) \rightarrow (A, Z+2) + 2e^- + 2\bar{\nu}_e$. The latter decay mode is suppressed by the small phase space associated with the four light particles in the final state, so we have a chance to observe the neutrinoless mode, $(A, Z) \rightarrow (A, Z+2) + 2e^-$.

While $0\nu\beta\beta$ can in principle receive contributions from a variety of mechanisms (R-parity-violating supersymmetric couplings, for example), it is easy to show explicitly that the observation of $0\nu\beta\beta$ at any non-vanishing rate would imply that nature contains at least one Majorana neutrino mass term [45]. Now, quarks and charged leptons cannot have Majorana mass terms, because such terms mix fermion and antifermion, and $q \leftrightarrow \bar{q}$ or $\ell \leftrightarrow \bar{\ell}$ would not conserve electric charge. Thus, the discovery of $0\nu\beta\beta$ would demonstrate that the physics of neutrino masses is unlike that of the masses of all other fermions.

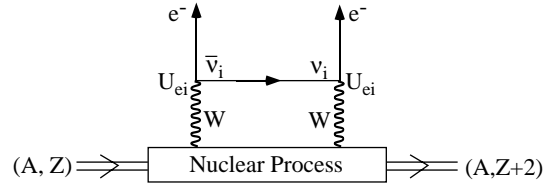


Figure 13.5: The dominant mechanism for $0\nu\beta\beta$. The diagram does not exist unless $\bar{\nu}_i = \nu_i$.

The dominant mechanism for $0\nu\beta\beta$ is expected to be the one depicted in Fig. 13.5. There, a pair of virtual W bosons are emitted by the parent nucleus, and then these W bosons exchange one or another of the light neutrino mass eigenstates ν_i to produce the outgoing electrons. The $0\nu\beta\beta$ amplitude is then a sum over the contributions of the different ν_i . It is assumed that the interactions at the two leptonic W vertices are those of the SM.

Since the exchanged ν_i is created together with an e^- , the left-handed SM current that creates it gives it the helicity we associate, in common parlance, with an “anti-neutrino.” That is, the ν_i is almost totally right-handed, but has a small left-handed-helicity component, whose amplitude is of order m_i/E , where E is the ν_i energy. At the vertex where this ν_i is absorbed, the absorbing left-handed SM current can absorb only its small left-handed-helicity component without further suppression. Consequently, the ν_i -exchange contribution to the $0\nu\beta\beta$ amplitude is proportional to m_i . From Fig. 13.5, we see that this contribution is also proportional to U_{ei}^2 . Thus, summing over the contributions of all the ν_i , we conclude that the amplitude for $0\nu\beta\beta$ is proportional to the quantity

$$\left| \sum_i m_i U_{ei}^2 \right| \equiv | \langle m_{\beta\beta} \rangle | \quad , \quad (13.36)$$

commonly referred to as the “effective Majorana mass for neutrinoless double beta decay” [46].

That the $0\nu\beta\beta$ amplitude arising from the diagram in Fig. 13.5 is proportional to neutrino mass is no surprise, and illustrates our earlier general discussion. The diagram in Fig. 13.5 is manifestly L -nonconserving. But we are assuming that the interactions in this diagram are L -conserving. Thus, the L -nonconservation in the diagram as a whole must be coming from underlying Majorana neutrino mass terms. Hence, if all the neutrino masses vanish, the L -nonconservation will vanish as well.

To how small an $| \langle m_{\beta\beta} \rangle |$ should a $0\nu\beta\beta$ search be sensitive? In answering this question, it makes sense to assume there are only three neutrino mass eigenstates — if there are more, $| \langle m_{\beta\beta} \rangle |$ might be larger. Suppose that there are just three mass eigenstates, and that the solar pair, ν_1 and ν_2 , is at the top of the spectrum, so that we

have an inverted spectrum. If the various ν_i are not much heavier than demanded by the observed splittings Δm_{atm}^2 and Δm_{\odot}^2 , then in $|\langle m_{\beta\beta} \rangle|$, Eq. (13.36), the contribution of ν_3 may be neglected, because both m_3 and $|U_{e3}^2| = s_{13}^2$ are small. From Eqs. (13.36) and (13.33), we then have that

$$|\langle m_{\beta\beta} \rangle| \simeq m_0 \sqrt{1 - \sin^2 2\theta_{\odot} \sin^2 \left(\frac{\Delta\alpha}{2} \right)}. \quad (13.37)$$

Here, m_0 is the average mass of the members of the solar pair, whose splitting will be invisible in a practical $0\nu\beta\beta$ experiment, and $\Delta\alpha \equiv \alpha_2 - \alpha_1$ is a CP-violating phase. Although $\Delta\alpha$ is completely unknown, we see from Eq. (13.37) that

$$|\langle m_{\beta\beta} \rangle| \geq m_0 \cos 2\theta_{\odot}. \quad (13.38)$$

Now, in an inverted spectrum, $m_0 \geq \sqrt{\Delta m_{\text{atm}}^2}$. At 90% CL, $\sqrt{\Delta m_{\text{atm}}^2} > 36$ meV [16], while $\cos 2\theta_{\odot} > 0.28$ [21]. Thus, if neutrinos are Majorana particles, and the spectrum is as we have assumed, a $0\nu\beta\beta$ experiment sensitive to $|\langle m_{\beta\beta} \rangle| \gtrsim 10$ meV would have an excellent chance of observing a signal. If the spectrum is inverted, but the ν_i masses are larger than the Δm_{atm}^2 - and Δm_{\odot}^2 -demanded minimum values we have assumed above, then once again $|\langle m_{\beta\beta} \rangle|$ is larger than 10 meV [47], and an experiment sensitive to 10 meV still has an excellent chance of seeing a signal.

If the solar pair is at the bottom of the spectrum, rather than at the top, then $|\langle m_{\beta\beta} \rangle|$ is not as tightly constrained, and can be anywhere from the present bound of 0.3–1.0 eV down to invisibly small [47,48]. For a discussion of the present bounds, see the article by Vogel and Piepke in this *Review* [49].

V. Questions to be answered: The strong evidence for neutrino flavor metamorphosis — hence neutrino mass — opens many questions about the neutrinos. These questions, which hopefully will be answered by future experiments, include the following:

i) *Does neutrino flavor change truly oscillate?*

Where matter effects are unimportant, flavor change probabilities are predicted to have an oscillatory $\sin^2[1.27\Delta m^2(L/E)]$ dependence on L/E . This so-far-unobserved characteristic signature of flavor change could in principle be seen in reactor experiments for $\Delta m^2 = \Delta m_{\odot}^2$, long base-line (LBL) accelerator experiments for $\Delta m^2 = \Delta m_{\text{atm}}^2$, and short base-line (SBL) accelerator experiments for $\Delta m^2 = \Delta m_{\text{LSND}}^2$.

ii) *How many neutrino species are there? Do sterile neutrinos exist?*

This question is being addressed by the MiniBooNE experiment [50], whose purpose is to confirm or refute LSND.

iii) *What are the masses of the mass eigenstates ν_i ?*

The sizes of the squared-mass splittings Δm_{\odot}^2 , Δm_{atm}^2 , and, if present, one or more large splittings Δm_{LSND}^2 , can be determined more precisely than they are currently known through future neutrino oscillation measurements. If there are only three ν_i , then one can find out whether the solar pair, $\nu_{1,2}$, is at the bottom of the spectrum or at its top by exploiting matter effects in LBL neutrino and anti-neutrino oscillations. These matter effects will determine the sign one wishes to learn — that of $\{m_3^2 - [(m_2^2 + m_1^2)/2]\}$ — relative to a sign that is already known — that of the interaction energy of Eq. (13.20).

While flavor-change experiments can determine a spectral pattern such as the one in Fig. 13.3, they cannot tell us the distance of the entire pattern from the zero of squared-mass. One might discover that distance via study of the β energy spectrum in tritium β decay, if the mass of some ν_i with appreciable coupling to an electron is large enough to be within reach of a feasible experiment. One might also gain some information on the distance from zero by measuring $|\langle m_{\beta\beta} \rangle|$, the effective Majorana mass for neutrinoless double beta decay [47–49] (see Vogel and Piepke in this *Review*). Finally, one might obtain information on this distance from cosmology or astrophysics. Indeed, from relatively recent cosmological data and

some cosmological assumptions, it is already concluded that, at 95% CL [51],

$$\sum_i m_i < 0.71 \text{ eV}. \quad (13.39)$$

Here, the sum runs over the masses of all the light neutrino mass eigenstates ν_i that may exist and that were in thermal equilibrium in the early universe.

If there are just three ν_i , and they are heavy enough to be constrained by the bound of Eq. (13.39), then, given that $\Delta m_{\odot}^2 \ll \Delta m_{\text{atm}}^2 \ll 1 \text{ eV}^2$, the ν_i are approximately degenerate. Then Eq. (13.39) requires that the mass of each of them be less than $0.71 \text{ eV} / 3 = 0.23 \text{ eV}$. Now, the mass of the heaviest ν_i cannot be less than $\sqrt{\Delta m_{\text{atm}}^2}$, which in turn is not less than 0.036 eV [see Eq. (13.25)]. Thus, if the cosmological assumptions behind Eq. (13.39) are correct, then

$$0.03 \text{ eV} < \text{Mass [Heaviest } \nu_i] < 0.23 \text{ eV}. \quad (13.40)$$

iv) *Are the neutrino mass eigenstates Majorana particles?*

The confirmed observation of neutrinoless double beta decay would establish that the answer is “yes.” If there are only three ν_i , knowledge that the spectrum is inverted and a definitive upper bound on $|\langle m_{\beta\beta} \rangle|$ that is well below 0.01 eV would establish that it is “no” [see discussion after Eq. (13.38)] [47], [48].

v) *What are the mixing angles in the leptonic mixing matrix U ?*

The solar mixing angle θ_{\odot} can be determined more precisely through future solar and reactor neutrino measurements.

The atmospheric mixing angle θ_{atm} is constrained at 90% CL to lie in the region where $\sin^2 2\theta_{\text{atm}} > 0.9$ [see Eq. (13.26)], but this region is fairly large: 36° to 54° [52]. The value of θ_{atm} , and in particular, its deviation from maximal mixing, 45° , can be sought in precision LBL ν_{μ} disappearance experiments.

A knowledge of the small mixing angle θ_{13} is important not only to help complete our picture of leptonic mixing, but also because, as Eq. (13.32) makes clear, all CP-violating effects of the phase δ are proportional to $\sin\theta_{13}$. Thus, a knowledge of the order of magnitude of θ_{13} would help guide the design of experiments to probe CP violation. From Eq. (13.33), we see that $\sin^2\theta_{13}$ is the ν_e fraction of ν_3 . The ν_3 is the isolated neutrino that lies at one end of the atmospheric squared-mass gap Δm_{atm}^2 , so an experiment seeking to measure θ_{13} should have an L/E that makes it sensitive to Δm_{atm}^2 , and should involve ν_e . Possibilities include a sensitive search for the disappearance of reactor $\bar{\nu}_e$ while they travel a distance $L \sim 1$ km, and an accelerator neutrino search for $\nu_{\mu} \rightarrow \nu_e$ or $\nu_e \rightarrow \nu_{\mu}$ with a beamline $L >$ several hundred km.

If LSND is confirmed, then the matrix U is at least 4×4 , and contains many more than three angles. A rich program, including short baseline experiments with multiple detectors, will be needed to learn about both the squared-mass spectrum and the mixing matrix.

Given the large sizes of θ_{atm} and θ_{\odot} , we already know that leptonic mixing is very different from its quark counterpart, where all the mixing angles are small. This difference, and the striking contrast between the tiny neutrino masses and the very much larger quark masses, suggest that the physics underlying neutrino masses and mixing may be very different from the physics behind quark masses and mixing.

vi) *Does the behavior of neutrinos violate CP?*

From Eqs. (13.8), (13.12), and (13.33), we see that if the CP-violating phase δ and the small mixing angle θ_{13} are both non-vanishing, there will be CP-violating differences between neutrino and anti-neutrino oscillation probabilities. Observation of these differences would establish that CP violation is not a peculiarity of quarks.

The CP-violating difference $P(\nu_{\alpha} \rightarrow \nu_{\beta}) - P(\bar{\nu}_{\alpha} \rightarrow \bar{\nu}_{\beta})$ between “neutrino” and “anti-neutrino” oscillation probabilities is independent of whether the mass eigenstates ν_i are Majorana or Dirac particles. To study $\nu_{\mu} \rightarrow \nu_e$ with a super-intense but conventionally-generated neutrino beam, for example, one would create the beam via the process $\pi^+ \rightarrow \mu^+ \nu_{\mu}$, and detect it via $\nu_i + \text{target} \rightarrow e^- + \dots$. To study $\bar{\nu}_{\mu} \rightarrow \bar{\nu}_e$, one would create the beam via $\pi^- \rightarrow \mu^- \bar{\nu}_{\mu}$, and detect it

via $\bar{\nu}_i + \text{target} \rightarrow e^+ + \dots$. Whether $\bar{\nu}_i = \nu_i$ or not, the amplitudes for the latter two processes are proportional to $U_{\mu i}$ and $U_{e i}^*$, respectively. In contrast, the amplitudes for their $\nu_\mu \rightarrow \nu_e$ counterparts are proportional to $U_{\mu i}^*$ and $U_{e i}$. As this illustrates, Eq. (13.12) relates “neutrino” and “anti-neutrino” oscillation probabilities even when the neutrino mass eigenstates are their own antiparticles.

The baryon asymmetry of the universe could not have developed without some violation of CP during the universe’s early history. The one known source of CP violation — the complex phase in the quark mixing matrix — could not have produced sufficiently large effects. Thus, perhaps *leptonic* CP violation is responsible for the baryon asymmetry. The see-saw mechanism predicts very heavy Majorana neutral leptons N_i (see Sec. IV), which would have been produced in the Big Bang. Perhaps CP violation in the leptonic decays of an N_i led to the inequality

$$\Gamma(N_i \rightarrow \ell^+ + \dots) \neq \Gamma(N_i \rightarrow \ell^- + \dots), \quad (13.41)$$

which would have resulted in unequal numbers of ℓ^+ and ℓ^- in the early universe [53]. This leptogenesis could have been followed by nonperturbative SM processes that would have converted the lepton asymmetry, in part, into the observed baryon asymmetry [54].

While the connection between the CP violation that would have led to leptogenesis, and that which we hope to observe in neutrino oscillation, is model-dependent, it is not likely that we have either of these without the other [55]. This makes the search for CP violation in neutrino oscillation very interesting indeed. Depending on the rough size of θ_{13} , this CP violation may be observable with a very intense conventional neutrino beam, or may require a “neutrino factory,” whose neutrinos come from the decay of stored muons. The detailed study of CP violation may require a neutrino factory in any case.

The questions we have discussed, and other questions about the world of neutrinos, will be the focus of a major experimental program in the years to come.

Acknowledgements

I am grateful to Susan Kayser for her crucial role in the production of this manuscript.

References

- This matrix is sometimes referred to as the Maki-Nakagawa-Sakata matrix, or as the Pontecorvo-Maki-Nakagawa-Sakata matrix, in recognition of the pioneering contributions of these scientists to the physics of mixing and oscillation. See Z. Maki, M. Nakagawa, and S. Sakata, *Prog. Theor. Phys.* **28**, 870 (1962); B. Pontecorvo, *Zh. Eksp. Teor. Fiz.* **53**, 1717 (1967) [*Sov. Phys. JETP* **26**, 984 (1968)].
- D. Karlen in this *Review*.
- B. Kayser, *Phys. Rev.* **D24**, 110 (1981); F. Boehm and P. Vogel, *Physics of Massive Neutrinos* (Cambridge University Press, Cambridge, 1987) p. 87; C. Giunti, C. Kim, and U. Lee, *Phys. Rev.* **D44**, 3635 (1991); J. Rich, *Phys. Rev.* **D48**, 4318 (1993); H. Lipkin, *Phys. Lett.* **B348**, 604 (1995); W. Grimus and P. Stockinger, *Phys. Rev.* **D54**, 3414 (1996); T. Goldman, [hep-ph/9604357](#); Y. Grossman and H. Lipkin, *Phys. Rev.* **D55**, 2760 (1997); W. Grimus, S. Mohanty, and P. Stockinger, in *Proc. of the 17th Int. Workshop on Weak Interactions and Neutrinos*, eds. C. Dominguez and R. Viollier (World Scientific, Singapore, 2000) p. 355.
- L. Stodolsky, *Phys. Rev.* **D58**, 036006 (1998); C. Giunti, *Phys. Scripta* **67**, 29 (2003); M. Beuthe, *Phys. Rept.* **375**, 105 (2003) and *Phys. Rev.* **D66**, 013003 (2002), and references therein; H. Lipkin, [hep-ph/0304187](#).
- G. Fogli, E. Lisi, and G. Scioscia, *Phys. Rev.* **D52**, 5334 (1995).
- L. Wolfenstein, *Phys. Rev.* **D17**, 2369 (1978).
- S. Mikheyev and A. Smirnov, *Yad. Fiz.* **42**, 1441 (1985) [*Sov. J. Nucl. Phys.* **42**, 913 (1986)]; *Zh. Eksp. Teor. Fiz.* **91**, 7, (1986) [*Sov. Phys. JETP* **64**, 4 (1986)]; *Nuovo Cimento* **9C**, 17 (1986).
- The Bugey Collaboration (B. Achkar *et al.*), *Nucl. Phys.* **B434**, 503 (1995); The Palo Verde Collaboration (F. Boehm *et al.*), *Phys. Rev.* **D64**, 112001 (2001); The CHOOZ Collaboration (M. Apollonio *et al.*), *Eur. Phys. J.* **C27**, 331 (2003).
- P. Langacker, J. Leveille, and J. Sheiman, *Phys. Rev.* **D27**, 1228 (1983); The corresponding energy for anti-neutrinos is negative.
- G. L. Fogli, E. Lisi, and D. Montanino, *Phys. Rev.* **D54**, 2048 (1996); A. de Gouvêa, A. Friedland, and H. Murayama, *Phys. Lett.* **B490**, 125 (2000).
- J. Bahcall, *Neutrino Astrophysics*, (Cambridge Univ. Press, Cambridge, UK 1989).
- S. Parke, *Phys. Rev. Lett.* **57**, 1275 (1986).
- We thank J. Beacom and A. Smirnov for invaluable conversations on how LMA-MSW works. For an early description, see S. Mikheyev and A. Smirnov, Ref. 7 (first paper).
- D. Ayres *et al.*, in *Proc. of the 1982 DPF Summer Study on Elementary Particle Physics and Future Facilities*, p. 590; G. Dass and K. Sarma, *Phys. Rev.* **D30**, 80 (1984); J. Flanagan, J. Learned, and S. Pakvasa, *Phys. Rev.* **D57**, 2649 (1998); B. Kayser, in *Proc. of the 17th Int. Workshop on Weak Interactions and Neutrinos*, eds. C. Dominguez and R. Viollier (World Scientific, Singapore, 2000) p. 339.
- E. Kearns, in *Proc. of the 30th Int. Conf. on High Energy Physics*, eds. C. Lim and T. Yamanaka (World Scientific, Singapore, 2001) p. 172.
- K. Nishikawa, presented at the XXI Int. Symp. on Lepton and Photon Interactions at High Energies (Lepton Photon 2003), Fermilab, August, 2003.
- The MACRO Collaboration (M. Ambrosio *et al.*), *Phys. Lett.* **B566**, 35 (2003); The Soudan 2 Collaboration (M. Sanchez *et al.*), [hep-ex/0307069](#); For a review, see M. Goodman, *Proc. of the XXth Int. Conf. on Neutrino Physics and Astrophysics*, eds. F. von Feilitzsch and N. Schmitz, *Nucl. Phys. B (Proc. Suppl.)* **118**, 99 (2003).
- For additional discussion of the atmospheric data, see T. Gaisser and T. Stanev in this *Review*.
- M. Shiozawa, presented at the XXth Int. Conf. on Neutrino Physics and Astrophysics, Munich, May, 2002.
- The K2K Collaboration (M. Ahn *et al.*), *Phys. Rev. Lett.* **90**, 041801 (2003).
- The SNO Collaboration (S. Ahmed *et al.*), [nucl-ex/0309004](#).
- Y. Koshio, to appear in the Proceedings of 38th Rencontres de Moriond on Electroweak Interactions and Unified Theories, Les Arcs, France, March 15-22, 2003, [hep-ex/0306002](#).
- J. Bahcall, M. Pinsonneault, and S. Basu, *Astrophys. J.* **555**, 990 (2001).
- G. Fogli, E. Lisi, A. Marrone, and A. Palazzo, [hep-ph/0309100](#).
- The KamLAND Collaboration (K. Eguchi *et al.*), *Phys. Rev. Lett.* **90**, 021802 (2003).
- The latter include the data from the chlorine experiment: B. Cleveland *et al.*, *Astrophys. J.* **496**, 505 (1998); and from the gallium experiments: T. Kirsten (for the GNO Collaboration), *Proc. of the XXth Int. Conf. on Neutrino Physics*

- and *Astrophysics*, eds. F. von Feilitzsch and N. Schmitz, Nucl. Phys. B (Proc. Suppl.) **118**, 33 (2003);
V. Gavrin (for the SAGE collaboration), presented at the 4th Int. Workshop on Low Energy and Solar Neutrinos, Paris, May, 2003.
27. The SNO Collaboration, Ref. [21]. We thank the collaboration for allowing us to use their figure.
 28. Fits to the neutrino data incorporating the recent SNO results of Ref. [21] may be found in A.B. Balantekin and H. Yuksel, hep-ph/0309079;
A. Bandyopadhyay *et al.*, Phys. Rev. **D68**, 113002 (2003);
P. Holanda and Y. Smirnov, hep-ph/0309299;
M. Maltoni, T. Schwetz, M. Tortola, and J. Valle, Phys. Rev. **D68**, 113010 (2003).
 29. J. Bahcall, M.C. Gonzalez-Garcia, and C. Peña-Garay, JHEP **0302**, 009 (2003);
See also P. Holanda and A. Smirnov, hep-ph/0211264 and hep-ph/0307266.
 30. The LSND Collaboration (A. Aguilar *et al.*), Phys. Rev. **D64**, 112007 (2001).
 31. The KARMEN Collaboration (B. Armbruster *et al.*), Phys. Rev. **D65**, 112001 (2002).
 32. E. Church *et al.*, Phys. Rev. **D66**, 013001 (2003).
 33. For an alternative possibility entailing *CPT* violation, see H. Murayama and T. Yanagida, Phys. Lett. **B520**, 263 (2001);
G. Barenboim *et al.*, JHEP **0210**, 001 (2002);
However, after KamLAND, this alternative is disfavored. M. C. Gonzalez-Garcia, M. Maltoni, and T. Schwetz, Phys. Rev. **D68**, 053007 (2003);
G. Barenboim, L. Borisso, and J. Lykken, hep-ph/0212116 v2.
 34. J. Schechter and J. Valle, Phys. Rev. **D23**, 1666 (1981);
J. Nieves and P. Pal, Phys. Rev. **D64**, 076005 (2001);
A. de Gouvêa, B. Kayser, and R. Mohapatra, Phys. Rev. **D67**, 053004 (2003).
 35. L.-L. Chau and W.-Y. Keung, Phys. Rev. Lett. **53**, 1802 (1984);
H. Harari and M. Leurer, Phys. Lett. **B181**, 123 (1986);
F.J. Botella and L.-L. Chau, Phys. Lett. **B168**, 97 (1986);
H. Fritzsch and J. Plankl, Phys. Rev. **D35**, 1732 (1987).
 36. G. Fogli *et al.*, hep-ph/0308055.
 37. F. Dydak *et al.*, Phys. Lett. **B134**, 281 (1984).
 38. A trio with its solar pair at the top is an interesting possibility that could reflect new physics that approximately conserves $L_e - L_\mu - L_\tau$, where L_α is the lepton number for flavor α . See K. Babu and R. Mohapatra, Phys. Lett. **B532**, 77 (2002).
 39. O.L.G. Peres and A. Smirnov, Nucl. Phys. **B599**, 3 (2001);
M.C. Gonzalez-Garcia, M. Maltoni, and C. Peña-Garay, Phys. Rev. **D64**, 093001 (2001), and in *Budapest 2001, High Energy Physics (Proc. of the Int. Europhys. Conf. on High-Energy Physics)*.
 40. See, however, H. Paes, L. Song, and T. Weiler, Phys. Rev. **D67**, 073019 (2003).
 41. M. Maltoni, T. Schwetz, and J. Valle, Phys. Rev. **D65**, 093004 (2002);
G. Fogli, E. Lisi, and A. Marrone, Phys. Rev. **D63**, 053008 (2001);
References in these two papers.
 42. M. Sorel, J. Conrad, and M. Shaevitz, hep-ph/0305255.
 43. We thank Belen Gavela for introducing us to this argument.
 44. M. Gell-Mann, P. Ramond, and R. Slansky, in: *Supergravity*, eds. D. Freedman and P. van Nieuwenhuizen (North Holland, Amsterdam, 1979) p. 315;
T. Yanagida, in: *Proceedings of the Workshop on Unified Theory and Baryon Number in the Universe*, eds. O. Sawada and A. Sugamoto (KEK, Tsukuba, Japan, 1979);
R. Mohapatra and G. Senjanovic: Phys. Rev. Lett. **44**, 912 (1980) and Phys. Rev. **D23**, 165 (1981).
 45. J. Schechter and J. Valle, Phys. Rev. **D25**, 2951 (1982).
 46. The physics of Majorana neutrinos and $0\nu\beta\beta$ are discussed in S. Bilenky and S. Petcov, Rev. Mod. Phys. **59**, 671 (1987) [Erratum—*ibid.* **61**, 169 (1987)];
B. Kayser, *The Physics of Massive Neutrinos* (World Scientific, Singapore, 1989).
 47. S. Pascoli and S.T. Petcov, Phys. Lett. **B580**, 280 (2003).
 48. Analyses of the possible values of $| \langle m_{\beta\beta} \rangle |$ have been given by H. Murayama and C. Peña-Garay, hep-ph/0309114;
S. Pascoli and S. Petcov, Phys. Lett. **B544**, 239 (2002);
S. Bilenky, S. Pascoli, and S. Petcov, Phys. Rev. **D64**, 053010 (2001), and Phys. Rev. **D64**, 113003 (2001);
H. Klapdor-Kleingrothaus, H. Päs, and A. Smirnov, Phys. Rev. **D63**, 073005 (2001);
S. Bilenky *et al.*, Phys. Lett. **B465**, 193 (1999);
References in these papers.
 49. See also S. Elliott and P. Vogel, Ann. Rev. Nucl. Part. Sci. **52**, 115 (2002), and references therein.
 50. The MiniBooNE Collaboration (E. Church *et al.*) FERMLAB-P-0898 (1997), available at <http://library.fnal.gov/archive/test-proposal/0000/fermilab-proposal-0898.shtml>.
 51. D. Spergel *et al.*, Astrophys. J. Supp. **148**, 175 (2003).
 52. This point has been stressed by S. Parke, private communication.
 53. M. Fukugita and T. Yanagida, Phys. Lett. **B174**, 45 (1986).
 54. G. 't Hooft, Phys. Rev. Lett. **37**, 8 (1976);
V. Kuzmin, V. Rubakov, and M. Shaposhnikov, Phys. Lett. **155B**, 36 (1985).
 55. S. Pascoli, S. Petcov, and W. Rodejohann, Phys. Rev. **D68**, 093007 (2003);
S. Davidson, S. Pascoli, and S. Petcov, private communications.

14. QUARK MODEL

Revised January 2004 by C. Amsler (University of Zürich) and C.G. Wohl (LBNL).

14.1. Quantum numbers of the quarks

Quarks are strongly interacting fermions with spin 1/2 and, by convention, positive parity. Then antiquarks have negative parity. Quarks have the additive baryon number 1/3, antiquarks -1/3. Table 14.1 gives the other additive quantum numbers (flavors) for the three generations of quarks. They are related to the charge Q (in units of the elementary charge e) through the generalized Gell-Mann-Nishijima formula

$$Q = I_z + \frac{B + S + C + B + T}{2}, \quad (14.1)$$

where B is the baryon number. The convention is that the *flavor* of a quark (I_z , S , C , B , or T) has the same sign as its *charge* Q . With this convention, any flavor carried by a charged meson has the same sign as its charge, e.g. the strangeness of the K^+ is +1, the bottomness of the B^+ is +1, and the charm and strangeness of the D_s^- are each -1. Antiquarks have the opposite flavor signs.

Table 14.1: Additive quantum numbers of the quarks.

Property \ Quark	d	u	s	c	b	t
Q – electric charge	$-\frac{1}{3}$	$+\frac{2}{3}$	$-\frac{1}{3}$	$+\frac{2}{3}$	$-\frac{1}{3}$	$+\frac{2}{3}$
I – isospin	$\frac{1}{2}$	$\frac{1}{2}$	0	0	0	0
I_z – isospin z -component	$-\frac{1}{2}$	$+\frac{1}{2}$	0	0	0	0
S – strangeness	0	0	-1	0	0	0
C – charm	0	0	0	+1	0	0
B – bottomness	0	0	0	0	-1	0
T – topness	0	0	0	0	0	+1

14.2. Mesons

Mesons have baryon number $B = 0$. In the quark model they are $q\bar{q}'$ bound states of quarks q and antiquarks \bar{q}' (the flavors of q and q' may be different). If the orbital angular momentum of the $q\bar{q}'$ state is ℓ , then the parity P is $(-1)^{\ell+1}$. The meson spin J is given by the usual relation $|\ell - s| < J < |\ell + s|$ where s is 0 (antiparallel quark spins) or 1 (parallel quark spins). The charge conjugation, or C -parity $C = (-1)^{\ell+s}$, is defined only for the $q\bar{q}$ states made of quarks and their own antiquarks. The C -parity can be generalized to the G -parity $G = (-1)^{I+\ell+s}$ for mesons made of quarks and their own antiquarks (isospin $I_z = 0$) and for the charged $u\bar{d}$ and $d\bar{u}$ states (isospin $I = 1$).

The mesons are classified in J^{PC} multiplets. The $\ell = 0$ states are the pseudoscalars (0^{-+}) and the vectors ($1^{- -}$). The orbital excitations $\ell = 1$ are the scalars (0^{++}), the axial vectors (1^{+-}) and (1^{+-}), and the tensors (2^{++}). Assignments for many of the known mesons are given in Tables 14.2 and 14.3. Radial excitations are denoted by the principal quantum number n . The very short lifetime of the t quark makes it likely that bound state hadrons containing t quarks and/or antiquarks do not exist.

States in the natural spin-parity series $P = (-1)^J$ must, according to the above, have $s = 1$ and hence $CP = +1$. Thus mesons with natural spin-parity and $CP = -1$ (0^{+-} , 1^{-+} , 2^{+-} , 3^{-+} , etc) are forbidden in the $q\bar{q}'$ model. The $J^{PC} = 0^{- -}$ state is forbidden as well. Mesons with such *exotic* quantum numbers may exist, but would lie outside the $q\bar{q}'$ model (see section below on exotic mesons).

Following SU(3) the nine possible $q\bar{q}'$ combinations containing the light u , d , and s quarks are grouped into an octet and a singlet of light quark mesons:

$$3 \otimes \bar{3} = 8 \oplus 1. \quad (14.2)$$

A fourth quark such as charm c can be included by extending SU(3) to SU(4). However, SU(4) is badly broken owing to the much heavier c quark. Nevertheless, in an SU(4) classification the sixteen mesons are grouped into a 15-plet and a singlet:

$$4 \otimes \bar{4} = 15 \oplus 1. \quad (14.3)$$

The *weight diagrams* for the ground-state pseudoscalar (0^{-+}) and vector ($1^{- -}$) mesons are depicted in Fig. 14.1. The light quark mesons are members of nonets building the middle plane in Fig. 14.1(a) and (b).

Isoscalar states with the same J^{PC} will mix but mixing between the two light quark mesons and the much heavier charm or bottom states are generally assumed to be negligible. In the following we shall use the generic names a for the $I = 1$, K for the $I = 1/2$, f and f' for the $I = 0$ members of the light quark nonets. Thus the physical isoscalars are mixtures of the SU(3) wave function ψ_8 and ψ_1 :

$$f' = \psi_8 \cos \theta - \psi_1 \sin \theta, \quad (14.4)$$

$$f = \psi_8 \sin \theta + \psi_1 \cos \theta, \quad (14.5)$$

where θ is the nonet mixing angle and

$$\psi_8 = \frac{1}{\sqrt{6}}(u\bar{u} + d\bar{d} - 2s\bar{s}), \quad (14.6)$$

$$\psi_1 = \frac{1}{\sqrt{3}}(u\bar{u} + d\bar{d} + s\bar{s}). \quad (14.7)$$

The mixing angle has to be determined experimentally.

These mixing relations are often rewritten to exhibit the $u\bar{u} + d\bar{d}$ and $s\bar{s}$ components which decouple for the “ideal” mixing angle θ_i such that $\tan \theta_i = 1/\sqrt{2}$ (or $\theta_i = 35.3^\circ$). Defining $\alpha = \theta + 54.7^\circ$, one obtains the physical isoscalar in the flavor basis

$$f' = \frac{1}{\sqrt{2}}(u\bar{u} + d\bar{d}) \cos \alpha - s\bar{s} \sin \alpha, \quad (14.8)$$

and its orthogonal partner f (replace α by $\alpha - 90^\circ$). Thus for ideal mixing ($\alpha_i = 90^\circ$) the f' becomes pure $s\bar{s}$ and the f pure $u\bar{u} + d\bar{d}$. The mixing angle θ can be derived from the mass relation

$$\tan \theta = \frac{4m_K - m_a - 3m_{f'}}{2\sqrt{2}(m_a - m_K)}, \quad (14.9)$$

which also determines its sign or, alternatively, from

$$\tan^2 \theta = \frac{4m_K - m_a - 3m_{f'}}{-4m_K + m_a + 3m_{f'}}. \quad (14.10)$$

Eliminating θ from these equations leads to the sum rule [1]

$$(m_f + m_{f'})(4m_K - m_a) - 3m_f m_{f'} = 8m_K^2 - 8m_K m_a + 3m_a^2. \quad (14.11)$$

This relation is verified for the ground-state vector mesons. We identify the $\phi(1020)$ with the f' and the $\omega(783)$ with the f . Thus

$$\phi(1020) = \psi_8 \cos \theta_V - \psi_1 \sin \theta_V, \quad (14.12)$$

$$\omega(782) = \psi_8 \sin \theta_V + \psi_1 \cos \theta_V, \quad (14.13)$$

with the vector mixing angle $\theta_V = 35^\circ$ from Eq. (14.9), very close to ideal mixing. Thus $\phi(1020)$ is nearly pure $s\bar{s}$. For ideal mixing Eq. (14.9) and Eq. (14.10) lead to the relations

$$m_K = \frac{m_f + m_{f'}}{2}, \quad m_a = m_f, \quad (14.14)$$

Table 14.2: Suggested $q\bar{q}$ quark-model assignments for some of the observed light mesons. Mesons in bold face are included in the Meson Summary Table. The wave functions f and f' are given in the text. The singlet-octet mixing angles from the quadratic and linear mass formulae are also given for some of the nonets. The classification of the 0^{++} mesons is tentative and the mixing angle uncertain due to large uncertainties in some of the masses. The $f_0(1500)$ in the Meson Summary Table is not in this table as it is hard to accommodate in the scalar nonet. The light scalars $a_0(980)$, $f_0(980)$ and $f_0(600)$ are often considered as meson-meson resonances or four-quark states and are therefore not included in the table. See the “Note on Non- $q\bar{q}$ Mesons” at the end of the Meson Listings.

$n^{2s+1}\ell_J$	J^{PC}	$l = 1$ $ud, \bar{u}d, \frac{1}{\sqrt{2}}(d\bar{d} - u\bar{u})$	$l = \frac{1}{2}$ $u\bar{s}, d\bar{s}; \bar{d}s, -\bar{u}s$	$l = 0$ f'	$l = 0$ f	θ_{quad} [°]	θ_{lin} [°]
1^1S_0	0^{-+}	π	K	η	$\eta'(958)$	-11.5	-24.6
1^3S_1	1^{--}	$\rho(770)$	$K^*(892)$	$\phi(1020)$	$\omega(782)$	38.7	36.0
1^1P_1	1^{+-}	$b_1(1235)$	K_{1B}^\dagger	$h_1(1380)$	$h_1(1170)$		
1^3P_0	0^{++}	$a_0(1450)$	$K_0^*(1430)$	$f_0(1710)$	$f_0(1370)$		
1^3P_1	1^{++}	$a_1(1260)$	K_{1A}^\dagger	$f_1(1420)$	$f_1(1285)$		
1^3P_2	2^{++}	$a_2(1320)$	$K_2^*(1430)$	$f_2'(1525)$	$f_2(1270)$	29.6	28.0
1^1D_2	2^{-+}	$\pi_2(1670)$	$K_2(1770)^\dagger$	$\eta_2(1870)$	$\eta_2(1645)$		
1^3D_1	1^{--}	$\rho(1700)$	$K^*(1680)^\ddagger$		$\omega(1650)$		
1^3D_2	2^{--}		$K_2(1820)^\ddagger$				
1^3D_3	3^{--}	$\rho_3(1690)$	$K_3^*(1780)$	$\phi_3(1850)$	$\omega_3(1670)$	32.0	31.0
1^3F_4	4^{++}	$a_4(2040)$	$K_4^*(2045)$		$f_4(2050)$		
1^3G_5	5^{--}	$\rho_5(2350)$					
1^3H_6	6^{++}	$a_6(2450)$			$f_6(2510)$		
2^1S_0	0^{-+}	$\pi(1300)$	$K(1460)$	$\eta(1475)$	$\eta(1295)$	-22.4	-22.6
2^3S_1	1^{--}	$\rho(1450)$	$K^*(1410)^\ddagger$	$\phi(1680)$	$\omega(1420)$		

[†] The 1^{+-} and 2^{-+} isospin $\frac{1}{2}$ states mix. In particular, the K_{1A} and K_{1B} are nearly equal (45°) mixtures of the $K_1(1270)$ and $K_1(1400)$.

[‡] The $K^*(1410)$ could be replaced by the $K^*(1680)$ as the 2^3S_1 state.

Table 14.3: $q\bar{q}$ quark-model assignments for the observed heavy mesons. Mesons in bold face are included in the Meson Summary Table.

$n^{2s+1}\ell_J$	J^{PC}	$l = 0$ $c\bar{c}$	$l = 0$ $b\bar{b}$	$l = \frac{1}{2}$ $c\bar{u}, \bar{c}d; \bar{c}u, \bar{c}d$	$l = 0$ $c\bar{s}; \bar{c}s$	$l = \frac{1}{2}$ $b\bar{u}, \bar{b}d; \bar{b}u, \bar{b}d$	$l = 0$ $b\bar{s}; \bar{b}s$	$l = 0$ $b\bar{c}; \bar{b}c$
1^1S_0	0^{-+}	$\eta_c(1S)$	$\eta_b(1S)$	D	D_s^\pm	B	B_s	B_c^\pm
1^3S_1	1^{--}	$J/\psi(1S)$	$\Upsilon(1S)$	D^*	$D_s^{*\pm}$	B^*	$B_s^{*\pm}$	
1^1P_1	1^{+-}	$h_c(1P)$		$D_1(2420)$	$D_{s1}(2536)^\pm$			
1^3P_0	0^{++}	$\chi_{c0}(1P)$	$\chi_{b0}(1P)$		$D_{sJ}^*(2317)^\pm$			
1^3P_1	1^{++}	$\chi_{c1}(1P)$	$\chi_{b1}(1P)$		$D_{sJ}^*(2460)^\pm$			
1^3P_2	2^{++}	$\chi_{c2}(1P)$	$\chi_{b2}(1P)$	$D_2(2460)$	$D_{s2}^*(2573)^\pm$			
1^3D_1	1^{--}	$\psi(3770)$						
2^1S_0	0^{-+}	$\eta_c(2S)$						
2^3S_1	1^{--}	$\psi(2S)$	$\Upsilon(2S)$					
$2^3P_{0,1,2}$	$0^{++}, 1^{++}, 2^{++}$		$\chi_{b0,1,2}(2P)$					

[†] The masses of these states are considerably smaller than most theoretical predictions. They have also been considered as four-quark states (See the “Note on Non- $q\bar{q}$ Mesons” at the end of the Meson Listings)

14.3. Exotic mesons

The existence of a light nonet composed of four quarks with masses below 1 GeV was suggested a long time ago [8]. Coupling two triplets of light quarks u , d and s one obtains nine states, of which the six symmetric (uu , dd , ss , $ud + du$, $us + su$, $ds + sd$) form the six dimensional representation $\mathbf{6}$, while the three antisymmetric ($ud - du$, $us - su$, $ds - sd$) form the three dimensional representation $\bar{\mathbf{3}}$ of SU(3):

$$\mathbf{3} \otimes \mathbf{3} = \mathbf{6} \oplus \bar{\mathbf{3}}. \quad (14.20)$$

Combining with spin and color and requiring antisymmetry, one finds that the most deeply bound diquark (and hence the lightest) is the one in the $\bar{\mathbf{3}}$ and spin singlet state. The combination of the diquark with an antidiquark in the $\mathbf{3}$ representation then gives a light nonet of four-quark scalar states. Letting the number of strange quarks determine the mass splitting one obtains a mass inverted spectrum with a light isosinglet ($u\bar{d}\bar{u}\bar{d}$), a medium heavy isodoublet (e.g. $ud\bar{s}\bar{d}$) and a heavy isotriplet (e.g. $ds\bar{u}\bar{s}$) + isosinglet (e.g. $us\bar{u}\bar{s}$). It is then tempting to identify the lightest state with the $f_0(600)$, and the heaviest states with the $a_0(980)$, and $f_0(980)$. Then the meson with strangeness $\kappa(800)$ would lie in between.

QCD predicts the existence of isoscalar mesons which contain only gluons, the glueballs. The ground state glueball is predicted by lattice gauge theories to be 0^{++} , the first excited state 2^{++} . Errors on the mass predictions are large. Ref. 9 predicts a mass of about 1600 MeV for the ground state with an uncertainty of 160 MeV. As an example for the glueball mass spectrum we show in Figure 14.3 a recent calculation from the lattice [10]. The first excited state has a mass of about 2.4 GeV and the lightest glueball with exotic quantum numbers (2^{+-}) has a mass of about 4 GeV.

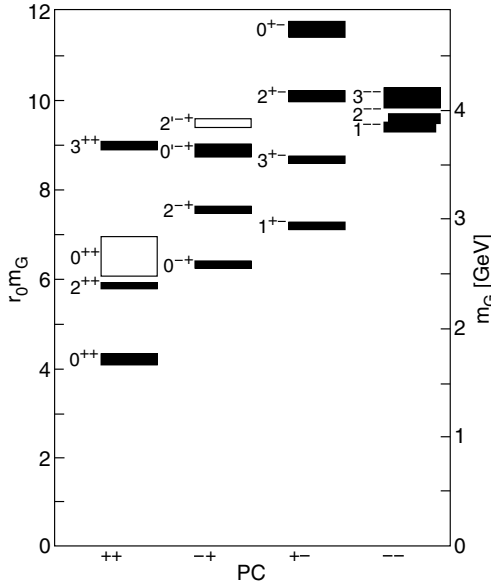


Figure 14.3: Predicted glueball mass spectrum from the lattice (from Ref. 10).

Lattice calculations assume that the quark masses are infinite and neglect $q\bar{q}$ loops. However, one expects that glueballs will mix with nearby $q\bar{q}$ states of the same quantum numbers [7,11]. For example, the two isoscalar 0^{++} mesons will mix with the pure ground state glueball to generate the observed physical states $f_0(1370)$, $f_0(1500)$, and $f_0(1710)$. Experimental evidence is mounting that the $f_0(1500)$ has considerable affinity for glue and that the $f_0(1370)$ and $f_0(1710)$ have large $u\bar{u} + d\bar{d}$ and $s\bar{s}$ components, respectively (See the “Note on Non- $q\bar{q}$ Mesons” at the end of the Meson Listings and Ref. 12).

Mesons made of $q\bar{q}$ pairs bound by excited gluons g , the hybrid states $q\bar{q}g$, are also predicted. They should lie in the 1.9 GeV mass

region, according to gluon flux tube models [13]. Lattice QCD also predicts the lightest hybrid, an exotic 1^{-+} , at a mass of 1.9 GeV [14]. However, the bag model predicts four nonets, among them an exotic 1^{-+} around 1.4 GeV [15]. Most hybrids are rather broad but some can be as narrow as 100 MeV. There are so far two prominent candidates for exotic states with quantum numbers 1^{-+} , the $\pi_1(1400)$ and $\pi_1(1600)$, which could be hybrids or four-quark states (See the “Note on Non- $q\bar{q}$ Mesons” at the end of the Meson Listings and Ref. 12).

14.4. Baryons: qqq states

All the established baryons are apparently 3-quark (qqq) states, and each such state is an SU(3) color singlet, a completely antisymmetric state of the three possible colors. Since the quarks are fermions, the state function for any baryon must be antisymmetric under interchange of any two equal-mass quarks (up and down quarks in the limit of isospin symmetry). Thus the state function may be written as

$$|qqq\rangle_A = |\text{color}\rangle_A \times |\text{space, spin, flavor}\rangle_S, \quad (14.21)$$

where the subscripts S and A indicate symmetry or antisymmetry under interchange of any two of the equal-mass quarks. Note the contrast with the state function for the three nucleons in ${}^3\text{H}$ or ${}^3\text{He}$:

$$|NNN\rangle_A = |\text{space, spin, isospin}\rangle_A. \quad (14.22)$$

This difference has major implications for internal structure, magnetic moments, *etc.* (For a nice discussion, see Ref. 16.)

The “ordinary” baryons are made up of u , d , and s quarks. The three flavors imply an approximate flavor SU(3), which requires that baryons made of these quarks belong to the multiplets on the right side of

$$\mathbf{3} \otimes \mathbf{3} \otimes \mathbf{3} = \mathbf{10}_S \oplus \mathbf{8}_M \oplus \mathbf{8}_M \oplus \mathbf{1}_A \quad (14.23)$$

(see Sec. 37, on “SU(n) Multiplets and Young Diagrams”). Here the subscripts indicate symmetric, mixed-symmetry, or antisymmetric states under interchange of any two quarks. The $\mathbf{1}$ is a uds state (Λ_1) and the octet contains a similar state (Λ_8). If these have the same spin and parity they can mix. An example is the mainly octet D_{03} $\Lambda(1690)$ and mainly singlet D_{03} $\Lambda(1520)$. In the ground state multiplet, the SU(3) flavor singlet Λ is forbidden by Fermi statistics. The mixing formalism is the same as for η - η' or ϕ - ω (see above), except that for baryons the mass M instead of M^2 is used. Section 36, on “SU(3) Isoscalar Factors and Representation Matrices”, shows how relative decay rates in, say, $\mathbf{10} \rightarrow \mathbf{8} \otimes \mathbf{8}$ decays may be calculated. A summary of results of fits to the observed baryon masses and decay rates for the best-known SU(3) multiplets is given in Appendix II of our 1982 edition [17].

The addition of the c quark to the light quarks extends the flavor symmetry to SU(4). Figures 14.4(a) and 14.4(b) show the (badly broken) SU(4) baryon multiplets that have as their bottom levels an SU(3) octet, such as the octet that includes the nucleon, or an SU(3) decuplet, such as the decuplet that includes the $\Delta(1232)$. All the particles in a given SU(4) multiplet have the same spin and parity. The charmed baryons are discussed in more detail in the “Note on Charmed Baryons” in the Particle Listings. The addition of a b quark extends the flavor symmetry to SU(5); it would require four dimensions to draw the multiplets.

For the “ordinary” baryons (no c or b quark), flavor and spin may be combined in an approximate flavor-spin SU(6) in which the six basic states are $d \uparrow, d \downarrow, \dots, s \downarrow$ (\uparrow, \downarrow = spin up, down). Then the baryons belong to the multiplets on the right side of

$$\mathbf{6} \otimes \mathbf{6} \otimes \mathbf{6} = \mathbf{56}_S \oplus \mathbf{70}_M \oplus \mathbf{70}_M \oplus \mathbf{20}_A. \quad (14.24)$$

These SU(6) multiplets decompose into flavor SU(3) multiplets as follows:

$$\mathbf{56} = \mathbf{4} \mathbf{10} \oplus \mathbf{2} \mathbf{8} \quad (14.25a)$$

$$\mathbf{70} = \mathbf{2} \mathbf{10} \oplus \mathbf{4} \mathbf{8} \oplus \mathbf{2} \mathbf{8} \oplus \mathbf{2} \mathbf{1} \quad (14.25b)$$

$$\mathbf{20} = \mathbf{2} \mathbf{8} \oplus \mathbf{4} \mathbf{1}, \quad (14.25c)$$

References:

1. J. Schwinger, Phys. Rev. Lett. **12**, 237 (1964).
2. A. Bramon, R. Escribano, and M.D. Scadron, Phys. Lett. **B403**, 339 (1997).
3. A. Aloisio *et al.*, Phys. Lett. **B541**, 45 (2002).
4. C. Amsler *et al.*, Phys. Lett. **B294**, 451 (1992).
5. C. Amsler, Rev. Mod. Phys. **70**, 1293 (1998).
6. T. Feldmann, Int. J. Mod. Phys. **A915**, 159 (2000).
7. C. Amsler and F.E. Close, Phys. Rev. **D53**, 295 (1996).
8. R.L. Jaffe, Phys. Rev. **D 15** 267, 281 (1977).
9. C. Michael, AIP Conf. Proc. **432**, 657 (1998).
10. C. Morningstar and M. Peardon, Phys. Rev. **D60**, 034509 (1999).
11. F.E. Close and A. Kirk, Eur. Phys. J. **C21**, 531 (2001).
12. C. Amsler and N.A. Törnqvist, Phys. Rev. **389**, 61 (2004).
13. N. Isgur and J. Paton, Phys. Rev. **D31**, 2910 (1985).
14. P. Lacock *et al.*, Phys. Lett. **B401**, 308 (1997);
C. Bernard *et al.*, Phys. Rev. **D56**, 7039 (1997).
15. T. Barnes, F.E. Close, F. de Viron Nucl. Phys. **B224**, 241 (1983).
16. F.E. Close, in *Quarks and Nuclear Forces* (Springer-Verlag, 1982), p. 56.
17. Particle Data Group, Phys. Lett. **111B** (1982).
18. R.H. Dalitz and L.J. Reinders, in *Hadron Structure as Known from Electromagnetic and Strong Interactions, Proceedings of the Hadron '77 Conference* (Veda, 1979), p. 11.
19. N. Isgur and G. Karl, Phys. Rev. **D18**, 4187 (1978); *ibid.* **D19**, 2653 (1979); *ibid.* **D20**, 1191 (1979);
K.-T. Chao, N. Isgur, and G. Karl, Phys. Rev. **D23**, 155 (1981).
20. C.P. Forsyth and R.E. Cutkosky, Z. Phys. **C18**, 219 (1983).
21. A.J.G. Hey and R.L. Kelly, Phys. Reports **96**, 71 (1983). Also see S. Gasiorowicz and J.L. Rosner, Am. J. Phys. **49**, 954 (1981).
22. N. Isgur, Int. J. Mod. Phys. **E1**, 465 (1992);
G. Karl, Int. J. Mod. Phys. **E1**, 491 (1992).

15. GRAND UNIFIED THEORIES

Written April 2002 by S. Raby (Ohio State University).

15.1. Grand Unification

15.1.1. Standard Model: An Introduction

In spite of all the successes of the Standard Model [SM], it is unlikely to be the final theory. It leaves many unanswered questions. Why the local gauge interactions $SU(3)_C \times SU(2)_L \times U(1)_Y$, and why 3 families of quarks and leptons? Moreover, why does one family consist of the states $[Q, u^c, d^c; L, e^c]$ transforming as $[(3, 2, 1/3), (\bar{3}, 1, -4/3), (\bar{3}, 1, 2/3); (1, 2, -1), (1, 1, 2)]$, where $Q = (u, d)$, and $L = (\nu, e)$ are $SU(2)_L$ doublets, and u^c, d^c, e^c are charge conjugate $SU(2)_L$ singlet fields with the $U(1)_Y$ quantum numbers given? [We use the convention that electric charge $Q_{EM} = T_{3L} + Y/2$ and all fields are left-handed.] Note the SM gauge interactions of quarks and leptons are completely fixed by their gauge charges. Thus, if we understood the origin of this charge quantization, we would also understand why there are no fractionally charged hadrons. Finally, what is the origin of quark and lepton masses, or the apparent hierarchy of family masses and quark mixing angles? Perhaps if we understood this, we would also know the origin of CP violation, the solution to the strong CP problem, the origin of the cosmological matter-antimatter asymmetry, or the nature of dark matter.

The SM has 19 arbitrary parameters; their values are chosen to fit the data. Three arbitrary gauge couplings: g_3, g, g' (where g, g' are the $SU(2)_L, U(1)_Y$ couplings, respectively) or equivalently, $\alpha_s = (g_3^2/4\pi), \alpha_{EM} = (e^2/4\pi)$ ($e = g \sin\theta_W$), and $\sin^2\theta_W = (g')^2/(g^2 + (g')^2)$. In addition, there are 13 parameters associated with the 9 charged fermion masses and the four mixing angles in the CKM matrix. The remaining 3 parameters are v, λ [the Higgs VEV (vacuum expectation value) and quartic coupling] (or equivalently, M_Z, m_h^0), and the QCD θ parameter. In addition, there are hints of new physics beyond the SM, such as neutrino masses. With 3 light Majorana neutrinos, there are at least 9 additional parameters in the neutrino sector; 3 masses and 6 mixing angles. In summary, the SM has too many arbitrary parameters, and leaves open too many unresolved questions to be considered complete. These are the problems which grand unified theories hope to address.

15.1.2. Charge Quantization

In the Standard Model, quarks and leptons are on an equal footing; both fundamental particles without substructure. It is now clear that they may be two faces of the same coin; unified, for example, by extending QCD (or $SU(3)_C$) to include leptons as the fourth color, $SU(4)_C$ [1]. The complete Pati-Salam gauge group is $SU(4)_C \times SU(2)_L \times SU(2)_R$, with the states of one family $[(Q, L), (Q^c, L^c)]$ transforming as $[(4, 2, 1), (\bar{4}, 1, \bar{2})]$, where $Q^c = (d^c, u^c), L^c = (e^c, \nu^c)$ are doublets under $SU(2)_R$. Electric charge is now given by the relation $Q_{EM} = T_{3L} + T_{3R} + 1/2(B-L)$, and $SU(4)_C$ contains the subgroup $SU(3)_C \times (B-L)$ where B (L) is baryon (lepton) number. Note ν^c has no SM quantum numbers and is thus completely "sterile." It is introduced to complete the $SU(2)_R$ lepton doublet. This additional state is desirable when considering neutrino masses.

Although quarks and leptons are unified with the states of one family forming two irreducible representations of the gauge group, there are still 3 independent gauge couplings (two if one also imposes parity, *i.e.*, $L \leftrightarrow R$ symmetry). As a result, the three low-energy gauge couplings are still independent arbitrary parameters. This difficulty is resolved by embedding the SM gauge group into the simple unified gauge group, Georgi-Glashow $SU(5)$, with one universal gauge coupling α_G defined at the grand unification scale M_G [2]. Quarks and leptons still sit in two irreducible representations, as before, with a $\mathbf{10} = [Q, u^c, e^c]$ and $\bar{\mathbf{5}} = [d^c, L]$. Nevertheless, the three low energy gauge couplings are now determined in terms of two independent parameters: α_G and M_G . Hence, there is one prediction.

In order to break the electroweak symmetry at the weak scale and give mass to quarks and leptons, Higgs doublets are needed which can sit in either a $\mathbf{5}_H$ or $\bar{\mathbf{5}}_H$. The additional 3 states are color triplet

Higgs scalars. The couplings of these color triplets violate baryon and lepton number, and nucleons decay via the exchange of a single color triplet Higgs scalar. Hence, in order not to violently disagree with the non-observation of nucleon decay, their mass must be greater than $\sim 10^{10-11}$ GeV. Note, in supersymmetric GUTs, in order to cancel anomalies, as well as give mass to both up and down quarks, both Higgs multiplets $\mathbf{5}_H, \bar{\mathbf{5}}_H$ are required. As we shall discuss later, nucleon decay now constrains the color triplet Higgs states in a SUSY GUT to have mass significantly greater than M_G .

Complete unification is possible with the symmetry group $SO(10)$, with one universal gauge coupling α_G , and one family of quarks and leptons sitting in the 16-dimensional-spinor representation $\mathbf{16} = [\mathbf{10} + \bar{\mathbf{5}} + \mathbf{1}]$ [3]. The $SU(5)$ singlet $\mathbf{1}$ is identified with ν^c . In Table 15.1 we present the states of one family of quarks and leptons, as they appear in the $\mathbf{16}$. It is an amazing and perhaps even profound fact that all the states of a single family of quarks and leptons can be represented digitally as a set of 5 zeros and/or ones or equivalently as the tensor product of 5 "spin" 1/2 states (see Table 15.1). The first three "spins" correspond to $SU(3)_C$ color quantum numbers, while the last two are $SU(2)_L$ weak quantum numbers. In fact, an $SU(3)_C$ rotation just raises one color index and lowers another, thereby changing colors $\{r, b, y\}$. Similarly an $SU(2)_L$ rotation raises one weak index and lowers another, thereby flipping the weak isospin from up to down or vice versa. In this representation, weak hypercharge Y is given by the simple relation $Y = 2/3(\sum \text{color spins}) - (\sum \text{weak spins})$ where the sum is over the spin values $\{\pm 1/2\}$. $SU(5)$ rotations then raise (or lower) a color index, while at the same time lowering (or raising) a weak index. It is easy to see that such rotations can mix the states $\{Q, u^c, e^c\}$ and $\{d^c, L\}$ among themselves, and ν^c is a singlet. The new $SO(10)$ rotations [not in $SU(5)$] are then given by either raising or lowering any two spins. For example, by lowering the two weak indices ν^c rotates into e^c , etc.

Table 15.1: The quantum numbers of the $\mathbf{16}$ dimensional representation of $SO(10)$ are represented as a tensor product of 5 "spin" 1/2 states with the values \pm denoting the spin states $|\pm \frac{1}{2}\rangle$ and with the condition that we have an even number of $-$ spins.

State	Y	Color	Weak
ν^c	0	+++	++
e^c	2	+++	--
u_r	1/3	-++	+-
d_r	1/3	-++	-+
u_b	1/3	+--	+-
d_b	1/3	+--	-+
u_y	1/3	++-	+-
d_y	1/3	++-	-+
u_r^c	-4/3	+--	++
u_b^c	-4/3	+--	++
u_y^c	-4/3	--+	++
d_r^c	2/3	+--	--
d_b^c	2/3	+--	--
d_y^c	2/3	--+	--
ν	-1	---	+-
e	-1	---	-+

$SO(10)$ has two inequivalent maximal breaking patterns: $SO(10) \rightarrow SU(5) \times U(1)_X$ and $SO(10) \rightarrow SU(4)_C \times SU(2)_L \times SU(2)_R$. In the first case, we obtain Georgi-Glashow $SU(5)$ if Q_{EM} is given in terms of $SU(5)$ generators alone, or so-called flipped $SU(5)$ [4] if Q_{EM} is partly in $U(1)_X$. In the latter case, we have the Pati-Salam symmetry. If $SO(10)$ breaks directly to the SM at M_G , then we

retain the prediction for gauge coupling unification. However, more possibilities for breaking (hence more breaking scales and more parameters) are available in $SO(10)$. Nevertheless with one breaking pattern $SO(10) \rightarrow SU(5) \rightarrow SM$, where the last breaking scale is M_G , the predictions from gauge coupling unification are preserved. The Higgs multiplets in minimal $SO(10)$ are contained in the fundamental $\mathbf{10}_H = [\mathbf{5}_H, \bar{\mathbf{5}}_H]$ representation. Note only in $SO(10)$ does the gauge symmetry distinguish quark and lepton multiplets from Higgs multiplets.

Finally, larger symmetry groups have been considered. For example, $E(6)$ has a fundamental representation $\mathbf{27}$, which under $SO(10)$ transforms as a $[\mathbf{16} + \mathbf{10} + \mathbf{1}]$. The breaking pattern $E(6) \rightarrow SU(3)_C \times SU(3)_L \times SU(3)_R$ is also possible. With the additional permutation symmetry $Z(3)$ interchanging the three $SU(3)$ s, we obtain so-called “trification [5],” with a universal gauge coupling. The latter breaking pattern has been used in phenomenological analyses of the heterotic string [6]. Note, in larger symmetry groups, such as $E(6)$, $SU(6)$, etc., there are now many more states which have not been observed and must be removed from the effective low-energy theory. In particular, three families of $\mathbf{27}$ s in $E(6)$ contain three Higgs type multiplets transforming as $\mathbf{10}$ s of $SO(10)$. This makes these larger symmetry groups unattractive starting points for model building.

15.1.3. Gauge coupling unification:

The biggest paradox of grand unification is to understand how it is possible to have a universal gauge coupling g_G in a grand unified theory [GUT], and yet have three unequal gauge couplings at the weak scale with $g_3 > g > g'$. The solution is given in terms of the concept of an effective field theory [EFT] [7]. The GUT symmetry is spontaneously broken at the scale M_G , and all particles not in the SM obtain mass of order M_G . When calculating Green’s functions with external energies $E \gg M_G$, we can neglect the mass of all particles in the loop and hence all particles contribute to the renormalization group running of the universal gauge coupling. However, for $E \ll M_G$, one can consider an effective field theory including only the states with mass $< E \ll M_G$. The gauge symmetry of the EFT is $SU(3)_C \times SU(2)_L \times U(1)_Y$, and the three gauge couplings renormalize independently. The states of the EFT include only those of the SM; 12 gauge bosons, 3 families of quarks and leptons, and one or more Higgs doublets. At M_G , the two effective theories [the GUT itself is most likely the EFT of a more fundamental theory defined at a higher scale] must give identical results; hence we have the boundary conditions $g_3 = g_2 = g_1 \equiv g_G$, where at any scale $\mu < M_G$, we have $g_2 \equiv g$ and $g_1 = \sqrt{5/3} g'$. Then using two low-energy couplings, such as $\alpha_s(M_Z)$, $\alpha_{EM}(M_Z)$, the two independent parameters α_G , M_G can be fixed. The third gauge coupling, $\sin^2 \theta_W$ in this case, is then predicted. This was the procedure up until about 1991 [8,9]. Subsequently, the uncertainties in $\sin^2 \theta_W$ were reduced tenfold. Since then, $\alpha_{EM}(M_Z)$, $\sin^2 \theta_W$ have been used as input to predict α_G , M_G , and $\alpha_s(M_Z)$ [10].

Note, the above boundary condition is only valid when using one-loop-renormalization group [RG] running. With precision electroweak data, however, it is necessary to use two-loop-RG running. Hence, one must include one-loop-threshold corrections to gauge coupling boundary conditions at both the weak and GUT scales. In this case, it is always possible to define the GUT scale as the point where $\alpha_1(M_G) = \alpha_2(M_G) \equiv \bar{\alpha}_G$ and $\alpha_3(M_G) = \bar{\alpha}_G (1 + \epsilon_3)$. The threshold correction ϵ_3 is a logarithmic function of all states with mass of order M_G and $\bar{\alpha}_G = \alpha_G + \Delta$, where α_G is the GUT coupling constant above M_G , and Δ is a one-loop-threshold correction. To the extent that gauge coupling unification is perturbative, the GUT threshold corrections are small and calculable. This presumes that the GUT scale is sufficiently below the Planck scale or any other strong coupling extension of the GUT, such as a strongly coupled string theory.

Supersymmetric grand unified theories [SUSY GUTs] are an extension of non-SUSY GUTs [11]. The key difference between SUSY GUTs and non-SUSY GUTs is the low-energy effective theory. The low-energy effective field theory in a SUSY GUT is assumed to satisfy $N = 1$ supersymmetry down to scales of order the weak scale, in addition to the SM gauge symmetry. Hence, the spectrum includes all the SM states, plus their supersymmetric partners. It also includes

one pair (or more) of Higgs doublets; one to give mass to up-type quarks, and the other to down-type quarks and charged leptons. Two doublets with opposite hypercharge Y are also needed to cancel fermionic triangle anomalies. Note, a low-energy SUSY-breaking scale (the scale at which the SUSY partners of SM particles obtain mass) is necessary to solve the gauge hierarchy problem.

Simple non-SUSY $SU(5)$ is ruled out, initially by the increased accuracy in the measurement of $\sin^2 \theta_W$, and by early bounds on the proton lifetime (see below) [9]. However, by now LEP data [10] has conclusively shown that SUSY GUTs is the new Standard Model; by which we mean the theory used to guide the search for new physics beyond the present SM. SUSY extensions of the SM have the property that their effects decouple as the effective SUSY-breaking scale is increased. Any theory beyond the SM must have this property simply because the SM works so well. However, the SUSY-breaking scale cannot be increased with impunity, since this would reintroduce a gauge hierarchy problem. Unfortunately there is no clear-cut answer to the question, “When is the SUSY-breaking scale too high?” A conservative bound would suggest that the third generation squarks and sleptons must be lighter than about 1 TeV, in order that the one-loop corrections to the Higgs mass from Yukawa interactions remain of order the Higgs mass bound itself.

At present, gauge coupling unification within SUSY GUTs works extremely well. Exact unification at M_G , with two-loop-RG running from M_G to M_Z , and one-loop-threshold corrections at the weak scale, fits to within 3 σ of the present precise low-energy data. A small threshold correction at M_G ($\epsilon_3 \sim -4\%$) is sufficient to fit the low-energy data precisely.* This may be compared to non-SUSY GUTs, where the fit misses by $\sim 12 \sigma$, and a precise fit requires new weak-scale states in incomplete GUT multiplets, or multiple GUT-breaking scales.**

15.1.4. Nucleon Decay

Baryon number is necessarily violated in any GUT [15]. In $SU(5)$, nucleons decay via the exchange of gauge bosons with GUT scale masses, resulting in dimension-6 baryon-number-violating operators suppressed by $(1/M_G^2)$. The nucleon lifetime is calculable and given by $\tau_N \propto M_G^4 / (\alpha_G^2 m_p^5)$. The dominant decay mode of the proton (and the baryon-violating decay mode of the neutron), via gauge exchange, is $p \rightarrow e^+ \pi^0$ ($n \rightarrow e^+ \pi^-$). In any simple gauge symmetry, with one universal GUT coupling and scale (α_G , M_G), the nucleon lifetime from gauge exchange is calculable. Hence, the GUT scale may be directly observed via the extremely rare decay of the nucleon. Experimental searches for nucleon decay began with the Kolar Gold Mine, Homestake, Soudan, NUSEX, Frejus, HPW, and IMB detectors [8]. The present experimental bounds come from Super-Kamiokande and Soudan II. We discuss these results shortly. Non-SUSY GUTs are also ruled out by the non-observation of nucleon decay [9]. In SUSY GUTs, the GUT scale is of order 3×10^{16} GeV, as compared to the GUT scale in non-SUSY GUTs, which is of order 10^{15} GeV. Hence, the dimension-6 baryon-violating operators are significantly suppressed in SUSY GUTs [11] with $\tau_p \sim 10^{34-38}$ yrs.

However, in SUSY GUTs, there are additional sources for baryon-number violation—dimension-4 and -5 operators [16]. Although the notation does not change, when discussing SUSY GUTs, all fields are implicitly bosonic superfields, and the operators

* This result implicitly assumes universal GUT boundary conditions for soft SUSY-breaking parameters at M_G . In the simplest case, we have a universal gaugino mass $M_{1/2}$, a universal mass for squarks and sleptons m_{16} , and a universal Higgs mass m_{10} , as motivated by $SO(10)$. In some cases, threshold corrections to gauge coupling unification can be exchanged for threshold corrections to soft SUSY parameters. See for example, Ref. 12 and references therein.

** Non-SUSY GUTs with a more complicated breaking pattern can still fit the data. For example, non-SUSY $SO(10) \rightarrow SU(4)_C \times SU(2)_L \times SU(2)_R \rightarrow SM$, with the second breaking scale of order an intermediate scale, determined by light neutrino masses using the see-saw mechanism, can fit the low-energy data for gauge couplings [13], and at the same time survive nucleon decay bounds [14], discussed in the following section.

considered are the so-called F terms, which contain two fermionic components, and the rest scalars or products of scalars. Within the context of $SU(5)$, the dimension-4 and -5 operators have the form $(\mathbf{10} \ \bar{\mathbf{5}} \ \bar{\mathbf{5}}) \supset (u^c d^c d^c) + (Q L d^c) + (e^c L L)$, and $(\mathbf{10} \ \mathbf{10} \ \mathbf{10} \ \bar{\mathbf{5}}) \supset (Q Q Q L) + (u^c u^c d^c e^c) + B$ and L conserving terms, respectively. The dimension-4 operators are renormalizable with dimensionless couplings; similar to Yukawa couplings. On the other hand, the dimension-5 operators have a dimensionful coupling of order $(1/M_G)$.

The dimension-4 operators violate baryon number or lepton number, respectively, but not both. The nucleon lifetime is extremely short if both types of dimension-4 operators are present in the low-energy theory. However, both types can be eliminated by requiring R parity. In $SU(5)$, the Higgs doublets reside in a $\mathbf{5}_H$, $\bar{\mathbf{5}}_H$, and R parity distinguishes the $\bar{\mathbf{5}}$ (quarks and leptons) from $\mathbf{5}_H$ (Higgs). R parity [17] (or more precisely, its cousin, family reflection symmetry (see Dimopoulos and Georgi [11] and DRW [18]) takes $F \rightarrow -F$, $H \rightarrow H$ with $F = \{\mathbf{10}, \bar{\mathbf{5}}\}$, $H = \{\mathbf{5}_H, \bar{\mathbf{5}}_H\}$. This forbids the dimension-4 operator $(\mathbf{10} \ \bar{\mathbf{5}} \ \bar{\mathbf{5}})$, but allows the Yukawa couplings of the form $(\mathbf{10} \ \bar{\mathbf{5}} \ \bar{\mathbf{5}}_H)$ and $(\mathbf{10} \ \mathbf{10} \ \mathbf{5}_H)$. It also forbids the dimension-3, lepton-number-violating operator $(\bar{\mathbf{5}} \ \mathbf{5}_H) \supset (L H_u)$, with a coefficient with dimensions of mass which, like the μ parameter, could be of order the weak scale and the dimension-5, baryon-number-violating operator $(\mathbf{10} \ \mathbf{10} \ \mathbf{10} \ \bar{\mathbf{5}}_H) \supset (Q Q Q H_d) + \dots$.

Note, in the MSSM, it is possible to retain R -parity-violating operators at low energy, as long as they violate either baryon number or lepton number only, but not both. Such schemes are natural if one assumes a low-energy symmetry, such as lepton number, baryon number, or a baryon parity [19]. However, these symmetries cannot be embedded in a GUT. Thus, in a SUSY GUT, only R parity can prevent unwanted dimension four operators. Hence, by naturalness arguments, R parity must be a symmetry in the effective low-energy theory of any SUSY GUT. This does not mean to say that R parity is guaranteed to be satisfied in any GUT.

Note also, R parity distinguishes Higgs multiplets from ordinary families. In $SU(5)$, Higgs and quark/lepton multiplets have identical quantum numbers; while in $E(6)$, Higgs and families are unified within the fundamental $\mathbf{27}$ representation. Only in $SO(10)$ are Higgs and ordinary families distinguished by their gauge quantum numbers. Moreover, the $Z(4)$ center of $SO(10)$ distinguishes $\mathbf{10}$ s from $\mathbf{16}$ s, and can be associated with R parity [20].

Dimension-5 baryon-number-violating operators may be forbidden at tree level by symmetries in $SU(5)$, etc. These symmetries are typically broken, however, by the VEVs responsible for the color triplet Higgs masses. Consequently, these dimension-5 operators are generically generated via color triplet Higgsino exchange. Hence, the color triplet partners of Higgs doublets must necessarily obtain mass of order the GUT scale. The dominant decay modes from dimension-5 operators are $p \rightarrow K^+ \bar{\nu}$ ($n \rightarrow K^0 \bar{\nu}$). This is due to a simple symmetry argument; the operators $(Q_i Q_j Q_k L_l)$, $(u_i^c u_j^c d_k^c e_l^c)$ (where $i, j, k, l = 1, 2, 3$ are family indices, and color and weak indices are implicit) must be invariant under $SU(3)_C$ and $SU(2)_L$. As a result, their color and weak doublet indices must be anti-symmetrized. However, since these operators are given by bosonic superfields, they must be totally symmetric under interchange of all indices. Thus, the first operator vanishes for $i = j = k$, and the second vanishes for $i = j$. Hence, a second or third generation member must exist in the final state [18].

Recent Super-Kamiokande bounds on the proton lifetime severely constrain these dimension-6 operators with dimension-5 operators with $\tau_{(p \rightarrow e^+ \pi^0)} > 5.0 \times 10^{33}$ yrs (79.3 ktyr exposure), $\tau_{(n \rightarrow e^+ \pi^-)} > 5 \times 10^{33}$ yrs (61 ktyr), and $\tau_{(p \rightarrow K^+ \bar{\nu})} > 1.6 \times 10^{33}$ yrs (79.3 ktyr), $\tau_{(n \rightarrow K^0 \bar{\nu})} > 1.7 \times 10^{32}$ yrs (61 ktyr) at (90% CL) based on the listed exposures [21]. These constraints are now sufficient to rule out minimal SUSY $SU(5)$ [22]. Non-minimal Higgs sectors in $SU(5)$ or $SO(10)$ theories still survive [24,25]. The upper bound on the proton lifetime from these theories is approximately a factor of 5 above the experimental bounds. They are also being pushed to their theoretical limits. Hence, if SUSY GUTs are correct, then nucleon decay must be seen soon.

Is there a way out of this conclusion? String theories, and recent field theoretic constructions [26,27], contain grand unified symmetries realized in higher dimensions. In most heterotic string models, when compactifying all but four of these extra dimensions, only the MSSM is recovered as a symmetry of the effective four dimensional field theory. [Of course, this is not required by string theory, and string theory models exist whose low-energy field theory is a SUSY GUT [28].] In the process of compactification and GUT symmetry breaking, color triplet Higgs states are removed (projected out of the massless sector of the theory). In addition, the same projections, in heterotic string models, typically rearrange the quark and lepton states so that the massless states which survive emanate from different GUT multiplets. In these models, proton decay due to dimension-5 operators can be severely suppressed, or eliminated completely. In addition, proton decay due to dimension-6 operators may be enhanced due to threshold corrections at the GUT scale which effectively lower the GUT scale [27], or eliminate it altogether, if the states of one family come from different irreducible representations. Hence, the observation of proton decay may distinguish extra-dimensional GUTs from four-dimensional ones.

Before concluding the topic of baryon-number violation, consider the status of $\Delta B = 2$ neutron- anti-neutron oscillations. Generically, the leading operator for this process is the dimension-9 six-quark operator $G_{(\Delta B=2)} (u^c d^c d^c u^c d^c d^c)$, with dimensionful coefficient $G_{(\Delta B=2)} \sim 1/M^3$. The present experimental bound $\tau_{n-\bar{n}} \geq 0.86 \times 10^8$ sec. at 90% CL [30] probes only up to the scale $M \leq 10^6$ GeV. For $M \sim M_G$, $n-\bar{n}$ oscillations appear to be unobservable for any GUT (for a recent discussion see Ref. 29).

15.1.5. Yukawa coupling unification

15.1.5.1. 3rd generation, $b-\tau$ or $t-b-\tau$ unification:

If quarks and leptons are two sides of the same coin, related by a new grand unified gauge symmetry, then that same symmetry relates the Yukawa couplings (and hence the masses) of quarks and leptons. In $SU(5)$, there are two independent renormalizable Yukawa interactions given by $\lambda_t (\mathbf{10} \ \mathbf{10} \ \mathbf{5}_H) + \lambda (\mathbf{10} \ \bar{\mathbf{5}} \ \bar{\mathbf{5}}_H)$. These contain the SM interactions $\lambda_t (Q u^c H_u) + \lambda (Q d^c H_d + e^c L H_d)$. Hence, at the GUT scale, we have the tree-level relation, $\lambda_b = \lambda_\tau \equiv \lambda$ [31]. In $SO(10)$, there is only one independent renormalizable Yukawa interaction given by $\lambda (\mathbf{16} \ \mathbf{16} \ \mathbf{10}_H)$, which gives the tree-level relation, $\lambda_t = \lambda_b = \lambda_\tau \equiv \lambda$ [32,33]. Note, in the discussion above, we assume the minimal Higgs content, with Higgs in $\mathbf{5}$, $\bar{\mathbf{5}}$ for $SU(5)$ and $\mathbf{10}$ for $SO(10)$. With Higgs in higher-dimensional representations, there are more possible Yukawa couplings.

In order to make contact with the data, one now renormalizes the top, bottom, and τ Yukawa couplings, using two-loop-RG equations, from M_G to M_Z . One then obtains the running quark masses $m_t(M_Z) = \lambda_t(M_Z) v_u$, $m_b(M_Z) = \lambda_b(M_Z) v_d$, and $m_\tau(M_Z) = \lambda_\tau(M_Z) v_d$, where $\langle H_u^0 \rangle \equiv v_u = \sin \beta v / \sqrt{2}$, $\langle H_d^0 \rangle \equiv v_d = \cos \beta v / \sqrt{2}$, $v_u/v_d \equiv \tan \beta$, and $v \sim 246$ GeV is fixed by the Fermi constant, G_μ .

Including one-loop-threshold corrections at M_Z , and additional RG running, one finds the top, bottom, and τ -pole masses. In SUSY, $b-\tau$ unification has two possible solutions, with $\tan \beta \sim 1$ or 40–50. The small $\tan \beta$ solution is now disfavored by the LEP limit, $\tan \beta > 2.4$ [34]. The large $\tan \beta$ limit overlaps the $SO(10)$ symmetry relation.

When $\tan \beta$ is large, there are significant weak-scale threshold corrections to down quark and charged lepton masses, from either gluino and/or chargino loops [35]. Yukawa unification (consistent with low energy data) is only possible in a restricted region of SUSY parameter space with important consequences for SUSY searches [36].

15.1.5.2. Three families:

Simple Yukawa unification is not possible for the first two generations, of quarks and leptons. Consider the $SU(5)$ GUT scale relation $\lambda_b = \lambda_\tau$. If extended to the first two generations, one would have $\lambda_s = \lambda_\mu$, $\lambda_d = \lambda_e$, which gives $\lambda_s/\lambda_d = \lambda_\mu/\lambda_e$. The last relation is a renormalization group invariant, and is thus satisfied at any scale. In particular, at the weak scale, one obtains $m_s/m_d = m_\mu/m_e$, which is in serious disagreement with the data, namely $m_s/m_d \sim 20$ and

$m_\mu/m_e \sim 200$. An elegant solution to this problem was given by Georgi and Jarlskog [37]. Of course, a three-family model must also give the observed CKM mixing in the quark sector. Note, although there are typically many more parameters in the GUT theory above M_G , it is possible to obtain effective low-energy theories with many fewer parameters making strong predictions for quark and lepton masses. Three-family models exist which fit all the data, including neutrino masses and mixing [38].

15.1.6. Neutrino Masses:

Atmospheric and solar neutrino oscillations require neutrino masses. Adding three “sterile” neutrinos ν^c with the Yukawa coupling $\lambda_\nu (\nu^c \mathbf{L} \mathbf{H}_u)$, one easily obtains three massive Dirac neutrinos with mass $m_\nu = \lambda_\nu v_u$. However, in order to obtain a tau neutrino with mass of order 0.1 eV, one needs $\lambda_{\nu\tau}/\lambda_\tau \leq 10^{-10}$. The see-saw mechanism, on the other hand, can naturally explain such small neutrino masses [15,39]. Since ν^c has no SM quantum numbers, there is no symmetry (other than global lepton number) which prevents the mass term $\frac{1}{2} \nu^c M \nu^c$. Moreover, one might expect $M \sim M_G$. Heavy “sterile” neutrinos can be integrated out of the theory, defining an effective low-energy theory with only light active Majorana neutrinos, with the effective dimension-5 operator $\frac{1}{2} (\mathbf{L} \mathbf{H}_u) \lambda_\nu^T M^{-1} \lambda_\nu (\mathbf{L} \mathbf{H}_u)$. This then leads to a 3×3 Majorana neutrino mass matrix $\mathbf{m} = m_\nu^T M^{-1} m_\nu$.

Atmospheric neutrino oscillations require neutrino masses with $\Delta m_\nu^2 \sim 3 \times 10^{-3} \text{ eV}^2$ with maximal mixing, in the simplest two-neutrino scenario. With hierarchical neutrino masses, $m_{\nu\tau} = \sqrt{\Delta m_\nu^2} \sim 0.055 \text{ eV}$. Moreover, via the “see-saw” mechanism, $m_{\nu\tau} = m_t(m_t)^2/(3M)$. Hence, one finds $M \sim 2 \times 10^{14} \text{ GeV}$ —remarkably close to the GUT scale. Note we have related the neutrino-Yukawa coupling to the top-quark-Yukawa coupling $\lambda_{\nu\tau} = \lambda_t$ at M_G , as given in $\text{SO}(10)$ or $\text{SU}(4) \times \text{SU}(2)_L \times \text{SU}(2)_R$. However, at low energies they are no longer equal, and we have estimated this RG effect by $\lambda_{\nu\tau}(M_Z) \approx \lambda_t(M_Z)/\sqrt{3}$.

15.1.7. Selected Topics:

15.1.7.1. Magnetic Monopoles:

In the broken phase of a GUT, there are typically localized classical solutions carrying magnetic charge under an unbroken $U(1)$ symmetry [40]. These magnetic monopoles with mass of order M_G/α_G are produced during the GUT phase transition in the early universe. The flux of magnetic monopoles is experimentally found to be less than $\sim 10^{-16} \text{ cm}^{-2} \text{ s}^{-1} \text{ sr}^{-1}$ [41]. Many more are predicted however, hence the GUT monopole problem. In fact, one of the original motivations for an inflationary universe is to solve the monopole problem by invoking an epoch of rapid inflation after the GUT phase transition [42]. This would have the effect of diluting the monopole density as long as the reheat temperature is sufficiently below M_G . Parenthetically, it was also shown that GUT monopoles can catalyze nucleon decay [43].

15.1.7.2. Baryogenesis via Leptogenesis:

Baryon-number-violating operators in $\text{SU}(5)$ or $\text{SO}(10)$ preserve the global symmetry $B-L$. Hence, the value of the cosmological $B-L$ density is an initial condition of the theory, and is typically assumed to be zero. On the other hand, anomalies of the electroweak symmetry violate $B+L$ while also preserving $B-L$. Hence, thermal fluctuations in the early universe, via so-called sphaleron processes, can drive $B+L$ to zero, washing out any net baryon number generated in the early universe at GUT temperatures.

One way out of this dilemma is to generate a net $B-L$ dynamically in the early universe. We have just seen that neutrino oscillations suggest a new scale of physics of order 10^{14} GeV . This scale is associated with heavy Majorana neutrinos with mass M . If in the early universe, the decay of the heavy neutrinos is out of equilibrium and violates both lepton number and CP , then a net lepton number may be generated. This lepton number will then be partially converted into baryon number via electroweak processes [44].

15.1.7.3. GUT symmetry breaking:

The grand unification symmetry is necessarily broken spontaneously. Scalar potentials (or superpotentials) exist whose vacua spontaneously break $\text{SU}(5)$ and $\text{SO}(10)$. These potentials are ad hoc (just like the Higgs potential in the SM), and, therefore it is hoped that they may be replaced with better motivated sectors. Gauge coupling unification now tests GUT-breaking sectors, since it is one of the two dominant corrections to the GUT threshold correction ϵ_3 . The other dominant correction comes from the Higgs sector and doublet-triplet splitting. This latter contribution is always positive $\epsilon_3 \propto \ln(M_T/M_G)$ (where M_T is an effective color triplet Higgs mass), while the low-energy data requires $\epsilon_3 < 0$. Hence, the GUT-breaking sector must provide a significant (of order -8%) contribution to ϵ_3 to be consistent with the Super-K bound on the proton lifetime [23,24,25,38].

In string theory (and GUTs in extra-dimensions), GUT breaking may occur due to boundary conditions in the compactified dimensions [26,27]. This is still ad hoc. The major benefits are that it does not require complicated GUT-breaking sectors, and it can suppress dimension-5 baryon-violating operators.

15.1.7.4. Doublet-triplet splitting:

The Minimal Supersymmetric Standard Model has a μ problem: why is the coefficient of the bilinear Higgs term in the superpotential $\mu (\mathbf{H}_u \mathbf{H}_d)$ of order the weak scale when, since it violates no low-energy symmetry, it could be as large as M_G ? In a SUSY GUT, the μ problem is replaced by the problem of *doublet-triplet* splitting—giving mass of order M_G to the color triplet Higgs, and mass μ to the Higgs doublets. Several mechanisms for natural doublet-triplet splitting have been suggested, such as the sliding singlet, missing partner or missing VEV [45], and pseudo-Nambu-Goldstone boson mechanisms. Particular examples of the missing partner mechanism for $\text{SU}(5)$ [25], the missing VEV mechanism for $\text{SO}(10)$ [24,38], and the pseudo-Nambu-Goldstone boson mechanism for $\text{SU}(6)$ [46], have been shown to be consistent with gauge coupling unification and proton decay. There are also several mechanisms for explaining why μ is of order the SUSY-breaking scale [47]. Finally, for a recent review of the μ problem and some suggested solutions in SUSY GUTs and string theory, see Ref. 48 and references therein.

15.2. Conclusion

Grand unification of the strong and electroweak interactions at a unique high energy scale $M_G \sim 3 \times 10^{16} \text{ GeV}$ requires

- gauge coupling unification,
- low-energy supersymmetry [with a large SUSY desert], and
- nucleon decay.

The first prediction has already been verified. Perhaps the next two will soon be seen. Whether or not Yukawa couplings unify is more model dependent. Nevertheless, the “digital” 16-dimensional representation of quarks and leptons in $\text{SO}(10)$ is very compelling, and may yet lead to an understanding of fermion masses and mixing angles.

In any event, the experimental verification of the first three pillars of SUSY GUTs would forever change our view of Nature. Moreover, the concomitant evidence for a vast SUSY desert would expose a huge lever arm for discovery. For then it would become clear that experiments probing the TeV scale could reveal physics at the GUT scale and perhaps beyond.

References:

1. J. Pati and A. Salam, Phys. Rev. **D8**, 1240 (1973);
For more discussion on the standard charge assignments in this formalism, see A. Davidson, Phys. Rev. **D20**, 776 (1979); and R.N. Mohapatra and R.E. Marshak, Phys. Lett. **B91**, 222 (1980).
2. H. Georgi and S.L. Glashow, Phys. Rev. Lett. **32**, 438 (1974).
3. H. Georgi, Particles and Fields, *Proceedings of the APS Div. of Particles and Fields*, ed. C. Carlson, p. 575 (1975);
H. Fritzsch and P. Minkowski, Ann. Phys. **93**, 193 (1975).
4. S.M. Barr, Phys. Lett. **B112**, 219 (1982).

5. A. de Rujula, H. Georgi, and S.L. Glashow, p. 88, *5th Workshop on Grand Unification*, ed. K. Kang, H. Fried, and P. Frampton, World Scientific, Singapore (1984);
See also earlier paper by Y. Achiman and B. Stech, p. 303, "New Phenomena in Lepton-Hadron Physics," ed. D.E.C. Fries and J. Wess, Plenum, NY (1979).
6. B.R. Greene *et al.*, Nucl. Phys. **B278**, 667 (1986), and Nucl. Phys. **B292**, 606 (1987);
B.R. Greene, C.A. Lutken, and G.G. Ross, Nucl. Phys. **B325**, 101 (1989).
7. H. Georgi, H. Quinn, and S. Weinberg, Phys. Rev. Lett. **33**, 451 (1974);
see also the definition of effective field theories by S. Weinberg, Phys. Lett. **91B**, 51 (1980).
8. See talks on proposed and running nucleon decay experiments, and theoretical talks by P. Langacker, p. 131, and W.J. Marciano and A. Sirlin, p. 151, in *The Second Workshop on Grand Unification*, eds. J.P. Leveille, L.R. Sulak, and D.G. Unger, Birkhäuser, Boston (1981).
9. W.J. Marciano, p. 190, *Eighth Workshop on Grand Unification*, ed. K. Wali, World Scientific Publishing Co., Singapore (1987).
10. U. Amaldi, W. de Boer, and H. Fürstenau, Phys. Lett. **B260**, 447 (1991);
J. Ellis, S. Kelly and D.V. Nanopoulos, Phys. Lett. **B260**, 131 (1991);
P. Langacker and M. Luo, Phys. Rev. **D44**, 817 (1991);
P. Langacker and N. Polonsky, Phys. Rev. **D47**, 4028 (1993);
M. Carena, S. Pokorski, and C.E.M. Wagner, Nucl. Phys. **B406**, 59 (1993);
see also the review by S. Dimopoulos, S. Raby, and F. Wilczek, Physics Today, 25–33, October (1991).
11. S. Dimopoulos, S. Raby, and F. Wilczek, Phys. Rev. **D24**, 1681 (1981);
S. Dimopoulos and H. Georgi, Nucl. Phys. **B193**, 150 (1981);
L. Ibanez and G.G. Ross, Phys. Lett. **105B**, 439 (1981);
N. Sakai, Z. Phys. **C11**, 153 (1981);
M.B. Einhorn and D.R.T. Jones, Nucl. Phys. **B196**, 475 (1982);
W.J. Marciano and G. Senjanovic, Phys. Rev. **D25**, 3092 (1982).
12. G. Anderson *et al.*, in *New directions for high-energy physics, Snowmass 1996*, eds. D.G. Cassel, L. Trindler Gennari, and R.H. Siemann, hep-ph/9609457.
13. R.N. Mohapatra and M.K. Parida, Phys. Rev. **D47**, 264 (1993).
14. D.G. Lee *et al.*, Phys. Rev. **D51**, 229 (1995).
15. M. Gell-Mann, P. Ramond, and R. Slansky, in *Supergravity*, eds. P. van Nieuwenhuizen and D.Z. Freedman, North-Holland, Amsterdam, 1979, p. 315.
16. S. Weinberg, Phys. Rev. **D26**, 287 (1982);
N. Sakai and T. Yanagida, Nucl. Phys. **B197**, 533 (1982).
17. G. Farrar and P. Fayet, Phys. Lett. **B76**, 575 (1978).
18. S. Dimopoulos, S. Raby, and F. Wilczek, Phys. Lett. **112B**, 133 (1982);
J. Ellis, D.V. Nanopoulos, and S. Rudaz, Nucl. Phys. **B202**, 43 (1982).
19. L.E. Ibanez and G.G. Ross, Nucl. Phys. **B368**, 3 (1992).
20. For a recent discussion, see C.S. Aulakh *et al.*, Nucl. Phys. **B597**, 89 (2001).
21. See talks by Matthew Earl, *NNN workshop*, Irvine, February (2000);
Y. Totsuka, *SUSY2K*, CERN, June (2000);
Y. Suzuki, *International Workshop on Neutrino Oscillations and their Origins*, Tokyo, Japan, December (2000), and *Baksan School, Baksan Valley*, Russia, April (2001), hep-ex/0110005. For published results see : Y. Hayato *et al.* (Super-Kamiokande Collab.), Phys. Rev. Lett. **83**, 1529 (1999).
22. H. Murayama and A. Pierce, Phys. Rev. **D65**, 055009 (2002).
23. K.S. Babu and S.M. Barr, Phys. Rev. **D48**, 5354 (1993);
V. Lucas and S. Raby, Phys. Rev. **D54**, 2261 (1996);
S.M. Barr and S. Raby, Phys. Rev. Lett. **79**, 4748 (1997) and references therein.
24. R. Dermíšek, A. Mafi, and S. Raby, Phys. Rev. **D63**, 035001 (2001);
K.S. Babu, J.C. Pati, and F. Wilczek, Nucl. Phys. **B566**, 33 (2000).
25. G. Altarelli, F. Feruglio, I. Masina, JHEP **0011**, 040 (2000);
see also earlier papers by A. Masiero *et al.*, Phys. Lett. **B115**, 380 (1982);
B. Grinstein, Nucl. Phys. **B206**, 387 (1982).
26. P. Candelas *et al.*, Nucl. Phys. **B258**, 46 (1985);
L.J. Dixon *et al.*, Nucl. Phys. **B261**, 678 (1985), and Nucl. Phys. **B274**, 285 (1986).
27. Y. Kawamura, Prog. Theor. Phys. **105**, 999 (2001);
L.J. Hall and Y. Nomura, Phys. Rev. **D64**, 055003 (2001);
R. Barbieri, L.J. Hall, and Y. Nomura, hep-ph/0106190 (2001).
28. Z. Kakushadze and S.H.H. Tye, Phys. Rev. **D54**, 7520 (1996);
Z. Kakushadze *et al.*, Int. J. Mod. Phys. **A13**, 2551 (1998).
29. K.S. Babu and R.N. Mohapatra, Phys. Lett. **B518**, 269 (2001).
30. M. Baldoceolin *et al.*, Z. Phys. **C63**, 409 (1994).
31. M. Chanowitz, J. Ellis, and M.K. Gaillard, Nucl. Phys. **B135**, 66 (1978);
For the corresponding SUSY analysis, see M. Einhorn and D.R.T. Jones, Nucl. Phys. **B196**, 475 (1982);
K. Inoue *et al.*, Prog. Theor. Phys. **67**, 1889 (1982);
L.E. Ibanez and C. Lopez, Nucl. Phys. **B233**, 511 (1984).
32. H. Georgi and D.V. Nanopoulos, Nucl. Phys. **B159**, 16 (1979);
J. Harvey, P. Ramond, and D.B. Reiss, Phys. Lett. **92B**, 309 (1980);
Nucl. Phys. **B199**, 223 (1982).
33. T. Banks, Nucl. Phys. **B303**, 172 (1988);
M. Olechowski and S. Pokorski, Phys. Lett. **B214**, 393 (1988);
S. Pokorski, Nucl. Phys. (Proc. Supp.) **B13**, 606 (1990);
B. Ananthanarayan, G. Lazarides, and Q. Shafi, Phys. Rev. **D44**, 1613 (1991);
Q. Shafi and B. Ananthanarayan, ICTP Summer School lectures (1991);
S. Dimopoulos, L.J. Hall, and S. Raby, Phys. Rev. Lett. **68**, 1984 (1992), and Phys. Rev. **D45**, 4192 (1992);
G. Anderson *et al.*, Phys. Rev. **D47**, 3702 (1993);
B. Ananthanarayan, G. Lazarides, and Q. Shafi, Phys. Lett. **B300**, 245 (1993);
G. Anderson *et al.*, Phys. Rev. **D49**, 3660 (1994);
B. Ananthanarayan, Q. Shafi, and X.M. Wang, Phys. Rev. **D50**, 5980 (1994).
34. LEP Higgs Working Group and ALEPH Collab., DELPHI Collab., L3 Collab., and OPAL Collab., Preliminary results, hep-ex/0107030 (2001).
35. L.J. Hall, R. Rattazzi, and U. Sarid, Phys. Rev. **D50**, 7048 (1994);
M. Carena *et al.*, Nucl. Phys. **B419**, 213 (1994);
R. Rattazzi and U. Sarid, Nucl. Phys. **B501**, 297 (1997).
36. T. Blažek, R. Dermíšek, and S. Raby, Phys. Rev. Lett. **88**, 111804 (2002) and hep-ph/0201081.
37. H. Georgi and C. Jarlskog, Phys. Lett. **86B**, 297 (1979).

38. K.S. Babu and R.N. Mohapatra, Phys. Rev. Lett. **74**, 2418 (1995);
 V. Lucas and S. Raby, Phys. Rev. **D54**, 2261 (1996);
 T. Blažek *et al.*, Phys. Rev. **D56**, 6919 (1997);
 R. Barbieri *et al.*, Nucl. Phys. **B493**, 3 (1997);
 T. Blažek, S. Raby, and K. Tobe, Phys. Rev. **D60**, 113001 (1999),
 and Phys. Rev. **D62**, 055001 (2000);
 Q. Shafi and Z. Tavartkiladze, Phys. Lett. **B487**, 145 (2000);
 C.H. Albright and S.M. Barr, Phys. Rev. Lett. **85**, 244 (2000);
 K.S. Babu, J.C. Pati, and F. Wilczek, Nucl. Phys. **B566**, 33 (2000);
 G. Altarelli, F. Feruglio, I. Masina, Ref. 25;
 Z. Berezhiani and A. Rossi, Nucl. Phys. **B594**, 113 (2001).
39. T. Yanagida, in *Proceedings of the Workshop on the Unified Theory and the Baryon Number of the Universe*, eds. O. Sawada and A. Sugamoto, KEK report No. 79-18, Tsukuba, Japan, 1979;
 R.N. Mohapatra and G. Senjanovic, Phys. Rev. Lett. **44**, 912 (1980).
40. G. 't Hooft, Nucl. Phys. **B79**, 276 (1974);
 A.M. Polyakov, Pis'ma Zh. Eksp. Teor. Fiz. **20**, 430 (1974) [JETP Lett. **20**, 194 (1974)];
 For a pedagogical introduction, see S. Coleman, in *Aspects of Symmetry*, Selected Erice Lectures, Cambridge University Press, Cambridge, (1985), and P. Goddard and D. Olive, Rep. Prog. Phys. **41**, 1357 (1978).
41. I. De Mitri, (MACRO Collab.), Nucl. Phys. (Proc. Suppl.) **B95**, 82 (2001).
42. For a review, see A.D. Linde, *Particle Physics and Inflationary Cosmology*, Harwood Academic, Switzerland (1990).
43. V. Rubakov, Nucl. Phys. **B203**, 311 (1982), Institute of Nuclear Research Report No. P-0211, Moscow (1981), unpublished;
 C. Callan, Phys. Rev. **D26**, 2058 (1982);
 F. Wilczek, Phys. Rev. Lett. **48**, 1146 (1982);
 See also, S. Dawson and A.N. Schellekens, Phys. Rev. **D27**, 2119 (1983).
44. M. Fukugita and T. Yanagida, Phys. Lett. **B174**, 45 (1986);
 see also the recent review by W. Buchmuller, hep-ph/0107153 (2001) and references therein.
45. S. Dimopoulos and F. Wilczek, *Proceedings Erice Summer School*, ed. A. Zichichi (1981);
 K.S. Babu and S.M. Barr, Phys. Rev. **D50**, 3529 (1994).
46. R. Barbieri, G.R. Dvali, and A. Strumia, Nucl. Phys. **B391**, 487 (1993);
 Z. Berezhiani, C. Csaki, and L. Randall, Nucl. Phys. **B444**, 61 (1995);
 Q. Shafi and Z. Tavartkiladze, Phys. Lett. **B522**, 102 (2001).
47. G.F. Giudice and A. Masiero, Phys. Lett. **B206**, 480 (1988);
 J.E. Kim and H.P. Nilles, Mod. Phys. Lett. **A9**, 3575 (1994).
48. L. Randall and C. Csaki, *Proceedings Pascos/Hopkins 1995*, hep-ph/9508208;
 E. Witten, hep-ph/0201018.

16. STRUCTURE FUNCTIONS

Written Summer 2001 by B. Foster (University of Bristol), A.D. Martin (University of Durham), M.G. Vincet (University of Alberta). Updated Summer 2003.

16.1. Deep inelastic scattering

High energy lepton-nucleon scattering (deep inelastic scattering) plays a key role in determining the partonic structure of the proton. The process $\ell N \rightarrow \ell' X$ is illustrated in Fig. 16.1. The filled circle in this figure represents the internal structure of the proton which can be expressed in terms of structure functions.

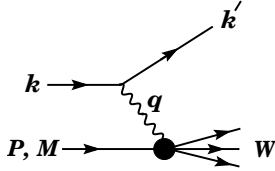


Figure 16.1: Kinematic quantities for the description of deep inelastic scattering. The quantities k and k' are the four-momenta of the incoming and outgoing leptons, P is the four-momentum of a nucleon with mass M , and W is the mass of the recoiling system X . The exchanged particle is a γ , W^\pm , or Z ; it transfers four-momentum $q = k - k'$ to the nucleon.

Invariant quantities:

$\nu = \frac{q \cdot P}{M} = E - E'$ is the lepton's energy loss in the nucleon rest frame (in earlier literature sometimes $\nu = q \cdot P$). Here, E and E' are the initial and final lepton energies in the nucleon rest frame.

$Q^2 = -q^2 = 2(EE' - \vec{k} \cdot \vec{k}') - m_\ell^2 - m_{\ell'}^2$ where m_ℓ ($m_{\ell'}$) is the initial (final) lepton mass. If $EE' \sin^2(\theta/2) \gg m_\ell^2, m_{\ell'}^2$, then

$\approx 4EE' \sin^2(\theta/2)$, where θ is the lepton's scattering angle in the nucleon rest frame with respect to the lepton beam direction.

$x = \frac{Q^2}{2M\nu}$ where, in the parton model, x is the fraction of the nucleon's momentum carried by the struck quark.

$y = \frac{q \cdot P}{k \cdot P} = \frac{\nu}{E}$ is the fraction of the lepton's energy lost in the nucleon rest frame.

$W^2 = (P + q)^2 = M^2 + 2M\nu - Q^2$ is the mass squared of the system X recoiling against the scattered lepton.

$s = (k + P)^2 = \frac{Q^2}{xy} + M^2 + m_\ell^2$ is the center-of-mass energy squared of the lepton-nucleon system.

The process in Fig. 16.1 is called deep ($Q^2 \gg M^2$) inelastic ($W^2 \gg M^2$) scattering (DIS). In what follows, the masses of the initial and scattered leptons, m_ℓ and $m_{\ell'}$, are neglected.

16.1.1. DIS cross sections:

$$\frac{d^2\sigma}{dx dy} = x(s - M^2) \frac{d^2\sigma}{dx dQ^2} = \frac{2\pi M\nu}{E'} \frac{d^2\sigma}{d\Omega_{\text{Nrest}} dE'} \quad (16.1)$$

In lowest-order perturbation theory, the cross section for the scattering of polarised leptons on polarised nucleons can be expressed in terms of the products of leptonic and hadronic tensors associated with the coupling of the exchanged bosons at the upper and lower vertices in Fig. 16.1 (see Refs. 1-4)

$$\frac{d^2\sigma}{dx dy} = \frac{2\pi y \alpha^2}{Q^4} \sum_j \eta_j L_j^{\mu\nu} W_{\mu\nu}^j \quad (16.2)$$

For neutral-current processes, the summation is over $j = \gamma, Z$ and γZ representing photon and Z exchange and the interference between them, whereas for charged-current interactions there is only W exchange, $j = W$. (For transverse nucleon polarization, there is a dependence on the azimuthal angle of the scattered lepton.) $L_{\mu\nu}$ is the lepton tensor associated with the coupling of the exchange boson to the leptons. For incoming leptons of charge $e = \pm 1$ and helicity $\lambda = \pm 1$,

$$\begin{aligned} L_{\mu\nu}^\gamma &= 2(k_\mu k'_\nu + k'_\mu k_\nu - k \cdot k' g_{\mu\nu} - i\lambda \varepsilon_{\mu\nu\alpha\beta} k^\alpha k'^\beta), \\ L_{\mu\nu}^{\gamma Z} &= (g_V^e + e\lambda g_A^e) L_{\mu\nu}^\gamma, \quad L_{\mu\nu}^Z = (g_V^e + e\lambda g_A^e)^2 L_{\mu\nu}^\gamma, \\ L_{\mu\nu}^W &= (1 + e\lambda)^2 L_{\mu\nu}^\gamma, \end{aligned} \quad (16.3)$$

where $g_V^e = -\frac{1}{2} - 2e \sin^2 \theta_W$, $g_A^e = -\frac{1}{2}$.

Although here the helicity formalism is adopted, an alternative approach is to express the tensors in Eq. (16.3) in terms of the polarization of the lepton.

The factors η_j in Eq. (16.2) denote the ratios of the corresponding propagators and couplings to the photon propagator and coupling squared

$$\begin{aligned} \eta_\gamma &= 1; \quad \eta_{\gamma Z} = \left(\frac{G_F M_Z^2}{2\sqrt{2}\pi\alpha} \right) \left(\frac{Q^2}{Q^2 + M_Z^2} \right); \\ \eta_Z &= \eta_{\gamma Z}^2; \quad \eta_W = \frac{1}{2} \left(\frac{G_F M_W^2}{4\pi\alpha} \frac{Q^2}{Q^2 + M_W^2} \right)^2. \end{aligned} \quad (16.4)$$

The hadronic tensor, which describes the interaction of the appropriate electroweak currents with the target nucleon, is given by

$$W_{\mu\nu} = \frac{1}{4\pi} \int d^4z e^{iq \cdot z} \langle P, S | [J_\mu^\dagger(z), J_\nu(0)] | P, S \rangle, \quad (16.5)$$

where S denotes the nucleon-spin 4-vector, with $S^2 = -M^2$ and $S \cdot P = 0$.

16.2. Structure functions of the proton

The structure functions are defined in terms of the hadronic tensor (see Refs. 1-3)

$$\begin{aligned} W_{\mu\nu} &= \left(-g_{\mu\nu} + \frac{q_\mu q_\nu}{q^2} \right) F_1(x, Q^2) + \frac{\hat{P}_\mu \hat{P}_\nu}{P \cdot q} F_2(x, Q^2) \\ &\quad - i\varepsilon_{\mu\nu\alpha\beta} \frac{q^\alpha P^\beta}{2P \cdot q} F_3(x, Q^2) \\ &\quad + i\varepsilon_{\mu\nu\alpha\beta} \frac{q^\alpha}{P \cdot q} \left[S^\beta g_1(x, Q^2) + \left(S^\beta - \frac{S \cdot q}{P \cdot q} P^\beta \right) g_2(x, Q^2) \right] \\ &\quad + \frac{1}{P \cdot q} \left[\frac{1}{2} (\hat{P}_\mu \hat{S}_\nu + \hat{S}_\mu \hat{P}_\nu) - \frac{S \cdot q}{P \cdot q} \hat{P}_\mu \hat{P}_\nu \right] g_3(x, Q^2) \\ &\quad + \frac{S \cdot q}{P \cdot q} \left[\frac{\hat{P}_\mu \hat{P}_\nu}{P \cdot q} g_4(x, Q^2) + \left(-g_{\mu\nu} + \frac{q_\mu q_\nu}{q^2} \right) g_5(x, Q^2) \right] \end{aligned} \quad (16.6)$$

where

$$\hat{P}_\mu = P_\mu - \frac{P \cdot q}{q^2} q_\mu, \quad \hat{S}_\mu = S_\mu - \frac{S \cdot q}{q^2} q_\mu. \quad (16.7)$$

In Ref. 2, the definition of $W_{\mu\nu}$ with $\mu \leftrightarrow \nu$ is adopted, which changes the sign of the $\varepsilon_{\mu\nu\alpha\beta}$ terms in Eq. (16.6), although the formulae given here below are unchanged. Ref. 1 tabulates the relation between the structure functions defined in Eq. (16.6) and other choices available in the literature.

The cross sections for neutral and charged-current deep inelastic scattering on unpolarized nucleons can be written in terms of the structure functions in the generic form

$$\frac{d^2\sigma^i}{dx dy} = \frac{4\pi\alpha^2}{xyQ^2} \eta^i \left\{ \left(1 - y - \frac{x^2 y^2 M^2}{Q^2} \right) F_2^i + y^2 x F_1^i \mp \left(y - \frac{y^2}{2} \right) x F_3^i \right\}, \quad (16.8)$$

where $i = \text{NC, CC}$ corresponds to neutral-current ($eN \rightarrow eX$) or charged-current ($eN \rightarrow \nu X$ or $\nu N \rightarrow eX$) processes, respectively. In the last term, the $-$ sign is taken for an incoming e^+ or $\bar{\nu}$ and the $+$ sign for an incoming e^- or ν . The factor $\eta^{\text{NC}} = 1$ for unpolarized e^\pm beams, whereas*

$$\eta^{\text{CC}} = (1 \pm \lambda)^2 \eta_W \quad (16.9)$$

with \pm for ℓ^\pm and where λ is the helicity of the incoming lepton. η_W is defined in Eq. (16.4). The CC structure functions, which derive exclusively from W exchange, are

$$F_1^{\text{CC}} = F_1^W, \quad F_2^{\text{CC}} = F_2^W, \quad xF_3^{\text{CC}} = xF_3^W. \quad (16.10)$$

The NC structure functions $F_2^\gamma, F_2^{\gamma Z}, F_2^Z$ are, for $e^\pm N \rightarrow e^\pm X$, given by Ref. 5,

$$F_2^{\text{NC}} = F_2^\gamma - (g_V^e \pm \lambda g_A^e) \eta_{\gamma Z} F_2^{\gamma Z} + (g_V^e \pm g_A^e \pm 2\lambda g_V^e g_A^e) \eta_Z F_2^Z \quad (16.11)$$

and similarly for F_1^{NC} , whereas

$$xF_3^{\text{NC}} = -(g_A^e \pm \lambda g_V^e) \eta_{\gamma Z} x F_3^{\gamma Z} + [2g_V^e g_A^e \pm \lambda (g_V^e \pm g_A^e)] \eta_Z x F_3^Z. \quad (16.12)$$

The polarized cross-section difference

$$\Delta\sigma = \sigma(\lambda_n = -1, \lambda_\ell) - \sigma(\lambda_n = 1, \lambda_\ell), \quad (16.13)$$

where λ_ℓ, λ_n are the helicities (± 1) of the incoming lepton and nucleon, respectively, may be expressed in terms of the five structure functions $g_{1,\dots,5}(x, Q^2)$ of Eq. (16.6). Thus,

$$\begin{aligned} \frac{d^2\Delta\sigma^i}{dx dy} &= \frac{8\pi\alpha^2}{xyQ^2} \eta^i \left\{ -\lambda_\ell y \left(2 - y - 2x^2 y^2 \frac{M^2}{Q^2} \right) x g_1^i + \lambda_\ell 4x^3 y^2 \frac{M^2}{Q^2} g_2^i \right. \\ &+ 2x^2 y \frac{M^2}{Q^2} \left(1 - y - x^2 y^2 \frac{M^2}{Q^2} \right) g_3^i \\ &\left. - \left(1 + 2x^2 y \frac{M^2}{Q^2} \right) \left[\left(1 - y - x^2 y^2 \frac{M^2}{Q^2} \right) g_4^i + x y^2 g_5^i \right] \right\} \quad (16.14) \end{aligned}$$

with $i = \text{NC or CC}$ as before. The Eq. (16.13) corresponds to the difference of antiparallel minus parallel spins of the incoming particles for e^- or ν initiated reactions, but parallel minus antiparallel for e^+ or $\bar{\nu}$ initiated processes. For longitudinal nucleon polarization, the contributions of g_2 and g_3 are suppressed by powers of M^2/Q^2 . These structure functions give an unsuppressed contribution to the cross section for transverse polarization [1], but in this case the cross-section difference vanishes as $M/Q \rightarrow 0$.

Because the same tensor structure occurs in the spin-dependent and spin-independent parts of the hadronic tensor of Eq. (16.6) in the $M^2/Q^2 \rightarrow 0$ limit, the differential cross-section difference of Eq. (16.14) may be obtained from the differential cross section Eq. (16.8) by replacing

$$F_1 \rightarrow -g_5, \quad F_2 \rightarrow -g_4, \quad F_3 \rightarrow 2g_1, \quad (16.15)$$

and multiplying by two, since the total cross section is the average over the initial-state polarizations. In this limit, Eq. (16.8) and Eq. (16.14) may be written in the form

$$\begin{aligned} \frac{d^2\sigma^i}{dx dy} &= \frac{2\pi\alpha^2}{xyQ^2} \eta^i \left[Y_+ F_2^i \mp Y_- x F_3^i - y^2 F_1^i \right], \\ \frac{d^2\Delta\sigma^i}{dx dy} &= \frac{4\pi\alpha^2}{xyQ^2} \eta^i \left[-Y_+ g_4^i \mp Y_- 2x g_1^i + y^2 g_5^i \right], \quad (16.16) \end{aligned}$$

with $i = \text{NC or CC}$, where $Y_\pm = 1 \pm (1-y)^2$ and

$$F_L^i = F_2^i - 2x F_1^i, \quad g_L^i = g_4^i - 2x g_5^i. \quad (16.17)$$

In the naive quark-parton model, the analogy with the Callan-Gross relations [6] $F_L^i = 0$, are the Dicus relations [7] $g_L^i = 0$. Therefore, there are only two independent polarized structure functions: g_1 (parity conserving) and g_5 (parity violating), in analogy with the unpolarized structure functions F_1 and F_3 .

16.2.1. Structure functions in the quark-parton model:

In the quark-parton model [8,9], contributions to the structure functions F^i and g^i can be expressed in terms of the quark distribution functions $q(x, Q^2)$ of the proton, where $q = u, \bar{u}, d, \bar{d}$ etc. The quantity $q(x, Q^2) dx$ is the number of quarks (or antiquarks) of designated flavor that carry a momentum fraction between x and $x + dx$ of the proton's momentum in a frame in which the proton momentum is large.

For the neutral-current processes $ep \rightarrow eX$,

$$\begin{aligned} [F_2^\gamma, F_2^{\gamma Z}, F_2^Z] &= x \sum_q [e_q^2, 2e_q g_V^q, g_V^{q^2} + g_A^{q^2}] (q + \bar{q}), \\ [F_3^\gamma, F_3^{\gamma Z}, F_3^Z] &= \sum_q [0, 2e_q g_A^q, 2g_V^q g_A^q] (q - \bar{q}), \\ [g_1^\gamma, g_1^{\gamma Z}, g_1^Z] &= \frac{1}{2} \sum_q [e_q^2, 2e_q g_V^q, g_V^{q^2} + g_A^{q^2}] (\Delta q + \Delta \bar{q}), \\ [g_5^\gamma, g_5^{\gamma Z}, g_5^Z] &= \sum_q [0, e_q g_A^q, g_V^q g_A^q] (\Delta q - \Delta \bar{q}), \quad (16.18) \end{aligned}$$

where $g_V^q = \pm \frac{1}{2} - 2e_q \sin^2 \theta_W$ and $g_A^q = \pm \frac{1}{2}$, with \pm according to whether q is a u - or d -type quark respectively. The quantity Δq is the difference $q \uparrow - q \downarrow$ of the distributions with the quark spin parallel and antiparallel to the proton spin.

For the charged-current processes $e^- p \rightarrow \nu X$ and $\bar{\nu} p \rightarrow e^+ X$, the structure functions are:

$$\begin{aligned} F_2^{W^-} &= 2x(u + \bar{d} + \bar{s} + c \dots), \\ F_3^{W^-} &= 2(u - \bar{d} - \bar{s} + c \dots), \\ g_1^{W^-} &= (\Delta u + \Delta \bar{d} + \Delta \bar{s} + \Delta c \dots), \\ g_5^{W^-} &= (-\Delta u + \Delta \bar{d} + \Delta \bar{s} - \Delta c \dots), \quad (16.19) \end{aligned}$$

where only the active flavors are to be kept and where CKM mixing has been neglected. For $e^+ p \rightarrow \bar{\nu} X$ and $\nu p \rightarrow e^- X$, the structure functions F^{W^+}, g^{W^+} are obtained by the flavor interchanges $d \leftrightarrow u, s \leftrightarrow c$ in the expressions for F^{W^-}, g^{W^-} . The structure functions for scattering on a neutron are obtained from those of the proton by the interchange $u \leftrightarrow d$. For both the neutral and charged-current processes, the quark-parton model predicts $2xF_1^i = F_2^i$ and $g_4^i = 2xg_5^i$.

Neglecting masses, the structure functions g_2 and g_3 contribute only to scattering from transversely polarized nucleons (for which $S \cdot q = 0$), and have no simple interpretation in terms of the quark-parton model. They arise from off-diagonal matrix elements $\langle P, \lambda' | [J_\mu^\dagger(z), J_\nu(0)] | P, \lambda \rangle$, where the proton helicities satisfy $\lambda' \neq \lambda$. In fact, the leading-twist contributions to both g_2 and g_3 are both twist-2 and twist-3, which contribute at the same order of Q^2 . The Wandzura-Wilczek relation [10] expresses the twist-2 part of g_2 in terms of g_1 as

$$g_2^i(x) = -g_1^i(x) + \int_x^1 \frac{dy}{y} g_1^i(y). \quad (16.20)$$

However, the twist-3 component of g_2 is unknown. Similarly, there is a relation expressing the twist-2 part of g_3 in terms of g_4 . A complete set of relations, including M^2/Q^2 effects, can be found in Ref. 11.

16.2.2. Structure functions and QCD:

One of the most striking predictions of the quark-parton model is that the structure functions F^i, g^i scale, *i.e.*, $F^i(x, Q^2) \rightarrow F^i(x)$ in the Bjorken limit that Q^2 and $\nu \rightarrow \infty$ with x fixed [12]. This property is related to the assumption that the transverse momentum of the partons in the infinite-momentum frame of the proton is small. In QCD, however, the radiation of hard gluons from the quarks violates this assumption, leading to logarithmic scaling violations, which are particularly large at small x , see Fig. 16.2. The radiation of gluons produces the evolution of both the structure functions and the parton distribution functions. As Q^2 increases, more and more gluons are radiated, which in turn split into $q\bar{q}$ pairs. This process leads both to the softening of the initial quark momentum distributions and to the growth of the gluon density and the $q\bar{q}$ sea as x decreases.

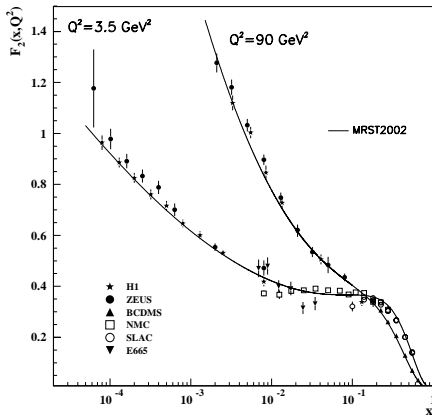


Figure 16.2: The proton structure function F_2^p given at two Q^2 values (3.5 GeV^2 and 90 GeV^2), which exhibit scaling at the ‘pivot’ point $x \sim 0.14$. See the caption in Fig. 16.6 for the references of the data. Also shown is the MRST2002 parameterization [13] given at the same scales.

In QCD, the above process is described in terms of scale-dependent parton distributions $f(x, \mu^2)$, where $f = g$ or q and, typically, μ is the scale of the probe Q . These distributions correspond, at a given x , to the density of partons in the proton integrated over transverse momentum k_t up to μ . Their evolution in μ is described in QCD by the DGLAP equations (see Refs. 14–17) which have the schematic form

$$\frac{\partial f}{\partial \ln \mu^2} \sim \frac{\alpha_s(\mu^2)}{2\pi} (P \otimes f), \quad (16.21)$$

where \otimes denotes the convolution integral

$$P \otimes f = \int_x^1 \frac{dy}{y} P(y) f\left(\frac{x}{y}\right). \quad (16.22)$$

Although perturbative QCD can predict, via Eq. (16.21), the evolution of the parton distribution functions from a particular scale, μ_0 , it cannot predict them *a priori* at any particular μ_0 . Thus they must be measured at a starting point μ_0 before the predictions of QCD can be compared to the data at other scales, μ . In general, all observables involving a hard hadronic interaction (such as structure functions) can be expressed as a convolution of calculable, process-dependent coefficient functions and these universal parton distributions.

It is often convenient to write the evolution equations in terms of the gluon, non-singlet (q^{NS}) and singlet (q^S) quark distributions, such that

$$q^{NS} = q_i - \bar{q}_i, \quad q^S = \sum_i (q_i + \bar{q}_i). \quad (16.23)$$

The non-singlet distributions have non-zero values of flavor quantum numbers, such as isospin and baryon number. The DGLAP evolution equations then take the form

$$\frac{\partial q^{NS}}{\partial \ln \mu^2} = \frac{\alpha_s(\mu^2)}{2\pi} P_{qq} \otimes q^{NS},$$

$$\frac{\partial}{\partial \ln \mu^2} \begin{pmatrix} q^S \\ g \end{pmatrix} = \frac{\alpha_s(\mu^2)}{2\pi} \begin{pmatrix} P_{qq} & 2n_f P_{qg} \\ P_{gq} & P_{gg} \end{pmatrix} \otimes \begin{pmatrix} q^S \\ g \end{pmatrix}, \quad (16.24)$$

where P are splitting functions that describe the probability of a given parton splitting into two others, and n_f is the number of (active) quark flavors. The leading-order Altarelli-Parisi [16] splitting functions are

$$P_{qq} = \frac{4}{3} \left[\frac{1+x^2}{(1-x)_+} \right] = \frac{4}{3} \left[\frac{1+x^2}{(1-x)_+} \right] + 2\delta(1-x), \quad (16.25)$$

$$P_{qg} = \frac{1}{2} [x^2 + (1-x)^2], \quad (16.26)$$

$$P_{gq} = \frac{4}{3} \left[\frac{1+(1-x)^2}{x} \right], \quad (16.27)$$

$$P_{gg} = 6 \left[\frac{1-x}{x} + x(1-x) + \frac{x}{(1-x)_+} \right] + \left[\frac{11}{2} - \frac{n_f}{3} \right] \delta(1-x), \quad (16.28)$$

where the notation $[F(x)]_+$ defines a distribution such that for any sufficiently regular test function, $f(x)$,

$$\int_0^1 dx f(x) [F(x)]_+ = \int_0^1 dx (f(x) - f(1)) F(x). \quad (16.29)$$

In general, the structure functions can be expressed as a power series in α_s . The series contains both terms proportional to $\ln \mu^2$ and to $\ln 1/x$. The leading $\ln \mu^2$ terms come, in an axial gauge, from evolution along the parton chain that is strongly ordered in transverse momenta, that is $\mu^2 \gg k_{t,n}^2 \gg k_{t,n-1}^2 \gg \dots$, where n denotes the n^{th} parton-branching process and k_t the parton transverse momentum. The leading-order DGLAP evolution sums up the $(\alpha_s \ln \mu^2)^n$ contributions. The next-to-leading order (NLO) sums up the $\alpha_s (\alpha_s \ln \mu^2)^{n-1}$ terms [18,19], which arise when two adjacent $k_{t,i}$ ’s are no longer strongly ordered but become comparable, thereby losing a factor of $\ln \mu^2$. The NNLO contributions are now almost all known (see Refs. 20–24).

In the small x kinematic region, it is essential to sum leading terms in $\ln 1/x$, independent of the value of $\ln \mu^2$. At leading order, this is done by the BFKL equation for the unintegrated distributions (see Refs. 25,26). The leading-order $(\alpha_s \ln(1/x))^n$ terms come from the configuration strongly ordered in x , *i.e.*, $x \ll x_n \ll x_{n-1} \ll \dots$

In general, however, QCD color coherence implies *angular* ordering along the chain, so that it is necessary to work in terms of $f_a(x, k_t^2, \mu^2)$, the parton distributions unintegrated over k_t . These distributions depend on two hard scales: k_t and the scale μ of the probe. Consequently they satisfy more complicated CCFM evolution equations [27,28]. The DGLAP and BFKL equations are two limits of angular-ordered evolution. In the DGLAP collinear approximation, the angle increases due to the growth of k_t , while, in the BFKL treatment, the angle ($\theta \simeq k_t/k_l$, where k_l is the longitudinal momentum) grows due to the decrease of the longitudinal-momentum fraction, x , along the chain of parton emissions from the proton.

As yet, there is no firm evidence in the data for $Q^2 \gtrsim 2 \text{ GeV}^2$ for any deviation from standard DGLAP evolution, except that some DGLAP parton sets predict an unphysical behavior for F_L at low x [29], see however Ref. 30.

The precision of the contemporary experimental data demands that NLO (or even NNLO) DGLAP evolution be used in comparisons between QCD theory and experiment. At higher orders, it is necessary to specify, and to use consistently, both a renormalization and a factorization scheme. Whereas the renormalization scheme used is almost universally the modified minimal subtraction (\overline{MS}) scheme,

there are two popular choices for factorization scheme, in which the form of the correction for each structure function is different. The two most-used factorization schemes are: DIS [31], in which there are no higher-order corrections to the F_2 structure function, and \overline{MS} (based on Refs. 32–34). They differ by how the higher-order gluon divergences are assimilated in the parton distribution functions.

Perturbative QCD predicts the Q^2 behavior of leading-twist (twist-2) contributions to the structure functions. Higher-twist terms, which involve their own non-perturbative input, can occur. These die off as powers of Q ; specifically twist- n terms are damped by $1/Q^{n-2}$. The higher-twist terms appear to be numerically unimportant for Q^2 above a few GeV^2 , except for x close to 1. At very large values of x , perturbative corrections proportional to $\log(1-x)$ can become important [35].

So far, it has been assumed that the quarks are massless. The effects of the c and b -quark masses on the evolution have been studied, for example, in Refs. 36–39. An approach using a variable flavor number is now generally adopted, in which evolution with $n_f = 3$ is matched to that with $n_f = 4$ at the charm threshold, with an analogous matching at the bottom threshold.

16.3. Determination of parton distributions

The parton distribution functions (PDFs) can be determined from data for deep inelastic lepton-nucleon scattering and for related hard-scattering processes initiated by nucleons. Table 16.1 given below (based on Ref. 40) highlights some processes and their primary sensitivity to PDFs.

Table 16.1: Lepton-nucleon and related hard-scattering processes and their primary sensitivity to the parton distributions that are probed.

Process	Main Subprocess	PDFs Probed
$\ell^\pm N \rightarrow \ell^\pm X$	$\gamma^* q \rightarrow q$	$g(x \lesssim 0.01), q, \bar{q}$
$\ell^+(\ell^-)N \rightarrow \bar{\nu}(\nu)X$	$W^* q \rightarrow q'$	
$\nu(\bar{\nu})N \rightarrow \ell^-(\ell^+)X$	$W^* q \rightarrow q'$	
$\nu N \rightarrow \mu^+ \mu^- X$	$W^* s \rightarrow c \rightarrow \mu^+$	s
$pp \rightarrow \gamma X$	$qg \rightarrow \gamma q$	$g(x \sim 0.4)$
$pN \rightarrow \mu^+ \mu^- X$	$\bar{q}\bar{q} \rightarrow \gamma^*$	\bar{q}
$pp, pn \rightarrow \mu^+ \mu^- X$	$u\bar{u}, d\bar{d} \rightarrow \gamma^*$ $u\bar{d}, d\bar{u} \rightarrow \gamma^*$	$\bar{u} - \bar{d}$
$ep, en \rightarrow e\pi X$	$\gamma^* q \rightarrow q$	
$p\bar{p} \rightarrow W \rightarrow \ell^\pm X$	$ud \rightarrow W$	$u, d, u/d$
$p\bar{p} \rightarrow \text{jet} + X$	$gg, qg, q\bar{q} \rightarrow 2j$	$q, g(0.01 \lesssim x \lesssim 0.5)$

The kinematic ranges of fixed-target and collider experiments are complementary (as is shown in Fig. 16.3) which enables the determination of PDFs over a wide range in x and Q^2 . Recent determinations of the unpolarized PDFs from NLO global analyses are given in Refs. 29,13 and Ref. 41, and at NNLO in Refs. 42,30, see also Ref. 43. Recent studies of the uncertainties in the PDFs and observables can be found in Refs. 44,45 and Refs. 13,30, see also Ref. 46. The result of one analysis is shown in Fig. 16.4 at a scale $\mu^2 = 10 \text{ GeV}^2$. The polarized PDFs are obtained through NLO global analyses of measurements of the g_1 structure function in inclusive polarized deep inelastic scattering (for recent examples see Refs. 47–49). The inclusive data do not provide enough observables to determine all polarized PDFs. These polarized PDFs may be fully accessed via flavor tagging in semi-inclusive deep inelastic scattering. Fig. 16.5 shows several global analyses at a scale of 2.5 GeV^2 along with the data from semi-inclusive DIS.

Comprehensive sets of PDFs available as program-callable functions can be obtained from several sources *e.g.*, Refs. 52,53. As a result of a Les Houches Accord, a PDF package (LHAPDF) exists [54] which facilitates the inclusion of recent PDFs in Monte Carlo/Matrix Element programs in a very compact and efficient format.

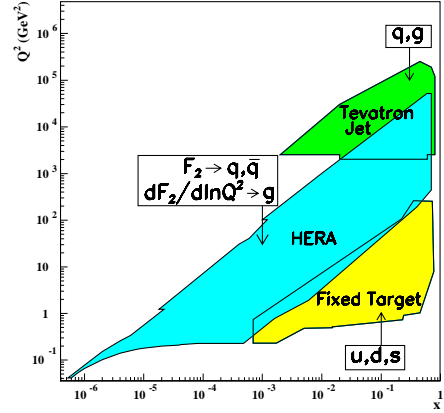


Figure 16.3: Kinematic domains in x and Q^2 probed by fixed-target and collider experiments, shown together with the important constraints they make on the various parton distributions.

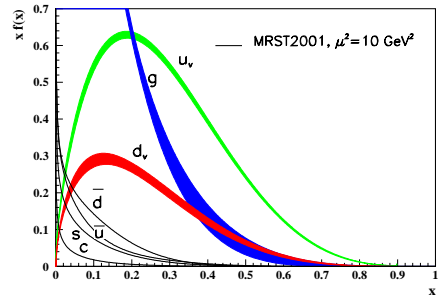


Figure 16.4: Distributions of x times the unpolarized parton distributions $f(x)$ (where $f = u_v, d_v, \bar{u}, \bar{d}, s, c, g$) using the MRST2001 parameterization [29,13] (with uncertainties for u_v, d_v , and g) at a scale $\mu^2 = 10 \text{ GeV}^2$.

16.4. DIS determinations of α_s

Table 16.2 shows the values of $\alpha_s(M_Z^2)$ found in recent fits to DIS and related data in which the coupling is left as a free parameter.

There have been several other studies of α_s at NNLO, and beyond, using subsets of DIS data (see, for example, Refs. 57–59). Moreover, there exist global NLO analyses of polarised DIS data which give $\alpha_s(M_Z^2) = 0.120 \pm 0.009$ [60] and 0.114 ± 0.009 [49].

16.5. The hadronic structure of the photon

Besides the *direct* interactions of the photon, it is possible for it to fluctuate into a hadronic state via the process $\gamma \rightarrow q\bar{q}$. While in this state, the partonic content of the photon may be *resolved*, for example, through the process $e^+e^- \rightarrow e^+e^-\gamma^*\gamma \rightarrow e^+e^-X$ where the virtual photon emitted by the deep inelastic scattering lepton probes the hadronic structure of the quasi-real photon emitted by the other lepton. The perturbative LO contributions, $\gamma \rightarrow q\bar{q}$ followed by $\gamma^* q \rightarrow q$, are subject to QCD corrections due to the coupling of quarks to gluons.

Often the equivalent-photon approximation is used to express the differential cross section for deep inelastic electron-photon scattering

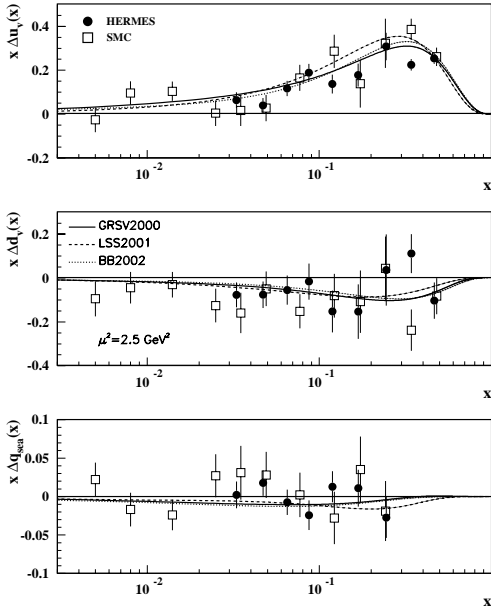


Figure 16.5: Distributions of x times the polarized parton distributions $\Delta q(x)$ (where $q = u_v, d_v, q_{sea}$) using the GRSV2000 [47], LSS2001 [48], and BB2002 [49] parameterizations at a scale $\mu^2 = 2.5 \text{ GeV}^2$. Points represent data from semi-inclusive positron (HERMES [50]) and muon (SMC [51]) deep inelastic scattering given at $Q^2 = 2.5 \text{ GeV}^2$.

Table 16.2: The values of $\alpha_S(M_Z^2)$ found in NLO and NNLO fits to DIS data. The experimental errors quoted correspond to an increase $\Delta\chi^2$ from the best fit value of χ^2 . CTEQ6 [41] and MRST03 [30] are global fits. H1 [56] fit only a subset of the F_2^{ep} data, while Alekhin [43] also includes F_2^{ed} and ZEUS [55] in addition include $x F_3^\nu$ data.

	$\Delta\chi^2$	$\alpha_S(M_Z^2) \pm \text{expt} \pm \text{theory} \pm \text{model}$
NLO		
CTEQ6	100	0.1165 ± 0.0065
ZEUS	50	$0.1166 \pm 0.0049 \pm 0.0018$
MRST03	5	$0.1165 \pm 0.002 \pm 0.003$
H1	1	$0.115 \pm 0.0017 \pm 0.005^{+0.0009}_{-0.0005}$
Alekhin	1	$0.1171 \pm 0.0015 \pm 0.0033$
NNLO		
MRST03	5	$0.1153 \pm 0.002 \pm 0.003$
Alekhin	1	$0.1143 \pm 0.0014 \pm 0.0009$

in terms of the structure functions of the transverse quasi-real photon times a flux factor N for the incoming quasi-real photons of transverse polarisation

$$\frac{d^2\sigma}{dx dQ^2} = N \frac{2\pi\alpha^2}{xQ^4} \left[\left(1 + (1-y)^2\right) F_2^\gamma(x, Q^2) - y^2 F_L^\gamma(x, Q^2) \right],$$

where we have used $F_2^\gamma = 2x F_T^\gamma + F_L^\gamma$. Complete formulae are given, for example, in the comprehensive review of Ref. 61.

The hadronic photon structure function F_2^γ evolves from the ‘hadron-like’ behavior, calculable via the vector-meson-dominance model, to the dominating ‘point-like’ behaviour, calculable in

perturbative QCD, with increasing Q^2 . Due to the point-like coupling, the logarithmic evolution of F_2^γ with Q^2 has a *positive* slope for all values of x , see Fig. 16.13. The ‘loss’ of quarks at large x due to gluon radiation is over-compensated by the ‘creation’ of quarks via the point-like $\gamma \rightarrow q\bar{q}$ coupling. The logarithmic evolution was first predicted in the quark-parton model ($\gamma^* \gamma \rightarrow q\bar{q}$) [62,63] and then in QCD in the limit of large Q^2 [64].

* The value of η^{CC} deduced from Ref. 1 is found to be a factor of two too small; η^{CC} of Eq. (16.9) agrees with Refs. 2,3.

References:

- J. Blümlein and N. Kochelev, Nucl. Phys. **B498**, 285 (1997).
- S. Forte, M.L. Mangano, and G. Ridolfi, Nucl. Phys. **B602**, 585 (2001).
- M. Anselmino, P. Gambino, and J. Kainowski, Z. Phys. **C64**, 267 (1994).
- M. Anselmino, A. Efremov, and E. Leader, Phys. Rep. **261**, 1 (1995).
- M. Klein and T. Riemann, Z. Phys. **C24**, 151 (1984).
- C.G. Callan and D.J. Gross, Phys. Rev. Lett. **22**, 156 (1969).
- D.A. Dicus, Phys. Rev. **D5**, 1367 (1972).
- J.D. Bjorken and E.A. Paschos, Phys. Rev. **185**, 1975 (1969).
- R.P. Feynman, Photon Hadron Interactions (Benjamin, New York, 1972).
- S. Wandzura and F. Wilczek, Phys. Rev. **B72**, 195 (1977).
- J. Blümlein and A. Tkabladze, Nucl. Phys. **B553**, 427 (1999).
- J.D. Bjorken, Phys. Rev. **179**, 1547 (1969).
- A.D. Martin, R.G. Roberts, W.J. Stirling, and R.S. Thorne, Eur. Phys. J. **C28**, 455 (2003).
- V.N. Gribov and L.N. Lipatov, Sov. J. Nucl. Phys. **15**, 438 (1972).
- L.N. Lipatov, Sov. J. Nucl. Phys. **20**, 95 (1975).
- G. Altarelli and G. Parisi, Nucl. Phys. **B126**, 298 (1977).
- Yu.L. Dokshitzer, Sov. Phys. JETP **46**, 641 (1977).
- G. Curci, W. Furmanski, and R. Petronzio, Nucl. Phys. **B175**, 27 (1980).
- R.K. Ellis, W.J. Stirling, and B.R. Webber, QCD and Collider Physics (Cambridge UP, 1996).
- E.B. Zijlstra and W.L. van Neerven, Nucl. Phys. **B383**, 525 (1992).
- S. Moch and J.A.M. Vermaseren, Nucl. Phys. **B573**, 853 (2000).
- S.A. Larin, P. Nogueira, T. van Ritbergen and J.A.M. Vermaseren, Nucl. Phys. **B492**, 338 (1997).
- A. Rerey and J.A.M. Vermaseren, Nucl. Phys. **B604**, 281 (2001).
- S. Moch, J.A.M. Vermaseren and A. Vogt, Nucl. Phys. **B646**, 181 (2002).
- E.A. Kuraev, L.N. Lipatov, and V.S. Fadin, Phys. Lett. **B60**, 50 (1975); Sov. Phys. JETP **44**, 443 (1976); Sov. Phys. JETP **45**, 199 (1977).
- Ya.Ya. Balitsky and L.N. Lipatov, Sov. J. Nucl. Phys. **28**, 822 (1978).
- M. Ciafaloni, Nucl. Phys. **B296**, 49 (1988).
- S. Catani, F. Fiorani, and G. Marchesini, Phys. Lett. **B234**, 339 (1990); Nucl. Phys. **B336**, 18 (1990).
- A.D. Martin, R.G. Roberts, W.J. Stirling, and R.S. Thorne, Eur. Phys. J. **C23**, 73 (2002).
- A.D. Martin, R.G. Roberts, W.J. Stirling and R.S. Thorne, (MRST2003) hep-ph/0308087.
- G. Altarelli, R.K. Ellis, and G. Martinelli, Nucl. Phys. **B143**, 521 (1978) and erratum: Nucl. Phys. **B146**, 544 (1978).
- G. ’t Hooft and M. Veltman, Nucl. Phys. **B44**, 189 (1972).

-
33. G. 't Hooft, Nucl. Phys. **B61**, 455 (1973).
 34. W.A. Bardeen *et al.*, Phys. Rev. **D18**, 3998 (1978).
 35. G. Sterman, Nucl. Phys. **B281**, 310 (1987).
 36. M.A.G. Aivazis *et al.*, Phys. Rev. **D50**, 3102 (1994).
 37. J.C. Collins, Phys. Rev. **D58**, 094002 (1998).
 38. R.S. Thorne and R.G. Roberts, Phys. Rev. **D57**, 1998 (1998); Phys. Lett. **B421**, 303 (1998); Eur. Phys. J. **C19**, 339 (2001).
 39. W.-K. Tung, S. Kretzer and C. Schmidt, J. Phys. **G28**, 983 (2002).
 40. A.D. Martin, R.G. Roberts, W.J. Stirling, and R.S. Thorne, Eur. Phys. J. **C4**, 463 (1998).
 41. CTEQ, J. Pumplin *et al.*, JHEP **0207**, 012 (2002).
 42. A.D. Martin, R.G. Roberts, W.J. Stirling, and R.S. Thorne, Phys. Lett. **B531**, 216 (2002).
 43. S. Alekhin, JHEP **0302**, 015 (2003).
 44. CTEQ, D. Stump *et al.*, Phys. Rev. **D65**, 014012 (2001).
 45. CTEQ, J. Pumplin *et al.*, Phys. Rev. **D65**, 014013 (2001).
 46. W.T. Giele, S. Keller and D.A. Kosower, hep-ph/0104052.
 47. M. Glück, E. Reya, M. Stratmann, and W. Vogelsang, Phys. Rev. **D63**, 094005 (2001).
 48. E. Leader, A.V. Sidorov and D.B. Stamenov, Eur. Phys. J. **C23**, 479 (2002).
 49. J. Blümlein and H. Böttcher, Nucl. Phys. **B636**, 225 (2002).
 50. HERMES, K. Ackerstaff *et al.*, Phys. Lett. **B464**, 123 (1999).
 51. SMC, B. Adeva *et al.*, Phys. Lett. **B420**, 180 (1998).
 52. H. Plothow-Besch, CERN PDFLIB, W5051 (2000).
 53. <http://durpdg.dur.ac.uk/HEPDATA/PDF>.
 54. <http://durpdg.dur.ac.uk/lhapdf/index.html>.
 55. ZEUS, S. Chenakov *et al.*, Phys. Rev. **D67**, 012007 (2003).
 56. H1, C. Adloff *et al.*, Eur. Phys. J. **C21**, 33 (2001).
 57. W.L. van Neerven and A. Vogt, Nucl. Phys. **B603**, 42 (2001).
 58. J. Santiago and F.J. Yndurain, Nucl. Phys. **B611**, 447 (2001).
 59. A.L. Kataev, G. Parente, and A.V. Sidorov, Nucl. Phys. Proc. Supp. **116**, 105 (2003).
 60. G. Altarelli, R.D. Ball, S. Forte, and G. Ridolfi, Nucl. Phys. **B496**, 337 (1997).
 61. R. Nisius, Phys. Reports **332**, 165 (2000).
 62. T.F. Walsh and P.M. Zerwas, Phys. Lett. **B44**, 195 (1973).
 63. R.L. Kingsley, Nucl. Phys. **B60**, 45 (1973).
 64. E. Witten, Nucl. Phys. **B120**, 189 (1977).

NOTE: THE FIGURES IN THIS SECTION ARE INTENDED TO SHOW THE REPRESENTATIVE DATA. THEY ARE NOT MEANT TO BE COMPLETE COMPILATIONS OF ALL THE WORLD'S RELIABLE DATA.

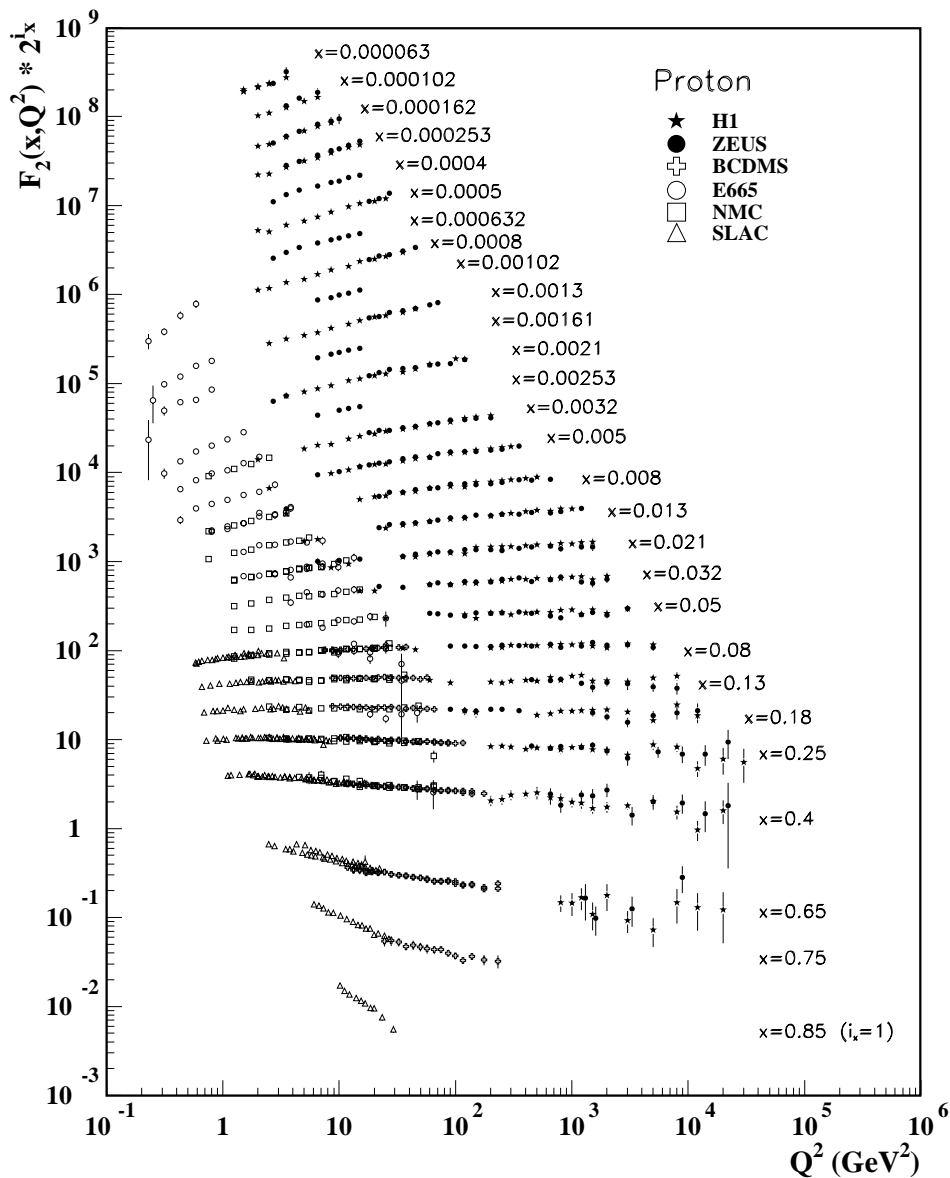


Figure 16.6: The proton structure function F_2^p measured in electromagnetic scattering of positrons on protons (collider experiments ZEUS and H1), in the kinematic domain of the HERA data, for $x > 0.00006$ (cf. Fig. 16.9 for data at smaller x and Q^2), and for electrons (SLAC) and muons (BCDMS, E665, NMC) on a fixed target. Statistical and systematic errors added in quadrature are shown. The data are plotted as a function of Q^2 in bins of fixed x . Some points have been slightly offset in Q^2 for clarity. The ZEUS binning in x is used in this plot; all other data are rebinned to the x values of the ZEUS data. For the purpose of plotting, F_2^p has been multiplied by 2^{i_x} , where i_x is the number of the x bin, ranging from $i_x = 1$ ($x = 0.85$) to $i_x = 28$ ($x = 0.000063$). References: **H1**—C. Adloff *et al.*, Eur. Phys. J. **C21**, 33 (2001); C. Adloff *et al.*, Eur. Phys. J. (accepted for publication) hep-ex/0304003; **ZEUS**—S. Chekanov *et al.*, Eur. Phys. J. **C21**, 443 (2001); **BCDMS**—A.C. Benvenuti *et al.*, Phys. Lett. **B223**, 485 (1989) (as given in [53]); **E665**—M.R. Adams *et al.*, Phys. Rev. **D54**, 3006 (1996); **NMC**—M. Arneodo *et al.*, Nucl. Phys. **B483**, 3 (97); **SLAC**—L.W. Whitlow *et al.*, Phys. Lett. **B282**, 475 (1992).

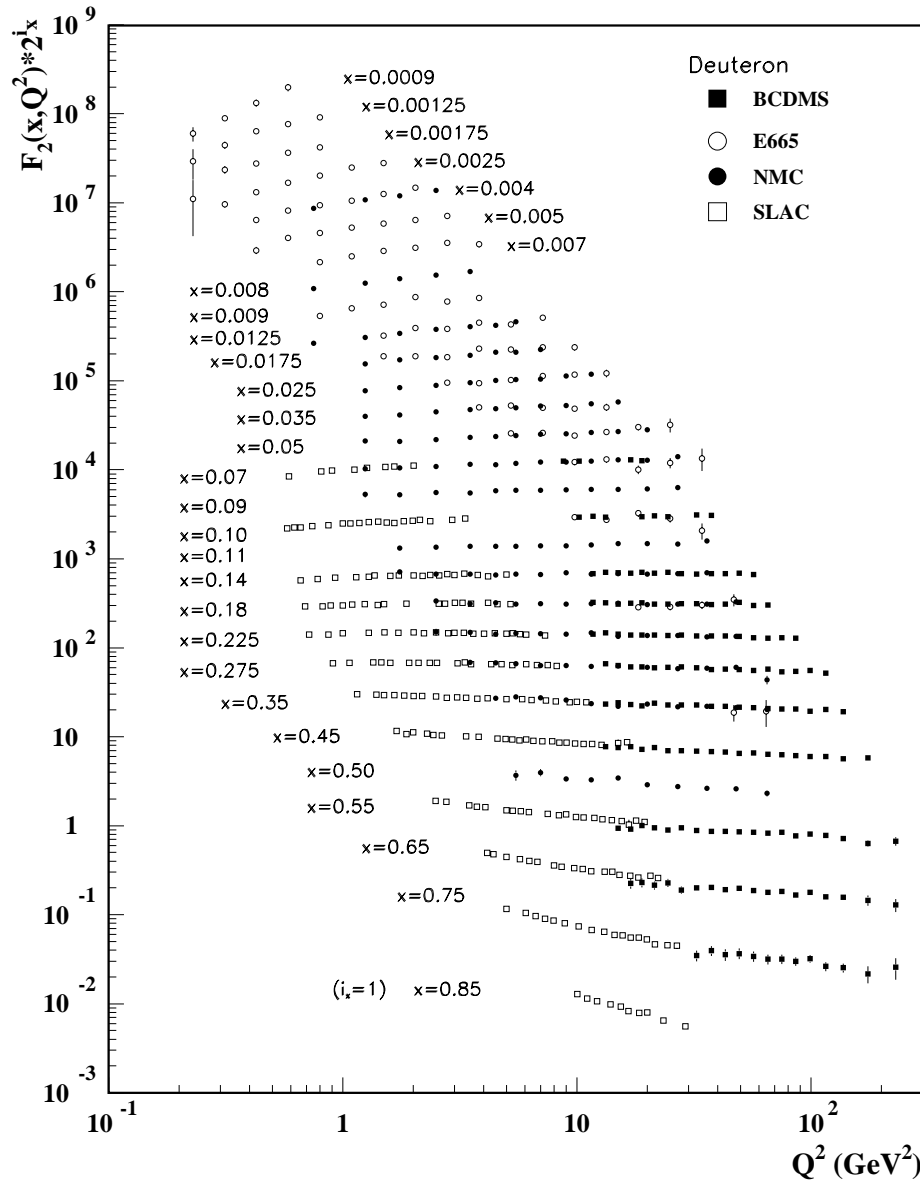


Figure 16.7: The deuteron structure function F_2^d measured in electromagnetic scattering of electrons (SLAC) and muons (BCDMS, E665, NMC) on a fixed target, shown as a function of Q^2 for bins of fixed x . Statistical and systematic errors added in quadrature are shown. For the purpose of plotting, F_2^d has been multiplied by 2^{i_x} , where i_x is the number of the x bin, ranging from 1 ($x = 0.85$) to 29 ($x = 0.0009$). References: **BCDMS**—A.C. Benvenuti *et al.*, Phys. Lett. **B237**, 592 (1990). **E665**, **NMC**, **SLAC**—same references as Fig. 16.6.

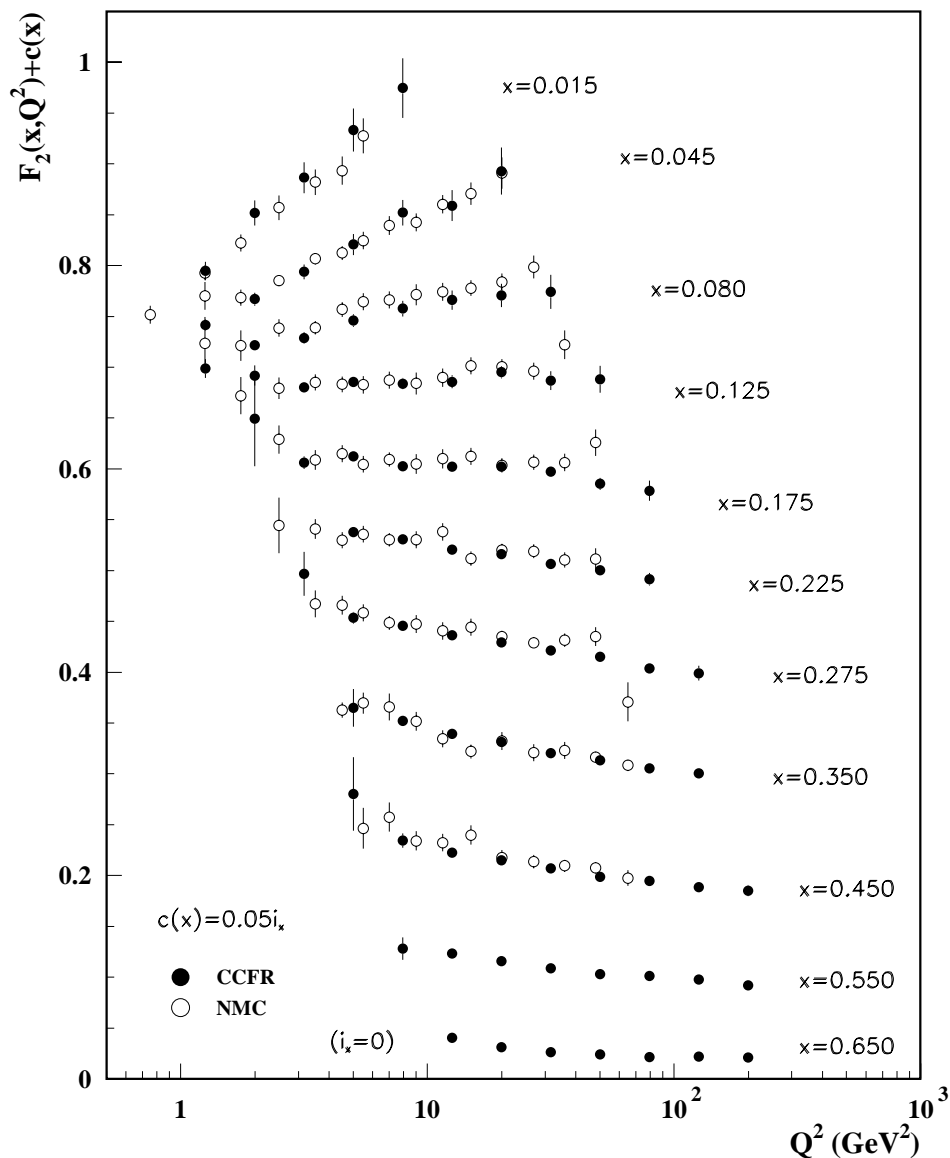


Figure 16.8: The deuteron structure function F_2 measured in deep inelastic scattering of muons on a fixed target (NMC) is compared to the structure function F_2 from neutrino-iron scattering (CCFR) using $F_2^{\mu} = (5/18)F_2^{\nu} - x(s + \bar{s})/6$, where heavy target effects have been taken into account. The data are shown versus Q^2 , for bins of fixed x . The NMC data have been rebinned to CCFR x values. Statistical and systematic errors added in quadrature are shown. For the purpose of plotting, a constant $c(x) = 0.05i_x$ is added to F_2 where i_x is the number of the x bin, ranging from 0 ($x = 0.65$) to 10 ($x = 0.015$). References: NMC—M. Arneodo *et al.*, Nucl. Phys. **B483**, 3 (97); CCFR/NuTeV—U.K. Yang *et al.*, Phys. Rev. Lett. **86**, 2741 (2001).

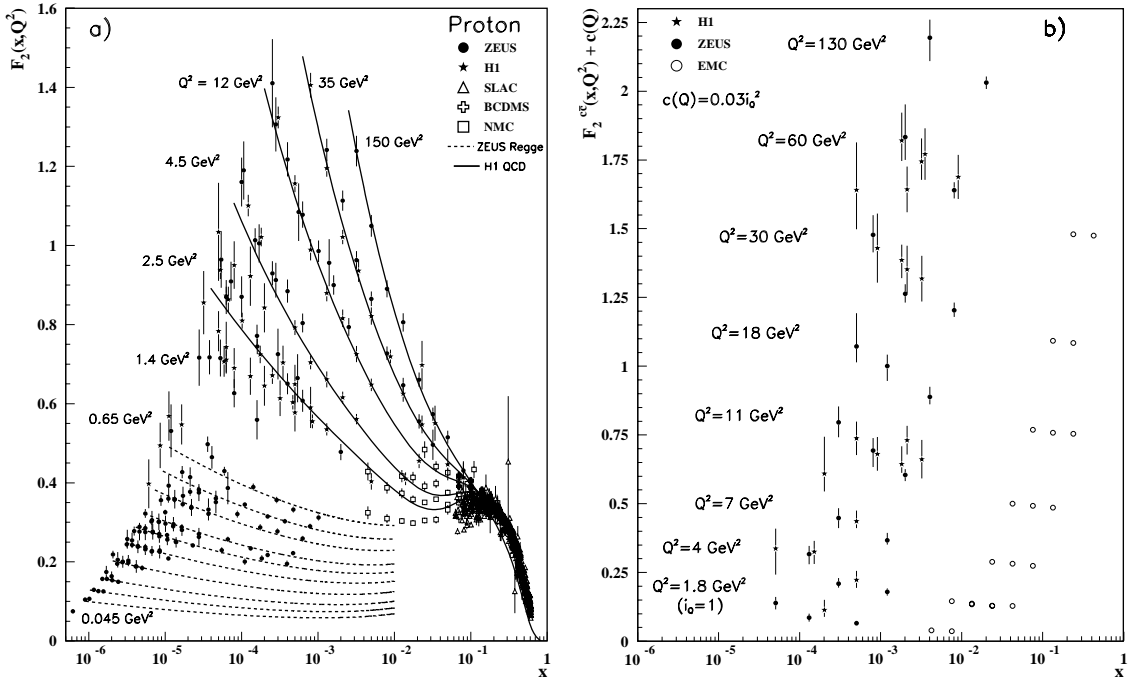


Figure 16.9: a) The proton structure function F_2^p mostly at small x and Q^2 , measured in electromagnetic scattering of positrons (H1, ZEUS), electrons (SLAC), and muons (BCDMS, NMC) on protons. Lines are ZEUS and H1 parameterizations for lower (Regge) and higher (QCD) Q^2 . Some points are only within 10% of the stated Q^2 . Some points have been slightly offset in x for clarity. References: **ZEUS**—J. Breitweg *et al.*, Phys. Lett. **B407**, 432 (1997); J. Breitweg *et al.*, Eur. Phys. J. **C7**, 609 (1999); J. Breitweg *et al.*, Phys. Lett. **B487**, 53 (2000) (both data and ZEUS Regge parameterization); S. Chekanov *et al.*, Eur. Phys. J. **C21**, 443 (2001); **H1**—C. Adloff *et al.*, Nucl. Phys. **B497**, 3 (1997); C. Adloff *et al.*, Eur. Phys. J. **C21**, 33 (2001) (both data and H1 QCD parameterization); **BCDMS**, **NMC**, **SLAC**—same references as Fig. 16.6.

b) The charm structure function $F_2^{c\bar{c}}(x)$, i.e. that part of the inclusive structure function F_2^p arising from the production of charm quarks, measured in electromagnetic scattering of positrons on protons (H1, ZEUS) and muons on iron (EMC). The H1 points have been slightly offset in x for clarity. For the purpose of plotting, a constant $c(Q) = 0.03i_Q^2$ is added to $F_2^{c\bar{c}}$ where i_Q is the number of the Q^2 bin, ranging from 1 ($Q^2 = 1.8 \text{ GeV}^2$) to 8 ($Q^2 = 130 \text{ GeV}^2$). References: **ZEUS**—J. Breitweg *et al.*, Eur. Phys. J. **C12**, 35 (2000); **H1**—C. Adloff *et al.*, Z. Phys. **C72**, 593 (1996); C. Adloff *et al.*, Phys. Lett. **B528**, 199 (2002); **EMC**—J.J. Aubert *et al.*, Nucl. Phys. **B213**, 31 (1983).

Statistical and systematic errors added in quadrature are shown for both plots. The data are given as a function of x in bins of Q^2 .

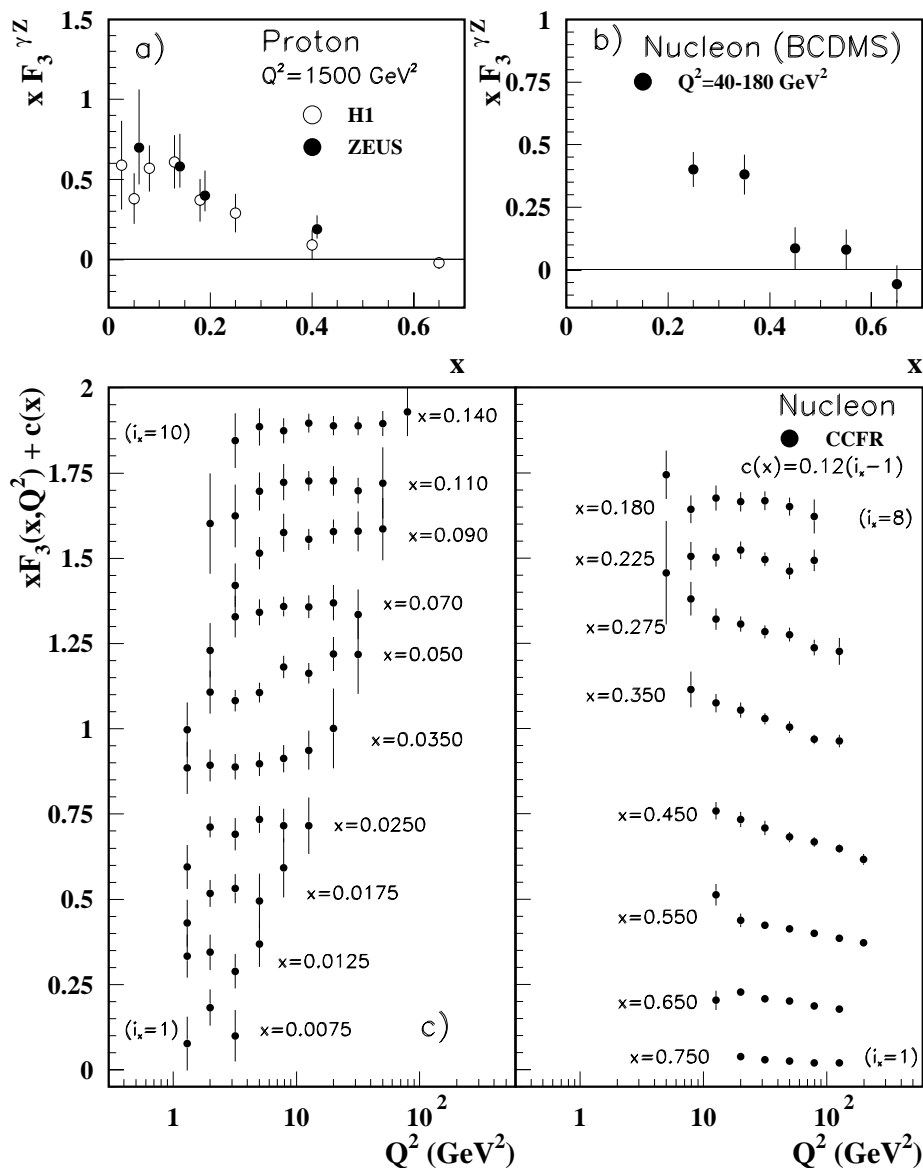


Figure 16.10: The structure function $x F_3^{\gamma Z}$ measured in electroweak scattering of a) electrons on protons (H1 and ZEUS) and b) muons on carbon (BCDMS). The ZEUS points have been slightly offset in x for clarity. References: **H1**—C. Adloff *et al.*, Eur. Phys. J. (accepted for publication) hep-ex/0304003; **ZEUS**—S. Chekanov *et al.*, Eur. Phys. J. **C28**, 175 (2003); **BCDMS**—A. Argento *et al.*, Phys. Lett. **B140**, 142 (1984).

c) The structure function $x F_3$ of the nucleon measured in ν -Fe scattering. The data are plotted as a function of Q^2 in bins of fixed x . For the purpose of plotting, a constant $c(x) = 0.12(i_x - 1)$ is added to $x F_3$, where i_x is the number of the x bin as shown in the plot. References: **CCFR**—W.G. Seligman *et al.*, Phys. Rev. Lett. **79**, 1213 (1997).

Statistical and systematic errors added in quadrature are shown for all plots.

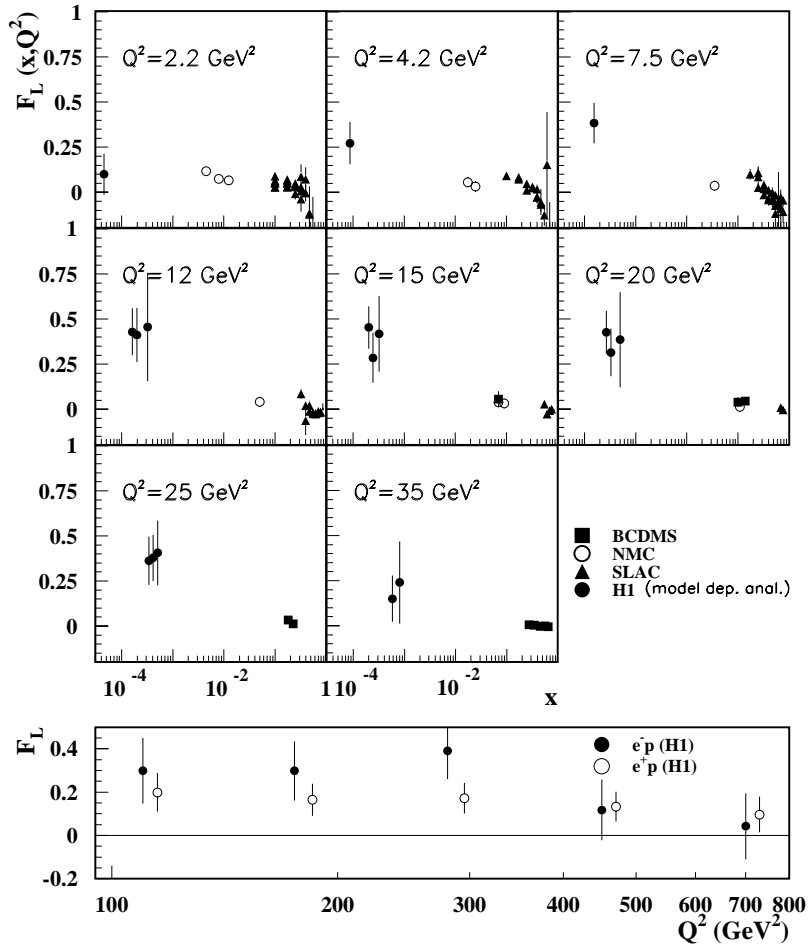


Figure 16.11: Top panel: The longitudinal structure function F_L as a function of x in bins of fixed Q^2 measured on the proton (except for the SLAC data which also contain deuterium data). BCDMS, NMC, and SLAC results are from measurements of R (the ratio of longitudinal to transverse photon absorption cross sections) which are converted to F_L by using the BCDMS parameterization of F_2 (A.C. Benvenuti *et al.*, Phys. Lett. **B223**, 485 (1989)). It is assumed that the Q^2 dependence of the fix-target data is small within a given Q^2 bin. References: **H1**—C. Adloff *et al.*, Eur. Phys. J. **C21**, 33 (2001); **BCDMS**—A. Benvenuti *et al.*, Phys. Lett. **B223**, 485 (1989); **NMC**—M. Arneodo *et al.*, Nucl. Phys. **B483**, 3 (1997); **SLAC**—L.W. Whitlow *et al.*, Phys. Lett. **B250**, 193 (1990) and numerical values from the thesis of L.W. Whitlow (SLAC-357).

Bottom panel: Higher Q^2 values of the longitudinal structure function F_L as a function of Q^2 given at the measured x for e^+/e^- -proton scattering. Points have been slightly offset in Q^2 for clarity. References: **H1**—C. Adloff *et al.*, Eur. Phys. J. (accepted for publication) hep-ex/0304003.

The H1 results shown in both plots require the assumption of the validity of the QCD form for the F_2 structure function in order to extract F_L . Statistical and systematic errors added in quadrature are shown for both plots.

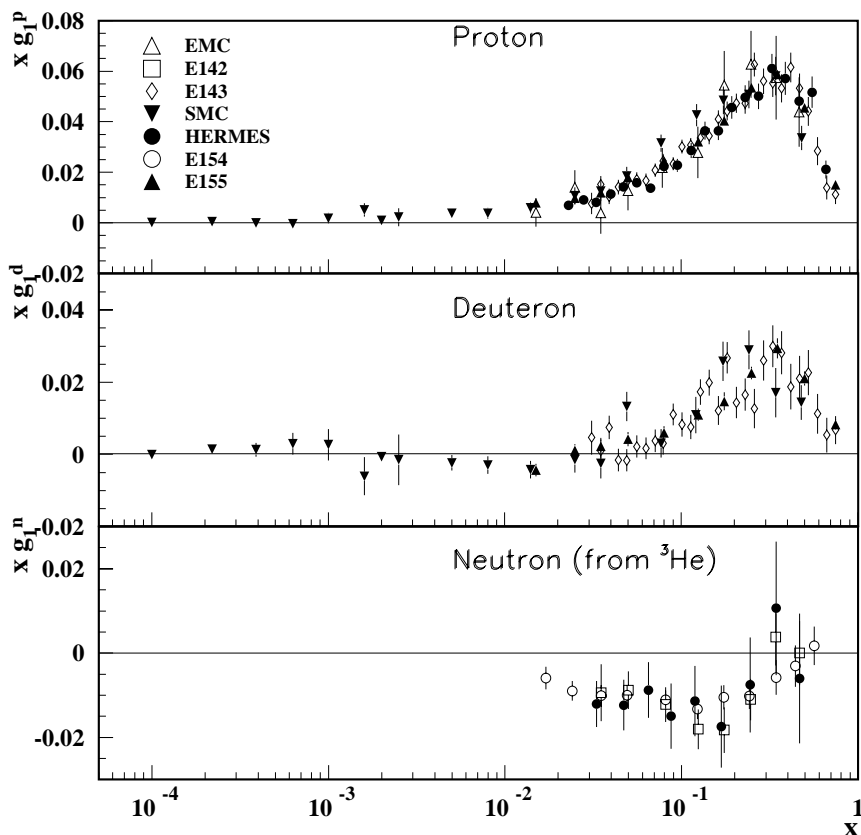


Figure 16.12: The spin-dependent structure function $xg_1(x)$ of the proton, deuteron, and neutron (from ^3He target) measured in deep inelastic scattering of polarized electrons/positrons: E142 ($Q^2 \sim 0.3 - 10 \text{ GeV}^2$), E143 ($Q^2 \sim 0.3 - 10 \text{ GeV}^2$), E154 ($Q^2 \sim 1 - 17 \text{ GeV}^2$), E155 ($Q^2 \sim 1 - 40 \text{ GeV}^2$), HERMES ($Q^2 \sim 0.8 - 20 \text{ GeV}^2$) and muons: EMC ($Q^2 \sim 1.5 - 100 \text{ GeV}^2$), SMC ($Q^2 \sim 0.01 - 100 \text{ GeV}^2$), shown at the measured Q^2 (except for EMC data given $Q^2 = 10.7 \text{ GeV}^2$ and E155 data given at $Q^2 = 5 \text{ GeV}^2$). Note that $g_1^n(x)$ may also be extracted by taking the difference between $g_1^d(x)$ and $g_1^p(x)$, but these values have been omitted in the bottom plot for clarity. Statistical and systematic errors added in quadrature are shown. References: **EMC**—J. Ashman *et al.*, Nucl. Phys. **B328**, 1 (1989); **E142**—P.L. Anthony *et al.*, Phys. Rev. **D54**, 6620 (1996); **E143**—K. Abe *et al.*, Phys. Rev. **D58**, 112003 (1998); **SMC**—B. Adeva *et al.*, Phys. Rev. **D58**, 112001 (1998), B. Adeva *et al.*, Phys. Rev. **D60**, 072004 (1999) and Erratum-Phys. Rev. **D62**, 079902 (2000); **HERMES**—A. Airapetian *et al.*, Phys. Lett. **B442**, 484 (1998) and K. Ackerstaff *et al.*, Phys. Lett. **B404**, 383 (1997); **E154**—K. Abe *et al.*, Phys. Rev. Lett. **79**, 26 (1997); **E155**—P.L. Anthony *et al.*, Phys. Lett. **B463**, 339 (1999) and P.L. Anthony *et al.*, Phys. Lett. **B493**, 19 (2000).

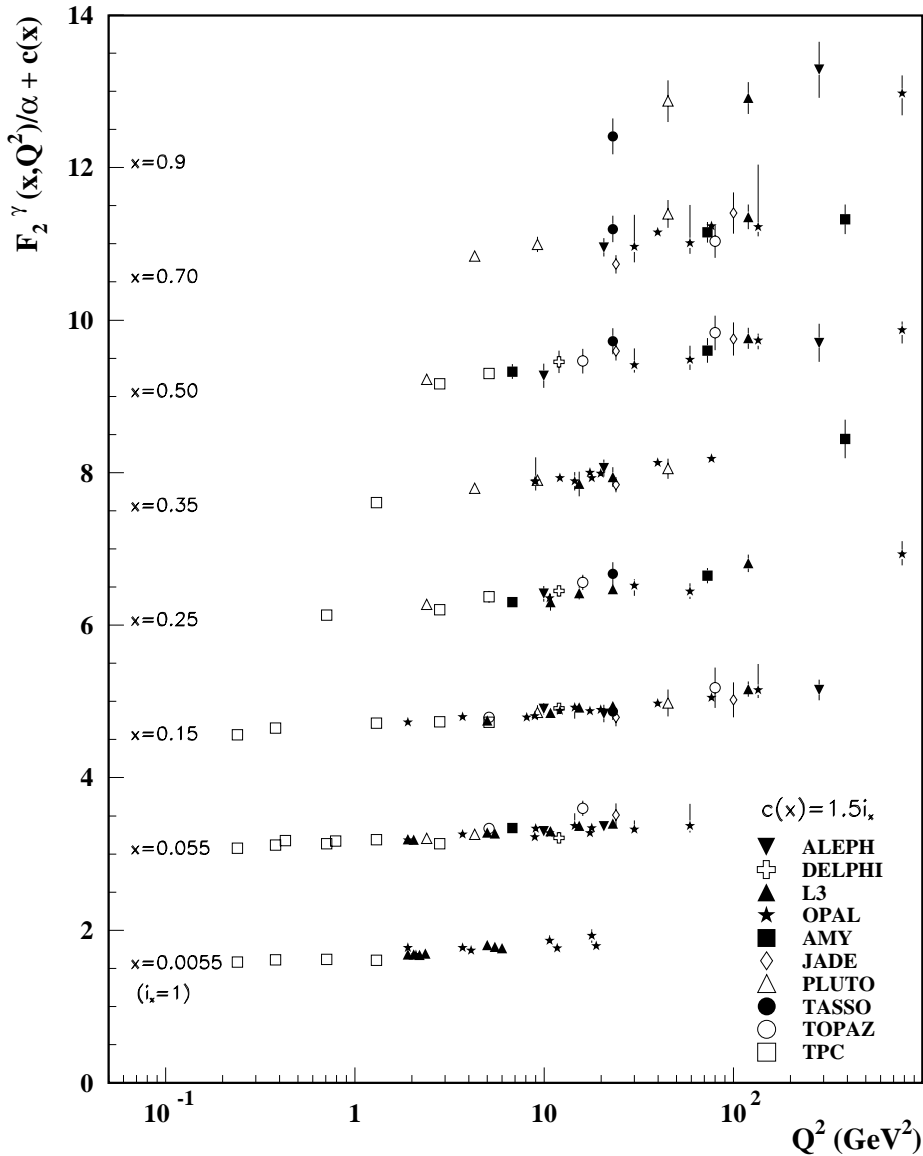


Figure 16.13: The hadronic structure function of the photon F_2^γ divided by the fine structure constant α measured in e^+e^- scattering, shown as a function of Q^2 for bins of x . Data points have been shifted to the nearest corresponding x bin as given in the plot. Some points have been offset in Q^2 for clarity. Statistical and systematic errors added in quadrature are shown. For the purpose of plotting, a constant $c(x) = 1.5i_x$ is added to F_2^γ/α where i_x is the number of the x bin, ranging from 1 ($x = 0.0055$) to 8 ($x = 0.9$). References: **ALEPH**—R. Barate *et al.*, Phys. Lett. **B458**, 152 (1999); **DELPHI**—P. Abreu *et al.*, Z. Phys. **C69**, 223 (1995); **L3**—M. Acciarri *et al.*, Phys. Lett. **B436**, 403 (1998); M. Acciarri *et al.*, Phys. Lett. **B447**, 147 (1999); M. Acciarri *et al.*, Phys. Lett. **B483**, 373 (2000); **OPAL**—A. Ackerstaff *et al.*, Phys. Lett. **B411**, 387 (1997); A. Ackerstaff *et al.*, Z. Phys. **C74**, 33 (1997); G. Abbiendi *et al.*, Eur. Phys. J. **C18**, 15 (2000); G. Abbiendi *et al.*, Phys. Lett. **B533**, 207 (2002) (note that there is some non-trivial statistical correlation between these last two papers); **AMY**—S.K. Sahu *et al.*, Phys. Lett. **B346**, 208 (1995); T. Kojima *et al.*, Phys. Lett. **B400**, 395 (1997); **JADE**—W. Bartel *et al.*, Z. Phys. **C24**, 231 (1984); **PLUTO**—C. Berger *et al.*, Phys. Lett. **142B**, 111 (1984); C. Berger *et al.*, Nucl. Phys. **B281**, 365 (1987); **TASSO**—M. Althoff *et al.*, Z. Phys. **C31**, 527 (1986); **TOPAZ**—K. Muramatsu *et al.*, Phys. Lett. **B332**, 477 (1994); **TPC/Two Gamma**—H. Aihara *et al.*, Z. Phys. **C34**, 1 (1987).

17. FRAGMENTATION FUNCTIONS IN e^+e^- ANNIHILATION

Revised September 2003 by O. Biebel (Max-Planck-Institut für Physik, Munich, Germany), P. Nason (INFN, Sez. di Milano, Milan, Italy), and B.R. Webber (Cavendish Laboratory, Cambridge, UK). An extended version of the 2001 version of this review can be found in Ref. 1

17.1. Introduction

Fragmentation functions are dimensionless functions that describe the final-state single-particle energy distributions in hard scattering processes. The total e^+e^- fragmentation function for hadrons of type h in annihilation at c.m. energy \sqrt{s} , via an intermediate vector boson $V = \gamma/Z^0$, is defined as

$$F^h(x, s) = \frac{1}{\sigma_{\text{tot}}} \frac{d\sigma}{dx} (e^+e^- \rightarrow V \rightarrow hX) \quad (17.1)$$

where $x = 2E_h/\sqrt{s} \leq 1$ is the scaled hadron energy (in practice, the approximation $x = x_p = 2p_h/\sqrt{s}$ is often used). Its integral with respect to x gives the average multiplicity of those hadrons:

$$\langle n_h(s) \rangle = \int_0^1 dx F^h(x, s). \quad (17.2)$$

Neglecting contributions suppressed by inverse powers of s , the fragmentation function (17.1) can be represented as a sum of contributions from the different parton types $i = u, \bar{u}, d, \bar{d}, \dots, g$:

$$F^h(x, s) = \sum_i \int_x^1 \frac{dz}{z} C_i(s; z, \alpha_S) D_i^h(x/z, s). \quad (17.3)$$

where D_i^h are the parton fragmentation functions. At lowest order in α_S the coefficient function C_g for gluons is zero, while for quarks $C_i = g_i(s)\delta(1-z)$ where $g_i(s)$ is the appropriate electroweak coupling. In particular, $g_i(s)$ is proportional to the charge-squared of parton i at $s \ll M_Z^2$, when weak effects can be neglected. In higher orders the coefficient functions and parton fragmentation functions are factorization-scheme dependent.

Parton fragmentation functions are analogous to the parton distributions in deep inelastic scattering (see sections on QCD and Structure Functions (9 and 16 of this *Review*). In both cases, the simplest parton-model approach would predict a scale-independent x distribution. Furthermore we obtain similar violations of this scaling behaviour when QCD corrections are taken into account.

17.2. Scaling violation

The evolution of the parton fragmentation function $D_i(x, t)$ with increasing scale $t = s$, like that of the parton distribution function $f_i(x, t)$ with $t = s$ (see Sec. 39 of this *Review*), is governed by the DGLAP equation [2]

$$t \frac{\partial}{\partial t} D_i(x, t) = \sum_j \int_x^1 \frac{dz}{z} \frac{\alpha_S}{2\pi} P_{ji}(z, \alpha_S) D_j(x/z, t). \quad (17.4)$$

In analogy to DIS, in some cases an evolution equation for the fragmentation function F itself (Eq. (17.3)) can be derived from Eq. (17.4) [3]. Notice that the splitting function is now P_{ji} rather than P_{ij} since here D_j represents the fragmentation of the final parton. The splitting functions again have perturbative expansions of the form

$$P_{ji}(z, \alpha_S) = P_{ji}^{(0)}(z) + \frac{\alpha_S}{2\pi} P_{ji}^{(1)}(z) + \dots \quad (17.5)$$

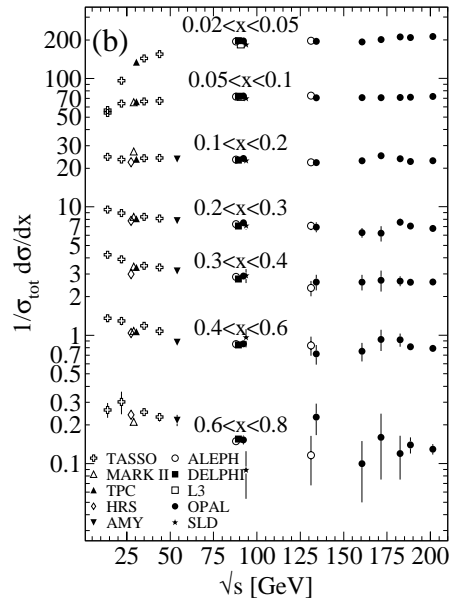
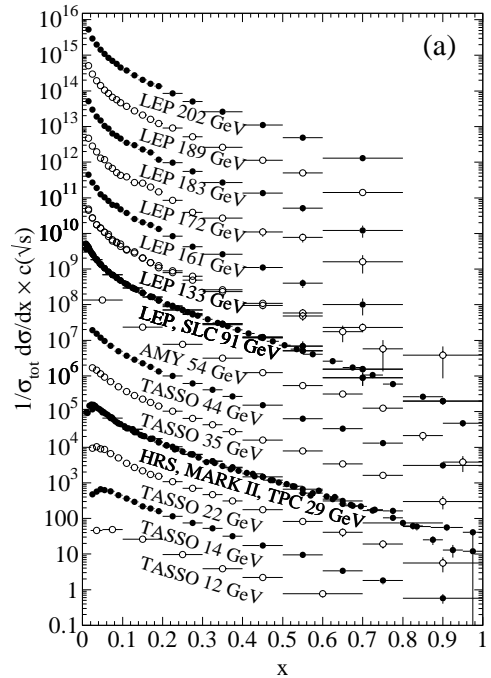


Figure 17.1: The e^+e^- fragmentation function for all charged particles is shown [6,7,8,9](a) for different c.m. energies, \sqrt{s} , versus x and (b) for various ranges of x versus \sqrt{s} . For the purpose of plotting (a), the distributions were scaled by $c(\sqrt{s}) = 10^i$ where i is ranging from $i = 0$ ($\sqrt{s} = 12$ GeV) to $i = 13$ ($\sqrt{s} = 202$ GeV).

where the lowest-order functions $P_{ji}^{(0)}(z)$ are the same as those in deep inelastic scattering but the higher-order terms [4]¹ are different. The effect of evolution is, however, the same in both cases: as the scale increases, one observes a scaling violation in which the x distribution is shifted towards lower values. This can be seen from Fig. 17.1.

The coefficient functions C_i in Eq. (17.3) and the splitting functions P_{ji} contain singularities at $z = 0$ and 1, which have important effects on fragmentation at small and large values of x , respectively. For details see *e.g.*, Ref. 1.

Quantitative results of studies of scaling violation in e^+e^- fragmentation are reported in Refs. 10,12. The values of α_S obtained are consistent with the world average (see section on QCD in Sec. 9 of this *Review*).

17.3. Longitudinal Fragmentation

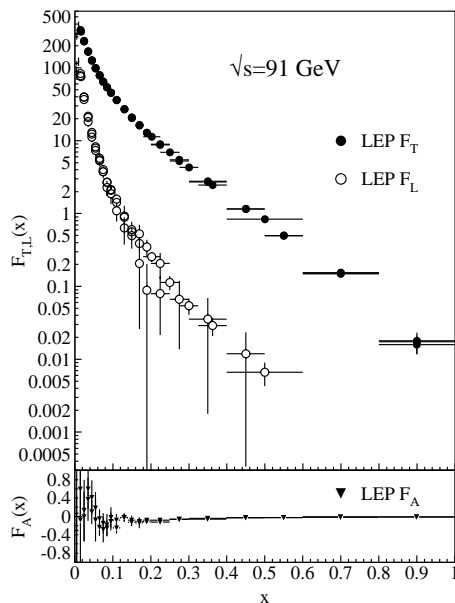


Figure 17.2: Transverse (F_T), longitudinal (F_L), and asymmetric (F_A) fragmentation functions are shown [8,11,13]. Data points with relative errors greater than 100% are omitted.

In the process $e^+e^- \rightarrow V \rightarrow hX$, the joint distribution in the energy fraction x and the angle θ between the observed hadron h and the incoming electron beam has the general form

$$\frac{1}{\sigma_{\text{tot}}} \frac{d^2\sigma}{dx d\cos\theta} = \frac{3}{8}(1 + \cos^2\theta) F_T(x) + \frac{3}{4}\sin^2\theta F_L(x) + \frac{3}{4}\cos\theta F_A(x), \quad (17.6)$$

where F_T , F_L and F_A are respectively the transverse, longitudinal and asymmetric fragmentation functions. All these functions also depend on the c.m. energy \sqrt{s} . Eq. (17.6) is the most general form of the inclusive single particle production from the decay of a massive vector boson [3]. As their names imply, F_T and F_L represent the contributions from virtual bosons polarized transversely or longitudinally with respect to the direction of motion of the hadron h . F_A is a parity-violating contribution which comes from the interference between vector and axial vector contributions. Integrating over all angles, we obtain the total fragmentation function, $F = F_T + F_L$. Each of these functions can be represented as a convolution of the parton fragmentation functions D_i with appropriate coefficient functions $C_i^{T,L,A}$ as in Eq. (17.3). This representation works in the

¹ There are misprints in the formulae in the published article. The correct expressions can be found in the preprint version or in Ref. 5.

high energy limit. As $x \cdot \sqrt{s}/2$ approaches hadronic scales $\simeq m_p$, power suppressed effects can no longer be neglected, and the fragmentation function formalism no longer accounts correctly for the separation of F_T , F_L , and F_A . In Fig. 17.2, F_T , F_L , and F_A measured at $\sqrt{s} = 91$ GeV are shown.

17.4. Gluon fragmentation

The gluon fragmentation function $D_g(x)$ can be extracted from the longitudinal fragmentation function defined in Eq. (17.6). Since the coefficient functions C_i^L for quarks and gluons are comparable in $\mathcal{O}(\alpha_S)$, F_L can be expressed in terms of F_T and D_g which allows one to obtain D_g from the measured F_L and F_T . It can also be deduced from the fragmentation of three-jet events in which the gluon jet is identified, for example by tagging the other two jets with heavy quark decays. To leading order the measured distributions of $x = E_{\text{had}}/E_{\text{jet}}$ for particles in gluon jets can be identified directly with the gluon fragmentation functions $D_g(x)$. The experimentally measured gluon fragmentation functions are shown in Fig. 17.3.

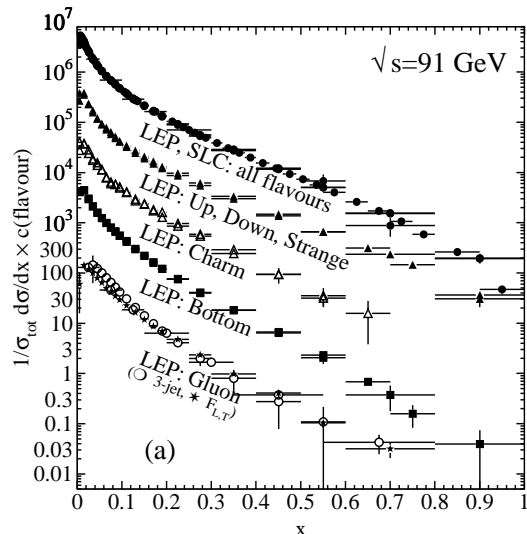


Figure 17.3: Comparison of the charged-particle and the flavour-dependent e^+e^- fragmentation functions obtained at $\sqrt{s} = 91$ GeV. The data [8,9,10,13,14] are shown for the inclusive, light (up, down, strange) quarks, charm quark, bottom quark, and the gluon versus x . For the purpose of plotting, the distributions were scaled by $c(\text{flavour}) = 10^i$ where i is ranging from $i = 0$ (Gluon) to $i = 4$ (all flavours).

17.5. Fragmentation models

Although the scaling violation can be calculated perturbatively, the actual form of the parton fragmentation functions is non-perturbative. Perturbative evolution gives rise to a shower of quarks and gluons (partons). Phenomenological schemes are then used to model the carry-over of parton momenta and flavour to the hadrons. Two of the very popular models are the *string fragmentation* [15,16], implemented in the JETSET [17] and UCLA [18] Monte Carlo event generation programs, and the *cluster fragmentation* of the HERWIG Monte Carlo event generator [19].

17.5.1. String fragmentation: The string-fragmentation scheme considers the colour field between the partons, *i.e.*, quarks and gluons, to be the fragmenting entity rather than the partons themselves. The string can be viewed as a colour flux tube formed by gluon self-interaction as two coloured partons move apart. Energetic gluon emission is regarded as energy-momentum carrying “kinks” on the string. When the energy stored in the string is sufficient, a $q\bar{q}$ pair may be created from the vacuum. Thus the string breaks up repeatedly

into colour singlet systems as long as the invariant mass of the string pieces exceeds the on-shell mass of a hadron. The $q\bar{q}$ pairs are created according to the probability of a tunnelling process $\exp(-\pi m_{q,\perp}^2/\kappa)$ which depends on the transverse mass squared $m_{q,\perp}^2 \equiv m_q^2 + p_{q,\perp}^2$ and the string tension $\kappa \approx 1$ GeV/fm. The transverse momentum $p_{q,\perp}$ is locally compensated between quark and antiquark. Due to the dependence on the parton mass m_q and/or hadron mass, m_h , the production of strange and, in particular, heavy-quark hadrons is suppressed. The light-cone momentum fraction $z = (E+p_{\parallel})_h/(E+p)_{q\bar{q}}$, where p_{\parallel} is the momentum of the formed hadron h along the direction of the quark q , is given by the string-fragmentation function

$$f(z) \sim \frac{1}{z}(1-z)^a \exp\left(-\frac{bm_{h,\perp}^2}{z}\right) \quad (17.7)$$

where a and b are free parameters. These parameters need to be adjusted to bring the fragmentation into accordance with measured data, e.g., $a = 0.11$ and $b = 0.52$ GeV $^{-2}$ as determined in Ref. 20 (for an overview on tuned parameters see Ref. 21).

17.5.2. Cluster fragmentation: Assuming a local compensation of colour based on the *pre-confinement* property of perturbative QCD [22], the remaining gluons at the end of the parton shower evolution are split non-perturbatively into quark-antiquark pairs. Colour singlet clusters of typical mass of a couple of GeV are then formed from quark and antiquark of colour-connected splittings. These clusters decay directly into two hadrons unless they are either too heavy (relative to an adjustable parameter CLMAX, default value 3.35 GeV), when they decay into two clusters, or too light, in which case a cluster decays into a single hadron, requiring a small rearrangement of energy and momentum with neighbouring clusters. The decay of a cluster into two hadrons is assumed to be isotropic in the rest frame of the cluster except if a perturbative-formed quark is involved. A decay channel is chosen based on the phase-space probability, the density of states, and the spin degeneracy of the hadrons. Cluster fragmentation has a compact description with few parameters, due to the phase-space dominance in the hadron formation.

17.6. Experimental studies

A great wealth of measurements of e^+e^- fragmentation into identified particles exists. A collection of references to find data on the fragmentation into identified particles is given for Table 40.1. As representatives of all the data, Fig. 17.4 shows fragmentation functions as the scaled momentum spectra of charged particles at several c.m. energies. Heavy flavour particles are dealt with separately in Sec. 17.7.

The measured fragmentation functions are solutions to the DGLAP equation (17.4) but need to be parametrized at some initial scale t_0 (usually 2 GeV 2 for light quarks and gluons). A general parametrization is [24]

$$D_{p \rightarrow h}(x, t_0) = N x^\alpha (1-x)^\beta \left(1 + \frac{\gamma}{x}\right) \quad (17.8)$$

where the normalization N , and the parameters α , β , and γ in general depend on the energy scale t_0 and also on the type of the parton, p , and the hadron, h . Frequently the term involving γ is left out [25]. The parameters of Eq. (17.8), listed in Ref. 25, were obtained by fitting data on various hadron types for different combinations of partons and hadrons in $p \rightarrow h$ in the range $\sqrt{s} \approx 5$ –200 GeV.

17.7. Heavy quark fragmentation

It was recognized very early [26] that a heavy flavoured meson should retain a large fraction of the momentum of the primordial heavy quark, and therefore its fragmentation function should be much harder than that of a light hadron. In the limit of a very heavy quark, one expects the fragmentation function for a heavy quark to go into any heavy hadron to be peaked near 1.

When the heavy quark is produced at a momentum much larger than its mass, one expects important perturbative effects, enhanced by powers of the logarithm of the transverse momentum over

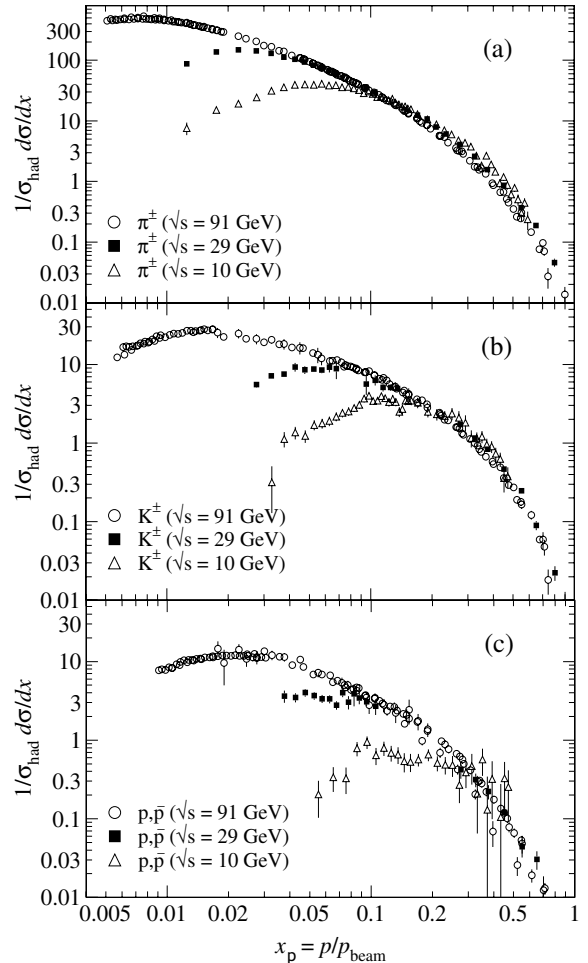


Figure 17.4: Scaled momentum spectra of (a) π^\pm , (b) K^\pm , and (c) p/\bar{p} at $\sqrt{s} = 10, 29$, and 91 GeV are shown [7,23].

the heavy quark mass, to intervene and modify the shape of the fragmentation function. In leading logarithmic order (*i.e.*, including all powers of $\alpha_S \log m_Q/p_T$) the total (*i.e.*, summed over all hadron types) perturbative fragmentation function is simply obtained by solving the leading evolution equation for fragmentation functions, Eq. (17.4), with the initial condition at a scale $\mu^2 = m_Q^2$ given by $D_Q(z, m_Q^2) = \delta(1-z)$ and $D_i(z, m_Q^2) = 0$ for $i \neq Q$ (the notation $D_i(z)$ stands for the probability to produce a heavy quark Q from parton i with a fraction z of the parton momentum).

Several extensions of the leading logarithmic result have appeared in the literature. Next-to-leading-log (NLL) order results for the perturbative heavy quark fragmentation function have been obtained in Ref. 27. At large z , phase space for gluon radiation is suppressed. This exposes large perturbative corrections due to the incomplete cancellation of real gluon radiation and virtual gluon exchange (Sudakov effects), which should be resummed in order to get accurate results. A leading-log (LL) resummation formula has been obtained in Refs. 27,28. Next-to-leading-log resummation has been performed in Ref. 29. Fixed-order calculations of the fragmentation function at order α_S^2 in e^+e^- annihilation have appeared in Ref. 30. This result does not include terms of order $(\alpha_S \log s/m^2)^k$ and $\alpha_S(\alpha_S \log s/m^2)^k$, but it does include correctly all terms up to the order α_S^2 , including terms without any logarithmic enhancements.

Inclusion of non-perturbative effects in the calculation of the heavy quark fragmentation function is done in practice by convolving the perturbative result with a phenomenological non-perturbative form. Among the most popular parametrizations we have the following:

$$\text{Peterson } et al. [3]: D_{np}(z) \propto \frac{1}{z} \left(1 - \frac{1}{z} - \frac{\epsilon}{1-z}\right)^{-2}, \quad (17.9)$$

$$\text{Kartvelishvili } et al. [32]: D_{np}(z) \propto z^\alpha (1-z), \quad (17.10)$$

$$\text{Collins\&Spiller [33]: } D_{np}(z) \propto \left(\frac{1-z}{z} + \frac{(2-z)\epsilon_C}{1-z}\right) \times (1+z^2) \left(1 - \frac{1}{z} - \frac{\epsilon_C}{1-z}\right)^{-2} \quad (17.11)$$

where ϵ , α , and ϵ_C are non-perturbative parameters, depending upon the heavy hadron considered. In general, the non-perturbative parameters do not have an absolute meaning. They are fitted together with some model of hard radiation, which can be either a shower Monte Carlo, a leading-log or NLL calculation (which may or may not include Sudakov resummation), or a fixed order calculation. In Ref. 30, for example, the ϵ parameter for charm and bottom production is fitted from the measured distributions of Refs. 34,35 for charm, and of Ref. 36 for bottom. If the leading-logarithmic approximation (LLA) is used for the perturbative part, one finds $\epsilon_c \approx 0.05$ and $\epsilon_b \approx 0.006$; if a second order calculation is used one finds $\epsilon_c \approx 0.035$ and $\epsilon_b \approx 0.0033$; if a NLLO calculation is used instead one finds $\epsilon_c \approx 0.022$ and $\epsilon_b \approx 0.0023$. The larger values found in the LL approximation are consistent with what is obtained in the context of parton shower models [37], as expected. The ϵ parameter for charm and bottom scales roughly with the inverse square of the heavy flavour mass. This behaviour can be justified by several arguments [26,38]. It can be used to relate the non-perturbative parts of the fragmentation functions of charm and bottom quarks [30,39].

The bulk of the available fragmentation function data on charmed mesons (excluding $J/\psi(1S)$) is from measurements in e^+e^- annihilation at $\sqrt{s} \approx 10$ GeV. Shown in Fig. 17.5(a) are the efficiency-corrected (but not branching ratio corrected) CLEO and ARGUS inclusive cross sections, $s \cdot B d\sigma/dx_p$, for the production of D^0 and D^{*+} . The variable x_p approximates the light-cone momentum fraction z in Eq. (17.9), but is not identical to it.

For the D^0 , B represents the product branching fraction: $D^{*+} \rightarrow D^0\pi^+$, $D^0 \rightarrow K^-\pi^+$. These inclusive spectra have not been corrected for cascades from higher states, nor for radiative effects. Since the momentum spectra are sensitive to QED and QCD radiative corrections, charm spectra at $\sqrt{s} = 10$ GeV cannot be compared directly with spectra at higher c.m. energies, and must be appropriately evolved. Tuning ϵ of (17.9) in the JETSET 7.4 Monte Carlo generator [17] using the parameter set of Ref. 20 and including radiative corrections to describe the combined CLEO and ARGUS D^0 and D^{*+} data gives $\epsilon_c = 0.043 \pm 0.004$; this is indicated in the solid curves.²

Experimental studies of the fragmentation function for b quarks, shown in Fig. 17.5(b), have been performed at LEP and SLD [36,41,42]. Commonly used methods identify the B meson through its semileptonic decay or based upon tracks emerging from the B secondary vertex. The most recent studies [42] fit the B spectrum using a Monte Carlo shower model supplemented with non-perturbative fragmentation functions yielding consistent results.

The experiments measure primarily the spectrum of B mesons. This defines a fragmentation function which includes the effect of the decay of higher mass excitations, like the B^* and B^{**} . In the literature there is sometimes ambiguity in what is defined to be the bottom fragmentation function. Instead of using what is directly measured (*i.e.*, the B meson spectrum) corrections are applied to account for B^* or B^{**} production in some cases. For a more detailed discussion see Ref. 1.

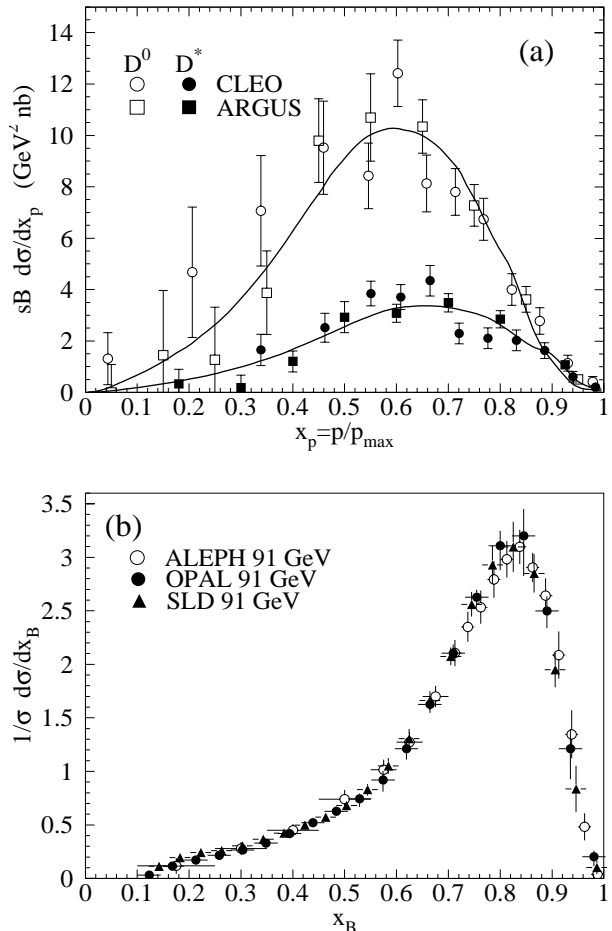


Figure 17.5: (a) Efficiency-corrected inclusive cross-section measurements for the production of D^0 and D^{*+} in e^+e^- annihilation at $\sqrt{s} \approx 10$ GeV [35,40]. (b) Measured e^+e^- fragmentation function of b quarks into B hadrons at $\sqrt{s} \approx 91$ GeV [41,42].

Besides degrading the fragmentation function by gluon radiation, QCD evolution can also generate soft heavy quarks, increasing in the small x region as s increases. Several theoretical studies are available on the issue of how often $b\bar{b}$ or $c\bar{c}$ pairs are produced indirectly, via a gluon splitting mechanism [43–45]. Experimental results from studies on charm production via gluon splitting [46,47], and measurements of $g \rightarrow b\bar{b}$ [48–50] are given in Table 17.1.

In Ref. 44 an explicit calculation of these quantities has been performed. Using these results, charm and bottom multiplicities as reported in Table 17.1 for different values of the masses and of $\Lambda_{\overline{\text{MS}}}^{(5)}$ were computed in Ref. 51. The averaged experimental result for charm, $(3.23 \pm 0.42)\%$, is 1–2 standard deviations above the theoretical prediction, preferring lower values of the quark mass and/or a larger value of $\Lambda_{\overline{\text{MS}}}^{(5)}$. However, higher-order corrections may well be substantial at the charm quark mass scale. Better agreement is achieved for bottom.

As reported in Ref. 44, Monte Carlo models are in qualitative agreement with these results, although the spread of the values they obtain is somewhat larger than the theoretical error estimated by the direct calculation. In particular, for charm one finds that while HERWIG [19] and JETSET [17] agree quite well with the theoretical calculation, ARIADNE [52] is higher by roughly a factor of 2, and

² This paragraph is adapted from D. Besson's contribution to C. Caso *et al.*, Eur. Phys. J. C3, 1 (1998).

Table 17.1: Measured fraction of events containing $g \rightarrow c\bar{c}$ and $g \rightarrow b\bar{b}$ subprocesses in Z decays, compared with theoretical predictions. The central/lower/upper values for the theoretical predictions are obtained with $m_c = (1.5 \pm 0.3)$ and $m_b = (4.75 \pm 0.25)$ GeV.

	$\overline{n}_{g \rightarrow c\bar{c}} (\%)$	$\overline{n}_{g \rightarrow b\bar{b}} (\%)$
OPAL	[46] $3.20 \pm 0.21 \pm 0.38$	
ALEPH	[47] $3.26 \pm 0.23 \pm 0.42$	[49] $0.277 \pm 0.042 \pm 0.057$
DELPHI		[48] $0.21 \pm 0.11 \pm 0.09$
SLD		[50] $0.307 \pm 0.071 \pm 0.066$
Theory [44]		
$\Lambda_{\overline{\text{MS}}}^{(5)} = 150$ MeV	$1.35^{+0.48}_{-0.30}$	0.20 ± 0.02
$\Lambda_{\overline{\text{MS}}}^{(5)} = 300$ MeV	$1.85^{+0.69}_{-0.44}$	0.26 ± 0.03

this is in better agreement with data. For bottom, agreement between theory, models and data is adequate. For a detailed discussion see Ref. 53.

The discrepancy with the charm prediction may be due to experimental cuts forcing the final state configuration to be more 3-jet like, which increases the charm multiplicity. Calculations that take this possibility into account are given in Ref. 45.

References:

- O. Biebel, P. Nason, and B.R. Webber, Bicocca-FT-01-20, Cavendish-HEP-01/12, MPI-PhE/2001-14, hep-ph/0109282.
- L.N. Lipatov, Sov. J. Nucl. Phys. **20**, 95 (1975); V.N. Gribov and L.N. Lipatov, Sov. J. Nucl. Phys. **15**, 438 (1972); G. Altarelli and G. Parisi, Nucl. Phys. **B126**, 298 (1977); Yu.L. Dokshitzer, Sov. Phys. JETP **46**, 641 (1977).
- P. Nason and B.R. Webber, Nucl. Phys. **B421**, 473 (1994); erratum *ibid.*; **B480**, 755 (1996).
- W. Furmanski and R. Petronzio, preprint TH.2933-CERN (1980), Phys. Lett. **97B**, 437 (1980).
- R.K. Ellis, J. Stirling, and B.R. Webber: *QCD and Collider Physics*, Cambridge University Press, Cambridge (1996).
- TASSO Collaboration: R. Brandelik *et al.*, Phys. Lett. **B114**, 65 (1982); W. Braunschweig *et al.*, Z. Phys. **C47**, 187 (1990); HRS Collaboration: D.Bender *et al.*, Phys. Rev. **D31**, 1 (1984); MARK II Collaboration: A. Petersen *et al.*, Phys. Rev. **D37**, 1 (1988); AMY Collaboration: Y.K. Li *et al.*, Phys. Rev. **D41**, 2675 (1990); ALEPH Collaboration: D. Buskulic *et al.*, Z. Phys. **C73**, 409 (1997); OPAL Collaboration: R. Akers *et al.*, Z. Phys. **C72**, 191 (1996); G. Abbiendi *et al.*, Eur. Phys. J. **C27**, 467 (2003); K. Ackerstaff *et al.*, Z. Phys. **C75**, 193 (1997); G. Abbiendi *et al.*, Eur. Phys. J. **C16**, 185 (2000).
- TPC Collaboration: H. Aihara *et al.*, Phys. Rev. Lett. **61**, 1263 (1988).
- DELPHI Collaboration: P. Abreu *et al.*, Eur. Phys. J. **C6**, 19 (1999).
- ALEPH Collaboration: E. Barate *et al.*, Phys. Reports **294**, 1 (1998); L3 Collaboration: B. Adeva *et al.*, Phys. Lett. **B259**, 199 (1991); OPAL Collaboration: K. Ackerstaff *et al.*, Eur. Phys. J. **C7**, 369 (1998); MARK II Collaboration: G.S. Abrams *et al.*, Phys. Rev. Lett. **64**, 1334 (1990).
- DELPHI Collaboration: P. Abreu *et al.*, Phys. Lett. **B398**, 194 (1997).
- ALEPH Collaboration: D. Barate *et al.*, Phys. Lett. **B357**, 487 (1995); erratum *ibid.*; **B364**, 247 (1995).
- DELPHI Collaboration: P. Abreu *et al.*, Eur. Phys. J. **C13**, 573 (2000); Phys. Lett. **B311**, 408 (1993); W. de Boer and T. Kufmaul, IEKP-KA/93-8, hep-ph/9309280;; B.A. Kniehl, G. Kramer, and B. Pötter, Phys. Rev. Lett. **85**, 5288 (2001).
- OPAL Collaboration: R. Akers *et al.*, Z. Phys. **C86**, 203 (1995).
- ALEPH Collaboration: R. Barate *et al.*, Eur. Phys. J. **C17**, 1 (2000); OPAL Collaboration: G. Abbiendi *et al.*, Eur. Phys. J. **C11**, 217 (1999); R. Akers *et al.*, Z. Phys. **C68**, 179 (1995).
- X. Artru and G. Mennessier, Nucl. Phys. **B70**, 93 (1974).
- B. Andersson, G. Gustafson, G. Ingelman, T. Sjöstrand, Phys. Reports **97**, 31 (1983).
- T. Sjöstrand and M. Bengtsson, Comp. Phys. Comm. **43**, 367 (1987); T. Sjöstrand, Comp. Phys. Comm. **82**, 74 (1994).
- S. Chun and C. Buchanan, Phys. Reports **292**, 239 (1998).
- G. Marchesini *et al.*, Comp. Phys. Comm. **67**, 465 (1992); G. Corcella *et al.*, JHEP **0101**, 010 (2001).
- OPAL Collaboration: G. Alexander *et al.*, Z. Phys. **C69**, 543 (1996).
- M. Schmelling, Phys. Scripta **51**, 683 (1995).
- D. Amati and G. Veneziano, Phys. Lett. **B83**, 87 (1979).
- ALEPH Collaboration: D. Buskulic *et al.*, Z. Phys. **C66**, 355 (1995); ARGUS Collaboration: H. Albrecht *et al.*, Z. Phys. **C44**, 547 (1989); DELPHI Collaboration: P. Abreu *et al.*, Eur. Phys. J. **C5**, 585 (1998); OPAL Collaboration: R. Akers *et al.*, Z. Phys. **C63**, 181 (1994); SLD Collaboration: K. Abe *et al.*, Phys. Rev. **D59**, 052001 (1999).
- B.A. Kniehl, G. Kramer and B. Pötter, Nucl. Phys. **B597**, 337 (2001).
- L. Bourhis *et al.*, Eur. Phys. J. **C19**, 89 (2001); B.A. Kniehl, G. Kramer, and B. Pötter, Nucl. Phys. **B582**, 514 (2000); J. Binnewies, B.A. Kniehl, and G. Kramer, Phys. Rev. **D52**, 4947 (1995); Z. Phys. **C65**, 471 (1995); J. Binnewies, Hamburg University PhD Thesis, DESY 97-128, hep-ph/9707269.
- V.A. Khoze, Ya.I. Azimov, and L.L. Frankfurt, Proceedings, Conference on High Energy Physics, Tbilisi 1976; J.D. Bjorken, Phys. Rev. **D17**, 171 (1978).
- B. Mele and P. Nason, Phys. Lett. **B245**, 635 (1990); Nucl. Phys. **B361**, 626 (1991).
- Y. Dokshitzer, V.A. Khoze, and S.I. Troyan, Phys. Rev. **D53**, 89 (1996).
- M. Cacciari and S. Catani, Nucl. Phys. **B617**, 253 (2001).
- P. Nason and C. Oleari, Phys. Lett. **B418**, 199 (1998) *ibid.*; **B447**, 327 (1999); Nucl. Phys. **B565**, 245 (2000).
- C. Peterson *et al.*, Phys. Rev. **D27**, 105 (1983).
- V.G. Kartvelishvili, A.K. Likheoded, and V.A. Petrov, Phys. Lett. **B78**, 615 (1978).
- P. Collins and T. Spiller, J. Phys. **G11**, 1289 (1985).
- OPAL Collaboration: R. Akers *et al.*, Z. Phys. **C67**, 27 (1995).
- ARGUS Collaboration: H. Albrecht *et al.*, Z. Phys. **C52**, 353 (1991).

-
36. ALEPH Collaboration: D. Buskulic *et al.*, Phys. Lett. **B357**, 699 (1995).
37. J. Chrin, Z. Phys. **C36**, 163 (1987).
38. R.L. Jaffe and L. Randall, Nucl. Phys. **B412**, 79 (1994);
P. Nason and B. Webber, Phys. Lett. **B395**, 355 (1997).
39. G. Colangelo and P. Nason, Phys. Lett. **B285**, 167 (1992);
L. Randall and N. Rius, Nucl. Phys. **B441**, 167 (1995).
40. CLEO Collaborations: D. Bortoletto *et al.*, Phys. Rev. **D37**, 1719 (1988).
41. OPAL Collaboration: G. Alexander *et al.*, Phys. Lett. **B364**, 93 (1995);
L3 Collaboration: B. Adeva *et al.*, Phys. Lett. **B261**, 177 (1991).
42. SLD Collaboration: K. Abe *et al.*, Phys. Rev. Lett. **84**, 4300 (2000);
K. Abe *et al.*, Phys. Rev. **D65**, 092006 (2002); erratum **D66**, 079905 (2002);
ALEPH Collaboration: A. Heister *et al.*, Phys. Lett. **B512**, 30 (2001);
OPAL Collaboration: G. Abbiendi *et al.*, Eur. Phys. J. **C29**, 463 (2003).
43. A.H. Mueller and P. Nason, Nucl. Phys. **B266**, 265 (1986);
M.L. Mangano and P. Nason, Phys. Lett. **B285**, 160 (1992).
44. M.H. Seymour, Nucl. Phys. **B436**, 163 (1995).
45. D.J. Miller and M.H. Seymour, Phys. Lett. **B435**, 213 (1998).
46. OPAL Collaboration: G. Abbiendi *et al.*, Eur. Phys. J. **C13**, 1 (2000).
47. ALEPH Collaboration: R. Barate *et al.*, Eur. Phys. J. **C16**, 597 (2000);
ALEPH Collaboration: R. Barate *et al.*, Phys. Lett. **B561**, 213 (2003).
48. DELPHI Collaboration: P. Abreu *et al.*, Phys. Lett. **B405**, 202 (1997).
49. ALEPH Collaboration: R. Barate *et al.*, Phys. Lett. **B434**, 437 (1998).
50. SLD Collaboration: K. Abe *et al.*, SLAC-PUB-8157, hep-ex/9908028.
51. S. Frixione, M.L. Mangano, P. Nason, and G. Ridolfi: Heavy Quark Production, in A.J. Buras and M. Lindner (eds.), *Heavy Flavours II*, World Scientific, Singapore (1998), hep-ph/9702287.
52. L. Lönnblad, Comp. Phys. Comm. **71**, 15 (1992).
53. A. Ballestrero *et al.*, CERN-2000-09-B, hep-ph/0006259.